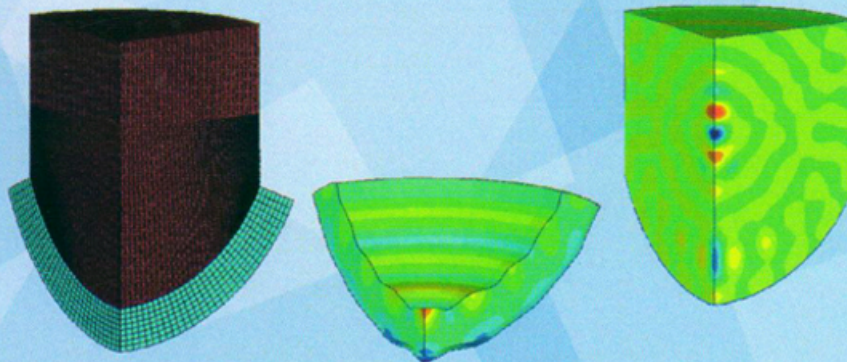


Icarus

---

A. V. Nasedkin, A. A. Nasedkina

# FINITE ELEMENT MODELING OF COUPLED PROBLEMS



FEDERAL STATE AUTONOMOUS EDUCATIONAL  
ESTABLISHMENT OF HIGHER EDUCATION  
SOUTHERN FEDERAL UNIVERSITY

**A. V. Nasedkin, A. A. Nasedkina**

**FINITE ELEMENT MODELING  
OF COUPLED PROBLEMS**

Rostov-on-Don  
2015

UDK 519.6+539.3+004.4

BBK 22.251

N24

*Published by decision of Editorial and Publishing Council of Southern  
Federal University*

**Reviewers:**

Soloviev A. N., Doctor of Physical and Mathematical Sciences,  
Associate Professor

Tkachev A. N., Doctor of Engineering, Professor

**Nasedkin A. V., Nasedkina A. A.**

N24 Finite element modeling of coupled problems: textbook /  
A. V. Nasedkin, A. A. Nasedkina. – Rostov-on-Don: publishing  
house of Southern Federal University, 2015. – 174 p.  
ISBN 978-5-9275-1611-7

This book partially corresponds to the lecture course “Finite element modeling of coupled problems” which is given in the framework of the Master degree program “IT in Biomechanics” in Institute of Mathematics, Mechanics and Computer Science of Southern Federal University. The book can be also used by students, post-graduate students and specialists who work in various areas of applied mathematics and mechanics.

The lecture course considers the issues of mathematical modeling of coupled physico-mechanical problems and application of finite element method for their solution. Special attention is given to coupled problems of electroelasticity, thermoelasticity, poroelasticity, and problems of interaction of deformable solids with acoustic media. Mathematical features of classical and generalized statements for the considered problems are given in details. Theoretical part of the book is supported by practical assignments for solving test problems of piezoelectricity, thermoelasticity and problems of interaction of solids with acoustic media in ANSYS 11.0 and higher versions.

Published in the original edition.

*The publishing of this textbook was carried out in the framework of the Tempus-IV project “Internationalized Curricula Advancement at Russian Universities in the Southern Region (ICARUS)”.*

ISBN 978-5-9275-1611-7

UDK 519.6+539.3+004.4

BBK 22.251

© Nasedkin A. V., Nasedkina A. A., 2015

# Contents

<b>Introduction</b>	<b>5</b>
<b>1 Some models of coupled problems for mechanics of solids</b>	<b>9</b>
1.1 Basic notations. Vectors and tensors . . . . .	9
1.1.1 Introduction to vectors and tensors . . . . .	9
1.1.2 Main notations and values in coupled problems of elasticity theory .	13
1.2 General issues . . . . .	15
1.3 Modeling of electroelasticity problems . . . . .	19
1.3.1 Classical statements of electroelasticity problems . . . . .	21
1.3.2 Generalized statements of electroelasticity problems . . . . .	28
1.3.3 Semi-discrete approximations in electroelasticity problems . . . . .	38
1.3.4 Summary of the main features of electroelasticity problems . . . . .	41
1.4 Modeling of thermoelasticity problems . . . . .	45
1.4.1 Classical statements of thermoelasticity problems . . . . .	45
1.4.2 Generalized statements of thermoelasticity problems . . . . .	49
1.4.3 Semi-discrete approximations in thermoelasticity problems . . . . .	52
1.5 Problems of poroelasticity. Porothermoelastic analogy . . . . .	54
1.6 Modeling of the interaction of deformable solids with acoustic media . . . . .	57
1.6.1 Classical statements of acoustic problems . . . . .	58
1.6.2 Semi-discrete approximations on the base of generalized statements and conjugation of acoustic equations with equations of solid structure	61
Exercises for Chapter 1 . . . . .	65
<b>2 Finite element method for coupled physico-mechanical problems</b>	<b>73</b>
2.1 General scheme of Galerkin method. Dynamic and static problems . . . . .	73
2.2 Finite element method as a version of Galerkin method. Main ideas of FEM	77
2.3 Basic finite element approximations . . . . .	85
Exercises for Chapter 2 . . . . .	99
<b>3 Practical assignments and examples of solving problems in ANSYS</b>	<b>103</b>
3.1 Practical assignment No. 1. Static deformation of a piezoceramic transducer with multi-electrode coating . . . . .	103
3.1.1 Example problem and solution methods . . . . .	104
3.1.2 Individual assignments . . . . .	129
3.2 Practical assignment No. 2. Plane problem of heating and cooling of a thermoelastic body . . . . .	132

---

3.2.1	Brief information on the solution techniques for the transient problems of thermoelasticity for isotropic bodies . . . . .	132
3.2.2	Example problem and solution methods . . . . .	135
3.2.3	Individual assignments . . . . .	145
3.3	Practical assignment No. 3. Steady-state oscillations of an elastic transmitter in acoustic medium . . . . .	146
3.3.1	Brief information on the solution techniques for the problems of interaction of solids with acoustic media . . . . .	147
3.3.2	Example problem and solution methods . . . . .	150
3.3.3	Individual assignments . . . . .	166
	<b>References</b>	<b>171</b>

# Introduction

The main goal of this book is to describe mathematical models and numerical methods of solving coupled physico-mechanical problems with the use of modern software, mainly ANSYS finite element package.

In accordance to this goal in the first chapter of this book we consider the issues of mathematical modeling of coupled physico-mechanical problems, such as the problems of electroelasticity, thermoelasticity, poroelasticity and the problems of interaction of deformable solids with acoustic media. The second chapter briefly describes the classical technique of finite element approximations and basic finite elements. The theoretical part of this book in the third chapter is supplemented by a set of practical assignments on solving coupled physico-mechanical problems in ANSYS of the version 11.0 and higher.

The methodology of studying coupled physico-mechanical problems includes the following common stages: the formulation of the classical problem statement (the system of differential equations and the boundary and initial conditions); the transition from the classical problem statements to the generalized problem statements; the application of discrete approximations by spatial variables; the obtaining of the corresponding system of discretized equations.

Despite of the common approach applied for simulating all problems considered in the first chapter, each type of these coupled problems has its own peculiarities.

The problems of electroelasticity are characterized by nonstandard boundary conditions for electroded surfaces, especially for the electrodes powered by the current generators. These conditions are the analogs to the boundary conditions of the contact type with rigid stamps for an elastic solid.

In the problems of electroelasticity the feasible problem statements include the statements for multilayer bodies with various physical properties: piezoelectric bodies, elastic bodies, dielectrics.

An important role for practical applications of piezoelectric devices belongs to the two sets of natural frequencies, namely, the frequencies of electric resonances and antiresonances. In order to find them, it is necessary to solve twice a generalized eigenvalue problem with slightly different boundary conditions for the electrodes. The necessity of solving these problems is significant for complete analysis of the majority of piezotransducers that work in dynamic modes.

The problems of thermoelasticity are characterized by the boundary conditions of the third kind, namely, the condition of the convective heat transfer. These boundary conditions give additional contribution to the symmetric bilinear forms of the generalized problem statement. The important classes of the problems of thermoelasticity are the weakly coupled problems, especially the problems of thermal stresses, in which the problem for the temperature field does not depend on the displacement field.

An interesting feature of the problems of poroelasticity is that an analysis of one class of problems can be performed using the tools developed for the other class of problems. Indeed, using porothermoelastic analogy, the problems of poroelasticity can be solved as the problems of thermoelasticity. An important methodological example is the demonstration of the effectiveness of the transition to a dimensionless statement of the problem of poroelasticity, which makes it possible to align the orders of the system coefficients and as a result increase the efficiency of numerical methods, especially for nonlinear problems.

The problems of the interaction of deformable solids with acoustic media are peculiar because they combine the problem statements for different field types, defined in different media: a solid structure and a surrounding acoustic (liquid or gaseous) medium. Here the coupling arises from the boundary conditions of the contact between the solid structure and the acoustic medium. Another feature of the problem is a nonreflecting or impedance boundary condition that determines the damping properties in the problem. Using the example of such problems, it can be shown how the choice of the main unknowns functions affects the form of the resulting system of discretized equations. It turns out that the statements of the acoustic problems on the base of the functions of the potential of acoustic velocity are more convenient for conjugation with the statements of the problems for the solid structure than the statements of the acoustic problems on the base of the functions of the excessive pressure.

The resulting boundary-value and initial boundary problems are rather complex and therefore require numerical methods that can effectively solve these problems for the domains of complex shape. Nowadays, one of such methods is the finite element method. In connection to this, in the second chapter we briefly describe the finite element method focusing on its application to the solution of coupled physico-mechanical problems.

We show that the finite element method is a special case of the general procedure of discretization by the Galerkin method with the choice of a special type of the basis from piecewise polynomial functions on canonical domains. Usually these functions are of low order and have a compact support. We note that the choice of the bases for the finite element methods determine the numerical effectiveness of the method: the sparsity of the matrix, the simplicity of the calculation of the finite element objects, the possibility of the implementation of the assembling procedure, the ease of taking into account the essential boundary conditions. The fact that the finite element method is constructed on the base of generalized problem statements that have energetic and variational meaning leads to the convergence of the approximate solutions by energy norms and also to the possibility of the implementation of the methods for searching the minimum of the quadratic functionals for the problems with positive definite symmetric operators.

The popularity of the finite element method is to a significant degree caused by its developed technology which is given some attention in this book. We consider the issues of forming the global finite element objects from the corresponding element objects using the procedure of assembling and the issues of the taking into account the essential boundary conditions.

In the framework of the general approach we describe isoparametric finite elements. Basic Lagrangian finite elements are considered for 1D, 2D and 3D problems. For 1D problems, the shape functions for linear and quadratic finite elements are provided. For 2D problems linear and quadratic finite elements are considered for the elements of the serendipity type. The ideology used for the construction of 2D problems is extended to 3D elements for tetrahedrons and hexahedrons with linear and quadratic approximations on canonical figures. The basis functions of finite elements are also provided in the form of prisms and pyramids. The issues of the consistency of the finite element meshes are also discussed.

In the third chapter we provide the practical assignments that support the theoretical part of this book. The assignments are devoted to solving the model problems of piezoelectricity, thermoelasticity and problems of



the interactions of solids with acoustic media using ANSYS version 11.0 and higher. Each assignment is supplied by a description of nonstandard methods and techniques of solving in ANSYS the specific types of coupled physico-mechanical problems. The programs in the command program language APDL ANSYS are provided with detailed comments. An analysis of the obtained results is also given. For independent work we provide a set of individual assignments for solving the model problems of piezoelectricity, thermoelasticity and problems of interaction of solids with acoustic media in ANSYS. It is assumed that the readers have basic knowledge of working with ANSYS [20, 30, 31] and are familiar with its program language APDL.

The book is intended in the first place as a support for the course “Finite element modeling of coupled problems”, that is given in the framework of the Master’s degree program ‘IT in Biomechanics’ in the Institute of Mathematics, Mechanics and Computer Science of Southern Federal University. The book can be also used by the under-graduate students and graduate students of various specializations who study Applied Mathematics, Numerical Methods or the problems of specific coupled physico-mechanical problems as well as by researches and engineers who wish to deepen their knowledge concerning the methodology of the mathematical modeling of coupled problems of mathematical physics and finite element technologies of their solution.

The authors express their gratitude to the Director of the Institute of Mathematics, Mechanics and Computer Science M. Karyakin who initiated the publication of the series of the monographs in the framework of the project of Tempus-IV program, which facilitated the intensification of the author’s work on this book.

# Chapter 1

## Some models of coupled problems for mechanics of solids

### 1.1 Basic notations. Vectors and tensors

This section serves for reference purposes and concerns the notations on vector and tensor values that we will use further. More details on vectors and tensors can be found in numerous publications (see, for example [38, 18, 19], etc.) Here we provide basic information on this issue.

#### 1.1.1 Introduction to vectors and tensors

Let  $\mathbb{R}^n$  be a Euclidian space. The elements of this space called *vectors* will be denoted here by bold and (as a rule) small letters:  $\mathbf{a} \in \mathbb{R}^n$ .

Let us select an orthonormal basis  $\mathbf{e}_i \in \mathbb{R}^n$ ,  $i = 1, 2, \dots, n$  in  $\mathbb{R}^n$ . Then any vector  $\mathbf{a} \in \mathbb{R}^n$  can be presented as a series expansion in the basis

$$\mathbf{a} = \sum_{i=1}^n a_i \mathbf{e}_i \stackrel{\text{def}}{=} a_i \mathbf{e}_i$$

with the coordinates  $a_1, a_2, \dots, a_n$ .

Hereinafter we use *Einstein summation rule over repeated indices* where upper and lower indices are not distinguished.

As  $\mathbb{R}^n$  is a linear space, then the operations of addition and multiplication by a scalar are already defined in it. Thus, if  $\lambda, \mu \in \mathbb{R}$ ;  $\mathbf{a} = a_i \mathbf{e}_i$ ,  $\mathbf{b} = b_i \mathbf{e}_i \in \mathbb{R}^n$ , then  $\lambda \mathbf{a} + \mu \mathbf{b} = (\lambda a_i + \mu b_i) \mathbf{e}_i \in \mathbb{R}^n$ .

The space  $\mathbb{R}^n$ , as a Euclidian space has an operation of *scalar multiplication*:

$$\mathbf{a} \cdot \mathbf{b} = (a_i \mathbf{e}_i) \cdot (b_j \mathbf{e}_j) = a_i b_j \mathbf{e}_i \cdot \mathbf{e}_j = a_i b_j \delta_{ij} = a_i b_i.$$

Here  $\delta_{ij}$  is the Kronecker delta ( $\delta_{ij} = 1$ , if  $i = j$ ;  $\delta_{ij} = 0$ , if  $i \neq j$ ), and we use that for the orthonormal basis  $\mathbf{e}_i \cdot \mathbf{e}_j = \delta_{ij}$ .

In vector-matrix notations we will write the set of vector coordinates  $\mathbf{a}$  in a form of a column vector  $\mathbf{a} = \{a_1, a_2, \dots, a_n\}$  or row vector  $\mathbf{a}^* = [a_1, a_2, \dots, a_n]$ . Whereas in tensor notations the column vector and the row vector can be not distinguished, in the matrix algebra we will denote the multiplication of a matrix  $\mathbf{K}$  by a column vector  $\mathbf{a}$  on the right as  $\mathbf{K} \cdot \mathbf{a}$ , and the multiplication of a matrix  $\mathbf{K}$  by a row vector  $\mathbf{a}^*$  on the left will be denoted as  $\mathbf{a}^* \cdot \mathbf{K}$ . Then if  $\mathbf{I}$  is a unit matrix, then  $\mathbf{b}^* \cdot \mathbf{I} \cdot \mathbf{a} = \mathbf{b}^* \cdot \mathbf{a}$ . Thus, the scalar multiplication of two vectors can be presented in different forms:  $\mathbf{b} \cdot \mathbf{a}$  (using tensor notation) or  $\mathbf{b}^* \cdot \mathbf{a}$  (using matrix notation).

If  $\mathbf{e}'_1, \mathbf{e}'_2, \dots, \mathbf{e}'_n$  is another orthonormal basis in  $\mathbf{R}^n$ , then we can introduce a matrix  $\mathbf{Q}$  (matrix of direction cosines)

$$[\mathbf{Q}]_{ij} = q_{ij} = \mathbf{e}_i^* \cdot \mathbf{e}'_j, \quad (1.1)$$

and represent the vectors of one basis by the vectors of another basis

$$\mathbf{e}_i = q_{ij} \mathbf{e}'_j, \quad \mathbf{e}'_i = \alpha_{ij} \mathbf{e}_j, \quad \alpha_{ij} = q_{ji}, \quad (1.2)$$

and obtain *the recalculation formulas for the coefficients of the vector  $\mathbf{a} = a_i \mathbf{e}_i = a'_j \mathbf{e}'_j$  under the change of the basis*

$$a_i = q_{ij} a'_j, \quad a'_i = \alpha_{ij} a_j, \quad (1.3)$$

or in the matrix form

$$\mathbf{a} = \mathbf{Q} \cdot \mathbf{a}', \quad \mathbf{a}' = \mathbf{A} \cdot \mathbf{a}, \quad \mathbf{A} = \mathbf{Q}^*, \quad (1.4)$$

where  $\mathbf{Q}^*$  is the transpose matrix.

As it can be easily proved, the transition matrix  $\mathbf{Q}$  is orthogonal:

$$\mathbf{Q}^* \cdot \mathbf{Q} = \mathbf{Q} \cdot \mathbf{Q}^* = \mathbf{I}, \quad \mathbf{Q} = (\mathbf{Q}^*)^{-1}.$$

As a result, the vector  $\mathbf{a}$  can be thought of as a set of numbers  $\{a_1, a_2, \dots, a_n\}$ , referred to the basis  $\{\mathbf{e}_1, \mathbf{e}_2, \dots, \mathbf{e}_n\}$  where with the transition to a different basis  $\{\mathbf{e}'_1, \mathbf{e}'_2, \dots, \mathbf{e}'_n\}$  the numbers change according to the laws (1.3), (1.4).

Let us now consider a Cartesian product of  $p$  Euclidean spaces  $\mathbf{R}^n$ :

$$\mathbf{T}_p^n \stackrel{\text{def}}{=} \underbrace{\mathbf{R}^n \otimes \mathbf{R}^n \otimes \dots \otimes \mathbf{R}^n}_p.$$

The elements of this space will be called *tensors* (Euclidean tensors) of the rank  $p$  and will be denoted, as vectors, in bold letters.

In  $T_p^n$  we can select a basis consisting of the elements

$$\underbrace{\mathbf{e}_{i_1} \otimes \mathbf{e}_{i_2} \otimes \dots \otimes \mathbf{e}_{i_p}}_p \stackrel{\text{def}}{=} \mathbf{e}_{i_1} \mathbf{e}_{i_2} \dots \mathbf{e}_{i_p},$$

where  $i_k \in \{1, 2, \dots, n\}$ ,  $\mathbf{e}_{i_k}$  are the vectors of an orthonormal basis in  $\mathbb{R}^n$ .

Then any element  $\mathbf{X} \in T_p^n$  can be presented as an expansion in the basis

$$\mathbf{X} = X_{i_1 i_2 \dots i_p} \mathbf{e}_{i_1} \mathbf{e}_{i_2} \dots \mathbf{e}_{i_p}$$

with the components  $X_{i_1 i_2 \dots i_p}$ , and it is obvious that  $\dim T_p^n = n^p$ .

The vectors can be considered as the tensors of the first rank, i. e.  $\mathbb{R}^n \equiv T_1^n$ ; and from the components of the second rank tensor  $\mathbf{X} = X_{ij} \mathbf{e}_i \mathbf{e}_j$  we can compose a square matrix  $[\mathbf{X}]_{ij} = X_{ij}$  of the order  $n \times n$ .

The Cartesian product of the Euclidean spaces is closely connected with the operation of *tensor multiplication (external multiplication)*

$$\mathbf{X} = X_{i_1 i_2 \dots i_p} \mathbf{e}_{i_1} \mathbf{e}_{i_2} \dots \mathbf{e}_{i_p} \in T_p^n, \quad \mathbf{Y} = Y_{j_1 j_2 \dots j_q} \mathbf{e}_{j_1} \mathbf{e}_{j_2} \dots \mathbf{e}_{j_q} \in T_q^n :$$

$$\mathbf{X} \mathbf{Y} \stackrel{\text{def}}{=} X_{i_1 i_2 \dots i_p} Y_{j_1 j_2 \dots j_q} \mathbf{e}_{i_1} \mathbf{e}_{i_2} \dots \mathbf{e}_{i_p} \mathbf{e}_{j_1} \mathbf{e}_{j_2} \dots \mathbf{e}_{j_q} \in T_{p+q}^n.$$

Accordingly, two vectors  $\mathbf{a} = a_i \mathbf{e}_i$ ,  $\mathbf{b} = b_j \mathbf{e}_j \in \mathbb{R}^n = T_1^n$  can constitute a second rank tensor  $\mathbf{a} \mathbf{b} = a_i b_j \mathbf{e}_i \mathbf{e}_j \in T_2^n$ , called *diad*. The components of this tensor constitute a matrix  $\mathbf{a} \mathbf{b}^*$ :  $[\mathbf{a} \mathbf{b}^*]_{ij} = a_i b_j$ .

For the second rank tensor  $\mathbf{X} = X_{ij} \mathbf{e}_i \mathbf{e}_j$  we will use the *operation of transposition*:

$$\mathbf{X}^* = X_{ji} \mathbf{e}_i \mathbf{e}_j,$$

which leads to the transposition of the matrix of the tensor coefficients.

The second rank tensor  $\mathbf{X} \in T_2^n$  is called *symmetric*, if  $\mathbf{X} = \mathbf{X}^*$ .

In a similar way we can speak of symmetry of an arbitrary rank tensor by a certain pair of indices. For example, the third rank tensors of piezomoduli  $\mathbf{e} = e_{ikl} \mathbf{e}_i \mathbf{e}_k \mathbf{e}_l$ , that will be used further in section 1.3, will be symmetric by the last two indices:  $e_{ikl} = e_{ilk}$ . For such tensors the transposition operation will denote the permutation of the first and the third indices or a pair of the first two indices and the third one:  $\mathbf{e}^* = e_{lki} \mathbf{e}_i \mathbf{e}_k \mathbf{e}_l = e_{lik} \mathbf{e}_i \mathbf{e}_k \mathbf{e}_l$ .

By analogy with vectors, for tensors of arbitrary rank we can consider the operations of addition and multiplication by a scalar. Namely,

$$\forall \lambda, \mu \in \mathbb{R}, \quad \mathbf{X} = X_{i_1 i_2 \dots i_p} \mathbf{e}_{i_1} \mathbf{e}_{i_2} \dots \mathbf{e}_{i_p}, \quad \mathbf{Y} = Y_{i_1 i_2 \dots i_p} \mathbf{e}_{i_1} \mathbf{e}_{i_2} \dots \mathbf{e}_{i_p} \in T_p^n :$$

$$\lambda \mathbf{X} + \mu \mathbf{Y} = (\lambda X_{i_1 i_2 \dots i_p} + \mu Y_{i_1 i_2 \dots i_p}) \mathbf{e}_{i_1} \mathbf{e}_{i_2} \dots \mathbf{e}_{i_p} \in T_p^n.$$

Although there is a specific concept of scalar multiplication for tensors, we will consider a more important for further application operation of *inner product* (*simple product* or *contraction*)

$$\forall \mathbf{X} = X_{i_1 i_2 \dots i_p} \mathbf{e}_{i_1} \mathbf{e}_{i_2} \dots \mathbf{e}_{i_p} \in \mathbb{T}_p^n, \quad \mathbf{Y} = Y_{j_1 j_2 \dots j_q} \mathbf{e}_{j_1} \mathbf{e}_{j_2} \dots \mathbf{e}_{j_q} \in \mathbb{T}_q^n :$$

$$\mathbf{X} \cdot \mathbf{Y} \stackrel{\text{def}}{=} X_{i_1 i_2 \dots i_{p-1} k} Y_{k i_p \dots i_{p+q-2}} \mathbf{e}_{i_1} \mathbf{e}_{i_2} \dots \mathbf{e}_{i_{p+q-2}} \in \mathbb{T}_{p+q-2}^n,$$

where there is a contraction of the last index of  $\mathbf{X}$  and the first index of  $\mathbf{Y}$  (summation over  $k$  in the last formula).

For the tensors  $\mathbf{X} \in \mathbb{T}_p^n$ ,  $\mathbf{Y} \in \mathbb{T}_q^n$  with  $p \geq 2$ ,  $q \geq 2$  we can define the operation of *double inner product* (*double contraction*)

$$\forall \mathbf{X} = X_{i_1 i_2 \dots i_p} \mathbf{e}_{i_1} \mathbf{e}_{i_2} \dots \mathbf{e}_{i_p} \in \mathbb{T}_p^n, \quad \mathbf{Y} = Y_{j_1 j_2 \dots j_q} \mathbf{e}_{j_1} \mathbf{e}_{j_2} \dots \mathbf{e}_{j_q} \in \mathbb{T}_q^n, \quad p, q \geq 2 :$$

$$\mathbf{X} : \mathbf{Y} \stackrel{\text{def}}{=} \mathbf{X} \cdot \cdot \mathbf{Y} \stackrel{\text{def}}{=} X_{i_1 i_2 \dots i_{p-2} l k} Y_{k l i_{p-1} \dots i_{p+q-4}} \mathbf{e}_{i_1} \mathbf{e}_{i_2} \dots \mathbf{e}_{i_{p+q-4}} \in \mathbb{T}_{p+q-4}^n,$$

which, as it can be seen, consists of successive application of the simple product (contraction) operation two times.

Thus, for the fourth rank tensor of elastic stiffness  $\mathbf{c}^E = c_{ijkl}^E \mathbf{e}_i \mathbf{e}_j \mathbf{e}_k \mathbf{e}_l \in \mathbb{T}_4^3$  and the second rank strain tensor  $\boldsymbol{\varepsilon} = \varepsilon_{rs} \mathbf{e}_r \mathbf{e}_s \in \mathbb{T}_2^3$  that will be introduced further in section 1.3 it holds that  $\mathbf{c}^E : \boldsymbol{\varepsilon} = c_{ijkl}^E \varepsilon_{lk} \mathbf{e}_i \mathbf{e}_j \in \mathbb{T}_2^3$ .

Under the transition to an orthonormal basis  $\mathbf{e}'_1, \mathbf{e}'_2, \dots, \mathbf{e}'_n$  in  $\mathbf{R}^n$  according to the laws (1.1), (1.2) the components of the tensor  $\mathbf{X} \in \mathbb{T}_p^n$  change according to the laws that generalize (1.3)

$$\mathbf{X} = X_{i_1 i_2 \dots i_p} \mathbf{e}_{i_1} \mathbf{e}_{i_2} \dots \mathbf{e}_{i_p} = X'_{j_1 j_2 \dots j_p} \mathbf{e}'_{j_1} \mathbf{e}'_{j_2} \dots \mathbf{e}'_{j_p},$$

$$X_{i_1 i_2 \dots i_p} = q_{i_1 j_1} q_{i_2 j_2} \dots q_{i_p j_p} X'_{j_1 j_2 \dots j_p}, \quad X'_{i_1 i_2 \dots i_p} = \alpha_{i_1 j_1} \alpha_{i_2 j_2} \dots \alpha_{i_p j_p} X_{j_1 j_2 \dots j_p}. \quad (1.5)$$

A change in the tensor components  $\mathbf{X} \in \mathbb{T}_p^n$  under the transition from one orthonormal basis to another according to the formulas (1.5) is a fundamental property that defines the very concept of the tensor.

Let  $\boldsymbol{\Phi} = \boldsymbol{\Phi}(\mathbf{x}) \in \mathbb{T}_p^3$  be a *tensor function* of the vector of spacial coordinates  $\mathbf{x} \in \mathbf{R}^3$ , that has sufficient properties of smoothness (*tensor field*). A *gradient operator*

$$\nabla = \mathbf{e}_k \frac{\partial}{\partial x_k},$$

is called *nabla operator* and has a rank of a vector (i. e. it is a first rank tensor).

A nabla operator and a tensor field can be used for various tensor operations. For example, a tensor product of the operator  $\nabla$  and the vector field  $\mathbf{a} = \mathbf{a}(\mathbf{x}) \in T_1^3$  gives the second rank tensor

$$\nabla \mathbf{a} = \frac{\partial a_j}{\partial x_i} \mathbf{e}_i \mathbf{e}_j.$$

Inner product of the nabla operator  $\nabla$  and the tensor field  $\Phi(\mathbf{x}) \in T_p^3$  gives the tensor of the rank  $p - 1$  which is called the *divergence* of the tensor field

$$\operatorname{div} \Phi \stackrel{\text{def}}{=} \nabla \cdot \Phi = \mathbf{e}_k \frac{\partial \Phi}{\partial x_k} = \frac{\partial \Phi_{ki_2 \dots i_p}}{\partial x_k} \mathbf{e}_{i_2 \dots i_p}.$$

In particular, the divergence of the vector field  $\mathbf{a} = \mathbf{a}(\mathbf{x})$  is a scalar value (zero rank tensor)

$$\nabla \cdot \mathbf{a} = \frac{\partial a_k}{\partial x_k} \stackrel{\text{def}}{=} a_{k,k}.$$

Finally, we provide the Gauss (Gauss-Ostrogradsky) formula for the tensor fields. If  $\Omega$  is a bounded volume in  $\mathbb{R}^3$ ,  $\Gamma = \partial\Omega$  is a closed piecewise smooth surface,  $\mathbf{n} = \mathbf{n}(\mathbf{x})$  is the vector of an external unit normal to the point  $\mathbf{x} \in \Gamma$ , then for continuously differentiable tensor field  $\Phi \in T_p^3$  of an arbitrary rank  $p$  the *Gauss (Gauss-Ostrogradsky) formula* holds:

$$\int_{\Omega} \nabla \cdot \Phi \, d\Omega = \int_{\Gamma} \mathbf{n} \cdot \Phi \, d\Gamma,$$

which generalize an analogous formula from mathematical analysis for vector fields.

### 1.1.2 Main notations and values in coupled problems of elasticity theory

This subsection contains main notations for the field characteristics, material properties and external influences, that are introduced and used further in sections 1.3 – 1.6. The description of each value contains its dimension in international system of units SI, where a dimensionless value is denoted by symbol “1”.

*Characteristics of mechanical, electric, thermal, filtration and acoustic fields:*

$\mathbf{u}$  – displacement vector, m;

$\varepsilon$  – strain tensor, 1;

$\sigma$  – stress tensor,  $\text{N/m}^2 = \text{Pa}$ ;

$\varphi$  – electric potential, V;

$\mathbf{E}$  – electric field intensity vector, V/m;

$\mathbf{D}$  – electric induction (electric displacement) vector, C/m<sup>2</sup>;

$T$  – temperature, K;

$T_0$  – temperature of the natural state, K;

$\theta$  – temperature increase, K;

$S$  – density of entropy (thermodynamic entropy), measured from the natural state, J/(K · m<sup>3</sup>) = N/(m<sup>2</sup> · K) = Pa/K;

$\mathbf{q}$  – heat flux vector (specific heat flux vector, heat flux density vector), W/m<sup>2</sup>;

$\phi$  – porosity, 1;

$\mathbf{v}$  – filtration velocity (in poroelasticity), acoustic velocity (in acoustics), m/s;

$p$  – pore pressure (in poroelasticity), excess acoustic pressure (in acoustics), N/m<sup>2</sup> = Pa;

$\psi$  – velocity potential, m<sup>2</sup>/s.

*Material properties:*

$\rho$  – density, kg/m<sup>3</sup>;

$\mathbf{c}^E$  ( $\mathbf{c}$ ) – elastic moduli tensor, calculated at constant electric field, N/m<sup>2</sup> = Pa;

$\mathbf{e}$  – piezomoduli tensor, C/m<sup>2</sup>;

$\boldsymbol{\epsilon}^S$  – tensor of dielectric permittivities, calculated at constant strains, F/m;

$\alpha_d$  – damping coefficient (the first damping coefficient with account for Rayleigh damping), 1/s;

$\beta_d$  – damping coefficient (the second damping coefficient with account for Rayleigh damping), s;

$\boldsymbol{\gamma}$  – tensor of thermal stress coefficients, J/(K · m<sup>3</sup>) = N/(m<sup>2</sup> · K) = Pa/K;

$c_\varepsilon$  – specific heat at constant strain, J/(kg · K) = m<sup>2</sup>/(s<sup>2</sup> · K);

$\mathbf{k}$  – tensor of thermal conductivities, W/(m · K);

$\rho_f$  – fluid density, kg/m<sup>3</sup>;

$\mathbf{b}$  – Biot's tensor, 1;

$N$  – Biot's modulus, m<sup>2</sup>/N = 1/Pa;

$\mathbf{K}$  – tensor of filtration coefficients, m/s;

$c_0$  – speed of sound in acoustic medium, m/s.

*External influences and couplings:*

$\mathbf{f}$  – mass force density vector, N/kg = m/s<sup>2</sup>;

$\sigma_\Omega$  – bulk density of the electric charges, C/m<sup>3</sup>;

$W$  – heat source intensity, W/m<sup>3</sup>;

$\mathbf{u}_\Gamma$  – displacement vector on the boundary, m;

$\mathbf{p}_\Gamma$  – stress vector,  $\text{N}/\text{m}^2 = \text{Pa}$ ;

$V_j$  – electric potential on the electrode  $\Gamma_{\varphi j}$ ,  $\text{V}$ ;

$Q_j$  – total electric charge on the electrode  $\Gamma_{\varphi j}$ ,  $\text{C}$ ;

$\sigma_\Gamma$  – surface density of electric charges,  $\text{C}/\text{m}^2$ ;

$\omega$  – circular frequency (angular frequency, radial frequency, rotation frequency),  $\text{rad}/\text{s} = \text{rad} \cdot \text{Hz}$ ;

$f = \omega/(2\pi)$  – frequency,  $1/\text{s} = \text{Hz}$ ;

$\theta_\Gamma$  – temperature (temperature increase) on the part of the boundary,  $\text{K}$ ;

$q_\Gamma$  – heat flux on the surface,  $\text{W}/\text{m}^2$ ;

$h_f$  – heat transfer coefficient on the surface,  $\text{W}/(\text{m}^2 \cdot \text{K})$ ;

$\theta_b$  – temperature (temperature increase) of external medium,  $\text{K}$ ;

$Z$  – impedance of the boundary,  $\text{N} \cdot \text{s}/\text{m}$ .

## 1.2 General issues

In classical problems of mathematical physics physical fields are usually considered to be of specific nature. For example, the problems of the elasticity theory for deformable solids study the mechanical fields arising from mechanical external influences, such as the displacement vector fields  $\mathbf{u} = \mathbf{u}(\mathbf{x}, t)$ , the tensor fields of strains  $\boldsymbol{\varepsilon} = \boldsymbol{\varepsilon}(\mathbf{x}, t)$ , stresses  $\boldsymbol{\sigma} = \boldsymbol{\sigma}(\mathbf{x}, t)$ , etc. The thermal conductivity problems consider the changes of the temperature field  $\theta = \theta(\mathbf{x}, t)$  under the thermal influences. The problems of electrostatics and quasielectrostatics investigate the electric fields, such as the scalar field of the electric potential  $\varphi = \varphi(\mathbf{x}, t)$ , the vector of the electric field intensity  $\mathbf{E} = \mathbf{E}(\mathbf{x}, t)$ , etc., that emerge in dielectrics under the electric external influences. The examples of similar problems can be easily extended.

All above cases can be attributed to the specific type of the problems of mathematical physics. Indeed, transient dynamic problems of the elasticity theory are described by the systems of equations of hyperbolic type (limiting case). Transient equations of thermal conductivity are the equations of parabolic type, and the equations for dielectrics have elliptical type. Note that for the problems with systems of differential equations (for example, the problems of elasticity theory), all equations usually contain spatial derivatives of the same order and time derivatives of the same order.

The coupled problems, where the fields of different nature are dependent on each other, are more complex from the mathematical viewpoint. For example, in the problems of thermoelasticity the mechanical and thermal fields are coupled with each other. In the problems of electroelasticity for



the piezoelectric media the mechanical and electric fields are coupled, in the problems of thermoelectroelasticity the coupled fields are the thermal, mechanical and electric ones.

The interaction of the fields of different nature is reflected in fundamental laws that form the basis of the theories of coupled physico-mechanical fields. This coupling has many forms and appears in essentially different ways for various situations and for various media. As a result, there are a lot of independent practically important theories of mechanics of solids with complex properties, which additionally can consider various mechanisms of coupling. For example, several theories can be considered in the framework of the theory of thermoelasticity, such as theory of thermal stresses, theory of thermal conductivity with a finite velocity of heat propagation, theory of thermal heating under steady-state oscillations, etc.

The computational results of the problems with coupled physico-mechanical fields are quite complex, because of both increasing number of the unknown field parameters and different scales changes in time for the main and associated fields. Nowadays, the most efficient numerical method that enables to conduct analysis of the problems of the elasticity theory with complicated properties is the finite element method (FEM).

There is a range of “heavy” commercial finite element (FE) packages (ANSYS, ABAQUS, COMSOL, MSC MARC, etc.) that allow performing computations of the coupled problems, as well as several specialized packages oriented to various classes of the elasticity theory problems with complicated physico-mechanical properties (for example, ICEPACK for the thermoelasticity problems, PZFlex, ATILA, ACELAN for piezoelectricity, etc.)

It is obvious, that in the view of complexity of the coupled problems both in the methodology and in the implementation of finite element calculations, there is still a wide field for research. The comparison of different finite element methods and their implementations in terms of accuracy, speed and efficiency is also of interest. Specific features of coupled physico-mechanical problems make relevant both mathematical studies and development of effective numerical methods, special software and modules for existing computational packages enabling to automate some of the important stages of coupled analysis.

Let us give a classification of the coupled problems on the example of two fields of different nature, such as the displacement field  $\mathbf{u}(\mathbf{x}, t)$  and the temperature field (more precisely, the temperature increase field)  $\theta(\mathbf{x}, t)$ .

The system of coupled differential equations for the main field  $\mathbf{u}(\mathbf{x}, t)$  and for the related field  $\theta(\mathbf{x}, t)$  in general case can be described in the form:

$$L_{uu}(\nabla, \partial_t)\mathbf{u} + L_{u\theta}(\nabla, \partial_t)\theta = \mathbf{f}_u,$$

$$L_{\theta u}(\nabla, \partial_t)\mathbf{u} + L_{\theta\theta}(\nabla, \partial_t)\theta = \mathbf{f}_\theta,$$

where  $L_{uu}$ ,  $L_{u\theta}$ ,  $L_{\theta u}$ ,  $L_{\theta\theta}$  are the differential operators, which can be nonlinear and dependent on the functions  $\mathbf{u}$  and  $\theta$ .

For classical problem settings this system should be supplied with the corresponding boundary and initial conditions. For further mathematical analysis and application of numerical method it is convenient to move to the generalized or weak problem settings usually represented by variational or energy relations, that express the principles of the equality of works and the energy balance of the system.

Let us apply semi-discrete approximations to the weak boundary-value problems setting in the corresponding finite-dimensional space that can be expressed as

$$\mathbf{u}(\mathbf{x}, t) \approx \mathbf{N}_u^*(\mathbf{x}) \cdot \mathbf{U}(t), \quad \theta(\mathbf{x}, t) \approx \mathbf{N}_\theta^*(\mathbf{x}) \cdot \mathbf{T}(t)$$

with the matrix of the basis functions  $\mathbf{N}_u(\mathbf{x})$ , the vector of the basis functions  $\mathbf{N}_\theta(\mathbf{x})$  and the vectors of the functions (constants) of approximation  $\mathbf{U}$  and  $\mathbf{T}$  (nodal degrees of freedom in the finite element method)

$$\mathbf{A}_{uu}(\partial_t) \cdot \mathbf{U} + \mathbf{A}_{u\theta}(\partial_t) \cdot \mathbf{T} = \mathbf{F}_u, \quad (1.6)$$

$$\mathbf{A}_{\theta u}(\partial_t) \cdot \mathbf{U} + \mathbf{A}_{\theta\theta}(\partial_t) \cdot \mathbf{T} = \mathbf{F}_\theta, \quad (1.7)$$

where  $\mathbf{A}_{uu} \neq 0$ ;  $\mathbf{A}_{\theta\theta} \neq 0$ .

The most important types of coupled problems are as follows:

- if  $\mathbf{A}_{u\theta} \neq 0$ ;  $\mathbf{A}_{\theta u} \neq 0$ , then we have the problems with full matrix coupling;
- if  $\mathbf{A}_{u\theta} = 0$ ;  $\mathbf{A}_{\theta u} = 0$ , and some diagonal blocks ( $\mathbf{A}_{uu}$  or  $\mathbf{A}_{\theta\theta}$ ) depend on the fields of different nature (for example,  $\mathbf{A}_{uu} = \mathbf{A}_{uu}(\mathbf{T})$ ), then we have the problems with block-diagonal matrix coupling;
- if one of the blocks  $\mathbf{A}_{u\theta}$  or  $\mathbf{A}_{\theta u}$  is equal to zero, than we have the problems with partial coupling.

Then, there are cases when the time derivatives are absent in certain matrix blocks and present in the others.

The classes of coupled physico-mechanical problems comprise the problems of thermoelasticity, electroelasticity, magnetoelasticity, acoustoelasticity, thermoelectroelasticity, acoustoelectroelasticity, etc.

The solution methods for coupled problems depend on the coupling type. The problems with full matrix coupling can be solved by conventional finite element algorithms, for example, the algorithms for a single vector of unknowns  $\mathbf{a} = \{\mathbf{U}, \mathbf{T}\}$ . In the problems with the time derivatives of different order the block algorithms, that use the reduction of quasi-static degrees of freedom, can be more suitable. For example, in the problems of electroelasticity, it can be convenient to reduce the electric potential degrees of freedom.

The problems with block-diagonal matrix coupling are usually nonlinear, and they can be solved with the use of the Newton-Raphson method for nonlinear problems.

In the problems with partial coupling, for example, when  $\mathbf{A}_{\theta u} = 0$ , the discretized problems are solved in two steps. First, we solve the problem for the related field  $\mathbf{T}$

$$\mathbf{A}_{\theta\theta}(\partial_t) \cdot \mathbf{T} = \mathbf{F}_\theta.$$

Second, the obtained values  $\mathbf{T}$  are substituted in the equation for the main field  $\mathbf{U}$ :

$$\mathbf{A}_{uu}(\partial_t) \cdot \mathbf{U} = \mathbf{F}_u - \mathbf{A}_{u\theta}(\partial_t) \cdot \mathbf{T}.$$

Essentially this problem is an ordinary problem for the main field, but it contains additional terms in the vector of the right-hand side.

Finally, there are coupled problems in which the right-hand side vectors depend on unknown functions, for example,  $\mathbf{F}_u = \mathbf{F}_u(\mathbf{U}, \mathbf{T})$ ,  $\mathbf{F}_\theta = \mathbf{F}_\theta(\mathbf{U}, \mathbf{T})$ . Such situations also arise when solving the problems with full matrix coupling using iterative algorithms. For example, problem (1.6), (1.7) with full matrix coupling can be written in the form

$$\mathbf{A}_{uu}(\partial_t) \cdot \mathbf{U} = \tilde{\mathbf{F}}_u, \tag{1.8}$$

$$\mathbf{A}_{\theta\theta}(\partial_t) \cdot \mathbf{T} = \tilde{\mathbf{F}}_\theta, \tag{1.9}$$

with  $\tilde{\mathbf{F}}_u = \mathbf{F}_u - \mathbf{A}_{u\theta}(\partial_t) \cdot \mathbf{T}$ ,  $\tilde{\mathbf{F}}_\theta = \mathbf{F}_\theta - \mathbf{A}_{\theta u}(\partial_t) \cdot \mathbf{U}$ , and it is possible to apply iterative methods to solve this problem.

In more general case, if  $\mathbf{A}_{uu} = \mathbf{A}_{uu}(\mathbf{U}, \mathbf{T})$ ,  $\mathbf{A}_{\theta\theta} = \mathbf{A}_{\theta\theta}(\mathbf{U}, \mathbf{T})$ ,  $\tilde{\mathbf{F}}_u = \tilde{\mathbf{F}}_u(\mathbf{U}, \mathbf{T})$ ,  $\tilde{\mathbf{F}}_\theta = \tilde{\mathbf{F}}_\theta(\mathbf{U}, \mathbf{T})$ , then problem (1.8), (1.9) is nonlinear and its solution requires special iterative methods. According to ANSYS terminology [1], such problem is called a problem with weak (sequential) coupling.

## 1.3 Modeling of electroelasticity problems

In this section, the main objects for investigation will be active dielectrics that have piezoelectric properties. The piezoelectric effect consists in the linear relation between electric and mechanical fields. The history of this phenomenon is described in many works, such as [7, 10] and others. Here we will only provide a brief history of the piezoelectric effect. In the 1880s, Pierre and Jacques Curie found that some crystals were exhibiting unusual properties under tension in certain directions: the electric charges were generated on the surfaces of these crystals, and these charges were proportional to the applied load. This phenomenon has been called the *direct piezoelectric effect* (from the Greek verb “piezein” meaning “to press”). Soon after this discovery in 1881 Gabriel Lippmann, using thermodynamic relations and his theorem of reversibility of physical phenomena, predicted an *inverse piezoelectric effect* that consisted in the following: the crystals that had piezoelectric properties under the presence of electric field should deform according to the linear law. In the same year the existence of the inverse piezoelectric effect was experimentally confirmed by Pierre and Jacques Curie who found that the piezoelectric modules (the proportionality factors) of the direct and inverse piezoelectric effect were the same.

Pierre Curie has also formulated the principles that relate the properties of symmetry and asymmetry in the phenomena to the causes that generate them [11]. According to the principles of Pierre Curie, the phenomenon has all elements of symmetry of the causes that generate it and can also has higher symmetry than its causes. Similarly, an asymmetry of the phenomenon is predetermined by an asymmetry of its causes. In other words, the phenomenon can exist only in the system that is the symmetry subgroup for this phenomenon.

According to these principles, in the system “crystal – external influences” the crystal changes its symmetry in such way that the only remaining elements are those common with the elements of the influence. Therefore, as the symmetrical tension has the center of symmetry, than for the crystals with the center of symmetry under symmetrical tension the central symmetry should remain. However, as the phenomenon of electric polarization does not have the central symmetry, than such asymmetry should be predetermined by asymmetry of the system. Therefore, from the Curie principle we can conclude that *only those crystals that do not have the centers of symmetry can have piezoelectric properties*. The connection of

the piezoelectric effect phenomenon with the crystal structure was studied in more details by V. Feucht in 1884. As it follows from the previous discussion, all these classes of crystals cannot have the center of symmetry. As a result, it was theoretically proved that the piezoelectric materials were necessarily bound to be anisotropic.

Over many years natural crystals were the only available piezoelectric materials, and many piezoelectric devices were constructed on their base. Later, approximately since the middle 60s of the twentieth century, artificial piezoceramic materials became to be developed and used. It was found that the materials on the base of barium titanate ( $\text{BaTiO}_3$ ) had rather strong piezoelectric effect. The subsequent developments showed that the PZT materials on the base of zirconate, or lead titanate, had even greater sensitivity and could work at rather high temperatures. As a result, this led to the emergence of a whole production technology for new piezoceramic materials and piezoelectric devices based on them. Modern piezoelectric ceramics is several times more sensitive to the electric and mechanical influences than natural piezocrystals. Varying the initial compounds of piezoceramics, it is possible to create materials with various properties that meet the needs of the consumer. Piezoceramics is strong enough, chemically inert and relatively cheap in production. Besides, it can be used to manufacture piezoelectric elements of almost any required shape and sizes.

At present the work of many piezoelectric devices is based on the effect of mechanical and electric field coupling. These devices are made of various specially designed formulations of piezoceramics. Modern piezoelectric manufacture has an extremely wide field of application.

Piezoelectric transducers transform electric external influence (electric voltage or current) into mechanical movements, usually, in sonic or ultrasonic vibrations. Piezoelectric transducers that generate ultrasonic acoustic vibrations, are used in medical diagnosis and therapy for spraying liquids, cleaning surfaces, as, for example, in ultrasound washing machines, in welding, in order to improve gas and oil recovery and for many other applications. The reversibility of the piezoelectric effect allows piezoelectric transducer not only to generate mechanical vibrations but also to receive and register them transforming mechanical signals into electrical. Therefore, piezoelectric transducers are widely used as distance sensors, liquid level sensors, parameters of environment, etc.

Other types of piezotechnical devices are generators, piezoelectric transformers, piezoelectric filters, delay lines, etc. Mathematical models

of piezoelectric devices are based on the equations of coupled theory of elasticity or piezoelectricity. The bibliography on piezoelectricity is wide enough and it can be subdivided in several groups, such as the works on physics aspects, the works devoted to application or technical issues of piezoelectric engineering which are the most numerous, and, lastly, the works that cover mechanical, mathematical and numerical problems of the electroelasticity theory. The classical works that describe in details the physical and mechanical aspects of piezoelectricity are [6, 7] and others. Various problems of the electroelasticity theory as the area of mechanics are presented in [17, 21, 26, 28], and numerical methods of solving the problems of electroelasticity are given in [17]. Modern approaches to the calculation of piezoelectric devices are based on the finite element technologies, the triangulation and assembly algorithms, and the methods for solving the problems of computational mathematics with large sparse matrices. The base for these approaches lies in the weak or variational statements for coupled problems of electroelasticity and their approximations. These issues will be discussed below.

### 1.3.1 Classical statements of electroelasticity problems

Let  $\Omega$  be a bounded domain in  $\mathbb{R}^3$ , occupied by a piezoelectric body;  $\Gamma = \partial\Omega$  is the boundary of the domain  $\Omega$ ;  $\mathbf{n} = \mathbf{n}(\mathbf{x})$  is the vector of the external unit normal to  $\Gamma$  ( $\mathbf{x} \in \Gamma$ ).

We will consider that the state of the piezoelectric medium is defined by the vector-function of displacements  $\mathbf{u} = \mathbf{u}(\mathbf{x}, t)$  and the scalar function of electric potential  $\varphi = \varphi(\mathbf{x}, t)$ .

The vector-function of displacements  $\mathbf{u}(\mathbf{x}, t)$  determines the tensor of small strains

$$\boldsymbol{\varepsilon} = (\nabla\mathbf{u} + \nabla\mathbf{u}^*)/2, \quad (1.10)$$

and the vector of electric field intensity depends on the function of electric potential

$$\mathbf{E} = -\nabla\varphi. \quad (1.11)$$

We note that the components  $\varepsilon_{ij}$  of the strain tensor and the components  $E_i$  of the electric field intensity vector are obtained through the first derivatives by spatial coordinates from the field functions  $u_i(\mathbf{x}, t)$  and  $\varphi(\mathbf{x}, t)$ , respectively,

$$\varepsilon_{ij} = \frac{1}{2} \left( \frac{\partial u_i}{\partial x_j} + \frac{\partial u_j}{\partial x_i} \right) = \frac{1}{2} (u_{i,j} + u_{j,i}), \quad (1.12)$$

$$E_i = -\frac{\partial\varphi}{\partial x_i} = -\varphi_{,i}. \quad (1.13)$$

In linear approximation, for piezoelectric medium there is a linear relation between the strain tensor  $\boldsymbol{\varepsilon}$  and the electric field intensity vector  $\mathbf{E}$  on one side and the stress tensor  $\boldsymbol{\sigma}$  and the electric induction vector  $\mathbf{D}$  on the other side. These dependences are called the constitutive relations and are given in the form:

$$\boldsymbol{\sigma} = \mathbf{c}^E : \boldsymbol{\varepsilon} - \mathbf{e}^* \cdot \mathbf{E}, \quad (1.14)$$

$$\mathbf{D} = \mathbf{e} : \boldsymbol{\varepsilon} + \boldsymbol{\epsilon}^S \cdot \mathbf{E}. \quad (1.15)$$

Here  $\mathbf{c}^E$  is the fourth rank tensor of the elastic moduli calculated at constant electric field ( $E$ );  $\mathbf{e}$  is the third rank tensor of piezomoduli;  $\boldsymbol{\epsilon}^S$  is the second rank tensor of dielectric permittivities, calculated at constant strains ( $S$ ).

In a component-wise setting, Eqs. (1.14), (1.15) can be written in the form:

$$\sigma_{ij} = c_{ijkl}^E \varepsilon_{kl} - e_{kij} E_k, \quad (1.16)$$

$$D_i = e_{ikl} \varepsilon_{kl} + \epsilon_{ik}^S E_k. \quad (1.17)$$

Let us note that the stress tensor  $\boldsymbol{\sigma}$  is the symmetric second rank tensor, i. e.  $\sigma_{ij} = \sigma_{ji}$ .

The elastic moduli tensor  $\mathbf{c}^E$  is the semi-symmetric fourth rank tensor

$$c_{ijkl}^E = c_{jikl}^E = c_{ijlk}^E = c_{klij}^E, \quad (1.18)$$

and the piezomoduli tensor  $\mathbf{e}$  of the third rank is symmetrical only by the last two indices

$$e_{ikl} = e_{ilk}. \quad (1.19)$$

The components  $c_{ijkl}^E$ ,  $e_{ijk}$ ,  $\epsilon_{ij}^S$  are the material constants that characterize the elastic (stiff), piezoelectric and dielectric properties of the body, respectively. In the majority of cases these values are constant (for homogeneous bodies) or piecewise constant (for piecewise homogeneous bodies). However, for inhomogeneous bodies the modules can be continuous or piecewise continuous functions of  $\mathbf{x}$ .

If we reduce Eq. (1.14), using double inner product (double contraction) by  $\boldsymbol{\varepsilon}$ , scalar multiply Eq. (1.15) by  $\mathbf{E}^*$ , and then add up the obtained relations, then we will get the expression for the density of the internal energy of piezoelectric body

$$\Pi = \frac{1}{2}(\boldsymbol{\varepsilon} : \boldsymbol{\sigma} + \mathbf{E}^* \cdot \mathbf{D}) = \frac{1}{2}(\boldsymbol{\varepsilon} : \mathbf{c}^E : \boldsymbol{\varepsilon} + \mathbf{E}^* \cdot \boldsymbol{\epsilon}^S \cdot \mathbf{E}). \quad (1.20)$$

From physical requirements of the positive definiteness for the internal energy the following conditions of the positive definiteness for the elastic moduli and dielectric permittivity tensors take place:

$$\exists \alpha_1 > 0 : \quad \forall \boldsymbol{\varepsilon} = \boldsymbol{\varepsilon}^*, \quad \boldsymbol{\varepsilon} : \mathbf{c}^E : \boldsymbol{\varepsilon} \geq \alpha_1 \boldsymbol{\varepsilon} : \boldsymbol{\varepsilon}, \quad (1.21)$$

$$\exists \alpha_2 > 0 : \quad \forall \mathbf{E}, \quad \mathbf{E}^* \cdot \boldsymbol{\epsilon}^S \cdot \mathbf{E} \geq \alpha_2 \mathbf{E}^* \cdot \mathbf{E}. \quad (1.22)$$

For a continuum the motion equations must hold, which in linear approximation and neglect of damping factors have the same form as in a conventional elasticity theory:

$$\nabla \cdot \boldsymbol{\sigma} + \rho \mathbf{f} = \rho \ddot{\mathbf{u}}, \quad (1.23)$$

where  $\rho = \rho(\mathbf{x})$  is the density of the material,  $\mathbf{f} = \mathbf{f}(\mathbf{x}, t)$  is the mass force density vector,  $\ddot{\mathbf{u}} = \partial^2 \mathbf{u} / \partial t^2$ .

As the velocities of elastic and electromagnetic waves differ in orders, and piezoelectric media are the non-conducting dielectrics, we can adopt the approximation equations of quasi-electrostatics

$$\nabla \cdot \mathbf{D} = \sigma_\Omega, \quad (1.24)$$

where  $\sigma_\Omega$  is the bulk density of electric charges, and usually in dielectrics  $\sigma_\Omega = 0$ .

In a component-wise setting, Eqs. (1.23), (1.24) take the form:

$$\sigma_{ij,j} + \rho f_i = \rho u_{i,tt}, \quad (1.25)$$

$$D_{i,i} = \sigma_\Omega. \quad (1.26)$$

Substituting (1.23), (1.24) into the constitutive relations (1.14), (1.15) and formulas (1.10), (1.11), we get the resulting system of differential equations for linear electroelasticity regarding the functions  $\mathbf{u}$  and  $\varphi$ :

$$\nabla \cdot (\mathbf{c}^E : \nabla \mathbf{u} + \mathbf{e}^* \cdot \nabla \varphi) + \rho \mathbf{f} = \rho \ddot{\mathbf{u}}, \quad (1.27)$$

$$\nabla \cdot (\mathbf{e} : \nabla \mathbf{u} - \boldsymbol{\epsilon}^S \cdot \nabla \varphi) = \sigma_\Omega. \quad (1.28)$$

(Here we have used the fact that, as a result of the symmetry properties (1.18), (1.19) of the tensors  $\mathbf{c}^E$  and  $\mathbf{e}$ , the following equalities hold:  $\mathbf{c}^E : \boldsymbol{\varepsilon} = \mathbf{c}^E : \nabla \mathbf{u}$ ;  $\mathbf{e} : \boldsymbol{\varepsilon} = \mathbf{e} : \nabla \mathbf{u}$ .)

In a component-wise setting, system (1.27), (1.28) will be written as follows:

$$(c_{ijkl}^E u_{k,l} + e_{kij} \varphi_{,k})_{,j} + \rho f_i = \rho u_{i,tt}, \quad i = 1, 2, 3, \quad (1.29)$$



$$(e_{ikl}u_{k,l} - \epsilon_{ik}^S \varphi_{,k})_{,i} = \sigma_{\Omega}. \quad (1.30)$$

As it is seen, for piezoelectric medium we have coupled system (1.29), (1.30) of four differential equations with respect to the four functions  $u_i = u_i(\mathbf{x}, t)$ ,  $i = 1, 2, 3$ ;  $\varphi = \varphi(\mathbf{x}, t)$ . All these equations are the equations of the second order in spatial variables. Meanwhile, time derivatives (of the second order) are present in Eqs. (1.29), but are absent in the equations of quasi-electrostatics (1.30). This fact is a significant feature of the electroelasticity equations.

In order to set an initial boundary value electroelasticity problem, system of equations (1.27), (1.28) or (1.29), (1.30) should be supplemented by boundary and initial conditions.

The boundary conditions can be split in two groups, mechanical and electric. To formulate mechanical boundary conditions, we assume that the boundary  $\Gamma$  is divided into two parts  $\Gamma_u$  and  $\Gamma_{\sigma}$ , where, respectively, the displacement vectors  $\mathbf{u}_{\Gamma}$  and the stress vectors  $\mathbf{p}_{\Gamma}$  are set:

$$\mathbf{u} = \mathbf{u}_{\Gamma}; \quad \mathbf{x} \in \Gamma_u, \quad (1.31)$$

$$\mathbf{p} = \mathbf{n} \cdot \boldsymbol{\sigma}; \quad \mathbf{p} = \mathbf{p}_{\Gamma}; \quad \mathbf{x} \in \Gamma_{\sigma}, \quad (1.32)$$

where, generally speaking, the external influences  $\mathbf{u}_{\Gamma}$  and  $\mathbf{p}_{\Gamma}$  can depend on  $\mathbf{x}$  and  $t$ .

Therefore, here we confine ourselves only to the main conditions of the first and second kind: condition (1.31) is the condition of the first kind or the condition of the Dirichlet type, and condition (1.32) is the condition of the second kind or the condition of the Neumann type. However, these conditions can be set on the parts of the boundary, i. e. it is not necessary that  $\Gamma = \Gamma_u$  or  $\Gamma = \Gamma_{\sigma}$ .

Important cases are the homogeneous boundary conditions of the first and second kind, when  $\mathbf{u}_{\Gamma} = 0$  or  $\mathbf{p}_{\Gamma} = 0$ . In the case of  $\mathbf{u}_{\Gamma} = 0$  the part of the boundary  $\Gamma_u$  is said to be rigidly fixed, and when  $\mathbf{p}_{\Gamma} = 0$  the part of the boundary  $\Gamma_{\sigma}$  is said to be free from stresses. In the same way as it holds for elastic body, in the electroelasticity theory the condition of the rigidly fixed boundary is the most common type of the boundary condition of the first kind (1.31), and on the major part of the boundary  $\Gamma = \Gamma_{\sigma}$  the vector  $\mathbf{p}_{\Gamma}$  is usually equal to zero.

We note that for the uniqueness of the solution it is convenient to require that the boundary  $\Gamma_u$  is not empty, i. e. the solutions of the homogeneous boundary-value problem in a form of rigid body motion are not allowed:  $\mathbf{u} = \mathbf{u}_{rigid} = \mathbf{u}_c + \boldsymbol{\omega}_c \times \mathbf{x}$ ,  $\mathbf{u}_c = \text{const}$ ,  $\boldsymbol{\omega}_c = \text{const}$ .

In order to set electric boundary conditions, we will assume that there exists another division of the boundary  $\Gamma$ :  $\Gamma = \Gamma_\varphi \cup \Gamma_D$ .

The part  $\Gamma_\varphi$  can in its turn consist of discontinuous parts  $\Gamma_{\varphi j}$ ;  $j = 0, 1, \dots, M$ , i. e.  $\Gamma_\varphi = \cup_j \Gamma_{\varphi j}$ . We will call these parts the electrode surfaces. In reality the regions  $\Gamma_{\varphi j}$  are the parts of the boundary of the piezoelectric body, that are covered with metallized surfaces that are called electrodes. The metal covering is usually very thin and can be mathematically considered to be infinitely thin. However, because of the assumption that is adopted in quasi-electrostatics, the electric potential  $\Phi_{\Gamma j}$  that falls to the electrode  $\Gamma_{\varphi j}$  immediately spreads to the entire part  $\Gamma_{\varphi j}$ , and therefore  $\Phi_{\Gamma j}$  does not depend on  $\mathbf{x}$  on  $\Gamma_{\varphi j}$ . Consequently, the electrode should be considered as an equipotential surface.

The presence of the electrodes is an important feature of the problems of quasi-electrostatics for dielectrics and more general problems of electroelasticity.

Besides, two important cases should be distinguished for electrodes. On some electrode surfaces  $\Gamma_{\varphi j}$  the values of potentials  $\Phi_{\Gamma j}$  can be considered to be known ( $\Phi_{\Gamma j} = V_j$ ), and such electrodes will be further referred to as the electrodes powered by voltage generators.

On the other electrode surfaces  $\Gamma_{\varphi j}$  the potentials  $\Phi_{\Gamma j}$ , that are still independent from  $\mathbf{x}$ , are the unknown values. However, for them the total electric charge  $Q_j$  or current  $I_j = \pm dQ_j/dt$  is considered to be unknown, where the sign “+” or “-” is determined by the direction of the current in the external circuit. The parts  $\Gamma_{\varphi j}$  of the second type will be called the electrodes powered by current generators.

For the electrodes of the first type, when  $V_j = 0$ , we will speak about short-circuited or grounded electrodes, and for the electrodes of the second type, when  $Q_j = 0$  we will speak about free electrodes that are not powered by electric current.

The described above boundary conditions for the electrodes can be mathematically formulated in the following way. Let  $\Gamma_\varphi = \Gamma_V \cup \Gamma_Q$ ;  $\Gamma_V = \cup \Gamma_{\varphi j}$ ,  $j \in J_V = \{0, m+1, \dots, M\}$ ;  $\Gamma_Q = \cup \Gamma_{\varphi j}$ ,  $j \in J_Q = \{1, 2, \dots, m\}$ , and the parts  $\Gamma_{\varphi j}$  do not touch each other. (The latter is required in order not to allow situations with discontinuous boundary conditions for electric potential.)

On the electrodes  $\Gamma_{\varphi j} \subseteq \Gamma_V$ , powered by voltage generators we set the potentials  $V_j$ :

$$\varphi = \Phi_{\Gamma j}; \quad \Phi_{\Gamma j} = \Phi_{\Gamma j}(t) = V_j(t); \quad \mathbf{x} \in \Gamma_{\varphi j}, \quad j \in J_V. \quad (1.33)$$

On the electrodes  $\Gamma_{\varphi_j} \subseteq \Gamma_Q$ , powered by current generators we set the following boundary conditions:

$$\varphi = \Phi_{\Gamma_j}; \quad \Phi_{\Gamma_j} = \Phi_{\Gamma_j}(t); \quad \mathbf{x} \in \Gamma_{\varphi_j}, \quad j \in J_Q, \quad (1.34)$$

$$\int_{\Gamma_{\varphi_j}} \mathbf{n} \cdot \mathbf{D} \, d\Gamma = -Q_j; \quad I_j = \pm \dot{Q}_j; \quad j \in J_Q. \quad (1.35)$$

The specificity of boundary conditions (1.34), (1.35) consists not only in the fact that the function  $\varphi(\mathbf{x}, t)$  should take constant values  $\Phi_{\Gamma_j}$  (at every fixed time moment  $t$ ) but also in the setting of a special integral condition that is actually an additional equation for finding  $\Phi_{\Gamma_j}$ .

In the elasticity theory an analogue of conditions (1.34), (1.35) is the contact boundary condition. If a rigid stamp is indented into the deformable body, than the stamp sediment is analogous to the potential  $\Phi_{\Gamma_j}$ , and an integral condition is set for finding the sediment, that expresses the equality of the integral of contact stresses under the stamp and the total force acting on the stamp (if we do not take into account the moments and rotations of the stamp).

Here the distinction from the problems of the elasticity theory consists in the following fact. For the problems of the elasticity theory the boundary conditions (1.34), (1.35) are adopted only for some types of problems, whereas for the problems of electroelasticity conditions (1.34), (1.35) are required to analyze the work of the majority of real-world piezoelectric devices.

Finally, on the non-electrode surfaces  $\Gamma_D$  the surface density of electric charges  $\sigma_\Gamma = \sigma_\Gamma(\mathbf{x}, t)$  is set

$$\mathbf{n} \cdot \mathbf{D} = -\sigma_\Gamma; \quad \mathbf{x} \in \Gamma_D. \quad (1.36)$$

Condition (1.36) clarifies (1.35). As it is known from electrostatics of dielectrics,  $(-\mathbf{n} \cdot \mathbf{D})$  is the surface density of electric charges, therefore an integration of the function  $(-\mathbf{n} \cdot \mathbf{D})$  over the whole part  $\Gamma_{\varphi_j}$  gives the total electric charge on this part.

Thus, the main types of the boundary conditions for electroelasticity are given by formulas (1.31) – (1.36).

As it is known, transient problems require initial conditions

$$\mathbf{u}(\mathbf{x}, +0) = \mathbf{u}_s(\mathbf{x}); \quad \dot{\mathbf{u}}(\mathbf{x}, +0) = \mathbf{v}_s(\mathbf{x}); \quad \mathbf{x} \in \Omega, \quad (1.37)$$

where  $\mathbf{u}_s, \mathbf{v}_s$  are respectively the initial displacements and velocities of the body points.

Thus, the statement of initial boundary-value problem of electroelasticity includes the system of differential equations (1.27), (1.28) or (1.29), (1.30), boundary conditions (1.31) – (1.36) and initial conditions (1.37).

We note that the described above system of differential equations of the dynamic electroelasticity theory (1.27), (1.28) or (1.29), (1.30) has one drawback for practical applications. This system does not take into account the effects of attenuation, damping or viscosity. (Hereinafter we will use these words as synonyms). By analogy with the classical problems of the elasticity theory here we adopt the Rayleigh method of account for damping, that is convenient for further application of numerical methods. We will add the term proportional to the velocity of the body points into the motion equation (1.23)

$$\nabla \cdot \boldsymbol{\sigma} + \rho \mathbf{f} = \rho \ddot{\mathbf{u}} + \alpha_d \rho \dot{\mathbf{u}}, \quad (1.38)$$

and constitutive relation (1.14) will be changed in the following way

$$\boldsymbol{\sigma} = \mathbf{c}^E : (\boldsymbol{\varepsilon} + \beta_d \dot{\boldsymbol{\varepsilon}}) - \mathbf{e}^* \cdot \mathbf{E}. \quad (1.39)$$

Here in (1.38), (1.39)  $\alpha_d$  and  $\beta_d$  are non-negative damping coefficients.

Then the system of differential equations of the electroelasticity theory with Rayleigh damping will be determined by Eqs. (1.10), (1.11), (1.39), (1.15), (1.38), (1.24), and therefore in the system (1.27), (1.28) instead of (1.27) we will have

$$\nabla \cdot (\mathbf{c}^E : (\nabla \mathbf{u} + \beta_d \nabla \dot{\mathbf{u}}) + \mathbf{e}^* \cdot \nabla \varphi) + \rho \mathbf{f} = \rho \ddot{\mathbf{u}} + \alpha_d \rho \dot{\mathbf{u}}. \quad (1.40)$$

The way of Rayleigh account for damping, that is adopted here, has many disadvantages. For example, adding of the term  $\alpha_d \rho \dot{\mathbf{u}}$  in (1.38) is not justified thermodynamically, and instead of (1.39) for anisotropic bodies it would be more logical to adopt the relation

$$\boldsymbol{\sigma} = \mathbf{c}^E : \boldsymbol{\varepsilon} + \tilde{\mathbf{c}}^E : \dot{\boldsymbol{\varepsilon}} - \mathbf{e}^* \cdot \mathbf{E},$$

where  $\tilde{\mathbf{c}}^E = \beta_d \mathbf{c}^E$  will be only a particular case of this more general relation. Other even more general forms of constitutive relations can be built in the frameworks of the theory of viscoelectroelasticity.

However, despite of all the drawbacks, the Rayleigh method of account for damping is one of the most simple and permit to describe qualitatively the main effects of the waves attenuation. This method is adopted in the models and implemented in such well-known finite element computational software, as ANSYS, ABAQUS and others.

With regard to the stated above, further when we need to account for damping in the electroelasticity problems, we will use the Rayleigh method of account for damping, i. e. initial boundary-value problems of electroelasticity will be described by Eqs. (1.10), (1.11), (1.39), (1.15), (1.38), (1.24), boundary conditions (1.31) – (1.36) and initial conditions (1.37).

In the case of static problems all external influences do not depend on time  $t$ , initial conditions are absent, and in the motion equations (1.23) or in (1.38), (1.39) the terms containing time derivatives should be omitted (as for the problems of statics  $\mathbf{u} = \mathbf{u}(\mathbf{x})$ , and  $\dot{\mathbf{u}} = 0$ ,  $\ddot{\mathbf{u}} = 0$ ).

We will call the pair of functions  $\mathbf{u}$ ,  $\varphi$ , that satisfy the differential equations, boundary conditions and initial conditions (for transient problems), the classical or ordinary solution.

The establishment of the smoothness properties of the solution depending on the smoothness of the external influences, the domain  $\Omega$ , its boundary  $\Gamma$ , the parts with various boundary conditions, material constants ( $c_{ijkl}^E$ ,  $e_{kij}$ ,  $\epsilon_{ik}^S$ ), external influences ( $\mathbf{f}$ ,  $\sigma_\Omega$ ,  $\mathbf{u}_\Gamma$ ,  $\mathbf{p}_\Gamma$ ,  $V_j$ ,  $Q_j$  or  $I_j$ ,  $\sigma_\Gamma$ ) and initial conditions ( $\mathbf{u}_s$ ,  $\mathbf{v}_s$ ) is the problem for a separate mathematical investigation. It is obvious that the functions  $\mathbf{u}(\mathbf{x}, t)$  and  $\varphi(\mathbf{x}, t)$  must be at least two times differentiable with respect to  $\mathbf{x}$  and  $t$ , as the second derivatives are present in the system of differential equations (1.29), (1.30). In the next section we will formulate another concept of the solution of the electroelasticity problem with weaker smoothness requirements than for the classical solution.

### 1.3.2 Generalized statements of electroelasticity problems

The transition from the classical problem statement to the generalized one is quite standard, and for the electroelasticity problems it consists in the same steps as for other boundary-value problems with the systems of differential equations of divergent type.

Considering transformations only in spatial coordinates, these stages consist in the following:

1) multiplication of differential equations by yet arbitrary, but sufficiently smooth projection functions and integration over the domain  $\Omega$ ;

2) integration in parts of the integrals with the divergence operator, reduction in the order of higher derivatives by spatial coordinates and obtaining (if possible) symmetrical integral forms;

3) application of the Gauss-Ostrogradskii formulas for transition from the integrals over domain with the divergence operator to the integrals over boundary;

4) transformation of the integrals over domain obtained after the application of the Gauss-Ostrogradskii formulas, using boundary conditions;

4.1) on the part of the boundary the restrictions on the projection functions are set that correspond to the homogeneous boundary conditions (essential boundary conditions) on these parts;

4.2) on other parts of the boundary the boundary conditions with the projection along the normal for the flow values ( $\mathbf{n} \cdot \boldsymbol{\sigma}$ ,  $\mathbf{n} \cdot \mathbf{D}$ , etc.) are used;

5) removal of inhomogeneity of essential boundary conditions by selecting the functions that satisfy inhomogeneous essential boundary conditions on the part of the boundary;

6) determination of the necessary functional spaces and formulation of a weak (generalized) problem statement.

We note that for the equations of the order  $2m$  the second stage is required to be repeated  $m$  times. For example, the problems of the beam bending are described by differential equations of the fourth order, and the procedure of integration by parts should be repeated two times.

The described scheme forms the base for such called semi-discrete numerical algorithms, when in the beginning no conversions in time are made and therefore the projection functions can depend only on  $\mathbf{x}$  but not on  $t$ . The weak or generalized statement of the problem in this case corresponds to the Lagrange variational principle.

An alternative approach consists in the integration over the domain  $\Omega$  and over time  $t$  on some interval  $[0, T]$ . In this case, the projection functions should depend both on  $\mathbf{x}$  and  $t$ , and for time integration the convolution operations can be used. Further transformations can lead to a completely different generalized problem statement that correspond to the Hamilton variational principle.

In the case of stationary (static) problems only the first scheme is possible, as there is no time dependence (apart from the problems with memory, such as the problems of viscoelasticity). Let us consider, for example, a static or quasi-static problem of electroelasticity, when in (1.23) there is no term with  $\rho \ddot{\mathbf{u}}$ , and the motion equation is reduced to the equilibrium equation. Following the scheme described above, let us multiply the equation of statics (1.23) without  $\rho \ddot{\mathbf{u}}$  scalarly by some yet arbitrary but sufficiently smooth vector-function  $\mathbf{v}^*(\mathbf{x})$  and integrate over

the domain  $\Omega$ . Analogously, we will multiply Eq. (1.24) by an arbitrary sufficiently smooth function  $\chi(\mathbf{x})$  and also integrate it over  $\Omega$ .

Using the formulas of tensor analysis

$$\mathbf{v}^* \cdot (\nabla \cdot \boldsymbol{\sigma}(\mathbf{u}, \varphi)) = \nabla \cdot (\mathbf{v}^* \cdot \boldsymbol{\sigma}(\mathbf{u}, \varphi)) - (\nabla \mathbf{v})^* : \boldsymbol{\sigma}(\mathbf{u}, \varphi), \quad (1.41)$$

$$\chi \nabla \cdot \mathbf{D}(\mathbf{u}, \varphi) = \nabla \cdot (\chi \mathbf{D}(\mathbf{u}, \varphi)) - (\nabla \chi)^* \cdot \mathbf{D}(\mathbf{u}, \varphi), \quad (1.42)$$

we get

$$\int_{\Omega} (\nabla \mathbf{v})^* : \boldsymbol{\sigma}(\mathbf{u}, \varphi) d\Omega = \int_{\Omega} \mathbf{v}^* \cdot \rho \mathbf{f} d\Omega + \int_{\Omega} \nabla \cdot (\mathbf{v}^* \cdot \boldsymbol{\sigma}(\mathbf{u}, \varphi)) d\Omega, \quad (1.43)$$

$$- \int_{\Omega} (\nabla \chi)^* \cdot \mathbf{D}(\mathbf{u}, \varphi) d\Omega = \int_{\Omega} \chi \sigma_{\Omega} d\Omega - \int_{\Omega} \nabla \cdot (\chi \mathbf{D}(\mathbf{u}, \varphi)) d\Omega. \quad (1.44)$$

The last integrals in (1.43), (1.44) are the integrals with the divergence operator and can be transformed to the surface integrals using the Gauss-Ostrogradskii formulas

$$\int_{\Omega} \nabla \cdot (\mathbf{v}^* \cdot \boldsymbol{\sigma}(\mathbf{u}, \varphi)) d\Omega = \int_{\Gamma} \mathbf{v}^* \cdot (\mathbf{n} \cdot \boldsymbol{\sigma}(\mathbf{u}, \varphi)) d\Gamma, \quad (1.45)$$

$$\int_{\Omega} \nabla \cdot (\chi \mathbf{D}(\mathbf{u}, \varphi)) d\Omega = \int_{\Gamma} \chi (\mathbf{n}^* \cdot \mathbf{D}(\mathbf{u}, \varphi)) d\Gamma. \quad (1.46)$$

Now we should try to account for boundary conditions in the integrals over the boundary  $\Gamma$ .

For mechanical boundary conditions, according to (1.32) the stress vector  $\mathbf{p}_{\Gamma} = \mathbf{n} \cdot \boldsymbol{\sigma}(\mathbf{u}, \varphi)$  is set on  $\Gamma = \Gamma_u \cup \Gamma_{\sigma}$ , and on  $\Gamma_{\sigma}$ . On  $\Gamma_u$  the variable  $\mathbf{n} \cdot \boldsymbol{\sigma}(\mathbf{u}, \varphi)$  is unknown, and the only possibility to exclude the dependence on  $\mathbf{u}, \varphi$  is the requirement that  $\mathbf{v}$  equals zero on  $\Gamma_u$ .

Thus, we must impose a homogeneous boundary condition corresponding to (1.31) on the projections function  $\mathbf{v}(\mathbf{x})$ :

$$\mathbf{v} = 0; \quad \mathbf{x} \in \Gamma_u. \quad (1.47)$$

The surface integral in (1.45) can be presented in the form

$$\int_{\Gamma} \mathbf{v}^* \cdot (\mathbf{n} \cdot \boldsymbol{\sigma}(\mathbf{u}, \varphi)) d\Gamma = \int_{\Gamma_{\sigma}} \mathbf{v}^* \cdot \mathbf{p}_{\Gamma} d\Gamma. \quad (1.48)$$

For electric boundary conditions  $\Gamma = \Gamma_{\varphi} \cup \Gamma_D$ ;  $\Gamma_{\varphi} = \Gamma_V \cup \Gamma_Q$ ;  $\Gamma_V = \cup \Gamma_{\varphi j}$ ,  $j \in J_V = \{0, m+1, \dots, M\}$ ;  $\Gamma_Q = \cup \Gamma_{\varphi j}$ ,  $j \in J_Q = \{1, 2, \dots, m\}$ ; and we get formulas (1.33)–(1.36).

On the part  $\Gamma_D$  the variable  $\mathbf{n}^* \cdot \mathbf{D}(\mathbf{u}, \varphi)$  is known from (1.36) and is equal to  $(-\sigma_\Gamma)$ .

On  $\Gamma_V$ , by analogy to the mechanical boundary condition on  $\Gamma_u$ , we require that the projection function  $\chi$  become zero:

$$\chi = 0; \quad \mathbf{x} \in \Gamma_{\varphi_j}, \quad j \in J_V. \quad (1.49)$$

On  $\Gamma_Q$  it is enough to impose a condition that the function  $\chi(\mathbf{x})$  take the values that do not depend on  $\mathbf{x}$ :

$$\chi = X_j; \quad X_j = \text{const}_j; \quad \mathbf{x} \in \Gamma_{\varphi_j}, \quad j \in J_Q. \quad (1.50)$$

Therefore, on the parts  $\Gamma_{\varphi_j}$ ,  $j \in J_Q$ , powered by current generators, we have:

$$\int_{\Gamma_{\varphi_j}} \chi(\mathbf{n}^* \cdot \mathbf{D}(\mathbf{u}, \varphi)) d\Gamma = X_j \int_{\Gamma_{\varphi_j}} \mathbf{n}^* \cdot \mathbf{D}(\mathbf{u}, \varphi) d\Gamma = -X_j Q_j, \quad j \in J_Q.$$

As a result, when the requirements (1.49), (1.50) for the projection function  $\chi$  are satisfied, the surface integral in (1.46) will take the form:

$$\int_{\Gamma} \chi(\mathbf{n}^* \cdot \mathbf{D}(\mathbf{u}, \varphi)) d\Gamma = - \int_{\Gamma_D} \chi \sigma_\Gamma d\Gamma - \sum_{j \in J_Q} X_j Q_j. \quad (1.51)$$

Thus, the last integrals in (1.43), (1.44) can be presented as functionals from  $\mathbf{v}$  and  $\chi$ , using (1.45), (1.46), (1.48), (1.51). Taking into account these transformations and (1.14), (1.15), relations (1.43), (1.44) will be written in the final form:

$$c(\mathbf{v}, \mathbf{u}) - e(\mathbf{v}, \varphi) = \tilde{L}_u(\mathbf{v}), \quad (1.52)$$

$$e(\mathbf{u}, \chi) + \epsilon(\chi, \varphi) = \tilde{L}_\varphi(\chi), \quad (1.53)$$

where

$$c(\mathbf{v}, \mathbf{u}) = \int_{\Omega} (\nabla \mathbf{v})^* : \mathbf{c}^E : \nabla \mathbf{u} d\Omega = \int_{\Omega} \boldsymbol{\varepsilon}(\mathbf{v}) : \mathbf{c}^E : \boldsymbol{\varepsilon}(\mathbf{u}) d\Omega, \quad (1.54)$$

$$e(\mathbf{v}, \varphi) = \int_{\Omega} \boldsymbol{\varepsilon}(\mathbf{v}) : \mathbf{e}^* \cdot \mathbf{E}(\varphi) d\Omega = \int_{\Omega} \mathbf{E}^*(\varphi) \cdot \mathbf{e} : \boldsymbol{\varepsilon}(\mathbf{v}) d\Omega, \quad (1.55)$$

$$\epsilon(\chi, \varphi) = \int_{\Omega} \nabla \chi \cdot \boldsymbol{\epsilon}^S \cdot \nabla \varphi d\Omega = \int_{\Omega} \mathbf{E}^*(\chi) \cdot \boldsymbol{\epsilon}^S \cdot \mathbf{E}(\varphi) d\Omega, \quad (1.56)$$

$$\tilde{L}_u(\mathbf{v}) = \int_{\Omega} \mathbf{v}^* \cdot \rho \mathbf{f} d\Omega + \int_{\Gamma_\sigma} \mathbf{v}^* \cdot \mathbf{p}_\Gamma d\Gamma, \quad (1.57)$$



$$\tilde{L}_\varphi(\chi) = \int_{\Omega} \chi \sigma_{\Omega} d\Omega + \int_{\Gamma_D} \chi \sigma_{\Gamma} d\Gamma + \sum_{j \in J_Q} X_j Q_j. \quad (1.58)$$

As it can be noted, if  $\{\mathbf{u}, \varphi\}$  is a classical solutions of a static electroelasticity problem, than for any sufficiently smooth functions  $\mathbf{v}$ , that satisfy (1.47), and functions  $\chi$ , that satisfy (1.49), (1.50), integral relations (1.52), (1.53) hold. However, the functions  $\mathbf{u}$ ,  $\varphi$  should satisfy inhomogeneous conditions (1.31), (1.33), (1.34).

It turns out that the projection functions  $\mathbf{v}$ ,  $\chi$  should satisfy homogeneous boundary conditions (1.47), (1.49), and the solution  $\{\mathbf{u}, \varphi\}$  satisfies analogous but inhomogeneous boundary conditions (1.31), (1.33). It is possible to remove the heterogeneity of these boundary conditions in the following way. Let us take such functions  $\mathbf{u}_n$ ,  $\varphi_n$ , that satisfy inhomogeneous conditions (1.31), (1.33), and also some conditions of type (1.34):

$$\mathbf{u}_n = \mathbf{u}_{\Gamma}; \quad \mathbf{x} \in \Gamma_u, \quad (1.59)$$

$$\varphi_n = \Phi_{n\Gamma j}; \quad \Phi_{n\Gamma j} = \text{const}_j = V_j; \quad \mathbf{x} \in \Gamma_{\varphi j}, \quad j \in J_V, \quad (1.60)$$

$$\varphi_n = \Phi_{n\Gamma j}; \quad \Phi_{n\Gamma j} = \text{const}_j; \quad \mathbf{x} \in \Gamma_{\varphi j}, \quad j \in J_Q, \quad (1.61)$$

where  $\Phi_{n\Gamma j}$  in (1.61) are, generally speaking, unknown variables that do not depend on  $\mathbf{x}$ .

We will seek the solution  $\{\mathbf{u}, \varphi\}$  in the form:

$$\mathbf{u} = \mathbf{u}_0 + \mathbf{u}_n, \quad \varphi = \varphi_0 + \varphi_n, \quad (1.62)$$

where now the functions  $\mathbf{u}_0$  and  $\varphi_0$  satisfy the conditions, that are analogous to the conditions for  $\mathbf{v}$  and  $\chi$ :

$$\mathbf{u}_0 = 0; \quad \mathbf{x} \in \Gamma_u, \quad (1.63)$$

$$\varphi_0 = 0; \quad \mathbf{x} \in \Gamma_{\varphi j}, \quad j \in J_V, \quad (1.64)$$

$$\varphi_0 = \Phi_{0\Gamma j}; \quad \Phi_{0\Gamma j} = \text{const}_j; \quad \mathbf{x} \in \Gamma_{\varphi j}, \quad j \in J_Q. \quad (1.65)$$

Using (1.62), let us present (1.52), (1.53) as relations for finding  $\mathbf{u}_0$  and  $\varphi_0$ :

$$c(\mathbf{v}, \mathbf{u}_0) - e(\mathbf{v}, \varphi_0) = L_u(\mathbf{v}), \quad (1.66)$$

$$e(\mathbf{u}_0, \chi) + \epsilon(\chi, \varphi_0) = L_\varphi(\chi), \quad (1.67)$$

where

$$L_u(\mathbf{v}) = \tilde{L}_u(\mathbf{v}) - c(\mathbf{v}, \mathbf{u}_n) + e(\mathbf{v}, \varphi_n), \quad (1.68)$$

$$L_\varphi(\chi) = \tilde{L}_\varphi(\chi) - e(\mathbf{u}_n, \chi) - \epsilon(\chi, \varphi_n). \quad (1.69)$$

In order to give strict definitions of a generalized solution, we only need to set the necessary functional spaces.

We introduce the scalar product on the set of vector-functions  $\mathbf{v} \in C^1$ , that satisfy (1.47)

$$(\mathbf{v}, \mathbf{u})_{H_u^1} = \int_{\Omega} (\nabla \mathbf{v})^* : \nabla \mathbf{u} \, d\Omega. \quad (1.70)$$

The closure of this set in the norm generated by the scalar product (1.70) will be called the  $H_u^1$  space.

By analogy, we introduce the scalar product on the set of functions  $\chi \in C^1$ , that satisfy (1.49), (1.50)

$$(\chi, \varphi)_{H_\varphi^1} = \int_{\Omega} (\nabla \chi)^* \cdot \nabla \varphi \, d\Omega. \quad (1.71)$$

The closure of this set in the norm generated by the scalar product (1.71) will be called the  $H_\varphi^1$  space.

Finally, we can strictly formulate the concept of a generalized solution of a static electroelasticity problem.

**Definition.** *A generalized or weak solution of a static boundary-value electroelasticity problem is a pair of functions  $\{\mathbf{u}, \varphi\}$ ;  $\mathbf{u} = \mathbf{u}_0 + \mathbf{u}_n$ ;  $\varphi = \varphi_0 + \varphi_n$ ;  $\mathbf{u}_0 \in H_u^1$ ;  $\varphi_0 \in H_\varphi^1$ , that satisfy the system of equations (1.66), (1.67) for  $\forall \mathbf{v} \in H_u^1$ ;  $\forall \chi \in H_\varphi^1$ . At that  $\mathbf{u}_n, \varphi_n$  are considered to be specially selected (known) functions for which conditions (1.59)–(1.61) hold.*

Let us note the distinction between the boundary conditions.

The boundary conditions (1.63)–(1.65) (or (1.47), (1.49), (1.50)) have entered the characterization of the spaces  $H_u^1, H_\varphi^1$ , in which we seek the generalized solution  $\mathbf{u}_0, \varphi_0$ . Therefore, *the boundary conditions that should be satisfied by the functions of the weak problem statement are called the essential boundary conditions.* In analogous inhomogeneous case as, for example, for (1.31), (1.33), (1.34), we will also speak about essential boundary conditions (which can be removed when selecting special functions  $\mathbf{u}_0$  and  $\varphi_0$ ).

The boundary conditions (1.32), (1.35), (1.36) take part only in forming the functionals  $\tilde{L}_u(\mathbf{u}), \tilde{L}_\varphi(\chi)$  in (1.57), (1.58), i. e. they are naturally included in the statement of the problem. For this reason such boundary conditions will be called the *natural boundary conditions*.

We note that conditions (1.34), (1.35), which should be considered in conjunction, here belong to different types of boundary conditions. Thus, the adopted classification for such complex forms of boundary conditions is fairly arbitrary.

It is obvious that if a pair of functions  $\{\mathbf{u}, \varphi\}$  is a classical solution of a static electroelasticity problem then integral relations (1.66), (1.67) hold for any sufficiently smooth functions  $\mathbf{v}, \chi$ , that satisfy (1.47), (1.49), (1.50).

Therefore, if there exists a classical solution, then it is a generalized solution.

The reverse statement, generally speaking, may not be satisfied, i. e. the generalized solution can exist, but the classical solution may not exist. For the generalized solution as a result of an integration by parts using the Gauss-Ostrogradskii formulas, compared with the classical solution, the smoothness requirements are reduced. Indeed, for existence of the integrals in (1.54)–(1.56) it is enough that the functions  $\mathbf{u}$  and  $\varphi$  have only the first derivatives in generalized sense, square-integrable, whereas the classical solution should be at least twice differentiable.

An important example, when the classical solution in the whole domain  $\Omega$  does not exist, but there exists a generalized solution, is the case of a piecewise-homogeneous medium. Let the body  $\Omega$  consist of two domains  $\Omega_1$  and  $\Omega_2$  ( $\Omega = \Omega_1 \cup \Omega_2$ ) with different homogeneous properties. Then some of the modules in  $\Omega_1$  and  $\Omega_2$  differ, for example,  $c_{ijkl}^{E(1)} \neq c_{ijkl}^{E(2)}$ , where the superscript (1) or (2) points to the belonging to the subdomain  $\Omega_1$  or  $\Omega_2$ .

On the interface of the media  $\Gamma_{12}$  for a rigid contact it is necessary that the continuity conditions are satisfied:

$$[\mathbf{u}] = 0, \quad [\varphi] = 0, \quad \mathbf{n} \cdot [\boldsymbol{\sigma}] = 0, \quad \mathbf{n} \cdot [\mathbf{D}] = 0, \quad \mathbf{x} \in \Gamma_{12}. \quad (1.72)$$

Here  $[\mathbf{a}]$  denotes a jump in the value of the vector or tensor  $\mathbf{a}$  over the interface  $\Gamma_{12}$ :  $[\mathbf{a}] = \mathbf{a}_2 - \mathbf{a}_1$ , where  $\mathbf{a}_2$  and  $\mathbf{a}_1$  are the limit values of  $\mathbf{a}$  on  $\Gamma_{12}$  when approaching  $\Gamma_{12}$ , respectively, from the positive or negative sides of the normal  $\mathbf{n}$ , external with regard to  $\Omega_1$ .

Then if  $\mathbf{n} \cdot \boldsymbol{\sigma}$  does not change when passing through the interface  $\Gamma_{12}$ , then because of (1.14) and inequality  $c_{ijkl}^{E(1)} \neq c_{ijkl}^{E(2)}$ , some of the components of the stress tensor  $\boldsymbol{\varepsilon}$  should be discontinuous. Therefore, the corresponding first derivatives undergo a jump, and the solution  $\mathbf{u}$  does not belong even to the class  $C^1$ . Thus, there is no classical solution for the whole piecewise-homogeneous medium. Meanwhile, there exists a generalized solution, as  $\mathbf{u}$  has the first derivatives in a generalized sense.

Naturally, the problems for piecewise-homogeneous media have many practical applications, and for the right statement their solutions must exist. In the case of the boundary-value problem statement, the reason

for the non-existence of an ordinary solution is that the classical solution should be sought separately in the domains  $\Omega_1$  and  $\Omega_2$  with the conjugation conditions between them. The classical solution  $\mathbf{u}^{(j)}$  will exist in each of the domains  $\Omega_j$ . In the same time, the generalized solution exists in the whole domain  $\Omega = \Omega_1 \cup \Omega_2$ , and in this sense it is closer to practice.

Another advantage of the generalized problem statement consists in its energy form.

The functions  $\mathbf{v}$  and  $\chi$  can be regarded as variations of the real fields of displacements  $\mathbf{u}$  and electric potential  $\varphi$ , respectively. Then, using the notations adopted in the variational calculus, let us set in (1.52), (1.53) or in (1.66), (1.67)  $\mathbf{v} = \delta\mathbf{u}$ ,  $\chi = \delta\varphi$ .

Let us note that  $\delta\mathbf{u} = \delta\mathbf{u}_0$ ,  $\delta\varphi = \delta\varphi_0$ , as  $\delta\mathbf{u}_n = 0$ ,  $\delta\chi_n = 0$ . In the terms of mechanics it means that the variations should be consistent with the kinematic relationships.

Then the weak problem statement based on (1.66), (1.67) or on (1.52), (1.53) can be interpreted as the Lagrange variational principle or as a variational principle of virtual work based on the principle of potential displacements and electric potentials. For example, from (1.52), (1.53), we have:

$$c(\delta\mathbf{u}, \mathbf{u}) - e(\delta\mathbf{u}, \varphi) = \tilde{L}_u(\delta\mathbf{u}), \quad (1.73)$$

$$e(\mathbf{u}, \delta\varphi) + \epsilon(\delta\varphi, \varphi) = \tilde{L}_\varphi(\delta\varphi). \quad (1.74)$$

The right-hand side of (1.73)

$$\tilde{L}_u(\delta\mathbf{u}) = \int_{\Omega} (\delta\mathbf{u})^* \cdot \rho\mathbf{f} \, d\Omega + \int_{\Gamma_\sigma} (\delta\mathbf{u})^* \cdot \mathbf{p}_\Gamma \, d\Gamma \quad (1.75)$$

is the work of the mass (bulk) and surface forces on the virtual displacements, i. e. the virtual work of external forces.

The right-hand side of (1.74)

$$\tilde{L}_\varphi(\delta\varphi) = \int_{\Omega} \delta\varphi\sigma_\Omega \, d\Omega + \int_{\Gamma_D} \delta\varphi\sigma_\Gamma \, d\Gamma + \sum_{j \in J_Q} \delta\Phi_{\Gamma j} Q_j \quad (1.76)$$

is the electric work of the charges on the virtual electric potentials.

The left-hand side of (1.73)

$$c(\delta\mathbf{u}, \mathbf{u}) - e(\delta\mathbf{u}, \varphi) = \int_{\Omega} \boldsymbol{\varepsilon}(\delta\mathbf{u}) : \boldsymbol{\sigma}(\mathbf{u}, \varphi) \, d\Omega \quad (1.77)$$

is the increment of the work of strains induced by the virtual displacement  $\delta\mathbf{u}$ , and the left-hand side of (1.74)

$$e(\mathbf{u}, \delta\varphi) + \epsilon(\delta\varphi, \varphi) = \int_{\Omega} \mathbf{E}(\delta\varphi) \cdot \mathbf{D}(\mathbf{u}, \varphi) \, d\Omega \quad (1.78)$$

is the increment of the work of electric field induced by the virtual electric potential  $\delta\varphi$ .

Thus, according to (1.75)–(1.78), relations (1.73), (1.74) determine the equalities of the virtual mechanical and electric works of external forces and the increments of the works of the virtual strains and electric field.

If we subtract (1.74) from (1.73), then we can obtain the variational principle of stationary virtual electric enthalpy

$$\delta H(\mathbf{u}, \varphi) = \delta[\tilde{L}_u(\mathbf{u}) - \tilde{L}_\varphi(\varphi)], \quad (1.79)$$

where

$$H(\mathbf{u}, \varphi) = \frac{1}{2}c(\mathbf{u}, \mathbf{u}) - e(\mathbf{u}, \varphi) - \frac{1}{2}\epsilon(\varphi, \varphi) = \frac{1}{2} \int_{\Omega} (\boldsymbol{\varepsilon} : \boldsymbol{\sigma} - \mathbf{E}^* \cdot \mathbf{D}) d\Omega \quad (1.80)$$

is the electric enthalpy.

We note that the electric enthalpy does not coincide with the internal energy

$$U(\mathbf{u}, \varphi) = \frac{1}{2}c(\mathbf{u}, \mathbf{u}) + \frac{1}{2}\epsilon(\varphi, \varphi) = \frac{1}{2} \int_{\Omega} (\boldsymbol{\varepsilon} : \boldsymbol{\sigma} + \mathbf{E}^* \cdot \mathbf{D}) d\Omega, \quad (1.81)$$

and the electric enthalpy is not positive definite by  $\mathbf{u}$  and  $\varphi$ .

In connection to this, from variational principle (1.79) it only follows that the functional

$$\Pi_e(\mathbf{u}, \varphi) = H(\mathbf{u}, \varphi) - \tilde{L}_u(\mathbf{u}) + \tilde{L}_\varphi(\varphi) \quad (1.82)$$

is stationary on the real (true) fields of displacements and electric potential.

There are no minimality properties, but the main forms  $c(\mathbf{u}, \mathbf{u})$  and  $\epsilon(\varphi, \varphi)$  are symmetrical and positive definite.

It is also important to note that the norms

$$\|\mathbf{v}\|_{\mathbb{W}_2^1}^2 = \int_{\Omega} [\mathbf{v}^* \cdot \mathbf{v} + (\nabla \mathbf{v})^* : \nabla \mathbf{v}] d\Omega, \quad \|\mathbf{v}\|_{\mathbb{H}_u^1}^2 = \int_{\Omega} (\nabla \mathbf{v})^* : \nabla \mathbf{v} d\Omega,$$

$$\|\mathbf{v}\|_c^2 = \int_{\Omega} \boldsymbol{\varepsilon}(\mathbf{v}) : \mathbf{c}^E : \boldsymbol{\varepsilon}(\mathbf{v}) d\Omega$$

are equivalent in  $\mathbb{H}_u^1$ . Here in order to prove the equivalence of the norms we can use one of the main results of the mathematical theory of elasticity, the inequality of Korn [13]. For the equivalence of the norms it is also important to exclude the solid body motions in the selected space, as it was adopted for  $\mathbb{H}_u^1$ .

By analogy, in  $H_\varphi^1$  the norms

$$\|\chi\|_{W_2^1}^2 = \int_{\Omega} [\chi^2 + (\nabla\chi)^* \cdot \nabla\chi] d\Omega, \quad \|\chi\|_{H_\varphi^1}^2 = \int_{\Omega} (\nabla\chi)^* \cdot \nabla\chi d\Omega,$$

$$\|\chi\|_{\epsilon}^2 = \int_{\Omega} \mathbf{E}^*(\chi) \cdot \boldsymbol{\epsilon}^S \cdot \mathbf{E}(\chi) d\Omega.$$

are equivalent.

The property of the positive definiteness of the forms  $c(\mathbf{u}, \mathbf{u})$  and  $\epsilon(\varphi, \varphi)$  are important both in theory and in justification of the numerical methods applied.

Thus, the weak problem settings are convenient instruments for proving the mathematical statements and also serve the basis for building effective numerical methods, based on the approximations of energy relations.

The generalized statements can be also constructed for transient problems with Rayleigh account for damping. Here the analogous transformations lead to the system

$$\rho(\mathbf{v}, \ddot{\mathbf{u}}_0) + d(\mathbf{v}, \dot{\mathbf{u}}_0) + c(\mathbf{v}, \mathbf{u}_0) - e(\mathbf{v}, \varphi_0) = L_u(\mathbf{v}), \quad (1.83)$$

$$e(\mathbf{u}_0, \chi) + \epsilon(\chi, \varphi_0) = L_\varphi(\chi), \quad (1.84)$$

where

$$\rho(\mathbf{v}, \mathbf{u}) = \int_{\Omega} \rho \mathbf{v}^* \cdot \mathbf{u} d\Omega, \quad d(\mathbf{v}, \mathbf{u}) = \alpha_d \rho(\mathbf{v}, \mathbf{u}) + \beta_d c(\mathbf{v}, \mathbf{u}), \quad (1.85)$$

$$L_u(\mathbf{v}) = \tilde{L}_u(\mathbf{v}) - \rho(\mathbf{v}, \ddot{\mathbf{u}}_n) - d(\mathbf{v}, \dot{\mathbf{u}}_n) - c(\mathbf{v}, \mathbf{u}_n) + e(\mathbf{v}, \varphi_n), \quad (1.86)$$

$$L_\varphi(\chi) = \tilde{L}_\varphi(\chi) - e(\mathbf{u}_n, \chi) - \epsilon(\chi, \varphi_n). \quad (1.87)$$

This system should be supplemented by initial conditions (1.37), that can be presented in the weak form

$$(\mathbf{v}, \mathbf{u}_0(\mathbf{x}, +0)) = (\mathbf{v}, \mathbf{u}_{sn}), \quad (\mathbf{v}, \dot{\mathbf{u}}_0(\mathbf{x}, +0)) = (\mathbf{v}, \mathbf{v}_{sn}), \quad (1.88)$$

where  $(\mathbf{v}, \mathbf{u}) = \int_{\Omega} \mathbf{v}^* \cdot \mathbf{u} d\Omega$  is an ordinary scalar product in  $L^2$ ;  $\mathbf{u}_{sn} = \mathbf{u}_s - \mathbf{u}_n(\mathbf{x}, +0)$ ;  $\mathbf{v}_{sn} = \mathbf{v}_s - \dot{\mathbf{u}}_n(\mathbf{x}, +0)$ .

Here relations (1.83)–(1.87) must hold when  $t \in (0, T)$  for any  $\mathbf{v} \in H_u^1$ ,  $\chi \in H_\varphi^1$ . At that for the solution  $\{\mathbf{u} = \mathbf{u}_0 + \mathbf{u}_n, \varphi = \varphi_0 + \varphi_n\}$  the displacements  $\mathbf{u}_0$  must belong to the space  $Q_u$ , and the electric potential  $\varphi_0$  must belong to the space  $Q_\varphi$ :

$$Q_u = L^2(0, T; H_u^1), \quad Q_\varphi = L^2(0, T; H_\varphi^1), \quad (1.89)$$

where for the Banach space  $X$  with the norm  $\|\cdot\|_X$  by  $L^2(0, T; X)$  we denote the space (of classes) of the functions  $t \rightarrow f(t)$  from  $[0, T]$  in  $X$  such that

$$\left( \int_0^T \|f(t)\|_X^2 dt \right)^{1/2} = \|f\|_{L^2(0, T; X)} < \infty.$$

The statement of the problem in the form (1.83), (1.84) has also the meaning of the energy principle of virtual work, that is analogous to the static case considered before. As in the elasticity theory, the form  $\rho(\mathbf{v}, \ddot{\mathbf{u}})$  is the virtual inertial force taken with the opposite sign.

The generalized or weak statement of dynamic electroelasticity problems in the form (1.83)–(1.88) serves the basis for building the semi-discrete approximations of the Galerkin (Bubnov-Galerkin) method, which will be considered in the next section.

### 1.3.3 Semi-discrete approximations in electroelasticity problems

The main issue that remained open in section 1.2.2 consists in the way of finding the weak solutions for the problems of electroelasticity. The general approach called the Bubnov-Galerkin method is based on the idea of finding solutions for the weak statements in finite-dimensional spaces.

When we consider transient problems with weak statements (1.83), (1.84), corresponding to the principle of virtual work, we seek semi-discrete approximations  $\mathbf{u}_{h0} \approx \mathbf{u}_0$ ,  $\varphi_{h0} \approx \varphi_0$  in the form

$$\mathbf{u}_{h0} = \mathbf{N}_u^*(\mathbf{x}) \cdot \mathbf{U}(t), \quad \varphi_{h0} = \mathbf{N}_\varphi^*(\mathbf{x}) \cdot \Phi(t), \quad (1.90)$$

where  $\mathbf{U}(t)$ ,  $\Phi(t)$  are the vectors of approximation constants (not depending on time),  $\mathbf{N}_u^*(\mathbf{x})$  is the matrix of the basis functions for  $\mathbf{u}_{h0}$ , and  $\mathbf{N}_\varphi^*(\mathbf{x})$  is the row-vector of the basis functions for  $\varphi_{h0}$ .

These approximations are called semi-discrete, because here the discretizations are made only in spatial variables, and there are no time discretizations in (1.90).

If the basis functions  $N_s(\mathbf{x})$  are the same for all three components of the displacements  $u_{h0j}$ ,  $j = 1, 2, 3$ , and electric potential  $\varphi_{h0}$  (in the case of the problem in  $\mathbb{R}^3$ ), then the matrix  $\mathbf{N}_u^*(\mathbf{x})$  and the row-vector  $\mathbf{N}_\varphi^*(\mathbf{x})$  have the form

$$\mathbf{N}_u^*(\mathbf{x}) = \begin{bmatrix} N_1(\mathbf{x}) & 0 & 0 & \dots & N_n(\mathbf{x}) & 0 & 0 \\ 0 & N_1(\mathbf{x}) & 0 & \dots & 0 & N_n(\mathbf{x}) & 0 \\ 0 & 0 & N_1(\mathbf{x}) & \dots & 0 & 0 & N_n(\mathbf{x}) \end{bmatrix}, \quad (1.91)$$

$$\mathbf{N}_\varphi^*(\mathbf{x}) = [N_1(\mathbf{x}), N_2(\mathbf{x}), \dots, N_n(\mathbf{x})], \quad (1.92)$$

where  $n$  is the number of the basis functions that are required to approximate one of the components of displacements or electric potential.

The basis functions must be linearly independent and have the property of completeness in  $H_u^1, H_\varphi^1$ . Naturally, they are assumed to be known, and the vectors  $\mathbf{U}(t), \Phi(t)$  in (1.90) are to be defined from the solution of the electroelasticity problem in the weak form.

We will take the probe functions  $\mathbf{v}(\mathbf{x})$  and  $\chi(\mathbf{x})$  from the same finite-dimensional spaces

$$\mathbf{v} = \mathbf{N}_u^*(\mathbf{x}) \cdot \delta\mathbf{U}, \quad \chi = \mathbf{N}_\varphi^*(\mathbf{x}) \cdot \delta\Phi, \quad (1.93)$$

where  $\delta\mathbf{U}, \delta\Phi$  are arbitrary vectors, for example, containing unit in one position and zero in all others.

Substituting (1.90), (1.93) into the weak problem statement (1.83), (1.84) and taking (1.54)–(1.58), (1.85)–(1.87) into account, we get the following system:

$$\delta\mathbf{U}^* \cdot (\mathbf{M}_{uu} \cdot \ddot{\mathbf{U}} + \mathbf{C}_{uu} \cdot \dot{\mathbf{U}} + \mathbf{K}_{uu} \cdot \mathbf{U} + \mathbf{K}_{u\varphi} \cdot \Phi) = \delta\mathbf{U}^* \cdot \mathbf{F}_u, \quad (1.94)$$

$$\delta\Phi^* \cdot (-\mathbf{K}_{u\varphi}^* \cdot \mathbf{U} + \mathbf{K}_{\varphi\varphi} \cdot \Phi) = \delta\Phi^* \cdot \mathbf{F}_\varphi. \quad (1.95)$$

Here

$$\mathbf{M}_{uu} = \int_{\Omega} \rho \mathbf{N}_u \mathbf{N}_u^* d\Omega, \quad \mathbf{C}_{uu} = \alpha_d \mathbf{M}_{uu} + \beta_d \mathbf{K}_{uu},$$

$$\mathbf{K}_{uu} = \int_{\Omega} \mathbf{B}_u^* : \mathbf{c}^E : \mathbf{B}_u d\Omega, \quad \mathbf{B}_u = \nabla \mathbf{N}_u^*,$$

$$\mathbf{K}_{u\varphi} = \int_{\Omega} \mathbf{B}_u^* : \mathbf{e}^* \cdot \mathbf{B}_\varphi d\Omega, \quad \mathbf{B}_\varphi = \nabla \mathbf{N}_\varphi^*, \quad (1.96)$$

$$\mathbf{K}_{\varphi\varphi} = \int_{\Omega} \mathbf{B}_\varphi^* \cdot \boldsymbol{\epsilon}^S \cdot \mathbf{B}_\varphi d\Omega,$$

$$\begin{aligned} \mathbf{F}_u &= \tilde{\mathbf{F}}_u - \int_{\Omega} \rho \mathbf{N}_u \cdot \ddot{\mathbf{u}}_n d\Omega - \alpha_d \int_{\Omega} \rho \mathbf{N}_u \cdot \dot{\mathbf{u}}_n d\Omega - \\ &- \int_{\Omega} \mathbf{B}_u^* : \mathbf{c}^E : (\nabla \mathbf{u}_n + \beta_d \nabla \dot{\mathbf{u}}_n) d\Omega - \int_{\Omega} \mathbf{B}_u^* : \mathbf{e}^* \cdot \nabla \varphi_n d\Omega, \end{aligned}$$

$$\tilde{\mathbf{F}}_u = \int_{\Omega} \mathbf{N}_u \cdot \rho \mathbf{f} d\Omega + \int_{\Gamma_\sigma} \mathbf{N}_u \cdot \mathbf{p}_\Gamma d\Gamma,$$

$$\mathbf{F}_\varphi = \tilde{\mathbf{F}}_\varphi + \int_{\Omega} \mathbf{B}_\varphi^* \cdot \mathbf{e} : \nabla \mathbf{u}_n d\Omega - \int_{\Omega} \mathbf{B}_\varphi^* \cdot \boldsymbol{\epsilon}^S \cdot \nabla \varphi_n d\Omega,$$



$$\tilde{\mathbf{F}}_\varphi = \int_{\Omega} \mathbf{N}_\varphi \sigma_\Omega d\Omega + \int_{\Gamma_D} \mathbf{N}_\varphi \sigma_\Gamma d\Gamma + \sum_{j \in J_Q} \mathbf{N}_\varphi|_{\Gamma_{\varphi j}} Q_j.$$

We note that every matrix in (1.96) reflects specific material characteristics of the body:  $\mathbf{M}_{uu}$  denotes the mass or the density,  $\mathbf{C}_{uu}$  denotes the damping,  $\mathbf{K}_{uu}$  denotes the stiffness,  $\mathbf{K}_{u\varphi}$  denotes the piezoelectric effect,  $\mathbf{K}_{\varphi\varphi}$  denotes the dielectric permeability.

Then by virtue of arbitrariness of the vectors  $\delta\mathbf{U}$ ,  $\delta\Phi$ , from (1.94), (1.95) we get the final system

$$\mathbf{M}_{uu} \cdot \ddot{\mathbf{U}} + \mathbf{C}_{uu} \cdot \dot{\mathbf{U}} + \mathbf{K}_{uu} \cdot \mathbf{U} + \mathbf{K}_{u\varphi} \cdot \Phi = \mathbf{F}_u, \quad (1.97)$$

$$-\mathbf{K}_{u\varphi}^* \cdot \mathbf{U} + \mathbf{K}_{\varphi\varphi} \cdot \Phi = \mathbf{F}_\varphi. \quad (1.98)$$

For transient problems system (1.97), (1.98) is a system of ordinary differential equations of the second order by time. It should be supplemented by initial conditions that can be obtained from (1.37) or from (1.88) and (1.90), (1.93). As a result, the initial conditions in a discrete form will be given in the following way:

$$\mathbf{U}(0) = \mathbf{U}_{sn}, \quad \dot{\mathbf{U}}(0) = \mathbf{V}_{sn}, \quad (1.99)$$

where  $\mathbf{U}_{sn}$ ,  $\mathbf{V}_{sn}$  are the unknown vectors obtained from initial data  $\mathbf{u}_{sn}(\mathbf{x})$ ,  $\mathbf{v}_{sn}(\mathbf{x})$  under their approximations in finite-dimensional spaces.

Numerical solution of the Cauchy problem (1.97)–(1.99) allows to take into account the features of system (1.97), (1.98), consisting in a possibility of the reduction of the vector  $\Phi$ . Indeed, finding  $\Phi$  from (1.98) and substituting it into (1.97), we get:

$$\Phi = \mathbf{K}_{\varphi\varphi}^{-1} \cdot \mathbf{K}_{u\varphi}^* \cdot \mathbf{U} + \mathbf{K}_{\varphi\varphi}^{-1} \cdot \mathbf{F}_\varphi, \quad (1.100)$$

$$\mathbf{M}_{uu} \cdot \ddot{\mathbf{U}} + \mathbf{C}_{uu} \cdot \dot{\mathbf{U}} + \bar{\mathbf{K}}_{uu} \cdot \mathbf{U} = \bar{\mathbf{F}}_u, \quad (1.101)$$

where

$$\bar{\mathbf{K}}_{uu} = \mathbf{K}_{uu} + \mathbf{K}_{u\varphi} \cdot \mathbf{K}_{\varphi\varphi}^{-1} \cdot \mathbf{K}_{u\varphi}^*, \quad (1.102)$$

$$\bar{\mathbf{F}}_u = \mathbf{F}_u - \mathbf{K}_{u\varphi} \cdot \mathbf{K}_{\varphi\varphi}^{-1} \cdot \mathbf{F}_\varphi. \quad (1.103)$$

As a result we obtain the problem (1.101), (1.99) but with respect to the vector  $\mathbf{U}$  with symmetric and at least non-negative definite matrix  $\bar{\mathbf{K}}_{uu}$ . This problem has almost the same properties as the problem for pure elastic medium. The distinction lies in the presence of the inverse matrix  $\mathbf{K}_{\varphi\varphi}^{-1}$ . If we use a sparse matrix technology [29] when implementing numerical algorithms for sparse matrices  $\mathbf{M}_{uu}$ ,  $\mathbf{K}_{uu}$ ,  $\mathbf{K}_{u\varphi}$ ,  $\mathbf{K}_{\varphi\varphi}$ , then it

is highly undesirable to form the matrix  $\mathbf{K}_{\varphi\varphi}^{-1}$  in explicit form, because, generally speaking, the matrix, that is inverse to the sparse one, is dense. Therefore, in order to implement the matrix-vector product  $\mathbf{K}_{u\varphi} \cdot \Phi$ , it is necessary every time to solve system (1.98) of linear algebraic equations with respect to  $\Phi$  and substitute the result into (1.97).

### 1.3.4 Summary of the main features of electroelasticity problems

In this section, we will summarize what we have considered in the previous sections regarding the problems of electroelasticity.

The classical statements of the electroelasticity problems include the systems of differential equations with dynamic motion equations (without account for coupling, hyperbolic type) and the equations of quasi-electrostatics (without account for coupling, elliptic type). Therefore, in total in the equations of linear dynamic theory of electroelasticity the orders of the higher time derivatives are different.

The boundary-value and initial boundary-value problems of electroelasticity are characterized by nonstandard electric boundary conditions, especially for the electrodes powered by the current generators. On separate electrode surfaces powered by voltage generators the electric potential should take the same values for all points of the electrode, and these values are known. On the electrodes powered by current generators the electric potential also should take the same values on every part, but these values are unknown, and finding them requires additional integral conditions that define total charges on the electrodes.

The generalized or weak statements of the electroelasticity problems obtained as a result of standard transformations, lead to a variational principle of stationary electric enthalpy (without the minimality property). Thus, for the electroelasticity problems, there is no conventional variational principle of virtual works with variation of the fields of displacement and electric potential that leads to a minimum of an energy functional.

The functional spaces  $H_{\varphi}^1$  that define the weak solutions of the electroelasticity problems are also rather unusual. For the space  $H_{\varphi}^1$  the functions should take stationary (not depending on  $\mathbf{x}$ ), but arbitrary values on some parts  $\Gamma_{\varphi j}$ , powered by current generators. Only the restrictions of homogeneity for the essential boundary conditions ( $\mathbf{u} = 0; \mathbf{x} \in \Gamma_u$ ) are set in a standard way, as, for example, for  $H_u^1$ . Here the essential boundary conditions may also be inhomogeneous.

The numerical solution by the Bubnov-Galerkin method for the static problems of electroelasticity gives a coupled system of equation with respect to the displacements and electric potentials with a common matrix that is not positive definite. The matrix of this system can be transformed to a quasi-definite symmetric matrix (matrices for the problems with a saddle point) [5]:

$$\mathbf{K} = \begin{bmatrix} \mathbf{K}_{uu} & \mathbf{K}_{u\varphi} \\ \mathbf{K}_{u\varphi}^* & -\mathbf{K}_{\varphi\varphi} \end{bmatrix}.$$

The reduction of the values of electric potentials permits to obtain the systems of equations with positive definite matrices for finding the displacements, which are similar to the equations of structural analysis (for pure elastic medium). At the same time the presence of the piezoelectric effect only enhances the properties of positive definiteness for the stiffness matrix, i. e.  $\bar{\mathbf{K}}_{uu} \geq \mathbf{K}_{uu}$ , as  $\bar{\mathbf{K}}_{uu} - \mathbf{K}_{uu} = \mathbf{K}_{u\varphi} \cdot \mathbf{K}_{\varphi\varphi}^{-1} \cdot \mathbf{K}_{u\varphi}^*$  is a non-negative definite matrix.

We note that hereinafter the inequalities  $\mathbf{A} > \mathbf{B}$  and  $\mathbf{A} \geq \mathbf{B}$  for the matrices mean that the matrix  $\mathbf{A} - \mathbf{B}$  is positive or non-negative definite, respectively. We will write the condition of the positive definiteness for the matrix  $\mathbf{A}$  in the form  $\mathbf{A} > 0$ , and the condition of the non-negative definiteness will be written in the form  $\mathbf{A} \geq 0$ .

For piezoelectric bodies, an important role is given to special sets of natural frequencies, namely the frequencies of electric resonances  $f_{rj}$  and the frequencies of electric anti-resonances  $f_{aj}$ .

Both the frequencies of electric resonances  $f_{rj}$  and electric anti-resonances  $f_{aj}$  are the natural frequencies, and the oscillations on them can be excited under electric external influences that change according to harmonic law. These external influences are different for the frequencies  $f_{rj}$  and  $f_{aj}$ .

In order to find the natural frequencies for a piezoelectric (electroelastic) body, we need to consider the mode of steady-state oscillations  $\mathbf{U} = \tilde{\mathbf{U}} \exp(i\omega t)$ ,  $\Phi = \tilde{\Phi} \exp(i\omega t)$  with the circular frequency  $\omega$  ( $\omega = f/2\pi$ ). Besides, for finding the natural frequencies we consider homogeneous problems with  $\mathbf{F}_u = 0$ ,  $\mathbf{F}_\varphi = 0$  without damping, i. e. with  $\mathbf{C}_{uu} = 0$ . Then from (1.97), (1.98) we get a generalized eigenvalue problem:

$$\mathbf{K}_{uu} \cdot \mathbf{U} + \mathbf{K}_{u\varphi} \cdot \Phi = \omega^2 \mathbf{M}_{uu} \cdot \mathbf{U}, \quad (1.104)$$

$$-\mathbf{K}_{u\varphi}^* \cdot \mathbf{U} + \mathbf{K}_{\varphi\varphi} \cdot \Phi = 0, \quad (1.105)$$

where the sign “~” for the amplitude values  $\tilde{\mathbf{U}}$ ,  $\tilde{\Phi}$  is dropped.

In (1.104), (1.105) the matrices  $\mathbf{K}_{u\varphi}$ ,  $\mathbf{K}_{\varphi\varphi}$  differ for the frequencies of electric resonances and anti-resonances. The difference in the problems of finding the natural frequencies of electric resonances and anti-resonances consists in the following. For the problem of finding the frequencies of electric resonances some electrodes  $\Gamma_{\varphi j}$  are considered to be short-circuited ( $\varphi = 0$ ,  $\mathbf{x} \in \Gamma_{\varphi j}$ ), and for the corresponding problems of finding the frequencies of electric anti-resonances these electrodes are considered to be free ( $\varphi = \Phi_{\Gamma j}$ ,  $\mathbf{x} \in \Gamma_{\varphi j}$ ;  $\int_{\Gamma_{\varphi j}} \mathbf{n} \cdot \mathbf{D} d\Gamma = 0$ ). Thus, in two corresponding eigenvalue problems we need to consider different electric boundary conditions on some (but not all!) electrode surfaces  $\Gamma_{\varphi j}$ .

Mathematically this difference consists in the different structures of the matrices  $\mathbf{K}_{u\varphi}$  and  $\mathbf{K}_{\varphi\varphi}$ . If for a problem of finding the frequencies of electric anti-resonances we present the matrices  $\mathbf{K}_{u\varphi}$ ,  $\mathbf{K}_{\varphi\varphi}$  and the vector  $\Phi$  in a block form

$$\mathbf{K}_{u\varphi} = \begin{bmatrix} \mathbf{K}_{u\varphi}^c & \mathbf{K}_{u\varphi}^s \end{bmatrix}, \quad \mathbf{K}_{\varphi\varphi} = \begin{bmatrix} \mathbf{K}_{\varphi\varphi}^c & \mathbf{K}_{\varphi\varphi}^{cs} \\ \mathbf{K}_{\varphi\varphi}^{cs*} & \mathbf{K}_{\varphi\varphi}^s \end{bmatrix}, \quad \Phi = \begin{Bmatrix} \Phi_c \\ \Phi_s \end{Bmatrix}, \quad (1.106)$$

than for the problem of finding the frequencies of electric resonances the matrices  $\mathbf{K}_{u\varphi}$ ,  $\mathbf{K}_{\varphi\varphi}$  and the vector  $\Phi$  will have the form

$$\mathbf{K}_{u\varphi} = \mathbf{K}_{u\varphi}^c, \quad \mathbf{K}_{\varphi\varphi} = \mathbf{K}_{\varphi\varphi}^c, \quad \Phi = \Phi_c. \quad (1.107)$$

Here in the vector  $\Phi$  in (1.106) we can separately allocate the degrees of freedom  $\Phi_s$ , when finding the frequencies of electric anti-resonances for which it is considered that the total electric charges on the corresponding electrodes are equal to zero, and when finding the frequencies of electric resonances we set  $\Phi_s = 0$ .

Therefore for finding the frequencies of electric resonances and anti-resonances we should solve the problems (1.104), (1.105) twice with different matrices  $\mathbf{K}_{u\varphi}$ ,  $\mathbf{K}_{\varphi\varphi}$  and the vector  $\Phi$  in the forms (1.106) and (1.107).

Let us denote by  $\omega_{aj}$  the natural frequencies for problem (1.104)–(1.106), and  $\omega_{rj}$  will denote the natural frequencies for problem (1.104), (1.105), (1.107). We note that by virtue of positive definiteness of the matrix  $\mathbf{M}_{uu}$  (problem 1.20) and at least non-negative definiteness of the matrix  $\bar{\mathbf{K}}_{uu}$  (problem 1.24) all these frequencies are real and can be chosen non-negative.

If we enumerate the frequencies in ascending order, then it is possible to show [4] that the following equalities hold

$$\omega_{rj} \leq \omega_{aj}; \quad j = 1, 2, \dots, m, \quad (1.108)$$

where  $m$  is the order of the matrix  $\mathbf{M}_{uu}$  or  $\overline{\mathbf{K}}_{uu}$ .

The value that is relevant in practice is the dynamic electromechanical coupling coefficient (DECC)  $k_{dj}$  for the  $j$ -th frequency that is given by the formula

$$k_{dj}^2 = \frac{\omega_{aj}^2 - \omega_{rj}^2}{\omega_{aj}^2}. \quad (1.109)$$

Dynamic electromechanical coupling coefficient defines the efficiency of the energy conversion at the  $j$ -th oscillation mode. Naturally, if  $k_{dj}$  is not equal to zero, then  $\omega_{rj} \neq \omega_{aj}$ , and these very frequencies are electrically active. (Some oscillation modes can be purely elastic, and for them  $\omega_{rj} = \omega_{aj}$ .)

Therefore, in order to analyze the work of piezoelectric devices in a steady-state oscillation mode it is often required to find the frequencies  $\omega_{rj}$ ,  $\omega_{aj}$ , solving slightly different generalized eigenvalue problems two times and finding the frequencies, for which  $\omega_{rj}$  and  $\omega_{aj}$  differ. This type of problems is a distinctive feature of the piezoelectric analysis of real-world piezoelectric devices.

Piezoelectric transducers can represent the bodies composed of a set of elastic and piezoelectric subdomains (for example, piezoelectric emitter in a case). Besides, for some devices, for example, for counter-pin transducers on the surface acoustic waves, it is necessary to account for the contact of piezoelectric body with the external medium (air). In such cases we have compound problems for multilayer medium  $\Omega = \cup \Omega_k$  with, generally speaking, different physico-mechanical properties. One part of these domains  $\Omega_k = \Omega_k^p$  can be piezoelectric, other part of these domains  $\Omega_k = \Omega_k^e$  can be elastic, and one more part  $\Omega_k = \Omega_k^d$  can be dielectric. For elastic and dielectric media we can use the same models of electroelasticity with the coupling coefficients  $\mathbf{e}$  equal to zero and apply either mechanical or dielectric part of the model. The conjugation conditions (continuity of  $\mathbf{u}$ ,  $\mathbf{n} \cdot \boldsymbol{\sigma}$ ,  $\varphi$ ,  $\mathbf{n} \cdot \mathbf{D}$  when crossing the interface) will then be naturally contained in the generalized problem statements. The numerical algorithms intended for solving the problems for compound bodies with different physico-mechanical properties will have peculiarities, related to the presence of the media with different field functions ( $\mathbf{u}$ ,  $\varphi$  for the piezoelectric media,  $\mathbf{u}$  for the elastic media,  $\varphi$  for the dielectric media). It is also worth noting that external dielectric media (surrounding air) can be very extensive and therefore should be modeled by unbounded domains. These unbounded dielectric media require the conditions for the field  $\varphi$  at infinity. Also, special numerical solution methods should be used for infinite domains.

Thus, the problems of electroelasticity have a number of significant features caused by both peculiarities of mathematical models and practical needs for calculation of real-world piezoelectric devices.

## 1.4 Modeling of thermoelasticity problems

The problems of thermoelasticity consider the coupling of mechanical and thermal fields. Concerning the mechanical part, it has much in common with ordinary elasticity theory and electroelasticity theory considered before. However, the equations for thermal fields significantly differ from the equations of quasi-electrostatics of dielectrics. There is an extensive literature on theory of thermoelasticity, among which the basic monographs of W. Nowacki [24, 25] are worth noting.

### 1.4.1 Classical statements of thermoelasticity problems

Let a thermoelastic body occupy the domain  $\Omega$  with the boundary  $\Gamma = \partial\Omega$ . The state of the body is characterized by the displacement vector  $\mathbf{u} = \mathbf{u}(\mathbf{x}, t)$  and the thermal field change  $\theta = \theta(\mathbf{x}, t)$ . The function  $\theta(\mathbf{x}, t)$  describes the temperature increase  $T(\mathbf{x}, t)$  from the natural state  $T_0$ :  $\theta = T - T_0$ .

The statement of the problems of linear thermoelasticity includes the following group of equations.

The field equations consist of the motion equations for continuum, which are identical to (1.23)

$$\nabla \cdot \boldsymbol{\sigma} + \rho \mathbf{f} = \rho \ddot{\mathbf{u}}, \quad (1.110)$$

and local conservation law of thermal energy

$$T_0 \dot{S} + \nabla \cdot \mathbf{q} = W. \quad (1.111)$$

Here for mechanical values we adopt the same notations as those in the electroelasticity theory in section 1.3 ( $\rho$  is the density;  $\boldsymbol{\sigma}$  is the second rank stress tensor;  $\mathbf{f}$  is the vector of mass force density), also, the following notations are introduced for thermal values:  $S$  is the density of entropy, measured from the natural state;  $\mathbf{q}$  is thermal flow vector;  $W = W(\mathbf{x}, t)$  is the intensity of heat sources.

The constitutive relations connect the stresses  $\boldsymbol{\sigma}$  and the entropy  $S$  with the strain tensor  $\boldsymbol{\varepsilon}$  and the temperature field  $\theta$ . For a linear medium the constitutive relations have the form:

$$\boldsymbol{\sigma} = \mathbf{c} : \boldsymbol{\varepsilon} - \gamma \theta, \quad (1.112)$$

$$S = \boldsymbol{\gamma} : \boldsymbol{\varepsilon} + \frac{\rho c_\varepsilon}{T_0} \theta, \quad (1.113)$$

where  $\mathbf{c}$  is the semi-symmetric fourth rank tensor of elastic moduli;  $\boldsymbol{\gamma}$  is the symmetric second rank tensor of thermal stresses;  $c_\varepsilon$  is the specific heat at constant strains.

Finally, the relations that connect the flow values  $\boldsymbol{\varepsilon}$  and  $\mathbf{q}$  with the field functions  $\mathbf{u}$  and  $\theta$  have the following form:

$$\boldsymbol{\varepsilon} = (\nabla \mathbf{u} + \nabla \mathbf{u}^*)/2, \quad (1.114)$$

$$\mathbf{q} = -\mathbf{k} \cdot \nabla \theta, \quad (1.115)$$

where  $\mathbf{k}$  is the second rank tensor of thermal conductivity coefficients.

Formula (1.115) expresses the Fourier law for the thermal conductive medium. The tensor  $\mathbf{k}$  in (1.115) should be symmetric and positive definite:

$$k_{ij} = k_{ji}; \quad \exists \alpha_k > 0 : \quad \forall \mathbf{a} \quad \mathbf{a}^* \cdot \mathbf{k} \cdot \mathbf{a} \geq \alpha_k \mathbf{a}^* \cdot \mathbf{a}.$$

Thus, the system of differential equations of thermoelasticity is given by formulas (1.110)–(1.115). If we present these equations as a system of equations with respect to the displacements  $\mathbf{u}$  and temperature increase  $\theta$ , then we will obtain:

$$\rho \ddot{\mathbf{u}} - \nabla \cdot (\mathbf{c} : \nabla \mathbf{u} - \boldsymbol{\gamma} \theta) = \rho \mathbf{f}, \quad (1.116)$$

$$\rho c_\varepsilon \dot{\theta} + T_0 \boldsymbol{\gamma} : \nabla \dot{\mathbf{u}} - \nabla \cdot (\mathbf{k} \cdot \nabla \theta) = W, \quad (1.117)$$

or in a component-wise form:

$$\rho u_{i,tt} - (c_{ijkl} u_{k,l} - \gamma_{ij} \theta)_{,j} = \rho f_i, \quad i = 1, 2, 3, \quad (1.118)$$

$$\rho c_\varepsilon \theta_{,t} + T_0 \gamma_{ij} u_{i,jt} - (k_{ij} \theta_{,j})_{,i} = W. \quad (1.119)$$

As it can be seen, the coupling of mechanical and thermal fields is determined by the thermal stress tensor  $\boldsymbol{\gamma}$ . If  $\boldsymbol{\gamma} = 0$ , then (1.116) is simply a motion equation in a dynamic elasticity theory, and (1.117) is a thermal conductivity equation. We note, that the motion equation in a theory of elasticity is an equation of hyperbolic type, and the thermal conductivity equation is an equation of parabolic type. The system of coupled equations keeps the different order of the higher time derivatives: (1.116) has the time derivatives of the second order, and (1.117) has the time derivatives of the first order.

System (1.116), (1.117) or (1.118), (1.119) requires the boundary conditions that are here subdivided into two groups, namely, mechanical and thermal boundary conditions.

We will adopt the same mechanical boundary conditions as those adopted in section 1.3 for the electroelastic body ( $\Gamma = \Gamma_u \cup \Gamma_\sigma$ ):

$$\mathbf{u} = \mathbf{u}_\Gamma; \quad \mathbf{x} \in \Gamma_u, \quad (1.120)$$

$$\mathbf{p} = \mathbf{n} \cdot \boldsymbol{\sigma}; \quad \mathbf{p} = \mathbf{p}_\Gamma; \quad \mathbf{x} \in \Gamma_\sigma, \quad (1.121)$$

where the mechanical sense of the values used is the same as for (1.31), (1.32).

In order to formulate the thermal boundary conditions, let us assume that the boundary  $\Gamma$  is divided in three parts  $\Gamma_\theta$ ,  $\Gamma_q$  and  $\Gamma_c$ :  $\Gamma = \Gamma_\theta \cup \Gamma_q \cup \Gamma_c$ .

We will consider that the temperature  $\theta_\Gamma(\mathbf{x}, t)$  is set on  $\Gamma_\theta$ :

$$\theta = \theta_\Gamma; \quad \mathbf{x} \in \Gamma_\theta. \quad (1.122)$$

On  $\Gamma_q$  we will set the heat flow, or the surface density of the heat source intensity  $q_\Gamma(\mathbf{x}, t)$ :

$$\mathbf{n}^* \cdot \mathbf{q} = -q_\Gamma; \quad \mathbf{x} \in \Gamma_q. \quad (1.123)$$

Finally, on  $\Gamma_c$  we will set the condition of convective heat exchange with the external environment:

$$\mathbf{n}^* \cdot \mathbf{q} = -h_f(\theta_b - \theta); \quad \mathbf{x} \in \Gamma_c, \quad (1.124)$$

where  $h_f$  is the heat exchange factor or heat transfer coefficient on  $h_f > 0$ ),  $\theta_b$  is the temperature of external environment.

According to (1.122)–(1.124), we have three types of thermal boundary conditions. The condition (1.122) is the condition of the first kind, the Dirichlet type or the essential boundary condition. The condition (1.123) is the condition of the second kind, the Neumann type or the natural boundary condition. The condition (1.124) is the condition of the third kind.

Boundary conditions (1.122)–(1.124) are the main conditions both in thermal conductivity problems and more general thermoelasticity problems. In addition to these conditions, other boundary conditions can be set, for example, nonlinear condition of radiative heat transfer on Stefan-Boltzmann law and so on. However, the most frequently used are the conditions (1.122)–(1.124), which we will consider hereinafter.

Let us note that the conditions of the third kind are specific mostly to the problems of thermal conductivity and thermoelasticity. These conditions have the features of both the first kind boundary conditions (at large  $h_f$  from (1.122) we have  $\theta - \theta_b = h_f^{-1} \mathbf{n}^* \cdot \mathbf{q} \approx 0$ ) and the second kind boundary



conditions (at small  $h_f$  (1.122) can be approximated by the condition  $\mathbf{n}^* \cdot \mathbf{q} = 0$ ).

If for an elastic body the larger part of its boundary is  $\Gamma_\sigma$  with a homogeneous boundary of the second kind, i. e. the larger part of the boundary  $\Gamma_\sigma$  is free from mechanical stresses  $\mathbf{p}_\Gamma$ , than for thermal boundary conditions the homogeneous conditions of the second kind ( $q_\Gamma = 0$  in (1.123)) indicate a thermally insulated boundary. The case of thermally insulated boundary is a much bigger abstraction than the condition of a convective heat exchange with external environment, i. e. than the condition of the third kind.

In the case of transient processes, in addition to the boundary conditions we need to set the initial conditions. Here, apart from setting the initial position of the body  $\mathbf{u}_s(\mathbf{x})$  and the initial velocity  $\mathbf{v}_s(\mathbf{x})$ , the initial temperature  $\theta_s(\mathbf{x})$  should be defined:

$$\mathbf{u} = \mathbf{u}_s, \quad \dot{\mathbf{u}} = \mathbf{v}_s, \quad \theta = \theta_s; \quad \mathbf{x} \in \Omega, \quad t = +0. \quad (1.125)$$

Thus, the conventional or classical statement of transient problems of thermoelasticity in linear approximation includes the system equations (1.116), (1.117), the boundary conditions (1.120)–(1.124) and initial conditions (1.125).

For stationary case there are no initial conditions;  $\mathbf{u} = \mathbf{u}(\mathbf{x})$ ,  $\theta = \theta(\mathbf{x})$ ; external influences do not depend on time, and the system of differential equations (1.116), (1.117) takes the form:

$$-\nabla \cdot (\mathbf{c} : \nabla \mathbf{u} - \gamma \theta) = \rho \mathbf{f}, \quad (1.126)$$

$$-\nabla \cdot (\mathbf{k} \cdot \nabla \theta) = W. \quad (1.127)$$

As it can be seen from (1.126), (1.127), a stationary case corresponds to a partial coupling of fields: the displacement field  $\mathbf{u}$  depends on  $\theta$ , but for the temperature field  $\theta$  we obtain an uncoupled problem of thermal conductivity (1.127), (1.122)–(1.124).

Another case of thermoelastic problem with partial coupling can be given with the use of the theory of thermal stresses [24, 25]. In this theory, the coupling for the temperature field is neglected in (1.117), and the term  $T_0 \gamma : \nabla \dot{\mathbf{u}}$  is omitted, however, for the mechanical fields the dynamic equation (1.116) is considered. As a result, the field equations of the thermal stress theory have the form:

$$\nabla \cdot \boldsymbol{\sigma} + \rho \mathbf{f} = \rho \ddot{\mathbf{u}}, \quad \boldsymbol{\sigma} = \mathbf{c} : \boldsymbol{\varepsilon} - \gamma \theta, \quad (1.128)$$

$$\rho c_\varepsilon \dot{\theta} + \nabla \cdot \mathbf{q} = W, \quad \mathbf{q} = -\mathbf{k} \cdot \nabla \theta. \quad (1.129)$$

The transfer from (1.116), (1.117) to (1.128), (1.129) can be justified by lots of experimental data and by the analysis of the coupling coefficients with appropriate nondimensionalization of thermoelasticity problem.

Therefore, both the equations of thermal stresses (1.128), (1.129) and the equations of stationary thermoelasticity (1.126), (1.127) give the problems with partial field coupling.

It is important to note the following issue. For the problems of coupled thermoelasticity (1.116), (1.117), (1.120)–(1.125) the presence of the term  $T_0\gamma : \nabla\dot{\mathbf{u}}$  with the first time derivative with respect to the displacements lead to the energy dissipation, and additional account for damping is not particularly necessary in this problem. Meanwhile, in a partially coupled problem of thermal stresses for mechanical fields there is no damping, and therefore we can adopt the Rayleigh account for damping similar to the one in section 1.3.1 for the problem of electroelasticity. Indeed, instead of (1.128) we can use the relations

$$\nabla \cdot \boldsymbol{\sigma} + \rho \mathbf{f} = \rho \ddot{\mathbf{u}} + \alpha_d \rho \dot{\mathbf{u}}, \quad \boldsymbol{\sigma} = \mathbf{c} : (\boldsymbol{\varepsilon} + \beta_d \dot{\boldsymbol{\varepsilon}}) - \gamma \theta \quad (1.130)$$

with the damping coefficients  $\alpha_d \geq 0$ ,  $\beta_d \geq 0$ . Regarding the advantages and disadvantages of this approach we can repeat the same arguments as those considered in section 1.3.1.

### 1.4.2 Generalized statements of thermoelasticity problems

Following the scheme described in section 1.3.2, we will obtain the generalized or weak statement for the coupled problem of thermoelasticity (1.116), (1.117), (1.120)–(1.125).

Let us scalar multiply Eq. (1.110) by a yet arbitrary but sufficiently smooth function  $\mathbf{v} = \mathbf{v}(\mathbf{x})$ , and Eq. (1.111) will be multiplied by a sufficiently smooth function  $\eta = \eta(\mathbf{x})$ . Then let us integrate the obtained equalities over  $\Omega$ , using the operations of tensor and vector analysis (1.41), (1.42), and the Gauss-Ostrogradskii formulas (1.45), (1.46). (In (1.42), (1.46)  $\chi$  is replaced by  $\eta$ , and  $\mathbf{D}$  is replaced by  $\mathbf{q}$ .)

Imposing a homogeneous boundary condition (1.47) on the function  $\mathbf{v}$

$$\mathbf{v} = 0; \quad \mathbf{x} \in \Gamma_u, \quad (1.131)$$

and using natural boundary condition (1.121), we receive:

$$\int_{\Omega} \rho \mathbf{v} \cdot \ddot{\mathbf{u}} \, d\Omega + \int_{\Omega} (\nabla \mathbf{v})^* : \boldsymbol{\sigma}(\mathbf{u}, \theta) \, d\Omega = \int_{\Omega} \mathbf{v}^* \cdot \rho \mathbf{f} \, d\Omega + \int_{\Gamma_{\sigma}} \mathbf{v}^* \cdot \mathbf{p}_{\Gamma} \, d\Gamma. \quad (1.132)$$

On the transformations of Eq. (1.111), taking (1.113) into account, we get:

$$T_0 \int_{\Omega} \eta \dot{S} d\Omega - \int_{\Omega} (\nabla \eta)^* \cdot \mathbf{q}(\mathbf{u}, \theta) d\Omega = \int_{\Omega} \eta W d\Omega - \int_{\Gamma} \eta \mathbf{n}^* \cdot \mathbf{q}(\mathbf{u}, \theta) d\Gamma. \quad (1.133)$$

Let us impose the zero condition on the function  $\Gamma_{\theta}$

$$\eta = 0; \quad \mathbf{x} \in \Gamma_{\theta}. \quad (1.134)$$

Then, using boundary conditions (1.123) on  $\Gamma_q$  and (1.124) on  $\Gamma_c$ , the last integral in (1.133) can be transformed in the following way:

$$- \int_{\Gamma} \eta \mathbf{n}^* \cdot \mathbf{q}(\mathbf{u}, \theta) d\Gamma = \int_{\Gamma_q} \eta q_{\Gamma} d\Gamma + \int_{\Gamma_c} \eta h_f \theta_b d\Gamma - \int_{\Gamma_c} h_f \eta \theta d\Gamma. \quad (1.135)$$

The integral identity (1.133) with account for (1.135) can be written in the form:

$$\begin{aligned} T_0 \int_{\Omega} \eta \dot{S} d\Omega - \int_{\Omega} (\nabla \eta)^* \cdot \mathbf{q}(\mathbf{u}, \theta) d\Omega + \int_{\Gamma_c} h_f \eta \theta d\Gamma = \\ \int_{\Omega} \eta W d\Omega + \int_{\Gamma_q} \eta q_{\Gamma} d\Gamma + \int_{\Gamma_c} \eta h_f \theta_b d\Gamma. \end{aligned} \quad (1.136)$$

Now we can use in (1.132), (1.136) the constitutive relations (1.112), (1.113) for thermoelastic medium and obtain the main integral relations

$$\rho(\mathbf{v}, \ddot{\mathbf{u}}) + c(\mathbf{v}, \mathbf{u}) - \gamma(\mathbf{v}, \theta) = \tilde{L}_u(\mathbf{v}), \quad (1.137)$$

$$T_0 \gamma(\dot{\mathbf{u}}, \eta) + s(\eta, \dot{\theta}) + k(\eta, \theta) = \tilde{L}_{\theta}(\eta), \quad (1.138)$$

where

$$\rho(\mathbf{v}, \mathbf{u}) = \int_{\Omega} \rho \mathbf{v}^* \cdot \mathbf{u} d\Omega, \quad (1.139)$$

$$c(\mathbf{v}, \mathbf{u}) = \int_{\Omega} (\nabla \mathbf{v})^* : \mathbf{c}^E : \nabla \mathbf{u} d\Omega = \int_{\Omega} \boldsymbol{\varepsilon}(\mathbf{v}) : \mathbf{c}^E : \boldsymbol{\varepsilon}(\mathbf{u}) d\Omega, \quad (1.140)$$

$$\gamma(\mathbf{v}, \theta) = \int_{\Omega} (\nabla \mathbf{v})^* : \boldsymbol{\gamma} \theta d\Omega = \int_{\Omega} \boldsymbol{\varepsilon}(\mathbf{v}) : \boldsymbol{\gamma} \theta d\Omega, \quad (1.141)$$

$$s(\eta, \theta) = \int_{\Omega} \rho c_{\varepsilon} \eta \theta d\Omega, \quad (1.142)$$

$$k(\eta, \theta) = \int_{\Omega} (\nabla \eta)^* \cdot \mathbf{k} \cdot \nabla \theta d\Omega + \int_{\Gamma_c} h_f \eta \theta d\Gamma, \quad (1.143)$$

$$\tilde{L}_u(\mathbf{v}) = \int_{\Omega} \mathbf{v}^* \cdot \rho \mathbf{f} d\Omega + \int_{\Gamma_{\sigma}} \mathbf{v}^* \cdot \mathbf{p}_{\Gamma} d\Gamma, \quad (1.144)$$

$$\tilde{L}_\theta(\eta) = \int_\Omega \eta W \, d\Omega + \int_{\Gamma_q} \eta q_\Gamma \, d\Gamma + \int_{\Gamma_c} \eta h_f \theta_b \, d\Gamma. \quad (1.145)$$

Now it remains to remove inhomogeneity in the essential boundary conditions (1.120), (1.122). In order to do this, we will seek the solution  $\{\mathbf{u}, \theta\}$  in the form

$$\mathbf{u} = \mathbf{u}_0 + \mathbf{u}_n, \quad \theta = \theta_0 + \theta_n, \quad (1.146)$$

where  $\mathbf{u}_n = \mathbf{u}_n(\mathbf{x}, t)$ ,  $\theta_n = \theta_n(\mathbf{x}, t)$  are specially selected functions that satisfy the inhomogeneous essential boundary conditions

$$\mathbf{u}_n = \mathbf{u}_\Gamma; \quad \mathbf{x} \in \Gamma_u, \quad (1.147)$$

$$\theta_n = \theta_\Gamma; \quad \mathbf{x} \in \Gamma_\theta, \quad (1.148)$$

and, therefore, the functions  $\mathbf{u}_0 = \mathbf{u}_0(\mathbf{x}, t)$ ,  $\theta_0 = \theta_0(\mathbf{x}, t)$  satisfy the homogeneous essential boundary conditions

$$\mathbf{u}_0 = 0; \quad \mathbf{x} \in \Gamma_u, \quad (1.149)$$

$$\theta_0 = 0; \quad \mathbf{x} \in \Gamma_\theta. \quad (1.150)$$

Substituting (1.146) into (1.137), (1.138), we get the final system written with respect to the unknown functions  $\mathbf{u}_0$  and  $\theta_0$ :

$$\rho(\mathbf{v}, \ddot{\mathbf{u}}_0) + c(\mathbf{v}, \mathbf{u}_0) - \gamma(\mathbf{v}, \theta_0) = L_u(\mathbf{v}), \quad (1.151)$$

$$T_0 \gamma(\dot{\mathbf{u}}_0, \chi) + s(\eta, \dot{\theta}_0) + k(\eta, \theta_0) = L_\theta(\eta), \quad (1.152)$$

where

$$L_u(\mathbf{v}) = \tilde{L}_u(\mathbf{v}) - \rho(\mathbf{v}, \ddot{\mathbf{u}}_n) - c(\mathbf{v}, \mathbf{u}_n) + \gamma(\mathbf{v}, \theta_n), \quad (1.153)$$

$$L_\theta(\eta) = \tilde{L}_\theta(\eta) - T_0 \gamma(\dot{\mathbf{u}}_n, \chi) - s(\eta, \dot{\theta}_n) - k(\eta, \theta_n). \quad (1.154)$$

Let us add to the system (1.137), (1.138) or to (1.151), (1.152) the initial conditions (1.125) in the weak form

$$\begin{aligned} (\mathbf{v}, \mathbf{u}(\mathbf{x}, +0)) &= (\mathbf{v}, \mathbf{u}_s), & (\mathbf{v}, \dot{\mathbf{u}}(\mathbf{x}, +0)) &= (\mathbf{v}, \mathbf{v}_s), \\ (\eta, \theta(\mathbf{x}, +0)) &= (\eta, \theta_s), \end{aligned} \quad (1.155)$$

where

$$\begin{aligned} (\mathbf{v}, \mathbf{u}_0(\mathbf{x}, +0)) &= (\mathbf{v}, \mathbf{u}_{sn}), & (\mathbf{v}, \dot{\mathbf{u}}_0(\mathbf{x}, +0)) &= (\mathbf{v}, \mathbf{v}_{sn}), \\ (\eta, \theta_0(\mathbf{x}, +0)) &= (\eta, \theta_{sn}), \end{aligned} \quad (1.156)$$

where  $\mathbf{u}_{sn}(\mathbf{x}) = \mathbf{u}_s(\mathbf{x}) - \mathbf{u}_n(\mathbf{x}, +0)$ , etc.

The comparison of (1.151), (1.152) with analogous system (1.83), (1.84) of the electroelasticity problem shows that for  $\mathbf{v}$  and  $\mathbf{u}_0$  we can select the same functional spaces as those selected in section 1.3:  $\mathbf{v} \in H_u^1$ ,  $\mathbf{u}_0 \in Q_u = L^2(0, T; H_u^1)$ .

For  $\eta$  and  $\theta_0$  let us introduce the spaces analogous to  $H_u^1$ ,  $Q_u$ , but in a scalar form.

Namely, on the set of functions  $\eta \in C^1$ , that satisfy (1.134), we introduce the scalar product

$$(\eta, \theta)_{H_\theta^1} = \int_{\Omega} (\nabla \eta)^* \cdot \nabla \theta \, d\Omega. \quad (1.157)$$

The closure of this set in the norm generated by the scalar product (1.157) will be called the space  $H_\theta^1$ , and we define the space  $Q_\theta = L^2(0, T; H_\theta^1)$ .

Now we can formulate a strict definition of a generalized solution for a transient problem of thermoelasticity.

**Definition.** *A generalized or weak solution of a transient problem of thermoelasticity is a pair of functions  $\{\mathbf{u}, \theta\}$ ;  $\mathbf{u} = \mathbf{u}_0 + \mathbf{u}_n$ ;  $\theta = \theta_0 + \theta_n$ , such that  $\mathbf{u}_n$ ,  $\theta_n$  satisfy boundary conditions (1.147), (1.148),  $\mathbf{u}_0 \in Q_u$ ,  $\theta_0 \in Q_\theta$ ;  $\mathbf{u}_0$ ,  $\theta_0$  satisfy initial conditions (1.156), and system of differential equations (1.151), (1.152) holds  $\forall t \in (0, T)$ ,  $\forall \mathbf{v} \in H_u^1$ ;  $\eta \in H_\theta^1$ .*

In a stationary case system (1.151), (1.152) takes the form

$$c(\mathbf{v}, \mathbf{u}_0) - \gamma(\mathbf{v}, \theta_0) = L_u(\mathbf{v}), \quad (1.158)$$

$$k(\eta, \theta_0) = L_\theta(\eta), \quad (1.159)$$

and we can give the corresponding definition of a generalized solution for a stationary problem.

**Definition.** *A generalized or weak solution of a stationary problem of thermoelasticity is a pair of functions  $\{\mathbf{u}, \theta\}$ ;  $\mathbf{u} = \mathbf{u}_0 + \mathbf{u}_n$ ;  $\theta = \theta_0 + \theta_n$ , such that  $\mathbf{u}_n$ ,  $\theta_n$  satisfy boundary conditions (1.147), (1.148),  $\mathbf{u}_0 \in H_u^1$ ,  $\theta_0 \in H_\theta^1$ ; and system of equations (1.158), (1.159) holds  $\forall \mathbf{v} \in H_u^1$ ;  $\eta \in H_\theta^1$ .*

Regarding the interrelation of generalized and classical solutions and the importance of the generalized solution, the arguments similar to those in section 1.3 are also valid here.

### 1.4.3 Semi-discrete approximations in thermoelasticity problems

By analogy to section 1.3.3, let us set semi-discrete approximations  $\mathbf{u}_{h0} \approx \mathbf{u}_0$ ,  $\theta_{h0} \approx \theta_0$  in the form

$$\mathbf{u}_{h0} = \mathbf{N}_u^*(\mathbf{x}) \cdot \mathbf{U}(t), \quad \theta_{h0} = \mathbf{N}_\theta^*(\mathbf{x}) \cdot \mathbf{T}(t), \quad (1.160)$$

where  $\mathbf{U}(t)$ ,  $\mathbf{T}(t)$  are the vectors of approximation constants (time dependent),  $\mathbf{N}_u^*(\mathbf{x})$  is the matrix of the basis functions for  $\mathbf{u}_{h0}$ , defined in (1.91),  $\mathbf{N}_\theta^*(\mathbf{x})$  is the row-vector of the basis functions for  $\theta_{h0}$ , that has the structure analogous to (1.92).

We will present the projection functions  $\mathbf{v}(\mathbf{x})$  and  $\eta(\mathbf{x})$  from the same finite-dimensional spaces in the form

$$\mathbf{v} = \mathbf{N}_u^*(\mathbf{x}) \cdot \delta \mathbf{U}, \quad \eta = \mathbf{N}_\theta^*(\mathbf{x}) \cdot \delta \mathbf{T}. \quad (1.161)$$

The substitution of (1.160), (1.161) into (1.151), (1.152) with account for (1.139)–(1.145), (1.153), (1.154) gives

$$\delta \mathbf{U}^* \cdot (\mathbf{M}_{uu} \cdot \ddot{\mathbf{U}} + \mathbf{K}_{uu} \cdot \mathbf{U} - \mathbf{K}_{u\theta} \cdot \mathbf{T}) = \delta \mathbf{U}^* \cdot \mathbf{F}_u, \quad (1.162)$$

$$\delta \mathbf{T}^* \cdot (T_0 \mathbf{K}_{u\theta}^* \cdot \dot{\mathbf{U}} + \mathbf{C}_{\theta\theta} \cdot \dot{\mathbf{T}} + \mathbf{K}_{\theta\theta} \cdot \mathbf{T}) = \delta \mathbf{T}^* \cdot \mathbf{F}_\theta. \quad (1.163)$$

Here the matrices  $\mathbf{M}_{uu}$  and  $\mathbf{K}_{uu}$  are those defined by (1.96) previously in section 1.3.3,

$$\mathbf{K}_{u\theta} = \int_{\Omega} \mathbf{B}_u^* : \gamma \mathbf{N}_\theta^* d\Omega, \quad \mathbf{C}_{\theta\theta} = \int_{\Omega} \rho c_\varepsilon \mathbf{N}_\theta \mathbf{N}_\theta^* d\Omega,$$

$$\mathbf{K}_{\theta\theta} = \int_{\Omega} \mathbf{B}_\theta^* \cdot \mathbf{k} \cdot \mathbf{B}_\theta d\Omega + \int_{\Gamma_c} h_f \mathbf{N}_\theta \mathbf{N}_\theta^* d\Gamma, \quad \mathbf{B}_\theta = \nabla \mathbf{N}_\theta^*, \quad (1.164)$$

$$\mathbf{F}_u = \tilde{\mathbf{F}}_u - \int_{\Omega} \rho \mathbf{N}_u \cdot \ddot{\mathbf{u}}_n d\Omega - \int_{\Omega} \mathbf{B}_u^* : \mathbf{c} : \nabla \mathbf{u}_n d\Omega + \int_{\Omega} \mathbf{B}_u^* : \gamma \theta_n d\Omega,$$

$$\begin{aligned} \mathbf{F}_\theta &= \tilde{\mathbf{F}}_\theta - T_0 \int_{\Omega} (\nabla \dot{\mathbf{u}}_n)^* : \gamma \mathbf{N}_\theta d\Omega - \int_{\Omega} \rho c_\varepsilon \mathbf{N}_\theta \dot{\theta}_n d\Omega - \\ &\quad - \int_{\Omega} \mathbf{B}_\theta^* \cdot \mathbf{k} \cdot \nabla \theta_n d\Omega - \int_{\Gamma_c} h_f \mathbf{N}_\theta \theta_n d\Gamma, \end{aligned}$$

$$\tilde{\mathbf{F}}_\theta = \int_{\Omega} \mathbf{N}_\theta W d\Omega + \int_{\Gamma_q} \mathbf{N}_\theta q_\Gamma d\Gamma + \int_{\Gamma_c} \mathbf{N}_\theta h_f \theta_b d\Gamma,$$

and the vector  $\tilde{\mathbf{F}}_u$  also was defined in (1.96) in section 1.3.3.

Taking into account the arbitrariness of  $\delta\mathbf{U}$ ,  $\delta\mathbf{T}$ , from (1.162), (1.163) we obtain the system of equations of transient thermoelasticity discretized by spacial variables:

$$\mathbf{M}_{uu} \cdot \ddot{\mathbf{U}} + \mathbf{K}_{uu} \cdot \mathbf{U} - \mathbf{K}_{u\theta} \cdot \mathbf{T} = \mathbf{F}_u, \quad (1.165)$$

$$T_0 \mathbf{K}_{u\theta}^* \cdot \dot{\mathbf{U}} + \mathbf{C}_{\theta\theta} \cdot \dot{\mathbf{T}} + \mathbf{K}_{\theta\theta} \cdot \mathbf{T} = \mathbf{F}_\theta, \quad (1.166)$$

This system should be supplemented by initial conditions

$$\mathbf{U}(0) = \mathbf{U}_{sn}, \quad \dot{\mathbf{U}}(0) = \mathbf{V}_{sn}, \quad \theta(0) = \theta_{sn}, \quad (1.167)$$

that follow from initial conditions (1.156) and approximations (1.160), (1.161).

We note that for the system (1.165), (1.166) the matrices  $\mathbf{M}_{uu}$  and  $\mathbf{C}_{\theta\theta}$  are positive definite ( $\mathbf{M}_{uu} > 0$ ,  $\mathbf{C}_{\theta\theta} > 0$ ), and the matrices  $\mathbf{K}_{uu}$  and  $\mathbf{K}_{\theta\theta}$  are at least non-negative definite (see problems 1.20, 1.21, 1.23, 1.30–1.32).

For static (stationary) problems system (1.165), (1.166) becomes only vector-coupled

$$\mathbf{K}_{uu} \cdot \mathbf{U} = \mathbf{F}_u + \mathbf{K}_{u\theta} \cdot \mathbf{T}, \quad (1.168)$$

$$\mathbf{K}_{\theta\theta} \cdot \mathbf{T} = \mathbf{F}_\theta. \quad (1.169)$$

Here we have uncoupled problem (1.169) for finding the vector  $\mathbf{T}$ , and problem (1.168) is almost the same as for purely elastic medium and differs only in the addition of the right-hand side vector  $\mathbf{K}_{u\theta} \cdot \mathbf{T}$ .

Finally, for the problem of thermal stresses with account for damping the system of FEM can be also written in a form of a vector-coupled system

$$\mathbf{M}_{uu} \cdot \ddot{\mathbf{U}} + \mathbf{C}_{uu} \cdot \dot{\mathbf{U}} + \mathbf{K}_{uu} \cdot \mathbf{U} = \mathbf{F}_u + \mathbf{K}_{u\theta} \cdot \mathbf{T}, \quad (1.170)$$

$$\mathbf{C}_{\theta\theta} \cdot \dot{\mathbf{T}} + \mathbf{K}_{\theta\theta} \cdot \mathbf{T} = \mathbf{F}_\theta, \quad (1.171)$$

where the damping matrix  $\mathbf{C}_{uu}$  is the same as in (1.96).

## 1.5 Problems of poroelasticity. Porothermoelastic analogy

In this section we will consider the issues of modeling the problems of geomechanics of deformable porous rocks with account of filtration. These problems are described by the systems of coupled equations of poroelasticity. The comparison of the equations of poroelasticity and thermoelasticity shows that there is a complete analogy between the system

of these equations. Consequently, using the analogy between the problems of poroelasticity and the problems of thermoelasticity, we can simulate complex coupled deformation and filtration processes in geomechanical media in the framework of the problems of thermoelasticity described in the previous section.

We will consider the poroelastic media to be heterogeneous with an elastic matrix and the pores filled by a fluid. Let us assume that the porosity is small and the distribution of a fluid in a matrix is subjected to the laws of filtration. The stress tensor  $\boldsymbol{\sigma}$  and the porosity  $\phi$  are expressed in terms of the strain tensor  $\boldsymbol{\varepsilon}$  and the pore pressure function  $p$  by the constitutive equations of poroelasticity [9]

$$\boldsymbol{\sigma} - \boldsymbol{\sigma}_0 = \mathbf{c} : \boldsymbol{\varepsilon} - \mathbf{b}(p - p_0) \quad (1.172)$$

$$\phi - \phi_0 = \mathbf{b} : \boldsymbol{\varepsilon} + \frac{1}{N}(p - p_0), \quad (1.173)$$

where  $\mathbf{c}$  is the fourth rank tensor of elastic stiffness,  $\mathbf{b}$  is the second rank Biot's tensor,  $N^{-1}$  is the inverse Biot's modulus, which connects the porosity change with the pressure change at constant strain,  $\boldsymbol{\sigma}_0$ ,  $\phi_0$ ,  $p_0$  are the initial stresses, porosity and pore pressure, respectively.

The deformation of the poroelastic matrix is described by the motion equations (1.23)

$$\nabla \cdot \boldsymbol{\sigma} + \rho \mathbf{f} = \rho \ddot{\mathbf{u}}. \quad (1.174)$$

To describe the filtration process, we will use the Darcy's law in a quasi-static approximation

$$\mathbf{v} = -\frac{\mathbf{K}}{\rho_f g} \cdot (\nabla p - \rho_f \mathbf{g}), \quad (1.175)$$

where  $\mathbf{v}$  is the filtration velocity,  $\mathbf{K}$  is the second rank tensor of filtration coefficients,  $\rho_f$  is the fluid density,  $\mathbf{g}$  is the vector of gravitational acceleration.

In order to obtain the equation for the porosity we use the continuity equation in the form

$$\frac{\partial(\rho_f \phi)}{\partial t} + \nabla \cdot (\rho_f \mathbf{v}) = 0 \quad (1.176)$$

and the fluid state equation

$$\frac{d\rho_f}{\rho_f} = \frac{dp}{K_f}, \quad (1.177)$$

where  $K_f$  is the fluid bulk modulus.



Substituting (1.175), (1.177), (1.173) in continuity equation (1.176) and assuming the changes in the compressibility and porosity to be small, we get

$$\mathbf{b} : \dot{\boldsymbol{\varepsilon}} + \frac{1}{M}\dot{p} - \nabla \cdot \left( \frac{\mathbf{K}}{\rho_{f0}g} \cdot \nabla p \right) = 0, \quad (1.178)$$

where  $\rho_{f0}$  is the initial fluid density,  $1/M = 1/N + \phi/K_f$ .

For a saturated porous medium the Biot's tensor can be taken unit ( $\mathbf{b} = \mathbf{I}$ ), and then with account for (1.172) and (1.178) Eq. (1.174) will give the following system of equations for poroelastic medium

$$\rho \ddot{\mathbf{u}} - \nabla \cdot (\mathbf{c} : \boldsymbol{\varepsilon} - p \mathbf{I}) = \rho \mathbf{f}, \quad (1.179)$$

$$\mathbf{I} : \dot{\boldsymbol{\varepsilon}} + \frac{1}{M}\dot{p} - \nabla \cdot \left( \frac{\mathbf{K}}{\rho_{f0}g} \cdot \nabla p \right) = 0, \quad (1.180)$$

where  $\mathbf{I}$  is the unit tensor and consequently  $\mathbf{I} : \dot{\boldsymbol{\varepsilon}} = \nabla \cdot \dot{\mathbf{u}} = \dot{\varepsilon}_{ii}$ .

System (1.179), (1.180) represents a coupled system of differential equations with different order of time derivatives and the values of material parameters and physical modules that significantly vary in magnitude. In simulation of the phenomenon of hydraulic disjuncting and failure of the rocks the filtration modules are adopted to be dependent on the pore pressure, and the elastic moduli can depend on the strains, which makes system (1.179), (1.180) nonlinear. To formulate the poroelastic problem statements, Eqs. (1.179), (1.180) should be supplemented by the boundary and initial conditions, and this finally leads to coupled transient linear or nonlinear initial boundary-value problems of geomechanics of poroelastic media.

In order to solve the problems of poroelasticity, we can use the analogy between the equations and boundary conditions for the poroelastic and the thermoelastic media.

As it was shown in section 1.4, the differential equations for thermoelastic media have the form

$$\rho \ddot{\mathbf{u}} - \nabla \cdot (\mathbf{c} : \nabla \mathbf{u} - \boldsymbol{\gamma} \theta) = \rho \mathbf{f}, \quad (1.181)$$

$$T_0 \boldsymbol{\gamma} : \nabla \dot{\mathbf{u}} + \rho c_\varepsilon \dot{\theta} - \nabla \cdot (\mathbf{k} \cdot \nabla \theta) = W. \quad (1.182)$$

The comparison of (1.179), (1.180) and (1.181), (1.182) shows that the equations of coupled poroelasticity after the multiplication of (1.180) by  $T_0$  are transformed into the equations of coupled thermoelasticity with  $W = 0$  under the changes

$$p \leftrightarrow \theta, \quad \mathbf{I} \leftrightarrow \boldsymbol{\gamma}, \quad \frac{T_0}{\rho M} \leftrightarrow c_\varepsilon, \quad \frac{T_0 \mathbf{K}}{\rho_{f0}g} \leftrightarrow \mathbf{k}, \quad (1.183)$$

where in the equations of poroelasticity it should be set  $T_0 = 1$ .

Thus, for solving the coupled initial boundary-value problems of poroelasticity we can solve the corresponding initial boundary-value problems of thermoelasticity and use the software developed for solving the problems of thermoelasticity.

For numerical calculation of the poroelasticity problems it is necessary to take into account that in the problems of geomechanics the values of the elastic moduli, filtration coefficients and porosity have substantially various orders and differ from the corresponding values (apart from the elastic moduli) of the problems of thermoelasticity. In connection to this in order to ensure the stability of the solution convergence for the numerical methods it is useful to make a transition to dimensionless parameters and notations.

Let us choose the characteristic length  $R$  of the domain as a parameter for nondimensionalization over spacial coordinates, the characteristic time  $t_*$  of the geomechanical process will be the parameter for nondimensionalization over time and the characteristic pressure  $p_*$  will be the parameter for nondimensionalization over pressure and stresses. We will mark the dimensionless variables by a “tilde” above.

$$\tilde{\mathbf{x}} = \mathbf{x}/R, \quad \tilde{\mathbf{u}} = \mathbf{u}/R, \quad \tilde{\nabla} = R\nabla, \quad \tilde{t} = t/t_*, \quad (1.184)$$

$$\tilde{\mathbf{c}} = \mathbf{c}/p_*, \quad \tilde{\boldsymbol{\sigma}} = \boldsymbol{\sigma}/p_*, \quad \tilde{p} = p/p_*. \quad (1.185)$$

Using these notations, equations of poroelasticity (1.179), (1.180) can be rewritten in the form

$$\tilde{\rho} \frac{\partial^2 \tilde{\mathbf{u}}}{\partial \tilde{t}^2} - \tilde{\nabla} \cdot (\tilde{\mathbf{c}} : \boldsymbol{\varepsilon} - \tilde{p} \mathbf{I}) = \tilde{\rho} \tilde{\mathbf{f}}, \quad (1.186)$$

$$T_0 \mathbf{I} : \frac{\partial \boldsymbol{\varepsilon}}{\partial \tilde{t}} + \tilde{\rho} \tilde{c}_p \frac{\partial \tilde{p}}{\partial \tilde{t}} - \tilde{\nabla} \cdot (\tilde{\mathbf{K}} \cdot \tilde{\nabla} \tilde{p}) = 0, \quad (1.187)$$

where

$$\tilde{\rho} = \frac{R^2}{p_2 t_*^2} \rho, \quad \tilde{\mathbf{f}} = \frac{t_*^2}{R} \mathbf{f}, \quad \tilde{c}_p = \frac{T_0 p_*}{M \tilde{\rho}}, \quad \tilde{\mathbf{K}} = \frac{T_0 p_* t_*}{R^2 \rho_f g} \mathbf{K}. \quad (1.188)$$

We note that the poroelastic equations in dimensionless form are transformed into the dimensionless equations of thermoelasticity under the change

$$\tilde{p} \leftrightarrow \tilde{\theta}, \quad \mathbf{I} \leftrightarrow \tilde{\boldsymbol{\gamma}}, \quad \tilde{c}_p \leftrightarrow \tilde{c}_\varepsilon, \quad \tilde{\mathbf{K}} \leftrightarrow \tilde{\mathbf{k}}, \quad (1.189)$$

with the corresponding notations for the dimensionless thermal values, where in the equations of thermoelasticity  $T_0 = 1$  can be set.

As the test calculations show, the transition to the dimensionless equations and values (1.184)–(1.189) enables to increase significantly the stability and accuracy of the numerical computations, as the system coefficients become aligned in orders.

## 1.6 Modeling of the interaction of deformable solids with acoustic media

Classical linear acoustics study the propagation of small amplitude sound waves in liquids and gases. Acoustic or sound waves are caused by elastic perturbations arising during the deformation of a solid structure that is in contact with an acoustic medium. In connection to this, typical problems of interest are the problems of interaction of elastic, piezoelectric or more complex solids with acoustic media. In these problems there are two adjacent domains,  $\Omega_s$  and  $\Omega_a$ .  $\Omega_s$  is the domain occupied by a solid structure, and  $\Omega_a$  is the domain occupied by an acoustic medium. In each of these domains the behaviour of the medium is simulated by the corresponding equations written with respect to various field functions. Thus, for the statement of the elasticity theory problem with respect to the displacement function the displacement vector  $\mathbf{u}(\mathbf{x}, t)$ ,  $\mathbf{x} \in \Omega_s$  is the unknown function. For the piezoelectric medium under the standard substitutions the unknowns are the functions of displacements  $\mathbf{u}(\mathbf{x}, t)$  and electric potential  $\varphi(\mathbf{x}, t)$ . Meanwhile, for the acoustic medium  $\Omega_a$  the main unknown is the function of excessive pressure  $p(\mathbf{x}, t)$  or the function of acoustic velocity potential  $\psi(\mathbf{x}, t)$ . Therefore on the boundary of the contact of two media  $\Gamma_{sa} = \Omega_s \cap \Omega_a$  it is necessary to use such conditions of fields conjugation that could be effectively included in various mathematical models of elastic, piezoelectric and acoustic media.

Simulation of coupled problems of interaction of elastic, piezoelectric or solid deformable bodies with acoustic media has certain difficulties and makes the scope of the next section.

### 1.6.1 Classical statements of acoustic problems

Let us firstly provide a brief derivation of the main equations of classical linear acoustics [12].

We denote the density of an acoustic medium (liquid or gas) as  $\tilde{\rho} = \tilde{\rho}(\mathbf{x}, t)$ , the pressure will be denoted by  $\tilde{p} = \tilde{p}(\mathbf{x}, t)$ , and the oscillating (acoustic) speed will be denoted by  $\mathbf{v} = \mathbf{v}(\mathbf{x}, t)$ .

As for any fluid, we have the continuity equation that expresses the law of mass conservation

$$\frac{\partial \tilde{\rho}}{\partial t} + \nabla \cdot (\mathbf{v} \tilde{\rho}) = 0. \quad (1.190)$$

Assuming the fluid to be ideal and neglecting its viscosity and thermal conductivity, we obtain the Euler's equation of motion

$$\tilde{\rho} \left( \frac{\partial \mathbf{v}}{\partial t} + (\mathbf{v} \cdot \nabla) \mathbf{v} \right) = -\nabla \tilde{p}. \quad (1.191)$$

In acoustic medium we study the excited or excessive values of pressure  $p(\mathbf{x}, t)$  and density  $\rho(\mathbf{x}, t)$  with respect to initial equilibrium states  $p_0$  and  $\rho_0$ :

$$\tilde{p} = p_0 + p, \quad \tilde{\rho} = \rho_0 + \rho, \quad (1.192)$$

where the values  $p/p_0$  and  $\rho/\rho_0$  are assumed to be small.

An acoustic fluid is considered to be compressible with the state law (Poisson's adiabatic)

$$\tilde{p} = p_0 \left( \frac{\tilde{\rho}}{\rho_0} \right)^\gamma. \quad (1.193)$$

Substituting (1.192) into (1.193) and taking into account the smallness of  $p/p_0$  and  $\rho/\rho_0$ , we get:

$$p + p_0 = p_0 \left( 1 + \frac{\rho}{\rho_0} \right)^\gamma \approx p_0 + \frac{p_0 \gamma}{\rho_0} \rho. \quad (1.194)$$

The value  $\sqrt{p_0 \gamma / \rho_0}$  is the main constant of the medium and is called the adiabatic speed of sound  $c_0$ :

$$c_0^2 = \frac{p_0 \gamma}{\rho_0}. \quad (1.195)$$

Thus, from (1.194), (1.195) we obtain the linear relation between the excessive pressure and the density

$$p = c_0^2 \rho. \quad (1.196)$$

Assuming the dimensionless velocity  $\mathbf{v}/c_0$  to be small, we linearize (1.190), (1.191) with account of (1.192)

$$\dot{\rho} + \rho_0 \nabla \cdot \mathbf{v} = 0, \quad (1.197)$$

$$\rho_0 \dot{\mathbf{v}} = -\nabla p. \quad (1.198)$$

Differentiating (1.197) by time and taking (1.198) and (1.196) into account, we obtain the wave equation for the function of excessive pressure

$$\frac{1}{c_0^2} \ddot{p} - \Delta p = 0. \quad (1.199)$$

This is the basic equation if the function of excessive pressure  $p(\mathbf{x}, t)$  is taken as the main field function. An alternative approach is the transition to an equation with respect to the acoustic velocity potential.

Let us vector multiply both parts of Eq. (1.198) by  $\nabla$ . Taking into account the identity  $\nabla \times \nabla p = 0$  we get:  $\text{rot } \mathbf{v} = 0$ . Thus, the acoustic velocity field is irrotational, and we can introduce the function of velocity potential  $\psi = \psi(\mathbf{x}, t)$ :

$$\mathbf{v} = \nabla \psi. \quad (1.200)$$

Then from (1.198) we get the relation that connect the functions  $p$  and  $\psi$ :

$$p = -\rho_0 \dot{\psi}. \quad (1.201)$$

Formulas (1.201), (1.199) show that the velocity potential  $\psi$  satisfies the wave equation

$$\frac{1}{c_0^2} \ddot{\psi} - \Delta \psi = 0. \quad (1.202)$$

For the differential equations (1.199) or (1.202) it is necessary to formulate the appropriate boundary conditions.

Let us assume that the boundary  $\Gamma_a = \partial\Omega_a$  of the acoustic medium is divided into four main parts:  $\Gamma_{af}$  is a free boundary;  $\Gamma_{ar}$  is a rigid boundary;  $\Gamma_{ai}$  is an impedance boundary;  $\Gamma_{as}$  is a boundary of a contact with a deformable solid.

On the free boundary the excessive pressure  $p$  should be equal to zero, and then according to (1.201) the velocity potential should be equal to zero:

$$p = 0, \quad \psi = 0; \quad \mathbf{x} \in \Gamma_{af}. \quad (1.203)$$

On the rigid boundary the normal component of the vector of acoustic velocity is equal to zero:  $\mathbf{n}_a \cdot \mathbf{v} = 0$ ,  $\mathbf{x} \in \Gamma_{ar}$ , where  $\mathbf{n}_a$  is the external with respect to  $\Omega_a$  unit normal to  $\Gamma_{ar}$ . Then by (1.200) the normal derivative of the function of velocity potential is equal to zero on  $\Gamma_{ar}$ , and consequently the same condition holds for the function of excessive pressure

$$\partial\psi/\partial n = \mathbf{n} \cdot \nabla \psi = 0, \quad \partial p/\partial n = \mathbf{n} \cdot \nabla p = 0; \quad \mathbf{x} \in \Gamma_{ar}. \quad (1.204)$$

The greatly extended domains should be limited by non-reflecting or absorbing boundaries. On these boundaries we can use an impedance

boundary condition:  $p = Zv_n$ ;  $\mathbf{x} \in \Gamma_{ai}$ , where  $Z$  is the impedance of the boundary  $\Gamma_{ai}$ . Using (1.201) this condition can be written as a condition for the function  $\psi$  or for the function  $p$ :

$$\mathbf{n} \cdot \nabla \psi = -\rho_0 Z^{-1} \dot{\psi}, \quad \mathbf{n} \cdot \nabla p = -\rho_0 Z^{-1} \dot{p}; \quad \mathbf{x} \in \Gamma_{ai}. \quad (1.205)$$

Finally, on the boundary  $\Gamma_{as}$  of the contact with a deformable solid the conjugation conditions should hold:

$$\mathbf{n} \cdot \mathbf{v} = \mathbf{n} \cdot \dot{\mathbf{u}}, \quad \mathbf{n} \cdot \boldsymbol{\sigma}_a = \mathbf{n} \cdot \boldsymbol{\sigma}_s; \quad \mathbf{x} \in \Gamma_{as}, \quad (1.206)$$

where  $\mathbf{v}$  is the acoustic velocity in the medium  $\Omega_a$ ;  $\mathbf{u}$  is the displacement vector in the body  $\Omega_s$ ;  $\mathbf{n} = \mathbf{n}_s$  is the external with respect to  $\Omega_s$  unit normal to  $\Gamma_{as}$  ( $\mathbf{n}_s = -\mathbf{n}_a$ ;  $\mathbf{n}_a$  is the external with respect to  $\Omega_a$  unit normal to  $\Gamma_{as}$ );  $\boldsymbol{\sigma}_s$  is the stress tensor in the solid structure;  $\boldsymbol{\sigma}_a = -p\mathbf{I}$  is the stress tensor in the acoustic medium ( $\mathbf{I}$  is the unit tensor).

The transient problems apart from the boundary conditions require the initial conditions for the values of field functions and their first time derivatives at  $t = +0$ .

Thus, the classical statement of the acoustic problem is possible with respect to both the excessive pressure function  $p = p(\mathbf{x}, t)$  and the acoustic velocity potential function  $\psi = \psi(\mathbf{x}, t)$ . This statement includes the wave equation (1.199) or (1.202), the boundary conditions (1.203)–(1.206) and the corresponding initial conditions. If there is a boundary  $\Gamma_{as}$  where a contact with a solid occurs, then this statement is not complete and it should be considered together with the corresponding problem for a deformable solid.

If the acoustic problem is considered separately, then at zero initial data its statement should be supplemented by the sources of excitation that should be added either to the right-hand sides of the wave equations or to the boundary conditions.

For the acoustic medium with dissipation we can consider a modification of Eq. (1.199)

$$\frac{1}{c_0^2} \ddot{p} - \Delta p - \varepsilon_a \Delta \dot{p} = 0, \quad (1.207)$$

where  $\varepsilon_a$  is the dissipation coefficient. Then it can be shown [22] that for the boundary conditions (1.206) it is possible to take:  $\boldsymbol{\sigma}_a \approx -(p + \varepsilon_a \dot{p})\mathbf{I}$ .

Such model of acoustic medium with dissipation obviously correlates with the models of solid structures with account of the Rayleigh damping. This model is convenient for construction of coupled systems of equations that describe the interrelation of various media with account of attenuation effects.

### 1.6.2 Semi-discrete approximations on the base of generalized statements and conjugation of acoustic equations with equations of solid structure

In order to move to a generalized statement for an acoustic problem formulated with respect to the pressure function, as usual we multiply the differential equation by a yet arbitrary sufficiently smooth function  $q = q(\mathbf{x})$ , then we integrate it over the domain  $\Omega_a$  and perform transformations related to the integration by parts. As a result from (1.199) we obtain:

$$\frac{1}{c_0^2} \int_{\Omega_a} q \ddot{p} d\Omega + \int_{\Omega_a} (\nabla q)^* \cdot \nabla p d\Omega = \int_{\Gamma_a} q \mathbf{n}_a \cdot \nabla p d\Gamma. \quad (1.208)$$

Now we need to transform the right-hand side of (1.208), using the boundary conditions and formulating the restrictions for the function  $q(\mathbf{x})$ .

On the part of the boundary  $\Gamma_{af}$  it is necessary to impose the same conditions (1.203) on  $q$  as those imposed on the function  $p$ :

$$q = 0; \quad \mathbf{x} \in \Gamma_{af}. \quad (1.209)$$

On the part  $\Gamma_{ar}$  according to (1.204) the normal derivative of the pressure is equal to zero, and therefore the integral in the right-hand side of (1.208) over the part  $\Gamma_{ar}$  vanishes.

The impedance boundary condition on  $\Gamma_{ai}$  by (1.205) leads to the following expression:

$$\int_{\Gamma_{ai}} q \mathbf{n}_a \cdot \nabla p d\Gamma = -\rho_0 Z^{-1} \int_{\Gamma_{ai}} q \dot{p} d\Gamma. \quad (1.210)$$

Finally, the representation of the right-hand side integral in (1.208) over the boundary  $\Gamma_{as}$  in contact with a solid structure depends on the possibility of the appropriate transformations for elastic (piezoelectric, thermoelastic, etc.) problems. Using the sequence of equalities

$$\mathbf{n}_a \cdot \nabla p = -\rho_0 \mathbf{n}_a \cdot \nabla \dot{\psi} = -\rho_0 \mathbf{n}_a \cdot \dot{\mathbf{v}} = -\rho_0 \mathbf{n}_a \cdot \ddot{\mathbf{u}}, \quad \mathbf{x} \in \Gamma_{as},$$

we get

$$\int_{\Gamma_{as}} q \mathbf{n}_a \cdot \nabla p d\Gamma = -\rho_0 \int_{\Gamma_{as}} q \mathbf{n}_a \cdot \ddot{\mathbf{u}} d\Gamma. \quad (1.211)$$

Then, when the constraint (1.209) holds, with account of (1.210), (1.211) the integral identity (1.208) will be written in the form

$$\frac{1}{c_0^2} \int_{\Omega_a} q \ddot{p} d\Omega + \frac{\rho_0}{Z} \int_{\Gamma_{ai}} q \dot{p} d\Gamma + \int_{\Omega_a} (\nabla q)^* \cdot \nabla p d\Omega + \rho_0 \int_{\Gamma_{as}} q \mathbf{n}_a \cdot \ddot{\mathbf{u}} d\Gamma = 0. \quad (1.212)$$

As our main goal is to construct numerical methods to analyze the work of solid structures interacting with acoustic medium, here we will not fully formulate the notion of the weak solution. Moreover, it can be easily done by analogy with the previous sections.

Therefore we proceed directly to the semi-discrete approximations that we will set in the form:

$$p \approx p_h = \mathbf{N}_p^*(\mathbf{x}) \cdot \mathbf{P}(t), \quad q = \mathbf{N}_p^*(\mathbf{x}) \cdot \delta \mathbf{P} = (\delta \mathbf{P})^* \cdot \mathbf{N}_p(\mathbf{x}), \quad (1.213)$$

$$\mathbf{u} \approx \mathbf{u}_h = \mathbf{u}_{0h} + \mathbf{u}_n, \quad \mathbf{u}_{0h} = \mathbf{N}_u^*(\mathbf{x}) \cdot \mathbf{U}(t), \quad (1.214)$$

where  $\mathbf{N}_p^*(\mathbf{x})$  is the row-vector of the shape functions for the pressure field;  $\mathbf{P}(t)$  is the vector of (time dependent) constants of approximation;  $\delta \mathbf{P}$  is an arbitrary vector;  $\mathbf{u}_n$ ,  $\mathbf{u}_{0h}$ ,  $\mathbf{N}_u^*(\mathbf{x})$ ,  $\mathbf{U}(t)$  are the same values that were defined previously in section 1.3.3.

Substituting (1.213), (1.214) into (1.212) and taking into account the independence of  $\delta \mathbf{P}$ , we receive

$$\mathbf{M}_{pp} \cdot \ddot{\mathbf{P}} + \mathbf{C}_{pp} \cdot \dot{\mathbf{P}} + \mathbf{K}_{pp} \cdot \mathbf{P} + \rho_0 \mathbf{R}_{pu} \cdot \ddot{\mathbf{U}} = -\rho_0 \dot{\mathbf{F}}_p, \quad (1.215)$$

where

$$\mathbf{M}_{pp} = \frac{1}{c_0^2} \int_{\Omega_a} \mathbf{N}_p \mathbf{N}_p^* d\Omega, \quad \mathbf{C}_{pp} = \frac{\rho_0}{Z} \int_{\Gamma_{ai}} \mathbf{N}_p \mathbf{N}_p^* d\Gamma, \quad (1.216)$$

$$\mathbf{K}_{pp} = \int_{\Omega_a} \mathbf{B}_p^* \cdot \mathbf{B}_p d\Omega, \quad \mathbf{B}_p = \nabla \mathbf{N}_p^*, \quad (1.217)$$

$$\mathbf{R}_{pu} = \int_{\Gamma_{as}} \mathbf{N}_p (\mathbf{n}^* \cdot \mathbf{N}_u^*) d\Gamma, \quad \mathbf{F}_p = \int_{\Gamma_{as}} \mathbf{N}_p (\mathbf{n}^* \cdot \dot{\mathbf{u}}_n) d\Gamma. \quad (1.218)$$

In order to conjugate these semi-discrete equations for an acoustic medium interacting with a solid structure, we need to obtain the corresponding equations for a deformable solid.

As it was shown in section 1.3, the right-hand side of the corresponding equation for a solid structure contained the integral  $\int_{\Gamma_s} \mathbf{v}^* \cdot (\mathbf{n}_s \cdot \boldsymbol{\sigma}_s) d\Gamma$ . Here  $\Gamma_s = \Gamma$  is the boundary of the solid structure domain  $\Omega_s = \Omega$ ,  $\mathbf{n}_s = \mathbf{n}$  is the external with respect to  $\Omega_s$  unit normal to  $\Gamma_s$ ,  $\boldsymbol{\sigma}_s = \boldsymbol{\sigma}$  is the stress tensor in the solid structure.

For the part of the boundary  $\Gamma_{as}$  with account of the contact conditions (1.206) and the equality  $\mathbf{n}_s = -\mathbf{n}_a$  at  $\boldsymbol{\sigma}_a = -p\mathbf{I}$  we get:

$$\mathbf{n}_s \cdot \boldsymbol{\sigma}_s = \mathbf{n}_s \cdot \boldsymbol{\sigma}_a = -\mathbf{n}_a \cdot \boldsymbol{\sigma}_a = \mathbf{n}_a^* \cdot (p\mathbf{I}) = p\mathbf{n}_a.$$

Thus, the equation similar to (1.52) of the weak problem statement for the solid structure in the right-hand side should be supplemented by an



integral over the surface of the contact with acoustic medium  $\int_{\Gamma_{as}} \mathbf{v}^* \cdot \mathbf{n}_a p d\Gamma$ . Then in the absence of the piezoelectric effect ( $\mathbf{e}=0$ ) Eq. (1.52) of the weak problem statement for a purely elastic medium will be written in the form:

$$c(\mathbf{v}, \mathbf{u}) = \tilde{L}_u(\mathbf{v}) + \int_{\Gamma_{as}} \mathbf{v}^* \cdot \mathbf{n}_a p d\Gamma.$$

Substituting the approximations (1.213) for  $p \approx p_h$  and (1.93) for  $\mathbf{v}$  into the last integral, we get:

$$\int_{\Gamma_{as}} \mathbf{v}^* \cdot \mathbf{n}_a p d\Gamma = \delta \mathbf{U}^* \cdot \mathbf{R}_{pu}^* \cdot \mathbf{P}.$$

Thus, the right-hand side of the discretized motion equations for the solid structure should be supplemented by the vector  $\mathbf{R}_{pu}^* \cdot \mathbf{P}$ . As a result, confining ourselves to an elastic case with the Rayleigh damping for the solid structure, we will have:

$$\mathbf{M}_{uu} \cdot \ddot{\mathbf{U}} + \mathbf{C}_{uu} \cdot \dot{\mathbf{U}} + \mathbf{K}_{uu} \cdot \mathbf{U} - \mathbf{R}_{pu}^* \cdot \mathbf{P} = \mathbf{F}_u. \quad (1.219)$$

Eqs (1.219), (1.215) should be solved simultaneously. These equations are the discretized by spacial variables motion equations for the solid structure and the acoustic medium that surrounds it.

In a single form these equations can be written as:

$$\mathbf{M} \cdot \ddot{\mathbf{a}} + \mathbf{C} \cdot \dot{\mathbf{a}} + \mathbf{K} \cdot \mathbf{a} = \mathbf{F}, \quad (1.220)$$

where

$$\mathbf{M} = \begin{bmatrix} \mathbf{M}_{uu} & 0 \\ \rho_0 \mathbf{R}_{pu} & \mathbf{M}_{pp} \end{bmatrix}, \quad \mathbf{C} = \begin{bmatrix} \mathbf{C}_{uu} & 0 \\ 0 & \mathbf{C}_{pp} \end{bmatrix}, \quad \mathbf{K} = \begin{bmatrix} \mathbf{K}_{uu} & -\mathbf{R}_{pu}^* \\ 0 & \mathbf{K}_{pp} \end{bmatrix}, \quad (1.221)$$

$$\mathbf{a} = \begin{Bmatrix} \mathbf{U} \\ \mathbf{P} \end{Bmatrix}, \quad \mathbf{F} = \begin{Bmatrix} \mathbf{F}_u \\ -\rho_0 \dot{\mathbf{F}}_p \end{Bmatrix}. \quad (1.222)$$

As it can be seen, the matrices  $\mathbf{M}$  and  $\mathbf{K}$  are not symmetric, and this fact somehow complicates the process of solving the problem (1.220).

We note that even in neglect of the attenuation mechanisms in a solid structure in the system (1.220) the damping remains if  $\mathbf{C}_{pp} \neq 0$ . Obviously, this takes place in the presence of the impedance boundary conditions, that permit the outflow of energy from the “solid – acoustic medium” system.

Let us see how the semi-discretized equations for acoustic medium will look like if we choose the acoustic potential  $\psi(\mathbf{x}, t)$  as an unknown function.

Let us adopt an appropriate approximation  $\psi \approx \psi_h = \mathbf{N}_\psi^*(\mathbf{x}) \cdot \Psi$  and take into account that by virtue of (1.201) at  $\mathbf{N}_\psi(\mathbf{x}) = \mathbf{N}_p(\mathbf{x})$

$$\mathbf{P} = -\rho_0 \dot{\Psi}. \quad (1.223)$$

Substituting (1.223) into (1.215) and integrating by time, we get

$$\mathbf{M}_{\psi\psi} \cdot \ddot{\Psi} + \mathbf{C}_{\psi\psi} \cdot \dot{\Psi} + \mathbf{K}_{\psi\psi} \cdot \Psi - \mathbf{R}_{\psi u} \cdot \dot{\mathbf{U}} = \mathbf{F}_\psi, \quad (1.224)$$

where  $\mathbf{M}_{\psi\psi} = \mathbf{M}_{pp}$ ,  $\mathbf{C}_{\psi\psi} = \mathbf{C}_{pp}$ ,  $\mathbf{K}_{\psi\psi} = \mathbf{K}_{pp}$ ,  $\mathbf{R}_{\psi u} = \mathbf{R}_{pu}$ ,  $\mathbf{F}_\psi = \mathbf{F}_p$ .

This equation in association with (1.219) and with account of (1.223) gives the system (1.220), in which now

$$\mathbf{M} = \begin{bmatrix} \mathbf{M}_{uu} & 0 \\ 0 & -\rho_0 \mathbf{M}_{\psi\psi} \end{bmatrix}, \quad \mathbf{C} = \begin{bmatrix} \mathbf{C}_{uu} & \rho_0 \mathbf{R}_{\psi u}^* \\ \rho_0 \mathbf{R}_{\psi u} & -\rho_0 \mathbf{C}_{\psi\psi} \end{bmatrix}, \quad (1.225)$$

$$\mathbf{K} = \begin{bmatrix} \mathbf{K}_{uu} & 0 \\ 0 & -\rho_0 \mathbf{K}_{\psi\psi} \end{bmatrix},$$

$$\mathbf{a} = \begin{Bmatrix} \mathbf{U} \\ \Psi \end{Bmatrix}, \quad \mathbf{F} = \begin{Bmatrix} \mathbf{F}_u \\ \rho_0 \mathbf{F}_\psi \end{Bmatrix}. \quad (1.226)$$

We note that system (1.220) with (1.225), (1.226) for the unknowns  $\{\mathbf{U}, \Psi\}$  has symmetric matrices of saddle structure (in order to insure the symmetry of the matrices, the equations for the acoustic medium (1.224) were specially multiplied by  $\rho_0$ ). Therefore in this form the system is numerically preferable than the system (1.220)–(1.222) for the unknowns  $\{\mathbf{U}, \mathbf{P}\}$ .

Nevertheless, a range of computational software [1] adopt exactly this approach (1.220)–(1.222), although there are implementations of the interaction of a solid structure with an acoustic medium on the base of Eqs. (1.220) with (1.225), (1.226).

## Exercises for Chapter 1

**1.1.** Show that in a sequence of equalities (1.18) one of the equalities follows from the others.

**1.2.** Find the maximum number of independent elastic moduli among the components  $c_{ijkl}^E$ , taking into account (1.18).

**1.3.** Find the maximum number of independent piezomoduli  $e_{ikl}$ , taking into account (1.19).

**1.4.** Show that from the condition of positive definiteness (1.21) of the fourth rank tensor of elastic moduli  $\mathbf{c}^E$  it follows that the components  $c_{iiii}^E$  with equal indices must be positive.

**1.5.** Show that by virtue of the condition of positive definiteness (1.22) of the second rank tensor of dielectric permittivities  $\epsilon^S$  it follows that the diagonal components  $\epsilon_{ii}^S$  must be positive. Should the nondiagonal components  $\epsilon_{ij}^S$  ( $i \neq j$ ) be positive as well?

**1.6.** By virtue of symmetry conditions (1.18) the elastic moduli  $c_{ijkl}^E$  can be arranged in the form of a symmetric matrix  $c_{\alpha\beta}^E = c_{ijkl}^E$  of the size  $6 \times 6$  ( $\alpha, \beta = 1, 2, \dots, 6$ ) with the following correspondence of the indices  $(ij) \leftrightarrow \alpha$ ,  $(ij) \leftrightarrow \beta$ :

$$(11) \leftrightarrow 1; \quad (22) \leftrightarrow 2; \quad (33) \leftrightarrow 3; \quad (23) = (32) \leftrightarrow 4;$$

$$(13) = (31) \leftrightarrow 5; \quad (12) = (21) \leftrightarrow 6.$$

Using this correspondence, the components of the strain tensor  $\epsilon$  can be represented in the form of a vector

$$\mathbf{S}^* = [\varepsilon_{11}, \varepsilon_{22}, \varepsilon_{33}, 2\varepsilon_{23}, 2\varepsilon_{13}, 2\varepsilon_{12}].$$

Show that from condition (1.21) it shows that the matrix  $c_{\alpha\beta}^E$  of the size  $6 \times 6$  must be positive definite.

**1.7.** Show that by virtue of condition (1.22) the matrix  $\epsilon^S$  composed of the components of the second rank tensor of dielectric permittivities  $\epsilon^S$  must be positive definite.

**1.8.** Prove that for the symmetric positive definite matrix  $\mathbf{K}$  for all  $i, j$  there holds an inequality  $|K_{ij}| \leq \sqrt{K_{ii}K_{jj}}$ .

**1.9.** Show that with the transition to vector-matrix notations described in problem 1.6 and introduction of the stress vector of the size 6

$$\mathbf{T}^* = [\sigma_{11}, \sigma_{22}, \sigma_{33}, \sigma_{23}, \sigma_{13}, \sigma_{12}]$$

and the matrix of the size  $3 \times 6$  for the piezomoduli  $e_{i\alpha} = e_{ikl}$ ,  $(kl) \leftrightarrow \alpha$ , the constitutive relations (1.16), (1.17) can be written in the form:

$$\mathbf{T} = \mathbf{c}^E \cdot \mathbf{S} - \mathbf{e}^* \cdot \mathbf{E},$$

$$\mathbf{D} = \mathbf{e} \cdot \mathbf{S} + \epsilon^S \cdot \mathbf{E}.$$

**1.10.** Show that for semi-symmetric fourth rank tensor the role of the unit tensor regarding the double contraction with the symmetric second rank tensor is performed by the tensor  $\Delta$ :

$$\Delta_{ijkl} = \frac{1}{2}(\delta_{ik}\delta_{jl} + \delta_{il}\delta_{jk}),$$

for which

$$\boldsymbol{\sigma} = \boldsymbol{\Delta} : \boldsymbol{\sigma}, \quad \forall \boldsymbol{\sigma} : \sigma_{ij} = \sigma_{ji}.$$

Check that if two fourth rank tensors  $\mathbf{c}^E$  and  $\mathbf{s}^E$  are connected by the relation

$$\mathbf{c}^E : \mathbf{s}^E = \mathbf{s}^E : \mathbf{c}^E = \boldsymbol{\Delta},$$

then from the equality  $\tilde{\boldsymbol{\sigma}} = \mathbf{c}^E : \tilde{\boldsymbol{\varepsilon}}$ ,  $\tilde{\boldsymbol{\varepsilon}} = \tilde{\boldsymbol{\varepsilon}}^*$  the equality  $\tilde{\boldsymbol{\varepsilon}} = \mathbf{s}^E : \tilde{\boldsymbol{\sigma}}$ ,  $\tilde{\boldsymbol{\sigma}} = \tilde{\boldsymbol{\sigma}}^*$  follows, and vice versa, i. e. the fourth rank tensors  $\mathbf{c}^E$  and  $\mathbf{s}^E$  can be regarded as reciprocal.

**1.11.** Show that the unit tensor  $\boldsymbol{\Delta}$  introduced in problem 1.10 is a semi-symmetric tensor, i. e. for this tensor the symmetry conditions similar to (1.18) hold. Is the tensor  $\boldsymbol{\Delta}$  positive definite in the sense of (1.21)?

**1.12.** Obtain an equivalent to (1.16), (1.17) form of the constitutive relations

$$\begin{aligned} \varepsilon_{ij} &= s_{ijkl}^E \sigma_{kl} + d_{kij} E_k, \\ D_i &= d_{ikl} \sigma_{kl} + \epsilon_{ik}^T E_k, \end{aligned}$$

where  $s_{ijkl}^E$  are the components of the tensor of elastic compliances calculated at constant electric field;  $d_{ikl}$  are the components of the tensor of piezomoduli;  $\epsilon_{ik}^T$  are the components of dielectric permittivities calculated at constant stress.

What are the properties of symmetry and positive definiteness for the tensors of elastic compliances  $\mathbf{s}^E$ , piezomoduli  $\mathbf{d}$  and dielectric permittivities  $\boldsymbol{\epsilon}^T$ ?

**1.13.** Show that with the introduction of vector-matrix notations for problems 1.6 and 1.9, the constitutive relation of problem 1.12 can be written in the form:

$$\begin{aligned} \mathbf{S} &= \mathbf{s}^E \cdot \mathbf{T} + \mathbf{d}^* \cdot \mathbf{E}, \\ \mathbf{D} &= \mathbf{d} \cdot \mathbf{T} + \boldsymbol{\epsilon}^T \cdot \mathbf{E}, \end{aligned}$$

where the components of the matrices  $s_{\alpha\beta}^E$  and  $d_{i\beta}$  are related to the components of the tensors  $s_{ijkl}^E$  and  $d_{ikl}$  by the laws

$$s_{\alpha\beta}^E = 2^{[\alpha/4]+[\beta/4]} s_{ijkl}^E, \quad d_{i\beta} = 2^{[\beta/4]} d_{ikl},$$

where  $[\gamma]$  is the integer part of  $\gamma$ .

**1.14.** Obtain an equivalent to (1.16), (1.17) form of the constitutive relations

$$\begin{aligned} \sigma_{ij} &= c_{ijkl}^D \varepsilon_{kl} - h_{kij} D_k, \\ E_i &= -h_{ikl} \varepsilon_{kl} + \beta_{ik}^S D_k, \end{aligned}$$

where  $c_{ijkl}^D$  are the components of the tensor of elastic moduli calculated at constant electric induction;  $h_{ikl}$  are the components of the tensor of piezoelectric constant strains;  $\beta_{ik}^S$  are the components of dielectric non-permittivities calculated at constant strain.

What are the properties of symmetry and positive definiteness for the tensor of elastic moduli  $\mathbf{c}^D$ , piezoelectric constant strains  $\mathbf{h}$  and dielectric non-permittivities  $\beta^S$ ?

**1.15.** Show that with the introduction of vector-matrix notation for problems 1.6 and 1.9 the constitutive relations in problem 1.14 can be written in the form:

$$\begin{aligned}\mathbf{T} &= \mathbf{c}^D \cdot \mathbf{S} - \mathbf{h}^* \cdot \mathbf{D}, \\ \mathbf{E} &= -\mathbf{h} \cdot \mathbf{S} + \beta^S \cdot \mathbf{D},\end{aligned}$$

where  $c_{\alpha\beta}^D = c_{ijkl}^D$  and  $h_{i\beta} = h_{ikl}$ .

**1.16.** Obtain an equivalent to (1.16), (1.17) form of the constitutive relations

$$\begin{aligned}\varepsilon_{ij} &= s_{ijkl}^D \sigma_{kl} + g_{kij} D_k, \\ E_i &= -g_{ikl} \sigma_{kl} + \beta_{ik}^T D_k,\end{aligned}$$

where  $s_{ijkl}^D$  are the components of the tensor of elastic compliances, calculated at constant electric induction;  $g_{ikl}$  are the components of the tensor of piezoelectric constant stresses;  $\beta_{ik}^T$  are the components of dielectric non-permittivities, calculated at constant stress.

What are the properties of symmetry and positive definiteness for the tensor of elastic compliances  $\mathbf{s}^D$ , piezoelectric constant stresses  $\mathbf{g}$  and dielectric non-permittivities  $\beta^T$ ?

**1.17.** Show that with the introduction of vector-matrix notation for problems 1.6 and 1.9 the constitutive relations in problem 1.16 can be written in the form:

$$\begin{aligned}\mathbf{S} &= \mathbf{s}^D \cdot \mathbf{T} + \mathbf{g}^* \cdot \mathbf{D}, \\ \mathbf{E} &= -\mathbf{g} \cdot \mathbf{T} + \beta^T \cdot \mathbf{D},\end{aligned}$$

where the components of the matrices  $s_{\alpha\beta}^D$  and  $g_{i\beta}$  are related to the components of the tensors  $s_{ijkl}^D$  and  $g_{ikl}$  by the laws

$$s_{\alpha\beta}^D = 2^{[\alpha/4]+[\beta/4]} s_{ijkl}^D, \quad g_{i\beta} = 2^{[\beta/4]} g_{ikl},$$

where  $[\gamma]$  is the integer part of  $\gamma$ .

**1.18.** Prove that for the strains of a deformable solid, that allows a rigid body motion, are equal to zero, i. e.  $\boldsymbol{\varepsilon} = 0$  for the displacements in the form  $\mathbf{u} = \mathbf{u}_{rigid} = \mathbf{u}_c + \boldsymbol{\omega}_c \times \mathbf{x}$ ,  $\mathbf{u}_c = \text{const}$ ,  $\boldsymbol{\omega}_c = \text{const}$ .

**1.19.** Show that in vector-matrix notation for problems 1.6 and 1.9 the Cauchy relation (1.10), motion equation (1.23) and boundary condition (1.32) can be presented in the form

$$\mathbf{S}(\mathbf{u}) = \mathbf{L}(\nabla) \cdot \mathbf{u},$$

$$\mathbf{L}^*(\nabla) \cdot \mathbf{T} + \rho \mathbf{f} = \rho \ddot{\mathbf{u}},$$

$$\mathbf{p} = \mathbf{L}^*(\mathbf{n}) \cdot \mathbf{T}; \quad \mathbf{p} = \mathbf{p}_\Gamma; \quad \mathbf{x} \in \Gamma_\sigma,$$

where

$$\mathbf{L}^*(\nabla) = \begin{bmatrix} \partial_1 & 0 & 0 & 0 & \partial_3 & \partial_2 \\ 0 & \partial_2 & 0 & \partial_3 & 0 & \partial_1 \\ 0 & 0 & \partial_3 & \partial_2 & \partial_1 & 0 \end{bmatrix}.$$

**1.20.** Prove that for a deformable solid with ordinary conditions for the density, when  $\rho \geq \rho_0 > 0$ , the mass matrix  $\mathbf{M}_{uu}$ , introduced in (1.96), is positive definite.

**1.21.** Prove that if the essential boundary conditions do not allow the motion of a solid as a rigid body, i. e. if  $\boldsymbol{\varepsilon}(\delta \mathbf{u}) \neq 0$  for any feasible displacements  $\delta \mathbf{u} \neq 0$ , compatible with the constraints ( $\delta \mathbf{u} = 0$ ,  $\mathbf{x} \in \Gamma_u$ ), then the stiffness matrix  $\mathbf{K}_{uu}$ , introduced in (1.96), is positive definite.

**1.22.** Show that if the electric potential is defined in at least one point of the boundary of piezoelectric body, then the matrix of dielectric permittivities  $\mathbf{K}_{\varphi\varphi}$ , introduced in (1.96), is positive definite.

**1.23.** Show that in a general case of the stiffness matrix  $\mathbf{K}_{uu}$  the dielectric permittivities  $\mathbf{K}_{\varphi\varphi}$ , introduced in (1.96), are non-negative definite.

**1.24.** Show that the matrix  $\bar{\mathbf{K}}_{uu} = \mathbf{K}_{uu} + \mathbf{K}_{u\varphi} \cdot \mathbf{K}_{\varphi\varphi}^{-1} \cdot \mathbf{K}_{u\varphi}^*$  from (1.102) is symmetric and positive definite if the essential boundary conditions do not allow the motion of a solid as a rigid body (see problem 1.21).

**1.25.** Prove the conclusion of Pierre Curie that the materials with piezoelectric effect cannot have the center of symmetry. In order to do this, consider the inversion transformation  $\mathbf{x} \rightarrow \mathbf{x}' = -\mathbf{x}$  with respect to the center of symmetry and apply the formulas of component conversion for the third rank tensor  $e_{ijk}$  under the transition from initial coordinate system  $Ox_1x_2x_3$  to another Cartesian coordinate system  $Ox'_1x'_2x'_3$ :

$$e'_{ijk} = \alpha_{il}\alpha_{jm}\alpha_{kn}e_{lmn},$$

where  $\alpha_{il}$  are the cosines of the angles between the axes  $x'_i$  and  $x_l$ . Then use the fact that for centrosymmetric materials under the transformations

with respect to the center of symmetry there holds an equality  $e'_{ijk} = e_{ijk}$  and show that in this case all the piezomoduli  $e_{ijk}$  must be equal to zero.

**1.26.** For the statement of transient electroelastic problem in section 1.3.1 initial conditions (1.37) were formulated only for the functions  $\mathbf{u}$  and  $\dot{\mathbf{u}}$ . Are the initial conditions for the electric potential  $\varphi$  required for this problem?

**1.27.** Show that in vector-matrix notation for problems 1.6 and 1.9 with the additionally introduced vector of thermal stress coefficients

$$\mathbf{G}^* = [\gamma_{11}, \gamma_{22}, \gamma_{33}, \gamma_{23}, \gamma_{13}, \gamma_{12}]$$

constitutive relations (1.112), (1.113) can be written in the form:

$$\begin{aligned}\mathbf{T} &= \mathbf{C} \cdot \mathbf{S} - \mathbf{G} \theta, \\ S &= \mathbf{G}^* \cdot \mathbf{S} + \frac{\rho c_\varepsilon}{T_0} \theta.\end{aligned}$$

**1.28.** Obtain an equivalent to (1.112), (1.113) form of the constitutive relations

$$\begin{aligned}\boldsymbol{\varepsilon} &= \mathbf{s} : \boldsymbol{\sigma} + \boldsymbol{\alpha} \theta, \\ S &= \boldsymbol{\alpha} : \boldsymbol{\sigma} + \frac{\rho c_\sigma}{T_0} \theta,\end{aligned}$$

where  $\mathbf{s}$  is the fourth rank semi-symmetric tensor of elastic compliances, inverse to  $\mathbf{c}$  in the sense of problem 1.10;  $\boldsymbol{\alpha}$  is the second rank symmetric tensor of thermal expansion coefficients;  $c_\sigma$  is the specific heat under constant stress. Which value is greater:  $c_\sigma$  or  $c_\varepsilon$  from (1.113)?

**1.29.** Show that with the introduction of vector-matrix notation for problems 1.6, 1.9 and the introduction of the vector of thermal expansion coefficients

$$\mathbf{A}^* = [\alpha_{11}, \alpha_{22}, \alpha_{33}, 2\alpha_{23}, 2\alpha_{13}, 2\alpha_{12}]$$

the constitutive relations in problem 1.28 can be written in the form:

$$\begin{aligned}\mathbf{S} &= \mathbf{s} \cdot \mathbf{T} + \mathbf{A} \cdot \theta, \\ S &= \mathbf{A}^* \cdot \mathbf{T} + \frac{\rho c_\sigma}{T_0} \theta,\end{aligned}$$

where the components of the matrix  $s_{\alpha\beta}$  are related (as in problem 1.17) to the components of the tensor  $s_{ijkl}$  by the law

$$s_{\alpha\beta} = 2^{[\alpha/4]+[\beta/4]} s_{ijkl},$$

where  $[\gamma]$  is the integer part of  $\gamma$ .

**1.30.** Prove that for a thermoelastic body under the ordinary conditions for the density  $\rho \geq \rho_0 > 0$  and specific heat  $c_\varepsilon \geq c_{\varepsilon 0} > 0$ , the heat capacity matrix  $\mathbf{C}_{\theta\theta}$ , introduced in (1.164), is positive definite.

**1.31.** Prove that in a general case the thermal conductivity matrix  $\mathbf{K}_{\theta\theta}$ , introduced in (1.164), is non-negative definite.

**1.32.** Formulate the conditions under which the thermal conductivity matrix  $\mathbf{K}_{\theta\theta}$ , introduced in (1.164), is positive definite (with a proof).

**1.33.** Prove that the matrices  $\mathbf{M}_{pp}$  and  $\mathbf{C}_{pp}$ , introduced in (1.216), are positive definite, and the matrix  $\mathbf{K}_{pp}$  from (1.217) is non-negative definite in a general case.

**1.34.** Formulate the conditions under which the acoustic matrix  $\mathbf{K}_{pp}$ , introduced in (1.217), is positive definite (with a proof).

**1.35.** By analogy to Eqs. (1.220)–(1.222) write the matrix semi-discrete equations for a piezoelectric body  $\Omega_s$ , interacting with an acoustic medium  $\Omega_a$ . Take the vectors  $\{\mathbf{U}, \Phi\}$  as the unknowns for approximations to model the processes in the medium  $\Omega_s$ , and take the vector  $\{\mathbf{P}\}$  as the unknown for approximations in the medium  $\Omega_a$ . As a result, obtain the system of equations with respect to the vectors  $\{\mathbf{U}, \Phi, \mathbf{P}\}$ . When solving the problem, take advantage of the fact that the behaviour of a solid piezoelectric structure is described by Eqs. (1.97), (1.98).

**1.36.** By analogy to Eqs. (1.220), (1.225), (1.226) write the matrix semi-discrete equations for a piezoelectric body  $\Omega_s$ , interacting with an acoustic medium  $\Omega_a$ . Take the vectors  $\{\mathbf{U}, \Phi\}$  as the unknowns for approximations to model the processes in the medium  $\Omega_s$ , and take the vector  $\{\Psi\}$  as the unknown for approximations in the medium  $\Omega_a$ . As a result, obtain the system of equations with respect to the vectors  $\{\mathbf{U}, \Phi, \Psi\}$ . When solving the problem, take advantage of the fact that the behaviour of a solid piezoelectric structure is described by Eqs. (1.97), (1.98).

**1.37.** By analogy to Eqs. (1.220)–(1.222) write the matrix semi-discrete equations for a thermoelastic body  $\Omega_s$ , interacting with an acoustic medium  $\Omega_a$  (without taking into account the temperature field in the acoustic medium). Take the vectors  $\{\mathbf{U}, \mathbf{T}\}$  as the unknowns for approximations to model the processes in the medium  $\Omega_s$ , and take the vector  $\{\mathbf{P}\}$  as the unknown for approximations in the medium  $\Omega_a$ . As a result, obtain the system of equations with respect to the vectors  $\{\mathbf{U}, \mathbf{T}, \mathbf{P}\}$ . When solving the problem, take advantage of the fact that the behaviour of a deformable thermoelastic body  $\Omega_s$  is described by Eqs. (1.165), (1.166).

**1.38.** By analogy to Eqs. (1.220), (1.225), (1.226) write the matrix semi-discrete equations for a thermoelastic body  $\Omega_s$ , interacting with an



acoustic medium  $\Omega_a$  (without taking into account the temperature field in the acoustic medium). Take the vectors  $\{\mathbf{U}, \mathbf{T}\}$  as the unknowns for approximations to model the processes in the medium  $\Omega_s$ , and take the vector  $\{\Psi\}$  as the unknown for approximations in the medium  $\Omega_a$ . As a result, obtain the system of equations with respect to the vectors  $\{\mathbf{U}, \mathbf{T}, \Psi\}$ . When solving the problem, take advantage of the fact that the behaviour of a deformable thermoelastic body  $\Omega_s$  is described by Eqs. (1.165), (1.166).

## Chapter 2

# Finite element method for coupled physico-mechanical problems

### 2.1 General scheme of Galerkin method. Dynamic and static problems

As it was shown in Chapter 1, in order to find weak solutions of coupled problems numerically, we can use the Galerkin method in a semidiscrete (for dynamic problems) setting. In general form all weak settings for the problem from Chapter 1 can be represented in a form

$$\rho_a(\mathbf{w}, \ddot{\mathbf{a}}) + d_a(\mathbf{w}, \dot{\mathbf{a}}) + c_a(\mathbf{w}, \mathbf{a}) = \tilde{L}_a(\mathbf{w}), \quad (2.1)$$

where  $\mathbf{a} = \mathbf{a}(\mathbf{x}, t) \in \mathbb{R}^k$ ,  $\mathbf{a} = \{a_1, a_2, \dots, a_k\}$ ,  $a_i$  are the unknown field functions;  $\mathbf{w} = \mathbf{w}(\mathbf{x}) \in \mathbb{R}^k$ ,  $\mathbf{w} = \{w_1, w_2, \dots, w_k\}$  are the projection functions;  $\rho_a$ ,  $d_a$ ,  $c_a$  are the bilinear forms, that contain integrals over the domain  $\Omega$  from the products  $\mathbf{w} \cdot \mathbf{a}$  and their derivations;  $\tilde{L}_a$  is the linear continuous functional.

For example, let us consider weak statements for three-dimensional problems of electroelasticity (1.83), (1.84), written without the procedures (1.62) for removal of inhomogeneous essential boundary conditions

$$\rho(\mathbf{v}, \ddot{\mathbf{u}}) + d(\mathbf{v}, \dot{\mathbf{u}}) + c(\mathbf{v}, \mathbf{u}) - e(\mathbf{v}, \varphi) = \tilde{L}_u(\mathbf{v}), \quad (2.2)$$

$$e(\mathbf{u}, \chi) + \epsilon(\chi, \varphi) = \tilde{L}_\varphi(\chi). \quad (2.3)$$

As in these equations  $\mathbf{v}$  and  $\chi$  are arbitrary functions of the required smoothness, then relations (2.2), (2.3) are equivalent to its sum. It is obvious that the termwise sum (2.2) and (2.3) can be written in the form (2.1) at  $k = 4$ ;  $\mathbf{a} = \{\mathbf{u}, \varphi\}$ ;  $a_1 = u_1 = u_x$ ;  $a_2 = u_2 = u_y$ ;  $a_3 = u_3 = u_z$ ;  $a_4 = \varphi$ ;  $\mathbf{w} = \{\mathbf{v}, \chi\}$ ;  $\rho_a(\mathbf{w}, \mathbf{a}) = \rho(\mathbf{v}, \mathbf{u})$ ;  $d_a(\mathbf{w}, \mathbf{a}) = d(\mathbf{v}, \mathbf{u})$ ;  $c_a(\mathbf{w}, \mathbf{a}) = c(\mathbf{v}, \mathbf{u}) - e(\mathbf{v}, \varphi) + e(\mathbf{u}, \chi) + \epsilon(\chi, \varphi)$ ;  $\tilde{L}_a(\mathbf{w}) = \tilde{L}_u(\mathbf{v}) + \tilde{L}_\varphi(\chi)$ .

Similarly, the weak statement for the thermoelasticity problem based on relations (1.137), (1.138), can be represented in the form (2.1) at  $k = 4$ ;  $\mathbf{a} = \{\mathbf{u}, \theta\}$ ;  $a_1 = u_1 = u_x$ ;  $a_2 = u_2 = u_y$ ;  $a_3 = u_3 = u_z$ ;  $a_4 = \theta$ ;  $\mathbf{w} = \{\mathbf{v}, \eta\}$ ;  $\rho_a(\mathbf{w}, \mathbf{a}) = \rho(\mathbf{v}, \mathbf{u})$ ;  $d_a(\mathbf{w}, \mathbf{a}) = T_0\gamma(\mathbf{u}, \eta) + s(\eta, \theta)$ ;  $c_a(\mathbf{w}, \mathbf{a}) = c(\mathbf{v}, \mathbf{u}) - \gamma(\mathbf{v}, \theta) + k(\eta, \theta)$ ;  $\tilde{L}_a(\mathbf{w}) = \tilde{L}_u(\mathbf{v}) + \tilde{L}_\theta(\eta)$ .

In order to remove the inhomogeneity of the essential boundary conditions, one can search the solution in the form

$$\mathbf{a} = \mathbf{a}_0 + \mathbf{a}_n, \quad (2.4)$$

where  $\mathbf{a}_0 = \{a_{01}, a_{02}, \dots, a_{0k}\}$  is an unknown function that satisfies homogeneous essential boundary conditions;  $\mathbf{a}_n = \{a_{n1}, a_{n2}, \dots, a_{nk}\}$  is the known (specially selected) function for which the same inhomogeneous essential boundary conditions as for the function  $\mathbf{a}$  are satisfied.

From (2.1), (2.4) it is obvious that after finding  $\mathbf{a}_0$  we have the relation

$$\rho_a(\mathbf{w}, \ddot{\mathbf{a}}_0) + d_a(\mathbf{w}, \dot{\mathbf{a}}_0) + c_a(\mathbf{w}, \mathbf{a}_0) = L_a(\mathbf{w}), \quad (2.5)$$

$$L_a(\mathbf{w}) = \tilde{L}_u(\mathbf{v}) - \rho_a(\mathbf{w}, \ddot{\mathbf{a}}_n) - d_a(\mathbf{w}, \dot{\mathbf{a}}_n) - c_a(\mathbf{w}, \mathbf{a}_n). \quad (2.6)$$

For the problems of electroelasticity Eq. (2.5) should be satisfied for  $\forall \mathbf{w} \in V$ ;  $V = \{H_u^1, H_\varphi^1\}$ ; and the unknown part of the solution  $\mathbf{a}_0$  should belong to the space  $Q = \{Q_u, Q_\varphi\}$ . Similar functional spaces can be also introduced for other coupled problems from Chapter 1.

The classical version of the Galerkin method assumes the choice of the finite by  $\mathbf{x}$  spaces  $V_h \subset V$ ,  $Q_h = L^2(0, T; V_h)$ ,  $Q_h \subset Q$  and the search for the approximate solution  $\mathbf{a}_{h0} \approx \mathbf{a}_0$ ,  $\mathbf{a}_{h0} \in Q_h$ , which satisfies (2.5) at  $\forall \mathbf{w} \in V_h$ .

In the space  $V_h$  an arbitrary vector-function  $\mathbf{w} = \{w_1, w_2, \dots, w_k\}$  can be expanded in the basis, and for an individual component  $w_i$  this expansion can be written in the form

$$w_i = \sum_{j=1}^{n_i} N_{aij}(\mathbf{x}) W_{ij} = \mathbf{N}_{ai}^* \cdot \mathbf{W}_i, \quad (2.7)$$

where  $N_{aij}(\mathbf{x})$  are the basis functions;  $W_{ij}$  are the coefficients at the basis functions;  $\mathbf{N}_{ai}^* = [N_{ai1}, N_{ai2}, \dots, N_{ain_i}]$ ;  $\mathbf{W}_i = \{W_{i1}, W_{i2}, \dots, W_{in_i}\}$ ; and there is no summation over  $i$  in (2.7).

As it can be seen, the dimension of the basis of the space  $V_h$  in the adopted notations is equal to  $n_{V_h} = n_1 + n_2 + \dots + n_k$ . The components  $a_{h0i}$  of the approximate solution vector  $\mathbf{a}_{h0}$  can be then searched in the

form

$$a_{h0i} = \sum_{j=1}^{n_i} N_{aij}(\mathbf{x}) A_{ij}(t) = \mathbf{N}_{ai}^* \cdot \mathbf{A}_i(t), \quad (2.8)$$

where  $\mathbf{A}_i(t) = \{A_{i1}(t), A_{i2}(t), \dots, A_{in_i}(t)\}$ ;  $A_{ij}(t)$  are the unknown scalar functions of approximation.

If we compose two single vectors  $\mathbf{W} = \{\mathbf{W}_1, \mathbf{W}_2, \dots, \mathbf{W}_k\}$ ;  $\mathbf{A}(t) = \{\mathbf{A}_1(t), \mathbf{A}_2(t), \dots, \mathbf{A}_k(t)\}$  out of the vectors  $\mathbf{W}_i$ ;  $\mathbf{A}_i(t)$ , then from (2.7), (2.8) we can obtain general representations for  $\mathbf{w}$  and  $\mathbf{a}_{h0}$

$$\mathbf{w} = \mathbf{N}_a^* \cdot \mathbf{W}, \quad \mathbf{a}_{h0} = \mathbf{N}_a^* \cdot \mathbf{A}(t), \quad (2.9)$$

where  $i$ -th row of the matrix of the basis functions  $\mathbf{N}_a^*$  has the following block structure:  $[\mathbf{0}, \dots, \mathbf{0}, \mathbf{N}_{ai}^*, \mathbf{0}, \dots, \mathbf{0}]$ . We should note here that the form of the matrix  $\mathbf{N}_a^*$  depends on the chosen way of collecting the vectors  $\mathbf{W}$  and  $\mathbf{A}$  from  $\mathbf{W}_i$  and  $\mathbf{A}_i$ .

Let us substitute (2.9) into (2.5) and take into account that in the integral forms  $\rho_a$ ,  $d_a$ ,  $c_a$  and in the linear functional  $L_a$  the values  $\mathbf{W}$  and  $\mathbf{A}(t)$  do not depend on the spacial variables  $\mathbf{x}$ , and, therefore, can not be moved outside the integral signs. As a result, we get an equation in the matrix form

$$\mathbf{W}^* \cdot (\mathbf{M} \cdot \ddot{\mathbf{A}} + \mathbf{C} \cdot \dot{\mathbf{A}} + \mathbf{K} \cdot \mathbf{A}) = \mathbf{W}^* \cdot \mathbf{F} \quad (2.10)$$

with the matrices  $\mathbf{M}$ ,  $\mathbf{C}$ ,  $\mathbf{K}$  and the vector  $\mathbf{F}$ , determined from  $\rho_a$ ,  $d_a$ ,  $c_a$  and  $L_a$ , respectively.

As  $\mathbf{W}$  is an arbitrary vector from  $V_h$ , then from (2.10) we have the resulting equation of motion

$$\mathbf{M} \cdot \ddot{\mathbf{A}} + \mathbf{C} \cdot \dot{\mathbf{A}} + \mathbf{K} \cdot \mathbf{A} = \mathbf{F}. \quad (2.11)$$

If we consider a *transient problem*, then it is necessary to add to (2.11) the initial conditions

$$\mathbf{A}(0) = \mathbf{A}_{sn}, \quad \dot{\mathbf{A}}(0) = \mathbf{V}_{sn} \quad (2.12)$$

with the known initial values  $\mathbf{A}_{sn}$ ,  $\mathbf{V}_{sn}$ , that are easy to find from the corresponding continuous initial conditions. Note that if for individual blocks  $\mathbf{A}_i$  in Eq. (2.11) the second time derivatives are absent, then for these blocks we do not set the initial conditions for their first derivatives by  $t$ .

Thus, the solutions of *transient problems* by the Galerkin method are reduced to the Cauchy problem (2.11), (2.12) for the system of ordinary

differential equations with respect to time. (In (2.11) there are  $n_{Vh}$  scalar equations with respect to the components  $A_{ij}(t)$ .)

We note that there are *three major types of dynamic problems: transient problems, problems of steady-state oscillations and eigenvalue problems.*

Transient problems (2.11), (2.12) usually are the most difficult and time-consuming. If all external influences (including essential boundary conditions) change according to the harmonic law with the same frequency  $f = \omega/2\pi$  so that  $\mathbf{F} = \tilde{\mathbf{F}}e^{i\omega t}$ , and the solution becomes steady in time by the same law  $\mathbf{A} = \tilde{\mathbf{A}}e^{i\omega t}$ , then we can omit the initial conditions and consider *the problem of steady-state oscillations.* It is obvious that the substitution of

$$\mathbf{A} = \tilde{\mathbf{A}}e^{i\omega t}, \quad \mathbf{F} = \tilde{\mathbf{F}}e^{i\omega t} \quad (2.13)$$

into (2.11) gives

$$(-\omega^2\mathbf{M} + i\omega\mathbf{C} + \mathbf{K}) \cdot \tilde{\mathbf{A}} = \tilde{\mathbf{F}}, \quad (2.14)$$

where  $\tilde{\mathbf{A}}$ ,  $\tilde{\mathbf{F}}$  are the complex amplitudes of the solution vectors and the external influences.

In the linear problem Eq. (2.14) represents a system of linear algebraic equations with complex arithmetic with respect to the complex vectors of unknowns  $\tilde{\mathbf{A}}$ . Note that even if there is no attenuation in the system, i. e.  $\mathbf{C} = 0$ , then the vector  $\tilde{\mathbf{F}}$  can be complex and, consequently, the vector  $\tilde{\mathbf{A}}$  will be complex.

Usually it is necessary to solve the problem of steady-state oscillations (2.14) several times, changing the frequency  $\omega$  in a certain interval  $[\omega_b, \omega_e]$ . In this case the values of interest are some characteristics of solution  $\tilde{\mathbf{A}}$  that depend on the frequency  $\omega$  (frequency characteristics). Of particular importance are the maximums of these characteristics and the frequencies at which the maximums are reached. These frequencies are called the *resonance frequencies.* In order to find feasible resonance frequencies, we can solve a separate *eigenvalue problem* when in (2.14)  $\tilde{\mathbf{F}} = 0$  and usually (but not always)  $\mathbf{C} = 0$ .

If  $\mathbf{C} = 0$ ,  $\tilde{\mathbf{F}} = 0$ , then (2.14) takes the form

$$\omega^2\mathbf{M} \cdot \tilde{\mathbf{A}} = \mathbf{K} \cdot \tilde{\mathbf{A}}. \quad (2.15)$$

In (2.15) the unknowns are the frequency  $\omega$  and the vector  $\tilde{\mathbf{A}}$ , where nontrivial solutions  $\tilde{\mathbf{A}} \neq 0$  are of interest. In this case  $\omega$  is called a *natural frequency* or *eigenfrequency*, and  $\tilde{\mathbf{A}}$  is called an *eigenvector* or *oscillation mode.* In numerical analysis problem (2.15) is also called a *generalized eigenvalue problem*, and the documentation on the finite element software refers to it as *modal analysis.*

The problem considered less often is an eigenvalue problem for a matrix bundle

$$(-\omega^2 \mathbf{M} + i\omega \mathbf{C} + \mathbf{K}) \cdot \tilde{\mathbf{A}} = 0, \quad (2.16)$$

where it is also necessary to find the pairs  $\{\omega, \tilde{\mathbf{A}}\}$ , at which (2.16) is satisfied, and  $\tilde{\mathbf{A}} \neq 0$ .

Finally, apart from dynamic problems we can also consider *static* or *stationary problems*, when in (2.11)  $\mathbf{A}$  and  $\mathbf{F}$  are not time-dependent, and in linear problems Eq. (2.11) is reduced to a system of linear algebraic equations

$$\mathbf{K} \cdot \mathbf{A} = \mathbf{F}. \quad (2.17)$$

As we have shown, the Galerkin method reduces dynamic and static problems to standard problems of numerical analysis, for solution of which a number of well-developed specialized numerical methods is available.

## 2.2 Finite element method as a version of Galerkin method. Main ideas of FEM

The main problem of practical application for the Galerkin method is the problem of finding the spaces  $V_h$  and their bases, suitable for the domains of fairly arbitrary shape. The finite element method (FEM) is a version of the Galerkin method where this problem is solved by dividing the domain  $\Omega$  (specifically,  $\Omega_h \subset \Omega$ ) into subdomains  $\Omega^{em}$  of standard shapes with simple basis functions.

As it has turned out, in the framework of FEM it is possible to implement a range of techniques, that allow to apply and implement them in programs for a variety of problems of mathematical physics. The procedures of *assembling and accounting for the essential boundary conditions* and *calculating the element matrices and vectors by numerical integration* can be attributed to these approaches. All this led to a wide application of FEM and its effective implementation in numerous computational complexes of both general and specialized purpose.

This book does not claim for the complete presentation of FEM. A reader is advised to consult numerous monographs where FEM is presented from the mathematical viewpoint [2, 8, 32], from the viewpoint of specific applications [27] and with specific attention to the program implementation. Often this division is difficult to make [3, 23, 33, 34, 35, 36, 37]. A range of monographs are oriented to the application of FEM for solving coupled problems of mechanics [14, 17]. Finally, very

useful information is contained in the documentation on the finite element software [1].

Now we pass to a brief description of FEM for classic Lagrangian finite elements in  $\mathbb{R}^3$ . Let  $\Omega_h \subset \Omega$ , and there is a division of the domain  $\Omega_h$  into a set of subdomains of a simple shape, the finite elements  $\Omega^{em}$ , i. e.  $\Omega_h = \cup_{m=1}^{n_{el}} \Omega^{em}$ , where  $m$  is the element number,  $n_{el}$  is the general number of subdomains  $\Omega^{em}$ .

We will consider weak statements of the problems on  $\Omega_h$ , changing the integration domains in them from  $\Omega$  to  $\Omega_h$  and moving the boundary conditions to the boundary  $\Gamma_h = \partial\Omega_h$  and its parts with various types of conditions ( $\Gamma_{hu}$ ,  $\Gamma_{h\sigma}$ , etc.)

The structure of the finite element mesh comprises finite elements and their *nodes*. A separate node is characterized by its number  $j$  and its coordinates  $\mathbf{x}_j = \{x_j, y_j, z_j\}$ . Each finite element  $\Omega^{em}$  has its own set of nodes  $\{\mathbf{x}_{r_1}^{em}, \mathbf{x}_{r_2}^{em}, \dots, \mathbf{x}_{r_n}^{em}\}$ ;  $\mathbf{x}_{r_s}^{em} \in \Omega^{em}$ ;  $s = 1, 2, \dots, n = n^{em}$ ;  $n^{em}$  is the number of element nodes.

For the simplest elements the nodes are the vertices of the geometrical figures  $\Omega^{em}$ . In more complex elements the vertices can lie on the edges and inside the domains  $\Omega^{em}$ . For example, in the elements with quadratic basis functions the nodes are located both in the vertices and usually in the middle of the edges of the figures  $\Omega^{em}$ .

Fig. 2.1 and 2.2 show 2D finite element meshes consisting of triangular and quadrilateral elements. Both variants of the mesh are built for the same solid model with the same parameters of finite element mesh. Therefore, almost all the domains  $\Omega^{em}$  and their numbers in both figures on the left coincide. Fig. 2.1 shows simple elements without midside nodes and Fig. 2.2 shows more complex elements with the nodes in the vertices and in the middle of the edges. As it can be seen from Fig. 2.2(b), the elements with middle nodes can have curvilinear sides, which allows to approximate the curved boundaries more precisely, compared to the elements with the nodes located only in the element vertices.

We will associate each node  $\mathbf{x}_j$  with its *basis function*  $N_j(\mathbf{x})$ , which has a range of important interrelated properties.

1) *Function  $N_j(\mathbf{x})$  is identically equal to zero on all elements  $\Omega^{el}$ , that do not include the node  $\mathbf{x}_j$  (both inside and on the boundaries  $\Omega^{el}$ ).*

2) Usually it is assumed that

$$N_j(\mathbf{x}_k) = \delta_{jk}, \quad (2.18)$$

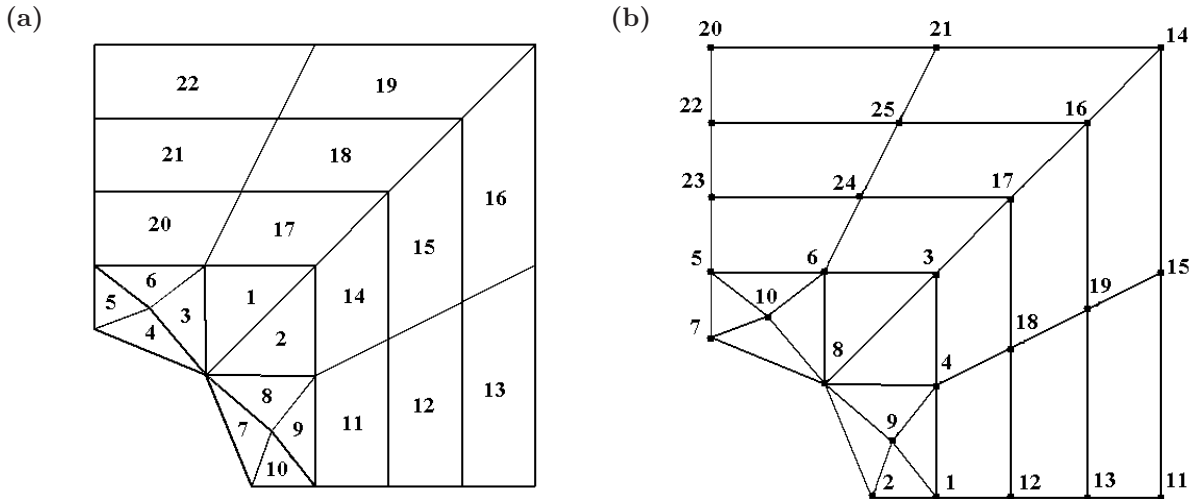


Figure 2.1. Example of 2D mesh with elements without midside nodes:  
 (a) with element numbering; (b) with node numbering

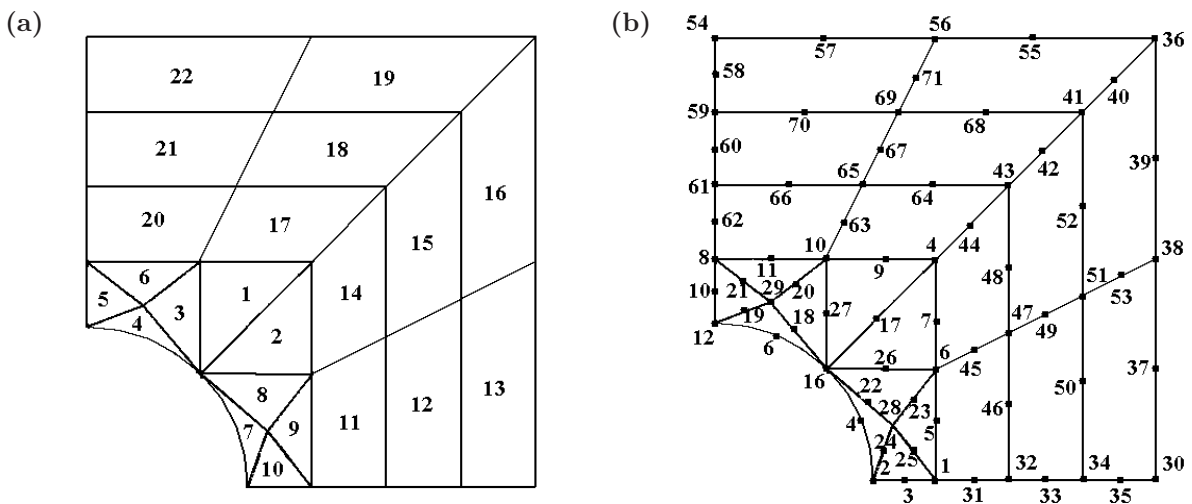


Figure 2.2. Example of 2D mesh with elements with midside nodes:  
 (a) with element numbering; (b) with node numbering

i. e. the basis function  $N_j(\mathbf{x})$  equals one in the node  $\mathbf{x}_j$  and zero in all other nodes.

3) The basis functions  $N_j(\mathbf{x})$ , probably together with parametric mappings (look further section 2.3), are defined by relatively simple polynomial expressions of low degree.

4) The use of consistent finite element meshes, when the adjacent elements  $\Omega^{em}$  have common nodes and sides and border each other without gaps and overlapping, ensures the  $C^0$ -smoothness of the approximated functions in  $\Omega_h$  for the elements with the same type of approximation on



the sides and/or edges and so called *completeness condition holds*:

$$\sum_{j=1}^{n_{nd}} N_j(\mathbf{x}) = 1, \quad \forall \mathbf{x} \in \Omega_h, \quad (2.19)$$

where  $n_{nd}$  is the total number of nodes.

These features of finite element meshes and bases determine a range of good computational properties of FEM.

As separate basis functions  $N_j(\mathbf{x})$  have the supports (i. e. the closures of the sets where  $N_j(\mathbf{x})$  are not equal to zero) related to a small number of finite elements, then the *finite element matrices*  $\mathbf{K}$ ,  $\mathbf{C}$  and  $\mathbf{M}$  are very *sparse*.

Fig. 2.3 shows the basis function  $N_9(\mathbf{x})$  for a finite element mesh identical to the one shown above in Fig. 2.1. Here the finite elements, where this function equals zero, are darkened. As it can be seen, only for four elements (with the numbers 7–10) this function is not equal to zero, and these elements are related to five nodes (with the numbers 1, 2, 4, 8, 9). Let us consider an example of a problem with one scalar unknown field function in the matrix  $\mathbf{K}$  of the size  $25 \times 25$  ( $n_{nd} = 25$  is the total number of nodes in the model). For such matrix in the ninth row only the elements  $K_{91}$ ,  $K_{92}$ ,  $K_{94}$ ,  $K_{98}$  and  $K_{99}$  will be not equal to zero, and in the ninth column only the elements  $K_{19}$ ,  $K_{29}$ ,  $K_{49}$ ,  $K_{89}$  and  $K_{99}$  will be not equal to zero. This holds, because the products of the functions  $N_9(\mathbf{x})$  on  $N_l(\mathbf{x})$  at  $l \neq \{1, 2, 4, 8, 9\}$  and the products of their derivatives are identically equal to zero on  $\Omega_h$ . Consequently, the integrals from these products that determine the components of the matrix  $\mathbf{K}$  will also be equal to zero. A similar result will be valid here for the matrices  $\mathbf{C}$  and  $\mathbf{M}$ .

From the property (2.18) we can determine the physical meaning of the unknowns in the vector  $\mathbf{A}$ . Having written the representation (2.8) for the

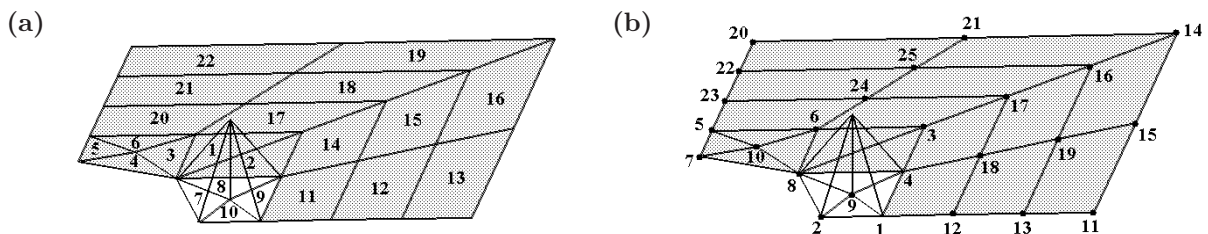


**Figure 2.3.** Basis function for triangular elements without midside nodes:  
(a) with element numbering; (b) with node numbering

component  $a_{h0i}$  of the approximate solution in the node  $\mathbf{x}_l$ , we get

$$a_{h0i}(\mathbf{x}_l, t) = \sum_{j=1}^{n_i} N_{aij}(\mathbf{x}_l) A_{ij}(t) = \sum_{j=1}^{n_i} \delta_{jl} A_{ij}(t) = A_{il}(t). \quad (2.20)$$

Here it is taken into account that the basis functions  $N_{aij}(\mathbf{x})$  for various components of the considered problems in FEM can be taken the same, i. e.  $N_{aij}(\mathbf{x}) = N_j(\mathbf{x})$ .

Formula (2.20) shows that *the component  $A_{il}$  of the vector  $\mathbf{A}$  is the value of an unknown function  $a_{h0i}$  (i. e. the displacements  $u_x, u_u, u_z$ , the potential  $\varphi$ , etc.) in the node  $\mathbf{x}_l$ .*

As it can be seen from (2.8), (2.20), the field function  $a_{h0i}(\mathbf{x}, t)$  in the domain  $\Omega_h$  is determined by FEM in the form

$$a_{h0i}(\mathbf{x}, t) = \sum_{j=1}^{n_i} N_j(\mathbf{x}) A_{ij}(t) = \sum_{j=1}^{n_i} N_j(\mathbf{x}) a_{h0i}(\mathbf{x}_j, t). \quad (2.21)$$

Thus, the function  $a_{h0i}(\mathbf{x}, t)$  in  $\Omega_h$  will be known as soon as its values in the nodes of the finite element mesh are calculated. In connection to this the values  $A_{ij}(t) = a_{h0i}(\mathbf{x}_j, t)$  are called the *nodal degrees of freedom* (degrees of freedom in the node  $\mathbf{x}_j$ ).

Let us note that in FEM the vector of unknowns  $\mathbf{A}$  is easy to collect by nodal degrees of freedom, and this approach differs from the approach explained in section 2.1 after (2.8). Namely, we form the *vector of nodal degrees of freedom*  $\mathbf{A}_j^{nd} = \{A_{1j}, A_{2j}, \dots, A_{kj}\}$  of the size  $k$ ; and from the vectors  $\mathbf{A}_j^{nd}$  we form a *global vector of nodal degrees of freedom*  $\mathbf{A} = \{\mathbf{A}_1^{nd}, \mathbf{A}_2^{nd}, \dots, \mathbf{A}_j^{nd}\}$ . Therefore, with the  $j$ -th node number in the global numbering we connect  $k$  degrees of freedom with the numbers  $\{k(j-1)+1, k(j-1)+2, \dots, k(j-1)+k = kj\}$ .

As  $\int_{\Omega_h} (\dots) d\Omega = \sum_m \int_{\Omega^{em}} (\dots) d\Omega$ , and for every finite element there is a small number  $n^{em}$  of nodes and nonzero basis functions, then the finite element matrices  $\mathbf{K}, \mathbf{C}, \mathbf{M}$  and some constituents of the vector  $\mathbf{F}$  can be gathered from the element matrices  $\mathbf{K}^{em}, \mathbf{C}^{em}, \mathbf{M}^{em}$  and the vectors  $\mathbf{F}_a^{em}$  of small sizes. Such approach to form the global finite element objects from the element objects is called an *assembling procedure*.

Let us consider an element  $\Omega^{em}$  with the nodes  $\mathbf{x}_{r_s}^{em}$ , where  $r_s = r_s^{em}$  are the global node numbers,  $s = 1, 2, \dots, n^{em}$  are the local numbers. Thus, we have a to-one correspondence among global and local node numbers:  $f^{em}(\mathbf{x}_{r_s}^{em}) = s$ .

Let  $J_L^{em}$  be a set of local numbers of the degrees of freedom of the dimension  $n_d^{em} = kn^{em}$ , consisting of the blocks  $\{k(s-1)+1, k(s-1)+2, \dots, k(s-1)+k=ks\}$ ,  $s = 1, 2, \dots, n^{em}$ .

In the general (global) numbering these degrees of freedom have certain numbers from the set  $J_G^{em}$ , that includes the corresponding blocks  $\{k(r_s^{em}-1)+1, k(r_s^{em}-1)+2, \dots, k(r_s^{em}-1)+k=kr_s^{em}\}$ .

Using the mapping  $f^{em}(\mathbf{x}_{r_s^{em}}) = s$ , we can build a one mapping  $g^{em}: J_G^{em} \rightarrow J_L^{em}$ , that transforms for the element  $\Omega^{em}$  the global number  $p$  of the degree of freedom from  $J_G^{em}$  into the local number  $i$  from  $J_L^{em}$ :

$$g^{em}(p) = i; \quad p \in J_G^{em}, \quad i \in J_L^{em}; \quad p = r_s. \quad (2.22)$$

The element matrices  $\mathbf{K}^{em}$ ,  $\mathbf{C}^{em}$ ,  $\mathbf{M}^{em}$  of the size  $n_d^{em} \times n_d^{em}$  and the element vector of the active external influences  $\mathbf{F}_a^{em}$  are determined by the formulas similar to those which were used to find the components of the global matrices  $\mathbf{K}$ ,  $\mathbf{C}$ ,  $\mathbf{M}$  and the vector  $\mathbf{F}$ . The only difference is that the volume integrals are now calculated over the domain  $\Omega^{em}$ , and the surface integrals are calculated over the parts of the boundary  $\Gamma^{em} = \partial\Omega^{em}$ . Besides, only the basis functions  $N_j(\mathbf{x})$  for  $k$  degrees of freedom of the element node  $j = r_s^{em}$ ,  $s = 1, 2, \dots, n^{em}$  take part in the calculation.

Then with account for the adopted numbering of global and element degrees of freedom the extended element matrix  $\mathbf{K}_G^{em}$  can be determined by the formula

$$K_{Gpq}^{em} = \begin{cases} K_{ij}^{em}; & i = g^{em}(p), \quad j = g^{em}(q); \quad (p \in J_G^{em}) \wedge (q \in J_G^{em}), \\ 0; & (p \notin J_G^{em}) \vee (q \notin J_G^{em}). \end{cases} \quad (2.23)$$

In a similar way we can set the extended matrices  $\mathbf{C}_G^{em}$ ,  $\mathbf{M}_G^{em}$  and the extended vector of active external influences  $\mathbf{F}_{Ga}^{em}$ .

A simple analysis show that

$$\mathbf{K} = \sum_{m=1}^{n_{el}} \mathbf{K}_G^{em}, \quad \mathbf{C} = \sum_{m=1}^{n_{el}} \mathbf{C}_G^{em}, \quad \mathbf{M} = \sum_{m=1}^{n_{el}} \mathbf{M}_G^{em}, \quad \mathbf{F} = \sum_{m=1}^{n_{el}} \mathbf{F}_{Ga}^{em}. \quad (2.24)$$

Formulas (2.24) that determine the assembling process in FEM are usually written in the form

$$\mathbf{K} = \sum_{m=1}^{n_{el}} {}^a \mathbf{K}^{em} = \sum_{m=1}^{n_{el}} \mathbf{K}_G^{em}, \quad (2.25)$$

and similarly for  $\mathbf{C}$ ,  $\mathbf{M}$  and  $\mathbf{F}$ .

In computational practice the extended element objects  $\mathbf{K}_G^{em}$ ,  $\mathbf{C}_G^{em}$ ,  $\mathbf{M}_G^{em}$  and  $\mathbf{F}_{Ga}^{em}$  usually are not constructed explicitly. Instead we can organize a loop over the element numbers where the process (2.25) of constructing global objects out of element objects is implemented with account for the location of the components of the element matrices and vectors under their summation into global objects by (2.22), (2.23). This assembling process is effectively implemented in computer programs for any types of finite elements, including the elements with various numbers of degrees of freedom in the nodes.

In FEM in the frameworks of global strategy of finite element mesh construction it is convenient to set both the approximate unknown functions  $\mathbf{a}_{h0}$  and the approximations of the specially selected function  $\mathbf{a}_{hn}$ , which satisfy inhomogeneous essential boundary conditions. Indeed, let us write an approximation for (2.4) and the second formula from (2.9), additionally marking  $\mathbf{N}_a(\mathbf{x})$  and  $\mathbf{A}$  by the subscript “0”:

$$\mathbf{a}_h = \mathbf{a}_{h0} + \mathbf{a}_{hn}, \quad \mathbf{a}_{h0} = \mathbf{N}_{a0}^* \cdot \mathbf{A}_0(t). \quad (2.26)$$

It is obvious that a complete finite element mesh in  $\bar{\Omega}_h$  contains both the nodes for  $\mathbf{a}_{h0}$  and the nodes for  $\mathbf{a}_{hn}$ . Using one-type basis functions for all nodes we can adopt a finite element approximation for  $\mathbf{a}_{hn}$

$$\mathbf{a}_{hn} = \mathbf{N}_{an}^* \cdot \mathbf{A}_n(t). \quad (2.27)$$

Then

$$\mathbf{a}_h = \mathbf{N}_{a0}^* \cdot \mathbf{A}_0(t) + \mathbf{N}_{an}^* \cdot \mathbf{A}_n(t) = \tilde{\mathbf{N}}_a^* \cdot \tilde{\mathbf{A}}(t), \quad (2.28)$$

$$\tilde{\mathbf{N}}_a^* = \{\mathbf{N}_{a0}^*, \mathbf{N}_{an}^*\}, \quad \tilde{\mathbf{A}}(t) = \{\mathbf{A}_0(t), \mathbf{A}_n(t)\}. \quad (2.29)$$

Here the components of the vector  $\mathbf{A}_n$  are known from inhomogeneous essential boundary conditions for  $\mathbf{a}_{hn}$  or  $\mathbf{a}_h$ , i. e. we can write

$$\mathbf{A}_n(t) = \mathbf{A}_\Gamma(t), \quad (2.30)$$

where  $\mathbf{A}_\Gamma(t)$  is the known vector of the values for the components of the field functions  $a_i$  in the corresponding nodes of the parts with essential boundary conditions.

Having analyzed the transformation of weak statements (2.2), (2.3) into (2.5), (2.6), we can note the following. If we formulate the finite element equations of motion for the whole ensemble of the nodes and finite elements in  $\bar{\Omega}_h$  without account for the essential boundary conditions, then we will have

$$\tilde{\mathbf{M}} \cdot \ddot{\tilde{\mathbf{A}}} + \tilde{\mathbf{C}} \cdot \dot{\tilde{\mathbf{A}}} + \tilde{\mathbf{K}} \cdot \tilde{\mathbf{A}} = \tilde{\mathbf{F}}, \quad (2.31)$$

$$\tilde{\mathbf{M}} = \begin{bmatrix} \mathbf{M}_{00} & \mathbf{M}_{0n} \\ \mathbf{M}_{0n}^* & \mathbf{M}_{nn} \end{bmatrix}, \quad \tilde{\mathbf{C}} = \begin{bmatrix} \mathbf{C}_{00} & \mathbf{C}_{0n} \\ \mathbf{C}_{0n}^* & \mathbf{C}_{nn} \end{bmatrix}, \quad \tilde{\mathbf{K}} = \begin{bmatrix} \mathbf{K}_{00} & \mathbf{K}_{0n} \\ \mathbf{K}_{0n}^* & \mathbf{K}_{nn} \end{bmatrix}, \quad (2.32)$$

$$\tilde{\mathbf{A}} = \begin{Bmatrix} \mathbf{A}_0 \\ \mathbf{A}_n \end{Bmatrix}, \quad \tilde{\mathbf{F}} = \begin{Bmatrix} \mathbf{F}_0 \\ \mathbf{F}_n \end{Bmatrix}. \quad (2.33)$$

In (2.31)–(2.33) the vector  $\mathbf{A}_0$  is unknown and the vector  $\mathbf{A}_n$  is known by (2.30). But from (2.31)–(2.33) and (2.30) it is easy to obtain an equation only for an unknown vector  $\mathbf{A}_0$

$$\mathbf{M}_{00} \cdot \ddot{\mathbf{A}}_0 + \mathbf{C}_{00} \cdot \dot{\mathbf{A}}_0 + \mathbf{K}_{00} \cdot \mathbf{A}_0 = \mathbf{F}_0 - \mathbf{M}_{0n} \cdot \ddot{\mathbf{A}}_\Gamma - \mathbf{C}_{0n} \cdot \dot{\mathbf{A}}_\Gamma - \mathbf{K}_{0n} \cdot \mathbf{A}_\Gamma. \quad (2.34)$$

Upon the change of notation, Eq. (2.34) coincides with the previously used Eq. (2.11) for the approximation (2.27) for  $\mathbf{a}_{hn}$ . Certain inconvenience of the transition from (2.31) to (2.34) consists in the change of the order and structure of the finite element matrices and vectors (under the transition from  $\tilde{\mathbf{M}}$  to  $\mathbf{M}_{00}$ , etc.)

One version of the *method of taking into account the essential boundary conditions*, that maintains the orders of the global finite element objects, consists only in their transformation which leads to the following resolving equations

$$\tilde{\mathbf{M}}_t \cdot \ddot{\tilde{\mathbf{A}}} + \tilde{\mathbf{C}}_t \cdot \dot{\tilde{\mathbf{A}}} + \tilde{\mathbf{K}}_t \cdot \tilde{\mathbf{A}} = \tilde{\mathbf{F}}_t, \quad (2.35)$$

$$\tilde{\mathbf{M}}_t = \begin{bmatrix} \mathbf{M}_{00} & \mathbf{0} \\ \mathbf{0} & \mathbf{0} \end{bmatrix}, \quad \tilde{\mathbf{C}}_t = \begin{bmatrix} \mathbf{C}_{00} & \mathbf{0} \\ \mathbf{0} & \mathbf{0} \end{bmatrix}, \quad \tilde{\mathbf{K}}_t = \begin{bmatrix} \mathbf{K}_{00} & \mathbf{0} \\ \mathbf{0} & \mathbf{K}_{nn}^d \end{bmatrix}, \quad (2.36)$$

$$\tilde{\mathbf{A}} = \begin{Bmatrix} \mathbf{A}_0 \\ \mathbf{A}_n \end{Bmatrix}, \quad \tilde{\mathbf{F}}_t = \begin{Bmatrix} \mathbf{F}_0 - \mathbf{M}_{0n} \cdot \ddot{\mathbf{A}}_\Gamma - \mathbf{C}_{0n} \cdot \dot{\mathbf{A}}_\Gamma - \mathbf{K}_{0n} \cdot \mathbf{A}_\Gamma \\ \mathbf{K}_{nn}^d \cdot \mathbf{A}_\Gamma \end{Bmatrix}, \quad (2.37)$$

where  $\mathbf{K}_{nn}^d$  is a diagonal block composed of the corresponding diagonal components of the matrix  $\mathbf{K}_{nn}$ .

It is obvious that formulas (2.35)–(2.37) are equivalent to (2.34), (2.30).

The second way (2.35)–(2.37) to take into account the essential boundary conditions is easier for the computer implementation than the first one ((2.34), (2.30)), as for this method it is not necessary to change the sizes of global finite element objects.

Thus, different ways of taking into account the essential boundary conditions can be suggested, in which firstly the finite element mesh is built without account for these boundary conditions, secondly the general FEM matrices and the main parts of the right-hand side vector are formed, and after that the procedure of taking account the essential boundary conditions is reduced to the transformation of the constructed matrices

and vectors. Such methods enable to automate the processes of taking into account the essential boundary conditions in the framework of the general concepts of FEM.

Concluding the description of the computational properties of FEM we note that the use of simple basis functions permits to calculate the element matrices  $\mathbf{K}^{em}$ ,  $\mathbf{C}^{em}$ ,  $\mathbf{M}^{em}$  and vectors  $\mathbf{F}_a^{em}$  fast enough and with high degree of accuracy by quadrature formulas of low order.

Besides, the resulting FEM global matrices will be, as a rule, well-conditioned and their condition numbers will not increase greatly with the increase of the order. It is also can be noted that these matrices are sparse and in many problems they are also symmetric and positive definite. Therefore in order to solve finite element problems we can effectively use powerful modern software for solving linear (and nonlinear) systems of algebraic equations, integrating the Cauchy problems by time and solving the eigenvalue problems with large sparse matrices.

In the next section we will provide a summary of basis functions for main finite elements used in modern finite element software.

## 2.3 Basic finite element approximations

This section describes main isoparametric finite elements for 1D, 2D and 3D problems.

Let  $\Omega^{em} = \Omega_x^{em}$  be a domain in  $\mathbb{R}^l$  occupied by a finite element with the number  $m$ . Here  $l = 1$  for 1D elements,  $l = 2$  for 2D elements and  $l = 3$  for 3D elements;  $\mathbf{x} = \{x\}$  at  $l = 1$ ,  $\mathbf{x} = \{x, y\}$  at  $l = 2$ ,  $\mathbf{x} = \{x, y, z\}$  at  $l = 3$ .

Let us denote by  $\mathbf{x}_{r_s}^{em} = \mathbf{x}_{r_s}$  a set of nodes of the element with the global numbering  $r_1, r_2, \dots, r_n$ . Then the total number of nodes for the element  $\Omega_x^{em}$  is equal to  $n = n^{em}$ .

We will consider that there is a parametric mapping  $\mathbf{x} = \mathbf{x}(\boldsymbol{\xi})$ ,  $\boldsymbol{\xi} \in \mathbb{R}^l$  ( $\boldsymbol{\xi} = \{\xi\}$  at  $l = 1$ ,  $\boldsymbol{\xi} = \{\xi, \eta\}$  at  $l = 2$ ,  $\boldsymbol{\xi} = \{\xi, \eta, \zeta\}$  at  $l = 3$ ), that transforms a certain canonical domain  $\Omega_\xi^{em}$  into the domain  $\Omega_x^{em}$ . For the canonical figure there is a set of nodes  $\boldsymbol{\xi}_s$  with local numbering  $s = 1, 2, \dots, n$ .

Let us consider some approximate vector-function  $\mathbf{a}_h(\mathbf{x}, t) \in \mathbb{R}^k$ ,  $\mathbf{a}_h = \{a_{h1}, a_{h2}, \dots, a_{hk}\}$ ,  $a_{hi} = a_{hi}(\mathbf{x}, t)$ ,  $i = 1, 2, \dots, k$ . We will consider that on the element  $\Omega_x^{em}$  each scalar component  $a_{hi}(\mathbf{x}, t)$  of this function can be

presented in the form

$$a_{hi}(\mathbf{x}, t) = a_{hi}(\mathbf{x}(\boldsymbol{\xi}), t) = a_{hi}(\boldsymbol{\xi}, t) = \sum_{s=1}^n N_s(\boldsymbol{\xi}) A_{is}(t), \quad (2.38)$$

where  $N_s = N_s(\boldsymbol{\xi})$  are the *basis functions* or the *shape functions* of the finite element;  $s = 1, 2, \dots, n$ .

Below for clarity we consider only one specific approximated function  $a_h$  for a fixed  $t$ , therefore we will omit the time dependence. Thus, instead of (2.38) we will use a simplified expression

$$a_h(\mathbf{x}) = \sum_{s=1}^n N_s(\boldsymbol{\xi}) A_s. \quad (2.39)$$

It is assumed that the parametric mapping of the canonical figure  $\Omega_{\boldsymbol{\xi}}^{em}$  on the domain  $\Omega_x^{em}$  can be presented in the form

$$\mathbf{x} = \mathbf{x}(\boldsymbol{\xi}) = \mathbf{N}_x^{em*}(\boldsymbol{\xi}) \cdot \mathbf{X}^{em}, \quad (2.40)$$

where for 1D elements ( $l = 1$ )

$$\mathbf{N}_x^{em*}(\boldsymbol{\xi}) = [N_1(\boldsymbol{\xi}), N_2(\boldsymbol{\xi}), \dots, N_n(\boldsymbol{\xi})], \quad (2.41)$$

$$\mathbf{X}^{em} = \{x_{r_1}, x_{r_2}, \dots, x_{r_n}\}, \quad (2.42)$$

for 2D elements ( $l = 2$ )

$$\mathbf{N}_x^{em*}(\boldsymbol{\xi}) = \begin{bmatrix} N_1 & 0 & N_2 & 0 & \dots & N_n & 0 \\ 0 & N_1 & 0 & N_2 & \dots & 0 & N_n \end{bmatrix}, \quad (2.43)$$

$$\mathbf{X}^{em} = \{x_{r_1}, y_{r_1}, x_{r_2}, y_{r_2}, \dots, x_{r_n}, y_{r_n}\}, \quad (2.44)$$

and for 3D elements ( $l = 3$ )

$$\mathbf{N}_x^{em*}(\boldsymbol{\xi}) = \begin{bmatrix} N_1 & 0 & 0 & N_2 & 0 & 0 & \dots & N_n & 0 & 0 \\ 0 & N_1 & 0 & 0 & N_2 & 0 & \dots & 0 & N_n & 0 \\ 0 & 0 & N_1 & 0 & 0 & N_2 & \dots & 0 & 0 & N_n \end{bmatrix}, \quad (2.45)$$

$$\mathbf{X}^{em} = \{x_{r_1}, y_{r_1}, z_{r_1}, x_{r_2}, y_{r_2}, z_{r_2}, \dots, x_{r_n}, y_{r_n}, z_{r_n}\}. \quad (2.46)$$

The finite elements of the form (2.39)–(2.46) are called *isoparametric*, as their characterization uses the parametric mapping  $\mathbf{x} = \mathbf{x}(\boldsymbol{\xi})$  and the sets of basis functions with the total number  $n$  are the same in the approximation (2.39) of the field function  $a_h$  and in the parametric mappings (2.40)–(2.46).

Obviously, the behaviour of the field  $a_h$  by  $\mathbf{x}$  is more important than its behaviour by  $\boldsymbol{\xi}$ . Therefore usually we need a bijective parametric mapping  $\mathbf{x} = \mathbf{x}(\boldsymbol{\xi})$  and require an existence of an inverse function  $\boldsymbol{\xi} = \boldsymbol{\xi}(\mathbf{x})$ . Then from (2.39)–(2.46) we will have a dependence  $a_h(\mathbf{x}) = a_h(\boldsymbol{\xi}(\mathbf{x}))$ . Here it should be noted that even for simple basis functions  $N_s(\boldsymbol{\xi})$  an inverse to (2.40) mapping can be rather cumbersome. However, despite of perhaps complex behaviour of the field  $a_h(\mathbf{x})$  on  $\Omega_x^{em}$ , this function usually has good approximation properties.

The basis functions of the main finite elements in total comprise full polynomials of the first or the second degree from each spatial variable.

### Linear finite element in the form of a segment with two nodes

In this 1D element shown in Fig. 2.4  $n = n^{em} = 2$ ;  $\Omega_x^{em} = [x_{r_1}, x_{r_2}]$ ;  $x_{r_1} < x_{r_2}$ ;  $\Omega_\xi^{em} = [-1, 1]$ ;  $\xi_1 = -1$ ;  $\xi_2 = 1$ .

The basis functions are defined by the formulas

$$N_1(\xi) = \frac{1}{2}(1 - \xi), \quad N_2(\xi) = \frac{1}{2}(1 + \xi), \quad (2.47)$$

or in the uniform notation

$$N_s(\xi) = \frac{1}{2}(1 + \xi_s \xi), \quad s = 1, 2. \quad (2.48)$$

The element ensures a linear representation of the function  $a_h$  when it depends either on  $\xi$  or on  $x$ . (The latter is true by virtue of linearity of the inverse mapping  $\xi = \xi(x)$  under the linear dependence on  $x = x(\xi)$ .)

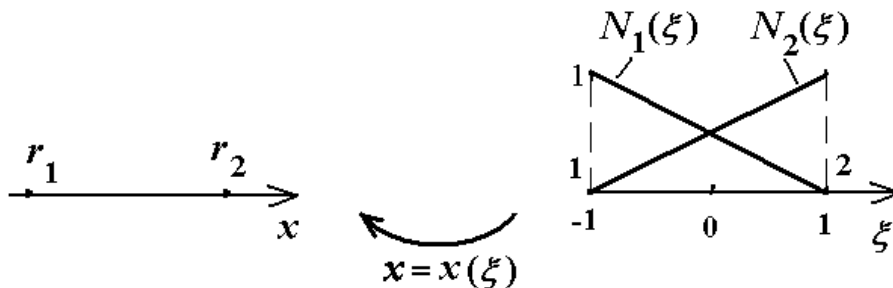


**Figure 2.4.** 1D element with two nodes: original segment (left) and canonical segment with basis functions (right)



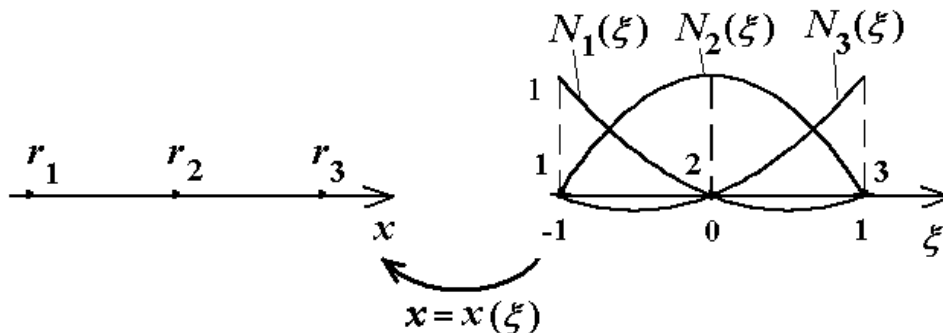


**Figure 2.5.** 1D element with three nodes: original segment (left) and canonical segment with basis functions (right)

### Quadratic finite element in the form of a segment with three nodes

For this 1D element (Fig. 2.5)  $n = n^{em} = 3$ ;  $\Omega_x^{em} = [x_{r_1}, x_{r_3}] = [x_{r_1}, x_{r_2}] \cup [x_{r_2}, x_{r_3}]$ ;  $x_{r_1} < x_{r_2} < x_{r_3}$ ;  $\Omega_\xi^{em} = [-1, 1] = [-1, 0] \cup [0, 1]$ ;  $\xi_1 = -1$ ;  $\xi_2 = 0$ ;  $\xi_3 = 1$ .

Here the basis functions are quadratic

$$N_1(\xi) = \frac{1}{2}\xi(1 - \xi), \quad N_2(\xi) = 1 - \xi^2, \quad N_3(\xi) = \frac{1}{2}\xi(1 + \xi), \quad (2.49)$$

or in the uniform notation

$$N_s(\xi) = \frac{1}{2}(3\xi_s^2 - 2)[\xi_s^2(1 + \xi_s\xi) - (1 - \xi^2)], \quad s = 1, 2, 3. \quad (2.50)$$

In order to ensure a bijective mapping  $x = x(\xi)$ , the internal node  $x_{r_2}$  must be located from the outermost nodes  $x_{r_1}$  and  $x_{r_3}$  at the distance greater than  $h_m/4$ , where  $h_m = x_{r_3} - x_{r_1}$  is the segment length.

In a general situation the behaviour of  $a_h$  from  $x$  is described by a complex transcendental expression. However, if an internal node is located in the middle of the segment, i. e.  $x_{r_2} = (x_{r_1} + x_{r_3})/2$ , then the quadratic parametric mapping  $x = x(\xi)$  is degenerated to a linear mapping. In this case each element gives a quadratic representation of the function  $a_h$  both by  $\xi$  and by  $x$ . Therefore almost always the node  $x_{r_2}$  is selected in the middle of the segment.

### Triangular finite element with 3 nodes

The figure  $\Omega_x^{em}$  on the plane  $Oxy$  has a form of triangle with the nodes  $\mathbf{x}_{r_s} = \{x_{r_s}, y_{r_s}\}$ ,  $s = 1, 2, 3$ , located in the counter-clockwise order of bypassing (Fig. 2.6). The canonical figure  $\Omega_\xi^{em}$  on the plane  $O\xi\eta$

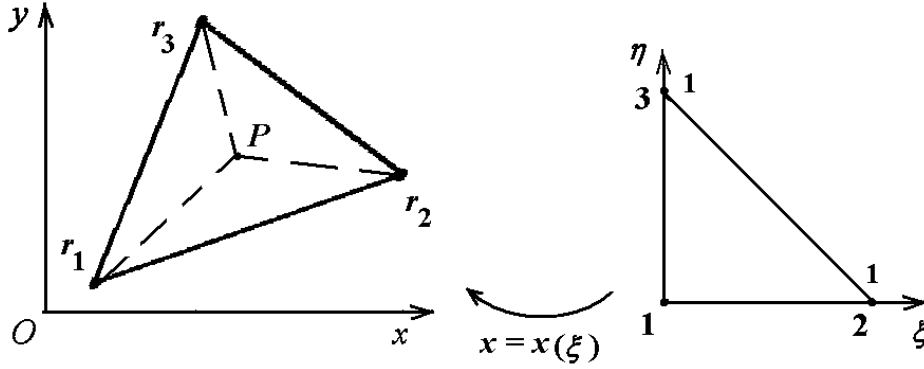


**Figure 2.6.** Triangular element with three nodes: original triangle (left) and canonical triangle (right)

$(\boldsymbol{\xi} = \{\xi, \eta\})$  is a rectangular triangle with the catheti equal to 1. Here  $n = 3$ ;  $\boldsymbol{\xi}_1 = \{0, 0\}$ ;  $\boldsymbol{\xi}_2 = \{1, 0\}$ ;  $\boldsymbol{\xi}_3 = \{0, 1\}$ .

In order to construct the shape functions, triangular coordinates or area coordinates are used

$$L_{r_1}(P) = \frac{S_{\Delta(P r_2 r_3)}}{S_{\Delta(r_1 r_2 r_3)}}, \quad L_{r_2}(P) = \frac{S_{\Delta(P r_3 r_1)}}{S_{\Delta(r_1 r_2 r_3)}}, \quad L_{r_3}(P) = \frac{S_{\Delta(P r_1 r_2)}}{S_{\Delta(r_1 r_2 r_3)}}, \quad (2.51)$$

where  $P = P(\mathbf{x}) = P(x, y)$  is the point inside triangle,  $S_{\Delta(P r_i r_j)}$  is the area of triangle with the vertices  $P(\mathbf{x})$ ,  $\mathbf{x}_{r_i}$ ,  $\mathbf{x}_{r_j}$ .

When bypassing the vertices in counter-clockwise direction, for calculation of the area the following formula can be used

$$S_{\Delta(P r_i r_j)} = \frac{1}{2} \begin{vmatrix} 1 & 1 & 1 \\ x & x_i & x_j \\ y & y_i & y_j \end{vmatrix}. \quad (2.52)$$

For canonical figure  $\Omega_{\boldsymbol{\xi}}^{em}$  the triangular coordinates  $L(\boldsymbol{\xi}) = L(\xi, \eta)$  have very simple form

$$L_1(\xi, \eta) = 1 - \xi - \eta, \quad L_2(\xi, \eta) = \xi, \quad L_3(\xi, \eta) = \eta. \quad (2.53)$$

These functions can be used as basis functions, i. e. for a triangular element with three nodes we have

$$N_s(\xi, \eta) = L_s(\xi, \eta), \quad s = 1, 2, 3. \quad (2.54)$$

The element has a linear behaviour of the field  $a_h$  both by  $\boldsymbol{\xi}$  and by  $\mathbf{x}$ , and triangular coordinates  $L_{r_s}(P)$  can be taken as basis functions from  $\mathbf{x}$ , i. e.  $L_{r_s}(P) = N_s(\boldsymbol{\xi}(\mathbf{x}))$ . From (2.52) it can be seen that the functions  $L_{r_s}(P)$  are linear by  $x$  and  $y$ . The graphs of these functions were presented before in Fig. 2.6, if we consider one of the elements.

### Quadrilateral finite element with four nodes

Let us consider a quadrangle  $\Omega_x^{em}$  on the plane  $Oxy$  with the nodes in its vertices  $\mathbf{x}_{r_s} = \{x_{r_s}, y_{r_s}\}$ ,  $s = 1, 2, 3, 4$ , located in the counter-clockwise order of bypassing (Fig. 2.7). The canonical figure  $\Omega_\xi^{em}$  on the plane  $O\xi\eta$  ( $\xi = \{\xi, \eta\}$ ) is a square with the center in the point  $\{0, 0\}$  and with the sides equal to 2. Here  $n = 4$ ;  $\xi_1 = \{-1, -1\}$ ;  $\xi_2 = \{1, -1\}$ ;  $\xi_3 = \{1, 1\}$ ;  $\xi_4 = \{-1, 1\}$ .

The shape functions are the products of the corresponding basis functions (2.47) of a 1D linear element that depend on  $\xi$  or  $\eta$

$$\begin{aligned} N_1(\xi, \eta) &= (1 - \xi)(1 - \eta)/4, & N_2(\xi, \eta) &= (1 + \xi)(1 - \eta)/4, \\ N_3(\xi, \eta) &= (1 + \xi)(1 + \eta)/4, & N_4(\xi, \eta) &= (1 - \xi)(1 + \eta)/4, \end{aligned} \quad (2.55)$$

or in a uniform notation

$$N_s(\xi) = (1 + \xi_s \xi)(1 + \eta_s \eta)/4, \quad s = 1, 2, 3, 4. \quad (2.56)$$

As it can be seen from (2.55), the basis functions are linear by  $\xi$  and  $\eta$ , i. e. bilinear. Therefore an element is also called a *bilinear quadrilateral finite element with four nodes*.

In order to ensure a bijective mapping  $\mathbf{x} = \mathbf{x}(\xi)$ , it is necessary [32] that a quadrangle is convex, i. e. all its internal nodes at the vertices are less than  $\pi$ .

The behaviour of the field  $a_h$  by  $\mathbf{x}$  here is quite complex, but on each side it is linear. For this reason the contact of two bilinear quadrilateral finite elements by a common side with shared nodes ensures a continuity of the field  $a_h(\mathbf{x})$ . This element can also contact by a common side with triangular finite element with three nodes. Here a continuity of the field

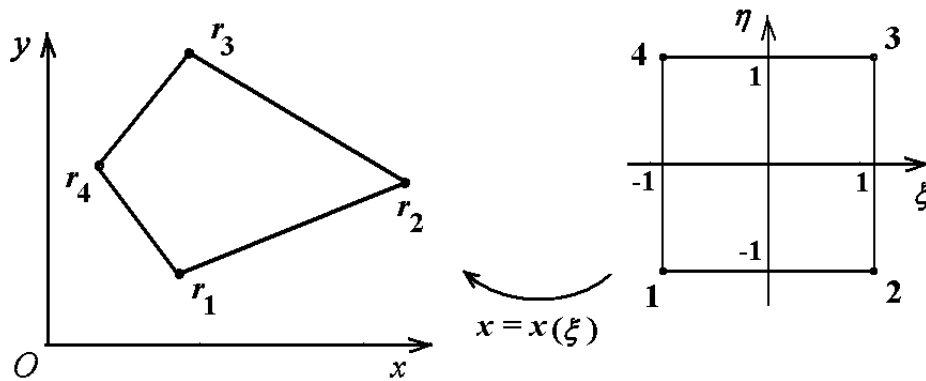


**Figure 2.7.** Quadrilateral element with four nodes: original quadrangle (left) and canonical quadrangle (right)

$a_h(\mathbf{x})$  is also ensured for the transition from bilinear quadrangle to a linear triangle.

This element has a simple shape for which we can demonstrate an importance of isoparametric approach. As it is known, for a quadrangle with four nodes and with the sides not parallel to the coordinate axes  $x$  and  $y$  it is not possible to construct polynomial representations  $a_h(\mathbf{x}) = a_h(x, y)$ , which ensure their continuity under the transition from one quadrangle to another. This continuity is ensured only for dependences (2.39)–(2.46) with isoparametric mappings.

In order to use more accurate quadratic approximations, it is necessary, as in 1D case, to consider the elements with the nodes on the element sides and quadratic basis functions.

### Triangular finite element with six nodes

Here a triangle  $\Omega_x^{em}$  on the plane  $Oxy$  has three nodes in the vertices  $\mathbf{x}_{r_s} = \{x_{r_s}, y_{r_s}\}$ ,  $s = 1, 2, 3$ , and another three nodes  $\mathbf{x}_{r_s}$  ( $s = 4, 5, 6$ ) on the sides (Fig. 2.8). The sides are usually rectilinear with the nodes  $\mathbf{x}_{r_s}$  ( $s = 4, 5, 6$ ) in the middle of the sides. However, for a range of cases as, for example, in a case of curvilinear boundaries, the side can be described by a quadratic parametric dependence defined by a replaced midside node (Fig. 2.8).

The canonical triangle  $\Omega_\xi^{em}$  is the same as in the case of a linear triangle but with additional nodes  $\xi_4 = \{1/2, 0\}$ ;  $\xi_5 = \{1/2, 1/2\}$ ;  $\xi_3 = \{0, 1/2\}$ .

The basis functions for the considered element are given by formulas

$$\begin{aligned} N_s &= (2L_s - 1)L_s, \quad s = 1, 2, 3, \\ N_4 &= 4L_1L_2, \quad N_5 = 4L_2L_3, \quad N_6 = 4L_1L_3. \end{aligned} \quad (2.57)$$

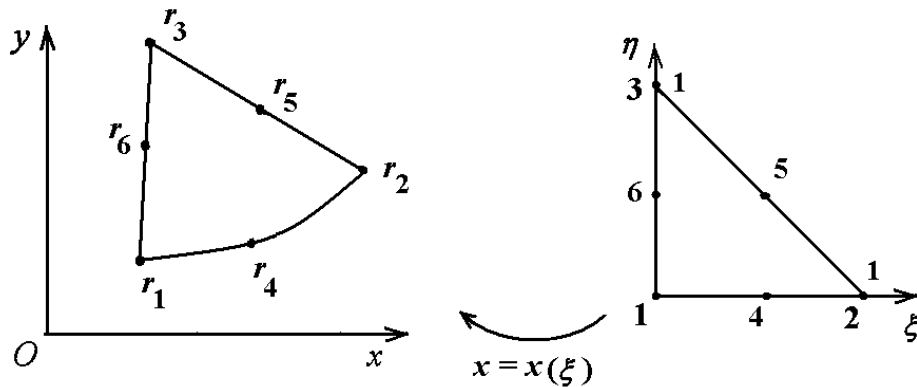


Figure 2.8. Triangular element with six nodes: original triangle (left) and canonical triangle (right)

The element ensures full quadratic approximation  $a_h(\boldsymbol{\xi})$  by  $\xi$  and  $\eta$ . If the sides of the triangle are rectilinear and the nodes  $\mathbf{x}_{r_s}$  at  $s = 4, 5, 6$  are located in the middle of the sides, then the parametric mapping becomes linear and therefore we get a quadratic approximation of the field  $a_h(\boldsymbol{\xi}(\mathbf{x}))$  by  $x, y$ . As a rule, the element is used in this particular form.

On the sides of the triangle there holds the approximation (2.39), (2.40), (2.43), (2.44) with (2.57) defined by the location of the nodes on the side and the value of the degree of freedom in these nodes. For a rectilinear side with a node in the middle, naturally, for  $a_h$  we have a quadratic behaviour by  $\mathbf{x}$ .

### Quadrilateral finite element with eight nodes

This famous element was suggested by J. Ergatoudis, B. Irons and O. Zienkiewicz and was called an element of *serendipity type* [33, 34]. Such elements do not have nodes inside the domain  $\Omega_x^{em}$ , but give the required representations of the field functions in the form of the polynomials of the required degree (in the framework of the isoparametric approach). It can be noted that a triangular finite element with six nodes is also an element of serendipity type, according to this terminology.

The considered element has a form of quadrangle  $\Omega_x^{em}$  on the plane  $Oxy$  with four nodes in the vertices  $\mathbf{x}_{r_s} = \{x_{r_s}, y_{r_s}\}$ ,  $s = 1, 2, 3, 4$ . Additional four nodes  $\mathbf{x}_{r_s}$  ( $s = 5, 6, 7, 8$ ) are located on the sides of the quadrangle (Fig. 2.9). Regarding the shape of the sides, here the same remarks hold as those for a triangle with six nodes. The canonical quadrangle  $\Omega_\xi^{em}$  is in fact the same square as it was for a quadrilateral finite element with four nodes ( $\boldsymbol{\xi}_1 = \{-1, -1\}$ ;  $\boldsymbol{\xi}_2 = \{1, -1\}$ ;  $\boldsymbol{\xi}_3 = \{1, 1\}$ ;  $\boldsymbol{\xi}_4 = \{-1, 1\}$ ), but with additional nodes  $\boldsymbol{\xi}_5 = \{0, -1\}$ ;  $\boldsymbol{\xi}_6 = \{1, 0\}$ ;  $\boldsymbol{\xi}_7 = \{0, 1\}$ ;  $\boldsymbol{\xi}_8 = \{-1, 0\}$ .

The basis functions have the form

$$\begin{aligned} N_5(\xi, \eta) &= (1 - \xi^2)(1 - \eta)/2, & N_6(\xi, \eta) &= (1 - \eta^2)(1 + \xi)/2, \\ N_7(\xi, \eta) &= (1 - \xi^2)(1 + \eta)/2, & N_8(\xi, \eta) &= (1 - \eta^2)(1 - \xi)/2, \\ N_1(\xi, \eta) &= (1 - \xi)(1 - \eta)/4 - (1/2)N_5(\xi, \eta) - (1/2)N_8(\xi, \eta), \\ N_2(\xi, \eta) &= (1 + \xi)(1 - \eta)/4 - (1/2)N_5(\xi, \eta) - (1/2)N_6(\xi, \eta), \\ N_3(\xi, \eta) &= (1 + \xi)(1 + \eta)/4 - (1/2)N_6(\xi, \eta) - (1/2)N_7(\xi, \eta), \\ N_4(\xi, \eta) &= (1 - \xi)(1 + \eta)/4 - (1/2)N_7(\xi, \eta) - (1/2)N_8(\xi, \eta). \end{aligned} \quad (2.58)$$

or in a uniform notation

$$\begin{aligned} N_s(\xi, \eta) &= \frac{1}{4}(3\xi_s^2\eta_s^2 - 2)[\xi_s^2\eta_s^2(1 + \xi_s\xi)(1 + \eta_s\eta) - \\ &\quad - \eta_s^2(1 - \xi^2)(1 + \eta_s\eta) - \xi_s^2(1 - \eta^2)(1 + \xi_s\xi)], \end{aligned} \quad (2.59)$$

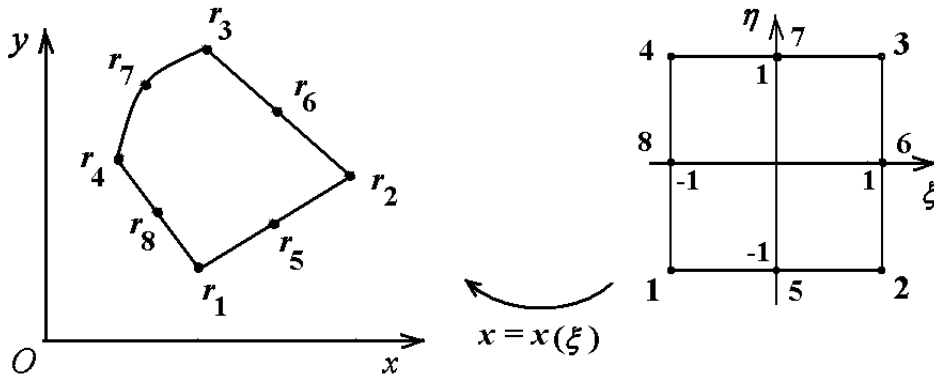


**Figure 2.9.** Quadrilateral element with eight nodes: original quadrangle (left) and canonical quadrangle (right)

where  $s = 1, 2, \dots, 8$ , and the nodes  $\xi_s = \{\xi_s, \eta_s\}$  were defined previously.

The element ensures quadratic behaviour of the field  $a_h$  by  $\xi$  and  $\eta$  on the canonical square. In the original quadrangle the field  $a_h(\mathbf{x})$  behaves in a complex way. However, on each side the change of the field  $a_h$  is the same as for a triangular element with six nodes. Therefore a quadrilateral element with eight nodes is consistent on the common side with shared nodes with the elements of the same type and with a triangular six-node element.

Many *3D finite elements* can be constructed by analogy with 2D elements. For this reason in 3D case we will provide only the main formulas of these elements. We will begin with the elements without intermediate midside nodes.

**Tetrahedron with four nodes (Fig. 2.10, left)**

The nodes (vertices) in a physical space:  $\mathbf{x}_{r_s} = \{x_{r_s}, y_{r_s}, z_{r_s}\}$ ,  $s = 1, 2, 3, 4$ .

The nodes (vertices) of the canonical tetrahedron  $\Omega_\xi^{em}$  in the space  $\xi\eta\zeta$ :  $\xi_1 = \{0, 0, 0\}$ ,  $\xi_2 = \{1, 0, 0\}$ ,  $\xi_3 = \{0, 1, 0\}$ ,  $\xi_4 = \{0, 0, 1\}$ .

The tetrahedral coordinates for a canonical tetrahedron:

$$L_1 = 1 - \xi - \eta - \zeta, \quad L_2 = \xi, \quad L_3 = \eta, \quad L_4 = \zeta. \quad (2.60)$$

The basis functions ( $L_s$  – tetrahedral coordinates):

$$N_s(\xi, \eta) = L_s(\xi, \eta), \quad s = 1, 2, 3, 4. \quad (2.61)$$

### Hexahedron (“brick”) with eight nodes (Fig. 2.10, right)

The nodes (vertices in a physical space:  $\mathbf{x}_{r_s} = \{x_{r_s}, y_{r_s}, z_{r_s}\}$ ,  $s = 1, 2, \dots, 8$ .

The nodes (vertices of a canonical hexahedron  $\Omega_\xi^{em}$  in the space  $\xi\eta\zeta$ :

$$\begin{aligned} \xi_1 &= \{-1, -1, -1\}, & \xi_2 &= \{1, -1, -1\}, \\ \xi_3 &= \{1, 1, -1\}, & \xi_4 &= \{-1, 1, -1\}, \\ \xi_5 &= \{-1, -1, 1\}, & \xi_6 &= \{1, -1, 1\}, \\ \xi_7 &= \{1, 1, 1\}, & \xi_8 &= \{-1, 1, 1\}. \end{aligned} \quad (2.62)$$

The basis functions:

$$N_s(\xi, \eta, \zeta) = \frac{1}{8}(1 + \xi_s\xi)(1 + \eta_s\eta)(1 + \zeta_s\zeta), \quad s = 1, 2, \dots, 8. \quad (2.63)$$

### Direct triangular prism with six nodes (Fig. 2.11, left)

The nodes (vertices) in a physical space:  $\mathbf{x}_{r_s} = \{x_{r_s}, y_{r_s}, z_{r_s}\}$ ,  $s = 1, 2, \dots, 6$ .

The nodes (vertices) of a canonical prism  $\Omega_\xi^{em}$  in the space  $\xi\eta\zeta$ :

$$\begin{aligned} \xi_1 &= \{0, 0, -1\}, & \xi_2 &= \{1, 0, -1\}, & \xi_3 &= \{0, 1, -1\}, \\ \xi_4 &= \{0, 0, 1\}, & \xi_5 &= \{1, 0, 1\}, & \xi_6 &= \{0, 1, 1\}. \end{aligned} \quad (2.64)$$

The basis functions:

$$N_s = L_s(1 - \zeta)/2, \quad N_{s+3} = L_s(1 + \zeta)/2, \quad s = 1, 2, 3, \quad (2.65)$$

where  $L_s$  are the coordinates of the area (2.51) for the triangle ( $L_1(\xi, \eta) = 1 - \xi - \eta$ ,  $L_2(\xi, \eta) = \xi$ ,  $L_3(\xi, \eta) = \eta$ ).

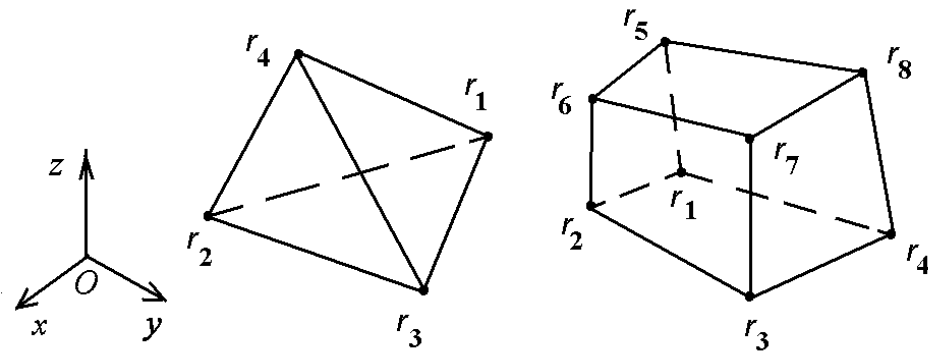


**Figure 2.10.** Tetrahedron and hexahedron without midside nodes: tetrahedron with four nodes (left) and hexahedron with eight nodes (right)

The prismatic element is used to model 3D problems for the bodies of a generalized cylindrical shape. For such problems good 3D meshes can be constructed by a translation of the corresponding plane meshes along the axis  $z$  (or curvilinear similar axis). Therefore, the prismatic elements are obtained through translation of plane triangular elements along this axis. As it can be seen from (2.65), the basis functions for a six-node prism are defined as a result of multiplication of the corresponding basis functions of the linear triangular element by the linear functions by  $\zeta$ .

### Quadrilateral pyramid with five nodes (Fig. 2.11, right)

The nodes (vertices) in a physical space:  $\mathbf{x}_{r_s} = \{x_{r_s}, y_{r_s}, z_{r_s}\}$ ,  $s = 1, 2, \dots, 5$ .

$\Omega_\xi^{em}$  is a canonical cube in the space  $\xi\eta\zeta$ , on the top edge of which only one node is chosen (the vertex):

$$\begin{aligned} \xi_1 &= \{-1, -1, -1\}, & \xi_2 &= \{1, -1, -1\}, \\ \xi_3 &= \{1, 1, -1\}, & \xi_4 &= \{-1, 1, -1\}, & \xi_5 &= \{0, 0, 1\}. \end{aligned} \quad (2.66)$$

The basis functions:

$$\begin{aligned} N_1 &= (1 - \xi)(1 - \eta)(1 - \zeta)/8, & N_2 &= (1 + \xi)(1 - \eta)(1 - \zeta)/8, \\ N_3 &= (1 + \xi)(1 + \eta)(1 - \zeta)/8, & N_4 &= (1 - \xi)(1 + \eta)(1 - \zeta)/8, \\ N_5 &= (1 + \zeta)/2. \end{aligned} \quad (2.67)$$

An element in a form of a pyramid is characterized by the fact that under a parametric mapping  $\mathbf{x} = \mathbf{x}(\boldsymbol{\xi})$  the canonical cube  $\Omega_\xi^{em}$  is transformed into a quadrilateral pyramid  $\Omega_x^{em}$ . Naturally, this mapping is not bijective, as all points of the edge of the cube  $\zeta = 1$  are transformed into one vertex  $\mathbf{x}_{r_5}$ .

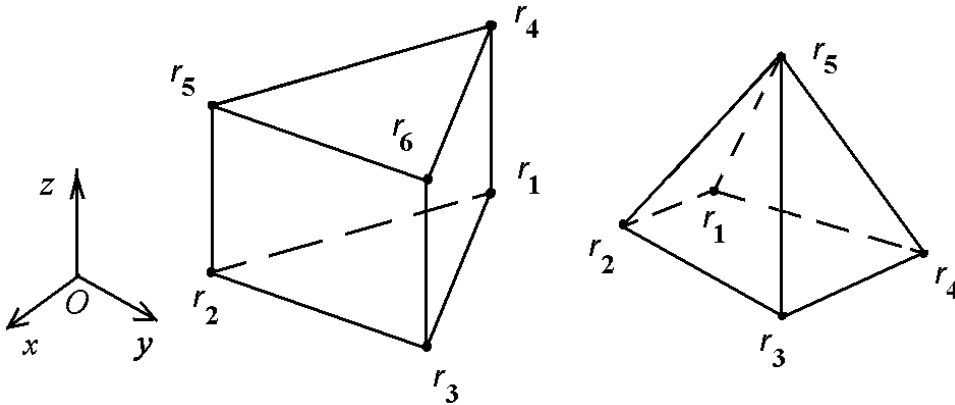


**Figure 2.11.** Prism and pyramid without midside nodes: prism with six nodes (left) and pyramid with five nodes (right)



Nevertheless, the highlighted feature of the parametric mapping for one point does not prevent the use of this element in practice. The prismatic element is necessary for transition from tetrahedral meshes to hexahedral meshes, and vice versa.

Regarding the meshes built of the described above tetrahedrons, hexahedrons, prisms and pyramids, one can make the following remark. All these elements can be stitched together with preserving the continuity of the field function  $a_h(\mathbf{x})$  at the transition from one element to another. It is only necessary that the elements have common edges and common shared nodes at the shared edges.

More accurate quadratic basis functions are used in 3D finite elements with additional nodes at the sides.

### Tetrahedron with 10 nodes (Fig. 2.12, left)

The nodes in a physical space:  $\mathbf{x}_{r_s} = \{x_{r_s}, y_{r_s}, z_{r_s}\}$ ,  $s = 1, 2, \dots, 10$ .

The nodes of the canonical tetrahedron  $\Omega_\xi^{em}$  in the space  $\xi\eta\zeta$ :  $\xi_1 = \{0, 0, 0\}$ ,  $\xi_2 = \{1, 0, 0\}$ ,  $\xi_3 = \{0, 1, 0\}$ ,  $\xi_4 = \{0, 0, 1\}$ ,  $\xi_5 = \{1/2, 0, 0\}$ ,  $\xi_6 = \{1/2, 1/2, 0\}$ ,  $\xi_7 = \{0, 1/2, 0\}$ ,  $\xi_8 = \{0, 0, 1/2\}$ ,  $\xi_9 = \{1/2, 0, 1/2\}$ ,  $\xi_{10} = \{0, 1/2, 1/2\}$ .

The basis functions ( $L_s$  are tetrahedral coordinates from (2.60)):

$$\begin{aligned} N_s &= (2L_s - 1)L_s, \quad s = 1, 2, 3, 4; \\ N_5 &= 4L_1L_2, \quad N_6 = 4L_2L_3, \quad N_7 = 4L_1L_3, \quad . \\ N_8 &= 4L_1L_4, \quad N_9 = 4L_2L_4, \quad N_{10} = 4L_3L_4. \end{aligned} \quad (2.68)$$

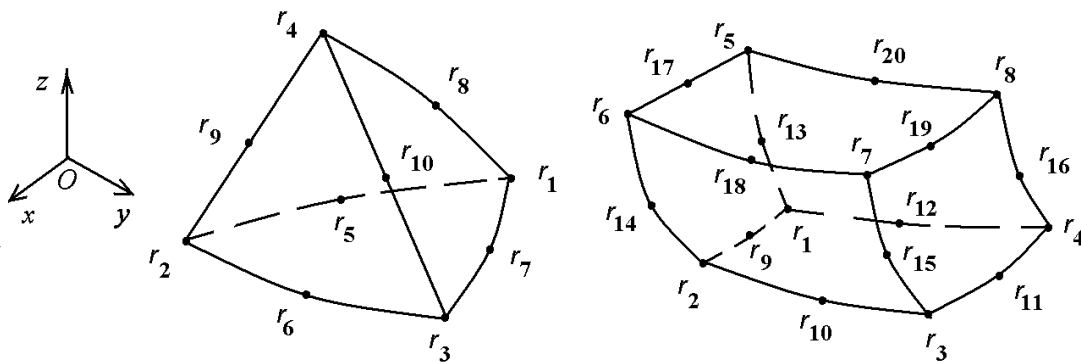


**Figure 2.12.** Tetrahedron and hexahedron with midside nodes: tetrahedron with 10 nodes (left) and hexahedron with 20 nodes (right)

### Hexahedron (“brick”) with 20 nodes (Fig. 2.12, right)

The nodes in a physical space:  $\mathbf{x}_{r_s} = \{x_{r_s}, y_{r_s}, z_{r_s}\}$ ,  $s = 1, 2, \dots, 20$ .

The nodes of the canonical hexahedron  $\Omega_\xi^{em}$  in the space  $\xi\eta\zeta$ : (2.62) – for  $s = 1, 2, \dots, 8$ , and

$$\begin{aligned} \boldsymbol{\xi}_9 &= \{0, -1, -1\}, & \boldsymbol{\xi}_{10} &= \{1, 0, -1\}, & \boldsymbol{\xi}_{11} &= \{0, 1, -1\}, \\ \boldsymbol{\xi}_{12} &= \{-1, 0, -1\}, & \boldsymbol{\xi}_{13} &= \{-1, -1, 0\}, & \boldsymbol{\xi}_{14} &= \{1, -1, 0\}, \\ \boldsymbol{\xi}_{15} &= \{1, 1, 0\}, & \boldsymbol{\xi}_{16} &= \{1, -1, 0\}, & \boldsymbol{\xi}_{17} &= \{0, -1, 1\}, \\ \boldsymbol{\xi}_{18} &= \{1, 0, 1\}, & \boldsymbol{\xi}_{19} &= \{0, 1, 1\}, & \boldsymbol{\xi}_{20} &= \{-1, 0, 1\}. \end{aligned} \quad (2.69)$$

The basis functions:

$$\begin{aligned} N_s(\xi, \eta, \zeta) &= \frac{1}{8}(3\xi_s^2\eta_s^2\zeta_s^2 - 2)[\xi_s^2\eta_s^2\zeta_s^2(1 + \xi_s\xi)(1 + \eta_s\eta)(1 + \zeta_s\zeta) - \\ &- \xi_s^2\eta_s^2(1 + \xi_s\xi)(1 + \eta_s\eta)(1 - \zeta^2) - \eta_s^2\zeta_s^2(1 + \eta_s\eta)(1 + \zeta_s\zeta)(1 - \xi^2) - \\ &- \xi_s^2\zeta_s^2(1 + \xi_s\xi)(1 + \zeta_s\zeta)(1 - \eta^2)], \end{aligned} \quad (2.70)$$

where  $s = 1, 2, \dots, 20$ .

### Right triangular prism with 15 nodes (Fig. 2.13, left)

The nodes in a physical space:  $\mathbf{x}_{r_s} = \{x_{r_s}, y_{r_s}, z_{r_s}\}$ ,  $s = 1, 2, \dots, 15$ .

By analogy with the prism with 5 nodes (see (2.64), (2.65)), the nodes of the canonical 15-node prism  $\Omega_\xi^{em}$  in the space  $\xi\eta\zeta$  and the basis functions are easily obtained as a result of the translation of a 6-node triangular element along the axis  $\zeta$  from  $-1$  to  $1$  and the multiplication of its basis functions by the basis functions of a 1D along the  $\zeta$ -axis quadratic element.

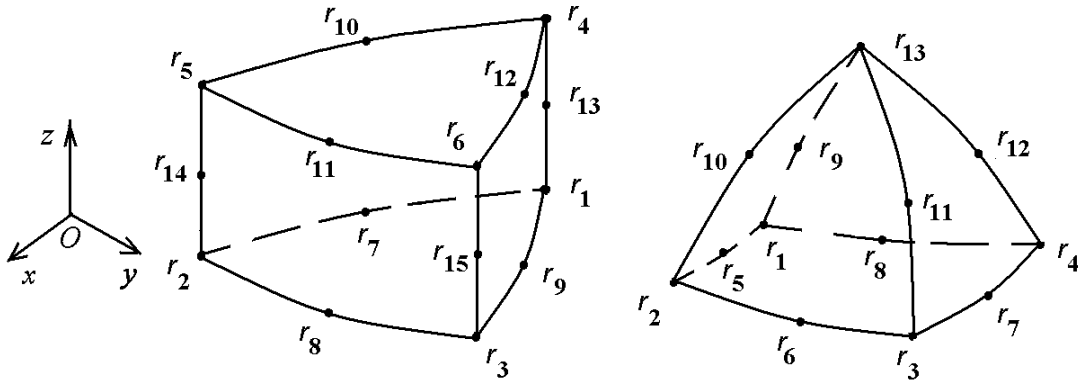


**Figure 2.13.** Prism and pyramid with midside nodes: prism with 15 nodes (left) and pyramid with 13 nodes (right)

### Quadrilateral pyramid with 13 nodes (Fig. 2.13, right)

The nodes in a physical space:  $\mathbf{x}_{r_s} = \{x_{r_s}, y_{r_s}, z_{r_s}\}$ ,  $s = 1, 2, \dots, 13$ .

$\Omega_\xi^{em}$  is a canonical cube in the space  $\xi\eta\zeta$ , on the top edge of which only one node is selected (the vertex):

$$\begin{aligned}
 \xi_1 &= \{-1, -1, -1\}, & \xi_2 &= \{1, -1, -1\}, \\
 \xi_3 &= \{1, 1, -1\}, & \xi_4 &= \{-1, 1, -1\}, \\
 \xi_5 &= \{0, -1, -1\}, & \xi_6 &= \{1, 0, -1\}, \\
 \xi_7 &= \{0, 1, -1\}, & \xi_8 &= \{-1, 0, -1\}, \\
 \xi_9 &= \{-1, -1, 0\}, & \xi_{10} &= \{1, -1, 0\}, \\
 \xi_{11} &= \{1, 1, 0\}, & \xi_{12} &= \{-1, 1, 0\}, \\
 \xi_{13} &= \{0, 0, 1\}.
 \end{aligned} \tag{2.71}$$

The basis functions:

$$\begin{aligned}
 N_1 &= (1 - \xi)(1 - \eta)(-1 - q\xi - q\eta)q/4, \\
 N_2 &= (1 + \xi)(1 - \eta)(-1 + q\xi - q\eta)q/4, \\
 N_3 &= (1 + \xi)(1 + \eta)(-1 + q\xi + q\eta)q/4, \\
 N_4 &= (1 - \xi)(1 + \eta)(-1 - q\xi + q\eta)q/4, \\
 N_5 &= (1 - \xi^2)(1 - \eta)q^2/2, & N_6 &= (1 + \xi)(1 - \eta^2)q^2/2, \\
 N_7 &= (1 - \xi^2)(1 + \eta)q^2/2, & N_8 &= (1 - \xi)(1 - \eta^2)q^2/2, \\
 N_9 &= (1 - \xi)(1 - \eta)q(1 - q), & N_{10} &= (1 + \xi)(1 - \eta)q(1 - q), \\
 N_{11} &= (1 + \xi)(1 + \eta)q(1 - q), & N_{12} &= (1 - \xi)(1 + \eta)q(1 - q), \\
 N_{13} &= (1 - q)(1 - 2q), & q &= (1 - \zeta)/2.
 \end{aligned} \tag{2.72}$$

Regarding the parametric mapping  $\mathbf{x} = \mathbf{x}(\boldsymbol{\xi})$ , here the same remarks hold as those for the pyramid with five nodes. The prismatic element with 13 nodes is required for the transition from tetrahedral meshes to hexahedral meshes for the elements with midside nodes.

For all elements with midside nodes (tetrahedrons, hexahedrons, prisms and pyramids) the continuity of the field function  $a_h(\mathbf{x})$  is ensured at the transition from one element to another. Here the elements must have common edges and common shared nodes on the shared edges (both in the vertices and on the sides).

It should be noted that both 2D and 3D elements with midside nodes cannot be stitched without the loss of the guarantee of the continuity of the field function  $a_h(\mathbf{x})$ . In order to move from an element with midside nodes to an element without midside nodes it is necessary to modify the element with midside nodes by deleting the nodes on the sides of the shared side (for 2D elements) or edge (for 3D elements). In order to do this, the values of the degrees of freedom in the midside nodes should be defined as

an arithmetic average of the values of the degrees of freedom in the nodes located in the vertices of the corresponding sides.

In conclusion we will formulate some general properties of the finite elements considered above and their basis functions.

For all basis functions  $\Omega_\xi^{em}$  condition (2.18) holds, i. e. all basis functions are equal to one in one node and are equal to zero in all other nodes of the element.

For all finite elements considered above the condition of completeness (2.19) is satisfied, i. e. the sum of all shape functions of the element is equal to 1. We note that the condition of completeness (2.19) for the isoparametric elements (2.39)–(2.46) ensures that an arbitrary linear by  $\mathbf{x}$  function on  $\Omega_x^{em}$  can be accurately represented by (2.39)–(2.46).

## Exercises for Chapter 2

**2.1.** Fig. 2.1(b) contains an example of a mixed mesh consisting of triangular and quadrilateral elements with the nodes located only in the vertices of the elements. How many nonzero elements will there be in a row 17 of a matrix  $\mathbf{K}$  of the size  $25 \times 25$  constructed for one scalar field function?

**2.2.** Fig. 2.2(b) contains an example of a mixed mesh consisting of triangular and quadrilateral elements with the nodes located both in the vertices of the elements and in the middle of the sides. How many nonzero elements will there be in a row 29 of a matrix  $\mathbf{K}$  of the size  $71 \times 71$  constructed for one scalar field function?

**2.3.** Answer the same question as in Problem 2.2, but for the row 18 of the matrix  $\mathbf{K}$ .

**2.4.** Answer the same question as in Problem 2.2, but for the column 69 of the matrix  $\mathbf{M}$ .

**2.5.** Answer the same question as in Problem 2.2, but for the column 68 of the matrix  $\mathbf{M}$ .

**2.6.** Show that the triangular coordinates  $L(\boldsymbol{\xi})$  on the canonical triangle  $\Omega_\xi^{em}$  indeed have the form (2.53), i. e. calculate using formulas (2.51) for canonical right triangle with the catheti equal to 1.

**2.7.** Show that the behavior of the field function  $a_h$  on a quadrangle with four nodes is linear on every side both by  $\boldsymbol{\xi}$  and  $\mathbf{x}$ . Which of the values  $A_s$  ( $s = 1, 2, 3, 4$ ) from (2.39) determine this behavior?

**2.8.** Show that the behavior of the field function  $a_h$  on a triangle with six nodes on the side is determined by an isoparametric quadratic dependence.

Also show that if the side is linear and the node is located in the middle of this side, than this behavior is quadratic by  $\mathbf{x}$ .

**2.9.** Show that the behavior of the field function  $a_h$  on a quadrangle of a serendipity type with 8 nodes on the side is determined by an isoparametric quadratic dependence. Also show that if the side is linear and the node is located in the middle of this side, than this behavior is quadratic by  $\mathbf{x}$ .

**2.10.** Build an isoparametric triangular finite element with five nodes (three nodes are located in the vertices of the canonical triangle and two (intermediate) nodes are located on two catheti), performing a reduction of the node 5 on the hypotenuse (Fig. 2.8). In order to do this, in the representation of the field function set  $A_5 = (A_2 + A_3)/2$ , and in the parametric mapping set  $x_5 = (x_2 + x_3)/2$ ,  $y_5 = (y_2 + y_3)/2$ . Obtain new basis functions instead of (2.57) and show that the resulting element will ensure linear behavior of the field function  $a_h$  on the side with reduced intermediate node.

**2.11.** Build an isoparametric triangular finite element with five nodes (three nodes are located in the vertices of the canonical triangle, one intermediate node is located on the cathetus  $\xi = 0$  and the other intermediate node is located on the hypotenuse), performing a reduction of the node 4 on the cathetus  $\eta = 0$  (Fig. 2.8). In order to do this, in the representation of the field function set  $A_4 = (A_1 + A_2)/2$ , and in the parametric mapping set  $x_4 = (x_1 + x_2)/2$ ,  $y_4 = (y_1 + y_2)/2$ . Obtain new basis functions instead of (2.57) and show that the resulting element will ensure linear behavior of the field function  $a_h$  on the side with reduced intermediate node.

**2.12.** Show that if for an isoparametric triangular element with 6 nodes we perform a reduction of all three nodes on the middle of the sides, using the methodology of problems 2.10, 2.11, then we will obtain a linear triangular finite element with three nodes.

**2.13.** Build an isoparametric finite element with 7 nodes, performing a reduction of an intermediate node on one side of an 8-node quadrilateral finite element, using the methodology of problems 2.10, 2.11. Obtain new basis functions instead of (2.58) and show that the resulting element will ensure linear behavior of the field function on the side with reduced intermediate node.

**2.14.** Show that if for an isoparametric quadrilateral finite element with 8 nodes we perform a reduction of all four nodes on the middle of the sides, using the methodology of problems 2.10, 2.11, then we will obtain a bilinear finite element with four nodes.

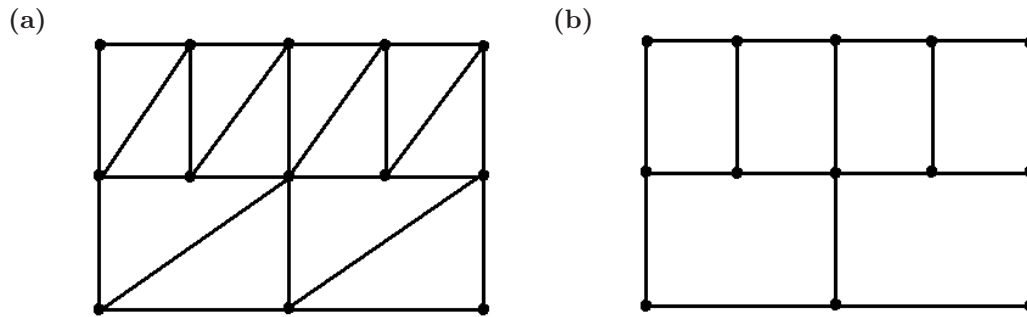


**Figure 2.14.** Meshes of elements without midside nodes:  
 (a) triangular mesh; (b) quadrilateral mesh

**2.15.** Show that the finite element in the form of a right triangular prism with 6 nodes is consistent by the side quadrilateral edges with similar elements and with 8-node hexahedrons.

**2.16.** Show that the finite element in the form of a right triangular prism with 6 nodes is consistent by the butt triangular edges with similar elements and with four-node tetrahedrons.

**2.17.** Write the shape functions of the right triangular prism with 15 nodes shown in Fig. 2.13 (left).

**2.18.** Do the meshes of linear triangular finite elements shown in Fig. 2.14(a) ensure the continuity of the field function when some of the nodal vertices of the smaller triangular elements lie on the sides of the bigger elements but are not their nodes? Explain your answer.

**2.19.** Do the meshes of bilinear quadrilateral finite elements shown in Fig. 2.14(b) ensure the continuity of the field function when some of the nodal vertices of the smaller quadrilateral elements lie on the sides of the bigger elements but are not their nodes? Explain your answer.

**2.20.** Do the meshes of 6-node triangular finite elements shown in Fig. 2.15(a) ensure the continuity of the field function when some of the nodal vertices of some finite elements coincide with the midside nodes of other elements? Explain your answer.

**2.21.** Do the meshes of 8-node quadrilateral finite elements shown in Fig. 2.15(b) ensure the continuity of the field function when some of the nodal vertices of some finite elements coincide with the midside nodes of other elements? Explain your answer.

**2.20.** Do the meshes of 3-node and 6-node triangular finite elements shown in Fig. 2.16(a) ensure the continuity of the field function? Explain your answer.

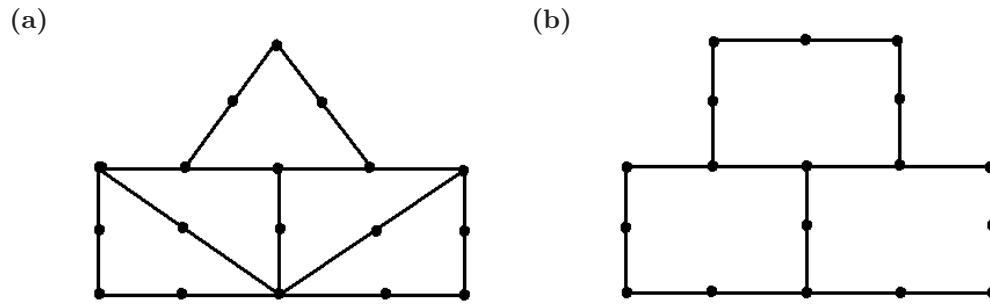


**Figure 2.15.** Meshes of elements with midside nodes:  
 (a) triangular mesh; (b) quadrilateral mesh

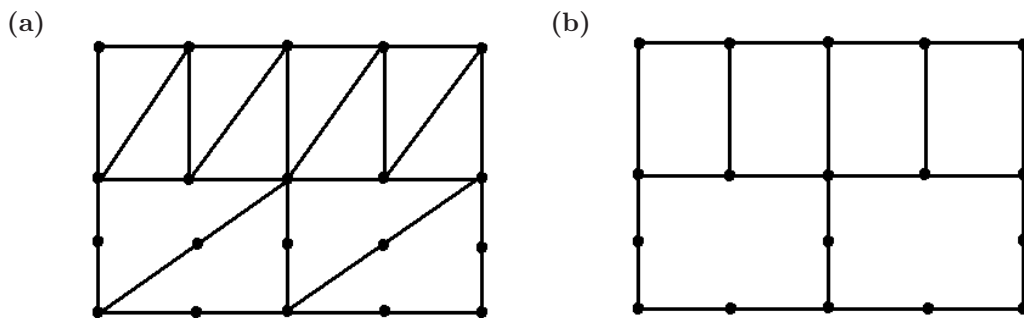


**Figure 2.16.** Meshes of elements without and with midside nodes:  
 (a) triangular mesh; (b) quadrilateral mesh

**2.21.** Do the meshes of 4-node and 8-node quadrilateral finite elements shown in Fig. 2.16(b) ensure the continuity of the field function? Explain your answer.

# Chapter 3

## Practical assignments and examples of solving problems in ANSYS

### 3.1 Practical assignment No. 1.

#### Static deformation of a piezoceramic transducer with multi-electrode coating

##### Objectives of the assignment

1. Study the main features of solving the problems of electroelasticity in ANSYS APDL:
  - setting the parameters of piezoelectric material
  - defining the element coordinate systems and using them to set anisotropic and piezoelectric properties of the material
  - using mapped finite element mesh
  - defining the electrode surfaces and setting the boundary conditions on them

The example problem is a two-dimensional static problem for a piezoelectric transducer with inhomogeneous polarization and multielectrode covering (input file FE\_Mod\_CP\_1.inp).

2. Write a program in ANSYS APDL for an individual assignment problem (static problem for a piezoelectric transducer with inhomogeneous polarization and multielectrode covering).
3. Perform computations, analyze the results and prepare a report.



### 3.1.1 Example problem and solution methods

#### Problem description

The piezoelectric disk of the radius  $R$  and the thickness  $H$  is assumed to be in a state of axisymmetric deformation in a cylindrical coordinate system ( $0 \leq r \leq R$ ,  $0 \leq z \leq H$ ). By virtue of axial symmetry, it is enough to consider only a meridional section of the disk. In accordance with ANSYS methodology,  $r$  is the  $X$ -axis and  $z$  is the  $Y$ -axis.

The disk has four electrode surfaces (Fig. 3.1): electrode 1 is  $0 \leq X \leq R_1$ ,  $Y = -H/2$ ; electrode 2 is  $0 \leq X \leq R_1$ ,  $Y = H/2$ ; electrode 3 is  $R_2 \leq X \leq R$ ,  $Y = -H/2$ ; electrode 4 is  $R_2 \leq X \leq R$ ,  $Y = H/2$ . The disk is made of piezoceramics PZT-4. Two of its zones  $\{0 \leq X \leq R_1, -H/2 \leq Y \leq H/2\}$  and  $\{R_1 \leq X \leq R_2, -H/2 \leq Y \leq H/2\}$  are polarized along the  $Y$ -axis, and the zone  $R_2 \leq X \leq R, -H/2 \leq Y \leq H/2\}$  is polarized opposite to the direction of the  $Y$ -axis (Fig. 3.2).

The disk is fixed in  $Y$ -direction in the middle points of its outer surface, i.e.  $u_y = 0$  at  $X = R$ ,  $Y = 0$ , the symmetry conditions hold at  $X = 0$ , and the rest of the boundaries are free from mechanical stresses.

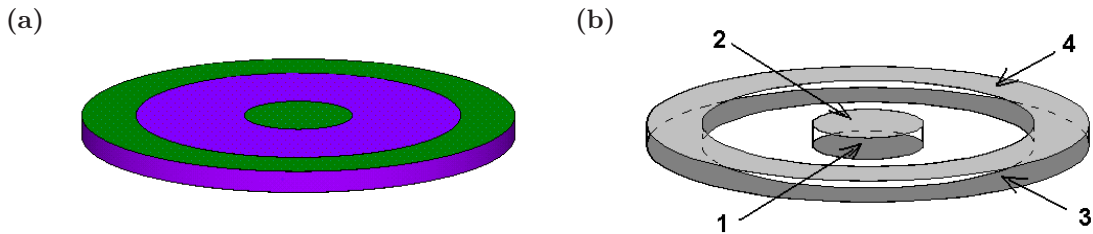


Figure 3.1. Piezoelectric disk (a) with four electrodes (b)

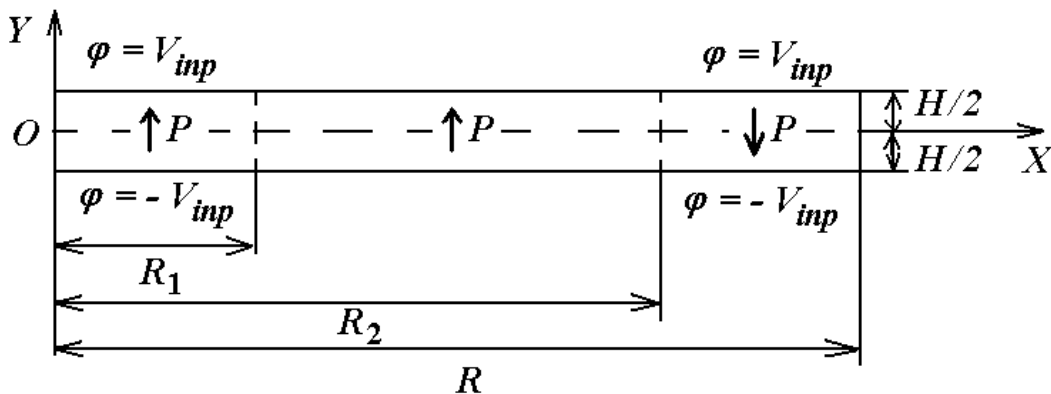


Figure 3.2. Meridional section of a piezoelectric disk

The disk is deformed by the applied electric voltage to the electrodes. The boundary conditions are:  $\varphi = -V_{inp}$  on the first electrode,  $\varphi = V_{inp}$  on the second electrode,  $\varphi = -V_{inp}$  on the third electrode, and  $\varphi = V_{inp}$  on the fourth electrode.

The objective of the problem is to determine the displacements of the disk caused by its deformation.

### Example of problem solving using ANSYS

The example of problem solving using ANSYS is provided in the file `FE_Mod_CP_1.inp` (see the listing below). The program is intended for use in command or batch mode. The text of the program contains detailed comments. Other examples of piezoelectricity problems can be found in ANSYS documentation: Coupled-Field Guide, 2.14. Sample Piezoelectric Analysis (Batch or Command Method), 2.16. Sample Electroelastic Analysis of a Dielectric Elastomer (Batch or Command Method); Verification Manual, files `Vm175.dat`, `Vm176.dat`, `Vm231.dat`, `Vm237.dat` (the references are provided for ANSYS 11.0).

ANSYS Product Launcher is the best option to start working with ANSYS. In ANSYS Product Launcher, select *Simulation Environment* → *ANSYS*, choose *Working Directory* for storing the working files and define *Job Name* for the project.

If there is an existing ANSYS database, then after the launch of ANSYS it can be resumed from *File* → *Resume*.

An ANSYS command file (text file with extension `.inp`, `.dat` or `.txt`), written in APDL ANSYS, can be executed from *File* → *Read Input from ...*. When creating a command file, it is useful to copy the commands from the input file into the command line, execute them step by step and look at the results in interactive mode.

It is recommended to save results from time to time! The current database should be cleared before performing new analysis (Menu path: *File* → *Clear and Start New*).

### Text of input file `FE_Mod_CP_1.inp`

```
! An exclamation point is a comment in ANSYS APDL.
! Any text after the sign ‘!’ is ignored

! File    FE\_Mod\_CP\_1.inp
! Test problem No.~1
```

```

! AXISYMMETRIC PROBLEM
! PIEZOELECTRIC DISK
! Static problem

! Invert background from black to white
/RGB,INDEX,100,100,100,0
/RGB,INDEX,0,0,0,15

! Title of the problem

/TITLE, PIEZOELECTRIC DISC

! Parameters for geometrical sizes (in SI system)

H=0.002 ! thickness of the disk
R=10*H  ! radius of the disk

! Additional geometrical parameters
R1=R/4  ! radius of the inner electrode surface
R23=R/4 ! size along the radius of the electrode ring

! The value of applied electric potential

VINP=1

! Parameters of finite element mesh
SM=1  ! scaling multiplier
HDIV=8*SM  ! Numbers of elements along the disk thickness
          ! (should be even number!)
R1DIV=16*SM ! Numbers of elements along the radial direction from 0 to R1
R12DIV=32*SM ! Numbers of elements along the radial direction from R1 to R2
R23DIV=16*SM ! Numbers of elements along the radial direction from R2 to R

! Parameters for material constants of piezoceramics PZT-4
! (all data in SI system)
R0=7.5e3      ! density
C11E=13.9e10  ! elastic moduli C\verb*"^"E\_ij
C12E=7.78e10
C13E=7.43e10
C33E=11.5e10
C66E=(C11E-C12E)/2.
C44E=2.56e10
E31=-5.2 ! piezomoduli
E33=15.1
E15=12.7
EPS11=730 ! dielectric permittivities,
          ! related to the permittivity of vacuum

```

EPS33=635

/PREP7 ! Enter Preprocessor

! Data tables for material constants of piezoelectric material

! (for the case of axisymmetric problem and piezoceramics

! polarized along the axis)

MP,DENS,1,R0

TB,ANEL,1

TBDATA,1,C11E,C13E,C12E

TBDATA,7,C33E,C13E

TBDATA,12,C11E

TBDATA,16,C44E

TB,PIEZ,1

TBDATA,2,E31

TBDATA,5,E33

TBDATA,8,E31

TBDATA,10,E15

MP,PERX,1,EPS11

MP,PERY,1,EPS33

! 2D quadrilateral finite element with 8 nodes for coupled analysis

ET,1,PLANE223,1001,,1

! KEYOPT(1)=1001 - degrees of freedom UX,UY,VOLT (piezoelectric FE)

! KEYOPT(3)=1 - axisymmetric problem

R2=R-R23 ! Auxiliary geometrical size

! Define keypoints

K,1,0,-H/2 ! Keypoint 1 with coordinates x=0, y=-H/2

K,2,R1,-H/2

K,3,R2,-H/2

K,4,R,-H/2

K,5,R,H/2

K,6,R2,H/2

K,7,R1,H/2

K,8,0,H/2

! Define straight lines

L,1,2 ! Line that connects keypoints 1 and 2 (will have number 1)

L,2,3 \$ L,3,4 ! Lines 2 and 3

!sign \$ separates the commands written in one command line

L,4,5 \$ L,5,6 \$ L,6,7 \$ L,7,8 \$ L,8,1 \$ L,6,3 ! Lines 4 and 9

! Define areas by keypoints

! Keypoints must be input in a clockwise or counterclockwise order

! around the area

A,1,2,3,6,7,8 ! Area 1

```
A,3,4,5,6 ! Area 2

! Define local coordinate system number 11, rotated at 180 degrees
! regarding z-axis
LOCAL,11,0,,180

! (Change System)
CSYS,0 ! Change active coordinate system to Cartesian (default number 0)

! Define element coordinate system 11 for area 2
! (to set the direction of polarization)
ASEL,S,AREA,,2 ! Select area 2
! AATT - Associate element attributes with selected unmeshed areas
AATT,1,,1,11 ! 11 - element coordinate system number for the selected area
! Optional commands
ASEL,S,AREA,,1
AATT,1,,1
ASEL,ALL ! select all areas

! Divide lines for mapped finite element mesh
! Important: total number of divisions for opposite lines of the area
! must be the same!

! Select all vertical lines (lines L8, L9, L4)
LSEL,S,LINE,,8,9
LSEL,A,LINE,,4

! Set the same number of divisions for all selected lines
! LESIZE - Set the number of divisions for unmeshed lines
LESIZE,ALL,,HDIV ! HDIV is the number of divisions

LSEL,S,LOC,X,0,R1 ! Select lines with coordinates  $0 \leq X \leq R1$ 
! (lines L1 and L7)
LESIZE,ALL,,R1DIV ! Set the number of divisions R1DIV
! for all selected lines

LSEL,S,LOC,X,R1,R2 ! Select lines with coordinates  $R1 \leq X \leq R2$ 
! (lines L2 and L6)
LESIZE,ALL,,R12DIV ! Set the number of divisions R2DIV
! for all selected lines

LSEL,S,LOC,X,R2,R ! Select lines with coordinates  $R2 \leq X \leq R$ 
! (lines L3 and L5)
LESIZE,ALL,,R23DIV ! Set the number of divisions R23DIV
! for all selected lines

LSEL,ALL ! Select all lines
```

```
! Prepare area 1 for mapped meshing
LCCAT,1,2 ! Concatenate lines L1 and L2 into one line (line L10)
LCCAT,7,6 ! Concatenate lines L6 and L7 into one line (line L11)

MSHKEY,1 ! Set mesh key
! (0 - free mesh, 1 - mapped mesh)
MSHAPE,0,2 ! Set finite element shapes
! 1st argument is a key indicating the element shape to be used
! (0 - quadrilateral-shaped elements)
! 2nd argument is the dimension of the model to be meshed (2D - area mesh)
AMESH,ALL ! Mesh all areas

FINISH ! Exit the preprocessor

/SOLU ! Enter the solver
ANTYPE,STAT ! Select the analysis type: static analysis

! Define the electrodes
! Select the nodes for the first electrode
! (with coordinates  $0 \leq X \leq R1$ ,  $Y = -H/2$ )
NSEL,S,LOC,Y,-H/2
NSEL,R,LOC,X,0,R1

! For all selected nodes define a set of coupled degrees of freedom VOLT
! (group number 1)
CP,1,VOLT,ALL

! Define the parameter N\_VOLT1 - minimal node number from group 1
! Node N\_VOLT1 will be the reference node for group 1
*GET,N\_VOLT1,NODE,,NUM,MIN

! Select the nodes for the second electrode
! (with coordinates  $0 \leq X \leq R1$ ,  $Y = H/2$ )

NSEL,S,LOC,Y,H/2
NSEL,R,LOC,X,0,R1

! For all selected nodes define a set of coupled degrees of freedom VOLT
! (group number 2)
CP,2,VOLT,ALL

! Define the parameter N\_VOLT2 - minimal node number from group 2
! Node with number N\_VOLT2 will be the reference node for group 2
*GET,N\_VOLT2,NODE,,NUM,MIN
```

```
! Select the nodes for the third electrode
! (with coordinates  $R/2 \leq X \leq R$ ,  $Y = -H/2$ )
NSEL,S,LOC,Y,-H/2
NSEL,R,LOC,X,R/2,R

! For all selected nodes define a set of coupled degrees of freedom VOLT
! (group number 3)
CP,3,VOLT,ALL

! Define the parameter N\_VOLT3 - minimal node number from group 3
! Node with number N\_VOLT3 will be the reference node for group 3
*GET,N\_VOLT3,NODE,,NUM,MIN

! Select the nodes for the fourth electrode
! (with coordinates  $R/2 \leq X \leq R$ ,  $Y = H/2$ )
NSEL,S,LOC,Y,H/2
NSEL,R,LOC,X,R/2,R

! For all selected nodes define a set of coupled degrees of freedom VOLT
! (group number 4)
CP,4,VOLT,ALL

! Define the parameter N\_VOLT4 - minimal node number from group 4
! Node with number N\_VOLT4 will be the reference node for group 4
*GET,N\_VOLT4,NODE,,NUM,MIN

NSEL,ALL ! Select all nodes

! Set the values of electric potential at the electrodes
D,N\_VOLT1,VOLT,-VINP
D,N\_VOLT2,VOLT,VINP
D,N\_VOLT3,VOLT,-VINP
D,N\_VOLT4,VOLT,VINP

! Conditions of symmetry with respect to OY-axis (axis along line 8)
DL,8,,SYMM

! Constraint of the middle point along the Y-axis
! Select node with coordinates  $X=R$ ,  $Y=0$ 
NSEL,S,LOC,Y,0
NSEL,R,LOC,X,R
D,ALL,UY,0 ! Define DOF constraint UY=0 for all selected nodes
NSEL,ALL ! Select all nodes

SOLVE ! Solve the system of finite element equations
FINISH ! Exit the solver
```

```

! Enter the postprocessor
/POST1
! Commands for graphical output
/SHOW,WIN32C ! Specify device for graphical output
/TRIAD,OFF      ! Do not show the global coordinate triad
/PLOPTS,INFO,2  ! Use Auto-legend format
/PLOPTS,LEG2,OFF
/PLOPTS,LOGO,OFF ! Do not show ANSYS logo
/PLOPTS,FRAME,OFF ! Do not show frame
/PLOPTS,DATE,OFF ! Do not show date

! Plot displacements UY
PLNSOL,U,Y

```

Now we will provide additional comments to the program.

Geometrical size, parameters for meshing (specific sizes of finite elements), and material constants are set as user-defined parameters. Then in the preprocessor (/PREP7 command enters the preprocessor) the matrices of elastic moduli, piezomoduli and dielectric permittivities are defined using the commands **MP**, **TB**, **TBDATA**. Let us have a closer look at the commands that define the piezoelectric material.

## Definition of material constants for piezoelectric materials

As it was noted before in section 1.3, the piezoelectric effect can be observed only in crystals that do not have the central symmetry. Therefore, the piezoelectric bodies must have anisotropic properties. In a general case, in order to set the material constants of piezoelectric bodies in ANSYS, the following values should be defined: the density  $\rho$ ; the symmetric matrix of elastic moduli  $c_{\alpha\beta}^E$ ;  $\alpha, \beta = 1, \dots, 6$ ;  $c_{\alpha\beta}^E = c_{\beta\alpha}^E$ ; the matrix of piezoelectric modules  $e_{i\alpha}$ ;  $i = 1, 2, 3$ ;  $\alpha = 1, \dots, 6$ ; and the matrix of dielectric permittivities  $\epsilon_{ij}^S$ ;  $i, j = 1, 2, 3$ , which is diagonal for most materials. These notations for the modules of piezoelectric body are conventional in the literature on piezoelectricity and technical applications [6, 7, 11, 17, 28], hence the values of these modules can be found in various reference books on piezoelectric materials.

We note that the transition from the tensor values  $c_{ijkl}^E$  and  $e_{ijk}$  to the matrix notations  $c_{\alpha\beta}^E$  and  $e_{i\alpha}$  was described in problems 1.6 and 1.9. However, as it is mentioned in ANSYS documentation [1], ANSYS uses nonstandard arrangement of the matrix components  $c_{\alpha\beta}^E$  and  $e_{i\alpha}$  in a form of one-dimensional arrays, which facilitates the transition from 3D to 2D problems. Besides, ANSYS enables to define alternative constant sets (problem 1.13), such as the elastic compliances  $s_{\alpha\beta}^E$  calculated at constant electric field; the strain piezomoduli  $s_{\alpha\beta}^E$  calculated at constant stress, and the dielectric permittivities  $\epsilon_{ij}^T$  calculated at constant stresses. Moreover, all components of the matrices  $s_{\alpha\beta}^E$  and  $d_{i\alpha}$  in ANSYS are arranged in a nonstandard way.

Let us describe the method of defining the modules  $c_{\alpha\beta}^E$  and  $e_{i\alpha}$  in ANSYS in more detail. The coefficients  $c_{\alpha\beta}^E$  are set in a form of  $6 \times 6$  matrix ( $4 \times 4$  for 2D problems). By virtue of symmetry, only the upper triangular part of the matrix of elastic moduli is used,



and the coefficients of the matrix are arranged in a specific way:

$$\mathbf{c}_{\text{ANSYS,3D}}^E \leftrightarrow \begin{array}{c|cccccc} & x & y & z & xy & yz & xz \\ \hline x & c_{11}^E & c_{12}^E & c_{13}^E & c_{16}^E & c_{14}^E & c_{15}^E \\ y & & c_{22}^E & c_{23}^E & c_{26}^E & c_{24}^E & c_{25}^E \\ z & & & c_{33}^E & c_{36}^E & c_{34}^E & c_{35}^E \\ xy & & & & c_{66}^E & c_{46}^E & c_{56}^E \\ yz & & \text{sym} & & & c_{44}^E & c_{45}^E \\ xz & & & & & & c_{55}^E \end{array} \quad (3.1)$$

$$\mathbf{c}_{\text{ANSYS,2D}}^E \leftrightarrow \begin{array}{c|cccc} & x & y & z & xy \\ \hline x & c_{11}^E & c_{12}^E & c_{13}^E & c_{16}^E \\ y & & c_{22}^E & c_{23}^E & c_{26}^E \\ z & & & c_{33}^E & c_{36}^E \\ xy & \text{sym} & & & c_{66}^E \end{array} \quad (3.2)$$

The components of the matrix  $\mathbf{c}_{\text{ANSYS,3(2)D}}^E$  in ANSYS are defined by the commands: **TB,ANISO,MAT** and **TBDATA,STLOC,C1,C2, ...,C6**; where *MAT* is the number of the material properties set, *STLOC* is the starting location in the data table for entering data values *C1, C2, ..., C6*. The data table for the coefficients that enter in (3.1), (3.2), is filled by rows (3.1) in a form of one-dimensional array with 21 components:

$$\begin{bmatrix} 1 & 2 & 3 & 4 & 5 & 6 \\ & 7 & 8 & 9 & 10 & 11 \\ & & 12 & 13 & 14 & 15 \\ & & & 16 & 17 & 18 \\ & & & & 19 & 20 \\ & & & & & 21 \end{bmatrix} \quad (3.3)$$

The resulting correspondence between the data from the data table defined by **TBDATA** command and the elasticity moduli  $c_{\alpha\beta}^E$  is presented in Table 3.1.

The most common type of piezoelectric materials is the piezoceramics polarized along the *Oz*-axis, which matrix of elastic moduli has the following structure (for the material of crystal class *6mm* [11])

$$\mathbf{c}^E = \begin{bmatrix} c_{11}^E & c_{12}^E & c_{13}^E & 0 & 0 & 0 \\ & c_{11}^E & c_{13}^E & 0 & 0 & 0 \\ & & c_{33}^E & 0 & 0 & 0 \\ & & & c_{44}^E & 0 & 0 \\ & \text{sym} & & & c_{44}^E & 0 \\ & & & & & c_{66}^E \end{bmatrix}, \quad (3.4)$$

**Table 3.1.** Arrangement of the elastic moduli  $c_{\alpha\beta}^E$  in the data table **TBDATA**

No.	1	2	3	4	5	6	7	8	9	10	11
$c_{\alpha\beta}^E$	$c_{11}^E$	$c_{12}^E$	$c_{13}^E$	$c_{16}^E$	$c_{14}^E$	$c_{15}^E$	$c_{22}^E$	$c_{23}^E$	$c_{26}^E$	$c_{24}^E$	$c_{25}^E$
No.	12	13	14	15	16	17	18	19	20	21	
	$c_{33}^E$	$c_{36}^E$	$c_{34}^E$	$c_{35}^E$	$c_{66}^E$	$c_{46}^E$	$c_{56}^E$	$c_{44}^E$	$c_{45}^E$	$c_{55}^E$	

**Table 3.2.** Nonzero elastic moduli  $c_{\alpha\beta}^E$  of piezoceramics in data table TBDDATA for 3D problems

No.	1	2	3	7	8	12	16	19	21
$c_{\alpha\beta}^E$	$c_{11}^E$	$c_{12}^E$	$c_{13}^E$	$c_{11}^E$	$c_{13}^E$	$c_{33}^E$	$c_{66}^E$	$c_{44}^E$	$c_{44}^E$

**Table 3.3.** Nonzero elastic moduli  $c_{\alpha\beta}^E$  of piezoceramics in data table TBDDATA for 2D problems

No.	1	2	3	7	8	12	16
$c_{\alpha\beta}^E$	$c_{11}^E$	$c_{13}^E$	$c_{12}^E$	$c_{33}^E$	$c_{13}^E$	$c_{11}^E$	$c_{44}^E$

where  $c_{66}^E = (c_{11}^E - c_{12}^E)/2$ .

Therefore, from comparison of (3.1), (3.3) and (3.4), we obtain that for 3D problems different nonzero elastic moduli for the piezoceramics polarized along the  $Oz$ -axis in the data table TBDDATA will have the numbers that are indicated in Table 3.2.

As it can be seen from comparison of (3.1)–(3.3), for 2D problems it is enough to specify the first 16 positions in a one-dimensional array of the moduli  $c_{\alpha\beta}^E$ .

We note that for plane and axisymmetric 2D problems the  $Oy$ -axis ( $z = (3)$  for the moduli  $c_{\alpha\beta}^E$ ) is usually considered to be the axis of polarization in the working plane  $Oxy$ . In this case for plane and axisymmetric problems different nonzero elastic moduli for piezoceramics in the data table TBDDATA will have the numbers that are indicated in Table 3.3.

Similarly, the piezomoduli  $e_{i\alpha}$  in ANSYS are also defined in an unusual way. The piezomoduli are arranged in a  $6 \times 3$  matrix ( $4 \times 2$  for 2D problems) in the following order:

$$\mathbf{e}_{\text{ANSYS,3D}} \leftrightarrow \begin{array}{c|ccc} & x & y & z \\ \hline x & e_{11} & e_{21} & e_{31} \\ y & e_{12} & e_{22} & e_{32} \\ z & e_{13} & e_{23} & e_{33} \\ xy & e_{16} & e_{26} & e_{36} \\ yz & e_{14} & e_{24} & e_{34} \\ xz & e_{15} & e_{25} & e_{35} \end{array}, \quad \mathbf{e}_{\text{ANSYS,2D}} \leftrightarrow \begin{array}{c|cc} & x & y \\ \hline x & e_{11} & e_{21} \\ y & e_{12} & e_{22} \\ z & e_{13} & e_{23} \\ xy & e_{16} & e_{26} \end{array} \quad (3.5)$$

After the execution of the command **TB,PIEZ,MAT** the data table TBDDATA for the piezomoduli will be filled by rows with the values from the matrix  $\mathbf{e}_{\text{ANSYS,3D}}$  as a one-dimensional array of the size 18. As a result, we obtain the correspondence between the data from the data table TBDDATA and the piezomoduli  $e_{i\alpha}$ , which can be seen in Table 3.4, where for 2D problems it is enough to define the elements with numbers 1,2,4,5,7,8,10 and 11.

For the piezoceramics polarized along the direction of  $Oz$ -axis the matrix of piezomoduli has the following structure

$$\mathbf{e} = \begin{bmatrix} 0 & 0 & 0 & 0 & e_{15} & 0 \\ 0 & 0 & 0 & e_{15} & 0 & 0 \\ e_{31} & e_{31} & e_{33} & 0 & 0 & 0 \end{bmatrix}, \quad (3.6)$$

**Table 3.4.** Arrangement of the moduli  $e_{i\alpha}$  in the data table TBDATA

No.	1	2	3	4	5	6	7	8	9
$e_{i\alpha}$	$e_{11}$	$e_{21}$	$e_{31}$	$e_{12}$	$e_{22}$	$e_{32}$	$e_{13}$	$e_{23}$	$e_{33}$
No.	10	11	12	13	14	15	16	17	18
	$e_{16}$	$e_{26}$	$e_{36}$	$e_{14}$	$e_{24}$	$e_{34}$	$e_{15}$	$e_{25}$	$e_{35}$

**Table 3.5.** Nonzero moduli  $e_{i\alpha}$  of piezoceramics in data table TBDATA for 3D problems

No.	3	6	9	14	16
$e_{i\alpha}$	$e_{31}$	$e_{31}$	$e_{33}$	$e_{15}$	$e_{15}$

**Table 3.6.** Nonzero moduli  $e_{i\alpha}$  of piezoceramics in data table TBDATA for 2D problems

No.	2	5	8	10
$e_{i\alpha}$	$e_{31}$	$e_{33}$	$e_{31}$	$e_{15}$

and therefore the nonzero piezomoduli of piezoceramic material for 3D problems in the data table TBDATA will have the numbers presented in Table 3.5.

Finally, for plane and axisymmetric problems in the cases, when in the plane  $Oxy$  the  $Oy$ -axis (the axis  $z = (3)$  for the piezomoduli  $e_{i\alpha}$ ) is the axis of preliminary polarization of piezoceramics, different nonzero piezomoduli in the data table TBDATA will have the numbers that are indicated in Table 3.6.

Summarizing the above, for the piezoceramic material we can write the following fragments of program code in ANSYS APDL, that define the sets of material constants  $MAT$  with number 1 for 3D and 2D problems, where for the latter case the piezoceramics is considered to be polarized along the  $Oy$ -axis of the working plane  $Oxy$ :

**Fragment 1 (3D)**

```

MP,DENS,1,RHO
TB,ANEL,1
TBDATA,1,C11E,C12E,C13E
TBDATA,7,C11E,C13E
TBDATA,12,C33E
TBDATA,16,C66E
TBDATA,19,C44E
TBDATA,21,C44E
TB,PIEZ,1
TBDATA,3,E31
TBDATA,6,E31
TBDATA,9,E33
TBDATA,14,E15
TBDATA,16,E15
MP,PERX,1,EPS11
MP,PERZ,1,EPS33

```

**Fragment 2 (2D)**

```

MP,DENS,1,RHO
TB,ANEL,1
TBDATA,1,C11E,C13E,C12E
TBDATA,7,C33E,C13E
TBDATA,12,C11E
TBDATA,16,C44E
TB,PIEZ,1
TBDATA,2,E31
TBDATA,5,E33
TBDATA,8,E31
TBDATA,10,E15
MP,PERX,1,EPS11
MP,PERY,1,EPS33

```

Here  $RHO = \rho$ ;  $C11E = c_{11}^E$  and so on. These values are scalar parameters in ANSYS APDL and their values should be defined beforehand. Besides, in the presented fragment of the program code we have added **MP** command, that defines the density and the dielectric permittivities of piezoceramics.

As it can be seen, the definition of piezoelectric materials requires some efforts. It should be emphasized that in the presented fragments the axes of  $Oxy(z)$ -plane are the axes of the element coordinate systems for the defined constant sets.

Let us now return to the listing of the input file for solving the test 2D static problem for piezoelectric transducer with inhomogeneous polarization and multi-electrode coating.

**ET,1,PLANE223,1001,,1** command defines the quadrilateral 8-node finite element **PLANE223** with the options of piezoelectric analysis and axisymmetry. This element will be used to solve the problem. For ANSYS user all the distinctions between axisymmetric problem and 2D plane stress problem consist in the third option of this finite element (the command **ET,1,PLANE223,1001,,0** will define the element for 2D plane stress problem). However, with this option ANSYS will use the equations of axisymmetric theory of piezoelectricity that are much more complex than the equations of plane stress or plane strain.

### Solid model of the meridional section of piezoelectric disk

In ANSYS APDL the solid model of the original domain with complex geometry is usually constructed “from bottom to top”, starting with the most simple objects (*Entities*), which are the *Keypoints*, and finishing with *Areas* for 2D problems or *Volumes* for 3D problems.

**K** command is used to build the keypoints. Its first argument is the reference number of the keypoint, and the remaining arguments are the coordinates of the keypoint. For example, **K,2,R1,-H/2** command defines a keypoint with the reference number 2 and coordinates  $x = R1$ ,  $y = -H/2$ ,  $z = 0$  (the last coordinate takes the default value). The *Line* between two keypoints can be defined by **L** command. For example, **L,2,3** command defines a line in the active coordinate system between the keypoints 2 and 3. The lines are numbered automatically, starting with the lowest available number. In order to construct the areas, we can use the commands **A** and **AL**, where the resulting areas are also numbered

automatically. **AL** command creates an area bounded by the previously defined lines. The lines (10 lines maximum) must be input in clockwise or counterclockwise order and must form a simply connected closed curve. **A** command defines an area by connecting the keypoints. The keypoints defining the area must be input in clockwise or counterclockwise order around the area (maximum 18 keypoints in the list). The existing lines between adjacent keypoints will be used; and the missing lines will be generated as “straight” lines in the active coordinate system and will be assigned the lowest available numbers.

According to Fig. 3.2 in the meridional section of the disk we can distinguish two zones with two different polarization directions. Therefore the axisymmetric model of the disk can be composed by two areas. Fig. 3.3 shows the areas A1 and A2 with indicated area numbers and keypoint numbers (Menu path *Plot* → *Areas*, to show the numbers of areas and keypoints select *PlotCtrls* → *Numbering* → and tick *Area numbers*, *Keypoint numbers*.)

The lines and the keypoints that constitute the areas A1 and A2 can be seen in Fig. 3.4 (Menu path *Plot* → *Lines*, before that in *Select* → *Entities* choose the lines L1–L9 and show the numbers of lines and keypoints by choosing: *PlotCtrls* → *Numbering* → *Line numbers*, *Keypoint numbers*). Here a rectangular area A2 is constructed in a standard way of four lines L3, L4, L5, L9 and four keypoints 3, 4, 5, 6. The upper and the lower boundaries of this area coincide with the lines of the electrodes location. The area A1 consists of six keypoints 1, 2, 3, 6, 7, 8 and six lines L1, L2, L9, L6, L7, L8. For this area both upper and lower boundaries must be constructed of two lines, and the keypoints of the lines L1 and L7 that simulate the electrodes must coincide with the ends of the electrodes. This requirement ensures that the ends of the electrodes will coincide with the nodes of finite elements. It is also worth noting, that the line L9 is common for the adjacent areas A1 and A2.

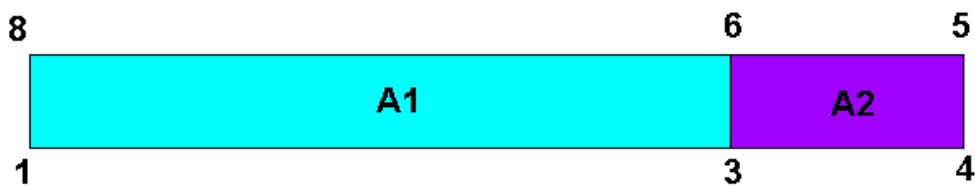


**Figure 3.3.** Area numbering in the model of a meridional section of piezoelectric disk

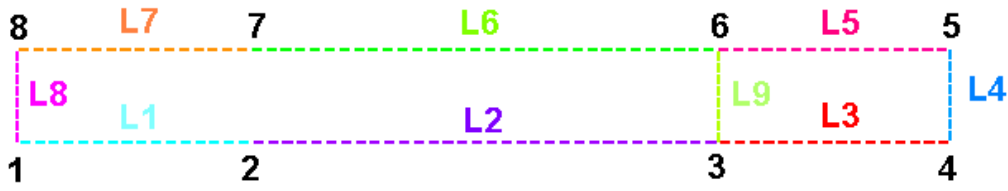


Figure 3.4. Keypoints and meshed lines of the disk section model

### Direction of the polarization vector for the areas of piezoelectric disk

All the moduli  $c_{\alpha\beta}^E$ ,  $e_{i\alpha}$ ,  $\epsilon_{ij}^S$  introduced for the piezoelectric materials, generally speaking are the moduli defined in crystallographic coordinate systems  $O\tilde{x}\tilde{y}\tilde{z}$ . These coordinate systems for piecewise-homogeneous domains can differ with the transition from one domain to another, and for the functionally-graded materials they can differ from point to point. Therefore, we can redenote the moduli defined previously in crystallographic coordinate system  $O\tilde{x}\tilde{y}\tilde{z}$  by  $\tilde{c}_{\alpha\beta}^E$ ,  $\tilde{e}_{i\alpha}$ ,  $\tilde{\epsilon}_{ij}^S$ . The computational formulas for finite element matrices use the tensor values  $\mathbf{c}^E$ ,  $\mathbf{e}$ ,  $\boldsymbol{\epsilon}^S$  calculated in global Cartesian coordinate system. If presented in a vector-matrix form, these formulas will contain the coefficients of the matrices  $c_{\alpha\beta}^E$ ,  $e_{i\alpha}$ ,  $\epsilon_{ij}^S$ , also written in global Cartesian coordinate system.

ANSYS uses the concept of element coordinate systems, in which every finite element can be assigned with its own coordinate system, and the material properties  $\tilde{c}_{\alpha\beta}^E$ ,  $\tilde{e}_{i\alpha}$ ,  $\tilde{\epsilon}_{ij}^S$ , etc. are defined in the element coordinate system. For every finite element ANSYS can recalculate the moduli  $\tilde{c}_{\alpha\beta}^E$ ,  $\tilde{e}_{i\alpha}$ ,  $\tilde{\epsilon}_{ij}^S$  into the moduli  $c_{\alpha\beta}^E$ ,  $e_{i\alpha}$ ,  $\epsilon_{ij}^S$ , presented in a global coordinate system. This recalculation can be performed without the participation of the user, if the element coordinate system is already defined for every finite element.

The orientation of the crystallographic coordinate system  $O\tilde{x}\tilde{y}\tilde{z}$  for piezoelectric materials is defined by the polarization vector  $\mathbf{P}$ . Namely, for piezoceramics (transversely isotropic material) the direction of the  $O\tilde{z}$ -axis coincides with the direction of the vector  $\mathbf{P}$ , and the axes  $O\tilde{x}$  and  $O\tilde{y}$  lie in the plane perpendicular to the vector  $\mathbf{P}$ .

For plane and axisymmetric 2D problems it is convenient to consider the  $O\tilde{y}$ -axis as the axis of preliminary polarization  $\mathbf{P}$  in the working plane  $O\tilde{x}\tilde{y}$ , and therefore in ANSYS for the piezomaterials with different polarization vectors it is enough to define for the corresponding areas the element

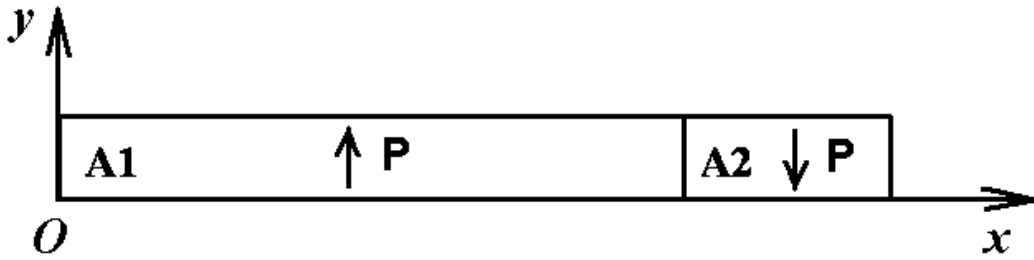


**Figure 3.5.** The directions of the polarization vectors  $\mathbf{P}$  for the areas of the disk section

coordinate systems that are rotated in the proper way with respect to the global coordinate system  $Oxy$ .

For our example problem (see Fig. 3.5) the direction of the polarization vector  $\mathbf{P}$  in the area A1 coincides with the direction of the  $Oy$ -axis of the global Cartesian coordinate system, therefore for the finite elements of this area it is not necessary to introduce special coordinate system. For the area A2 the direction of the polarization vector  $\mathbf{P}$  is opposite to the direction of the  $Oy$ -axis of the global Cartesian coordinate system, therefore for this area it is necessary to define the element coordinate system with the axis  $O\tilde{y}$ , directed along the polarization vector, i. e. the axis  $O\tilde{y}$  must be directed in the way opposite to the axis  $Oy$ .

To achieve this, we need to rotate the original element coordinate system to 180 degrees with respect to the global Cartesian coordinate system. The next block of commands creates the local coordinate system and defines it as an element coordinate system for finite elements that will be created in the area A2.

```
LOCAL,11,0,,,,180
ASEL,S,AREA,,2
AATT,1,,1,11
```

Fig. 3.6 shows an example of finite element mesh with the element coordinate systems. Here more coarse meshing is used than in the previously provided file FE\_Mod\_CP\_1.inp. (Menu path *Plot* → *Elements*, to show the polarization zones with different colours select *PlotCtrls* → *Numbering* → *Elem/Attrib numbering* → then select *Element CS num, Numbering shown with* → *Colors only*, to show the direction of the element coordinate system for every element select *PlotCtrls* → *Symbols* and tick *ESYS Element coordinate sys*).

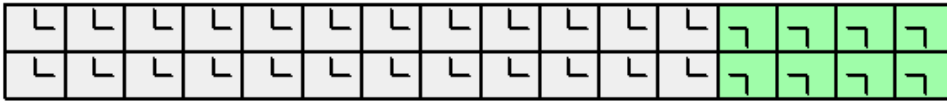


**Figure 3.6.** Element coordinate systems in the areas of meridional section of the disk

### Finite element mapped mesh

As the element **PLANE223** is a quadrilateral finite element and the simulated area of the meridional section of the disk is a quadrangle, more precisely, rectangle, it is therefore logical to use *mapped* finite element meshing in quadrangles (or, even better, in rectangles).

There are two main meshing methods in ANSYS: *Free Mesh* and *Mapped Mesh*. A free mesh does not follow any pattern and has no element shape restrictions. Free mesh is suitable for areas and volumes of complex shapes. Free mesh is usually defined by an average finite element size. On the contrary, a mapped mesh restricts the element shape (for example, quadrangles for areas, or hexahedrons for volumes) and typically has a regular pattern with obvious rows of elements. Mapped mesh is beneficial for areas and volumes of simple shape, such as rectangles or bricks. The use of a mapped mesh facilitates to reduce the computation time. Usually a mapped mesh is built on the base of the divisions and spacing ratio, which are specified for its constituting lines. Generally a mapped mesh is more precise than a free mesh with comparable number of elements and nodes.

In order to build a mapped quadrilateral finite element mesh for a quadrilateral area, this area must satisfy two conditions: 1) the area must consist of four lines, 2) the area must have equal numbers of element divisions specified on the opposite sides. If an area is bounded by more than four lines, then some of the lines can be combined (by **LComb** command) or concatenated (by **LCCAT** command) in order to reduce the total number of lines to four.

In our example problem there are at least two ways to construct a solid model of the meridional section of the disk that would accept mapped finite element mesh. For example, we could build an additional line between keypoints 2 and 7 and then create three rectangular areas, each of them consisting of four lines.

Here we use another way that allows us to reduce the number of the required areas to two. We create two areas A1 and A2, where A2 is a



regular area that accepts a mapped mesh, and A1 is irregular in the way that it does not accept a mapped mesh because it consists of six lines. In order to make area A1 regular, it is enough to concatenate lines L1 and L2 which constitute the lower boundary and lines L6 and L7 which constitute the upper boundary. This can be done by **LCCAT** command which concatenates multiple, adjacent lines into one line in preparation for mapped meshing. Note that **LCCAT** accepts only two arguments, so if it is necessary to concatenate more than two lines, the first argument should be set to *ALL*. In this case the second argument is ignored and all previously selected lines (by **LSEL** command) are concatenated. It is also worth noting that for a mapped mesh the total number of the line divisions must be the same for the opposite lines of the area. Fig. 3.7 shows the result of concatenation for the lines of the upper and lower boundaries of the area A1. The output lines L10 and L11 keep the element divisions of the input lines.

### Bondary conditions

**Boundary conditions on the electrode surfaces.** As it was noted in section 1.3, the metallized surfaces or electrodes on the surface of the piezoelectric body are equipotential surfaces, i. e. the electric potential  $\varphi(\mathbf{x}, t)$  on them must not depend on  $\mathbf{x}$ , and the boundary conditions (1.33) or (1.34), (1.35) must be satisfied.

The boundary conditions on the electrode surfaces can be set in the following way. The nodes of the finite element mesh that belong to one electrode  $\Gamma_{\varphi_j}$  can be combined in one node (coupled DOF) by **CP** command that will be a reference node for this electrode. Then for this reference node **N\_VOLT** we can either set the value of the electric potential  $VJ = V_j$  by the command **D,N\_VOLT,VOLT,VJ**, or define the total electric charge  $QJ = Q_j$  by the command **F,N\_VOLT,CHRG,QJ** (for finite elements **PLANE223**, **SOLID226**, **SOLID227**) or by



**Figure 3.7.** Line concatenation for a solid model of the meridional section of the disk

the command **F,N\_VOLT,AMPS,QJ** (for finite elements **PLANE13**, **SOLID5**, **SOLID98**).

The block of commands, that define a group of nodes and set the value of the electric potential on the first electrode, is presented below:

```
NSEL,S,LOC,Y,-H/2
NSEL,R,LOC,X,0,R1
CP,1,VOLT,ALL
*GET,N\_VOLT1,NODE,,NUM,MIN
D,N\_VOLT1,VOLT,-VINP
```

In order to define a free electrode, i. e. satisfy the conditions (1.34), (1.35) with  $Q_j = 0$ , it is enough to define a group of nodes by **CP** command with using **D** command.

**Mechanical boundary conditions.** In our example problem we need to set the symmetry boundary conditions with respect to the axis of rotation ( $Oy$ -axis) and the constraint on displacements along  $Oy$  for the middle point on the outer surface radius of the meridional section of the disk .

The degrees-of-freedom constraints (three DOFs **UX**, **UY**, **VOLT** for the element **PLANE223** with the options of piezoelectric analysis **KEYOPT(1) = 1001**) can be set either by **D** command that defines DOF constraints at nodes or by **DL** command that defines DOF constraints on lines. It should be noted that all solid boundary conditions will be transformed into finite element boundary conditions at the stage of the solution. The solid boundary conditions on a line have priority over the finite element boundary conditions for the nodes on the same line.

The condition of symmetry can be set either by **DL** command or by **D** command. **DL** command accepts a symmetry options (**SYMM**, as in the above example **DL,8,,SYMM**). Another way is to select all necessary nodes and use **D** command. We can select the nodes that lie on the line L8 by the following commands:

```
LSEL,S,LINE,,8
NSLL,S,1
```

where the last command selects the nodes associated with selected lines, and its second argument contains the key that specifies whether only interior line nodes are to be selected (0 – select only nodes interior to selected lines, 1 – select all nodes associated with selected lines).

**D,ALL,UX,0** command assigns zero **UX** displacements for all selected nodes, and this corresponds to the symmetry with respect to  $Ox$ -axis.

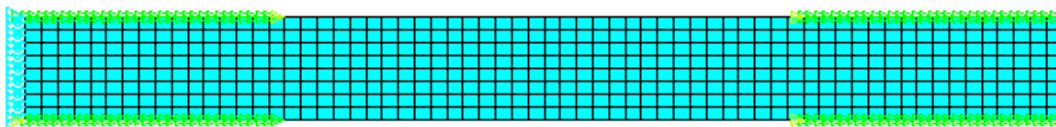


**Figure 3.8.** Finite element mesh with boundary conditions

We note that in the considered axisymmetric problem, as it can be easily checked in ANSYS, the symmetry boundary conditions on the line  $x = 0$  will be satisfied automatically, and the above command **DL,8,,SYMM** is provided for reliability and is therefore optional.

The condition of a rigidly fixed boundary assumes that for the given nodes the displacement vector is equal to zero, i. e. in a case of plane problem  $UX=0$  and  $UY=0$ . The corresponding block of commands will be written as:

```
D,ALL,UX,0
D,ALL,UY,0
```

Note that in our example problem we use only a constraint on displacements along  $Oy$ -axis, i. e.  $UY=0$ .

Finite element model of piezoelectric disk with boundary conditions is shown in Fig. 3.8 (Menu path *Plot*  $\rightarrow$  *Elements*, to show boundary conditions select *PltCtrls*  $\rightarrow$  *Symbols*  $\rightarrow$  and tick *All applied BC*.)

## Results

The solution results for the finite element problem can be accessed in ANSYS via postprocessor. There are two postprocessors in ANSYS, General Postprocessor and Time History Postprocessor.

General Postprocessor is used for reviewing results for a specifically defined combination of loads at a single time (or frequency). To enter the ANSYS general postprocessor, issue **/POST1** command or use menu path: *Main Menu*  $\rightarrow$  *General Postproc*. It is the only postprocessor available for static or steady state analysis.

Time History Postprocessor is used for reviewing results at specific locations in the model as a function of time, frequency, or some other change in the analysis parameters that can be related to time. Time History Postprocessor can be used to construct graphics displays, chart

representations or tabular listings, or to perform math operations on the data sets. Time History Postprocessor is available for transient, modal or harmonic analyses. A typical time-history task would be to graph result items versus time in a transient analysis, or to graph force versus deflection in a nonlinear structural analysis. To enter the ANSYS general postprocessor, issue **/POST26** command or use menu path: *Main Menu* → *TimeHist PostPro*, which will launch the Variable Viewer.

Here we provide menu paths for the results that can be reviewed for structural analysis (after entering *Main Menu*).

To display the deformed shape of the structure, select

- *General Postproc* → *Plot Results* → *Deformed Shape* (deformed shape of the structure).

In order to access the results for Degree of freedom solution (solution in terms of unknown variables), select:

- *General Postproc* → *Plot Results* → *Contour Plot* → *Nodal Solu...* → *DOF Solution* →
  - *X-Component of displacement* (distribution of the displacements  $u_x$ );
  - *Y-Component of displacement* (distribution of the displacements  $u_y$ );
  - *Displacement vector sum* (distribution of the displacement vector magnitude);
  - *Electric potential* (distribution of the electric potential);

To display the distribution of vector variables, select Vector Plot in General Postprocessor: • *General Postproc* → *Plot Results* → *Vector Plot* → *Predefined* →

- *DOF solution* → *Translation U* (distribution of the displacement vector);
- *Flux & gradient* → *Elec field EF* (distribution of the electric field vector).

The results of distribution of various components of stresses, strains, electric induction vector, etc. can be also reviewed in General Postprocessor.

There are several ways to save an image into a graphical file.

- *PlotCtrls* → *Capture Image*. An image will appear in a new window. Use menu path *File* → *Save as...* to save an image as a bmp graphical file without reversing black and white colors.
- *PlotCtrls* → *Hard Copy* → *To File*. Here one can choose a color scale (Monochrome, Gray Scale, Color) and an extension for the graphical file (.bmp, postscript, .tiff, .jpeg, .png), and also specify the file name and choose whether or not use a Reverse Video for reversing black and white

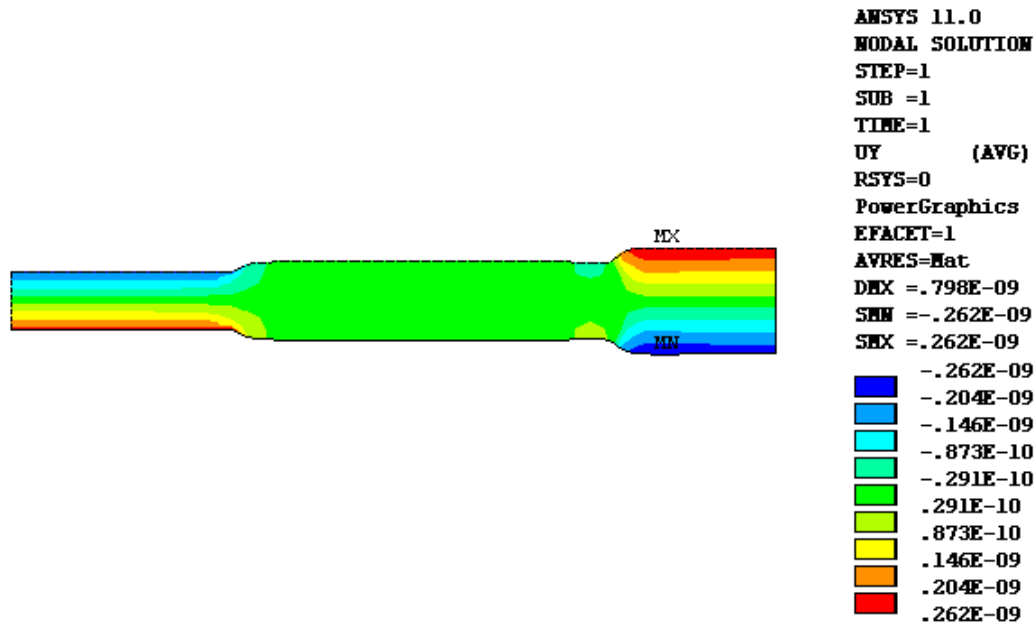


Figure 3.9. Distributions of the displacements UY

colors. There is no option to choose the place where to save the image. The graphical file will be saved in the working directory of ANSYS that was selected at the start.

- *PlotCtrls* → *Redirect Plots* → *To JPEG File ...* The program will open the window *Redirect Plots to JPEG*, where one can choose various saving modes for the graphical file (*Color* or *Monochromatic*, *Quality*, etc.) and save the file JPEG format;

- similarly instead of selecting *To JPEG File...* other formats of saving modes can also be selected.

- *PlotCtrls* → *Write Metafile*. It is recommended to tick *Invert White/Black* for reversing black and white colors. It is possible to specify the directory where to save the image. The graphical file will be saved as a Windows metafile with an extension *.emf* or *.wmf*.

The program code for solving the example problem in ANSYS ends with the command **PLNSOL,U,Y** which shows the picture of displacement UY distribution (Fig. 3.9, hereinafter the presented results were obtained in version ANSYS 11.0).

We note that the example problem is axisymmetric in meridional section, where *OY*-axis corresponds to *Oz*-axis in 3D, and *Ox*-axis corresponds to *Or*-axis. Therefore displacement UY is in fact the displacement  $u_z$ , displacement UX is the displacement  $u_r$  and so on.

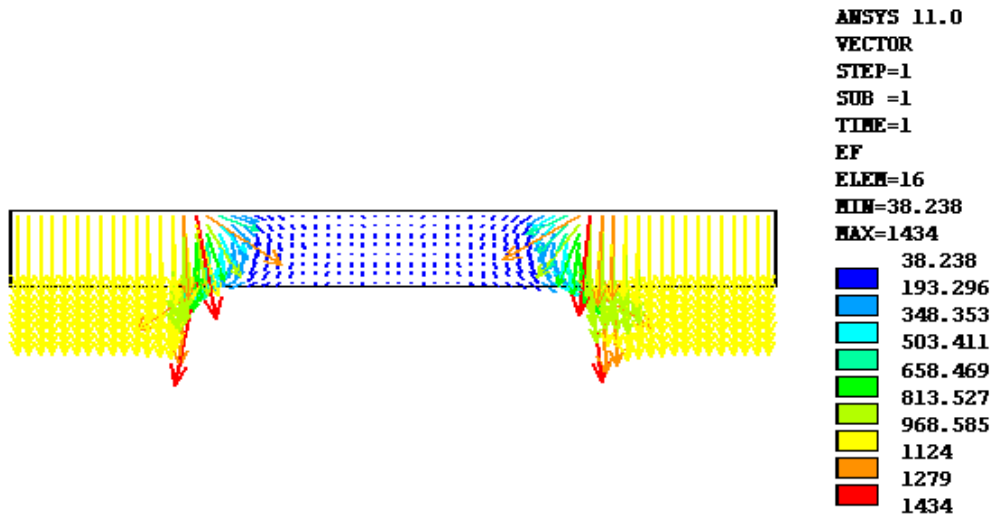


Figure 3.10. Distribution of the electric field vector

In postprocessor, it is also easy to obtain the pictures of distribution for other mechanical and electric field values. For example, Fig. 3.10 shows the distribution of the electric field vector.

Let us analyse the obtained results from both physical and mathematical viewpoints. The difference of potentials  $\Delta V = \varphi|_{Y=-H/2} - \varphi|_{Y=H/2} = -2V_{inp}$  is applied between the electrodes 1 and 2 (i. e. between continuous electrodes in the zone  $0 \leq X \leq R_1$ ) and between the electrodes 3 and 4 (i. e. between ring electrodes in the zone  $R_2 \leq X \leq R$ ). Then we can expect that in the areas between these electrodes an electric field will be formed  $E \sim \Delta V/H = -2V_{inp}/H = -1000$  (V/m), as  $V_{inp} = 1$  (V),  $H = 0.002$  (m). The same values of electric fields are indeed can be observed in Fig. 3.10 (yellow vectors). For the zone  $0 \leq X \leq R_1$  between continuous electrodes the direction of the polarization vector  $\mathbf{P}$  is opposite to the direction of the generated electric field  $\mathbf{E}$ . Therefore, due to the phenomenon of inverse piezoelectric effect (see section 1.3), piezoelectric elements in this area should shrink. On the contrary, in the zone  $R_2 \leq X \leq R$  between ring electrodes the direction of the polarization vector  $\mathbf{P}$  coincides with the direction of the generated electric field  $\mathbf{E}$ . Then again, due to the phenomenon of the inverse piezoelectric effect, piezoelectric elements in the area  $R_2 \leq X \leq R$  should expand. Indeed, such deformations of the zones under the electrodes can be clearly seen in Fig. 3.9. Thus, the expected physics of electromechanical processes in

the considered problem for a piezoceramic transducer with multielectrode coating is supported by the results presented in Fig. 3.9 and 3.10.

It is worth noting that finite element calculations are approximate. Therefore it is necessary to address the question on the accuracy of the obtained results and determine the situations in which it is not worth to expect the convergence. In the above program code, the characteristics of the finite element mesh were defined in the following block of commands:

```
! Parameters of finite element mesh
SM=1.00 ! scaling multiplier
HDIV=8*SM ! Numbers of elements along the disk thickness
! (should be even number!)
R1DIV=16*SM ! Numbers of elements along the radial direction from 0 to R1
R12DIV=32*SM ! Numbers of elements along the radial direction from R1 to R2
R23DIV=16*SM ! Numbers of elements along the radial direction from R2 to R
```

Therefore in order to analyze the convergence we can perform computations with different values of the parameter  $SM$ . The results of this computation series are presented in Table 3.7. As it can be seen from the table, the maximum values of the displacements get stabilized already at  $SM=0.75$  and continue stabilizing further with an increase of the parameter  $SM$ , i. e. when the sizes of finite elements become smaller the values of the displacements almost do not change. Thus, based on the data from Table 3.7 we can conclude that in order to estimate the maximal displacements for this problem it is enough to take  $SM=0.75$ . However, already at  $SM=0.25$  the relative error in the determination of displacements is less than 3 %, which is enough for the majority of practical applications.

The value  $SM=0.25$  means that we take two finite elements ( $HDIV = 2$ ) along the disk thickness . This rather coarse mesh is satisfactory to define the displacements, as the considered problem is static and has rather simple geometry, and the elements **PLANE223** are finite elements with quadratic approximation for each canonic variable.

Meanwhile, as it can be seen from Fig. 3.10, the electric field vector changes significantly in the vicinity of the boundaries of the electrode surfaces (red vectors). Data from Table 3.7 shows that, when the mesh

**Table 3.7.** Data to analyze the convergence of results

SM	0.25	0.50	0.75	1.00	1.25	1.50	1.75	2.00
$\max u_y \cdot 10^{-12}$ (m)	255	260	262	262	262	262	262	262
$\max  \mathbf{E} $ (V/m)	1001	1141	262	1293	1564	1685	1798	1904

density increases, the maximal values of the electric field vector magnitude also increase, and we observe no convergence for this values. This effect can be expected, as in the electroelasticity problems the surface electrodes are the concentrators for various components of the electromechanical fields of stresses, strains, electric field intensity and electric induction (i. e. for gradient or flow values defined by the derivatives of displacements and electric potential). The role of surface electrodes in these problems are similar to the roles of the stamps with non-smooth boundaries in contact problems. Therefore, as in analogous contact problems, in the vicinity of the electrode boundaries some components of stresses, strains, electric field intensity and electric induction can have root singularities, such as  $\bar{r}^{-1/2}$ , where  $\bar{r}$  is the distance from the electrode boundary. Naturally, when using conventional isoparametric finite elements, we will observe an increase of the values of these fields in the vicinity of the electrode boundaries. In practice it means that specific values of such flow variables in a small area near the electrode boundaries do not have much sense, but far away from the electrode boundaries the convergence will take place. The integral values (for example, the total electric charge) will also converge.

The idea stated above can be illustrated by a graph (Fig. 3.11) that shows the change of the axial component of the electric field intensity  $E_z$  (**EF**, **Y** in ANSYS) along the radius of the disk on its upper surface ( $0 \leq X \leq R$ ,  $Y = H/2$  in ANSYS). This graph can be plotted in ANSYS General Postprocessor by the following commands:

```
! File      FE_Mod_CP_1_Post.inp
! Postprocessor plot of the graphs
\
/PLOPTS,INFO,ON
/COLOR,CURVE,WHIT,1,6 ! color for the graphs - white
                        ! (will be black after inversion)
/COLOR,GRID,WHIT,    ! color for mesh - white
                        ! (will be black after inversion)

/PLOPTS,TITLE,OFF ! no title for the graph
/PLOPT,FRAME,OFF ! no frame
/AXLAB,X,r      ! label for the X-axis (r-axis)
/AXLAB,Y, E_Z  ! label for the Y-axis (z-axis)
/GROPT,DIVX,4 ! Number of divisions along X-axis
/GROPT,DIVY,4 ! Number of divisions along Y-axis
/GROPT,DIG2,1 ! Number of digits after decimal point

! Commands to define a path by a number of points
PATH,XX,4,,120
```



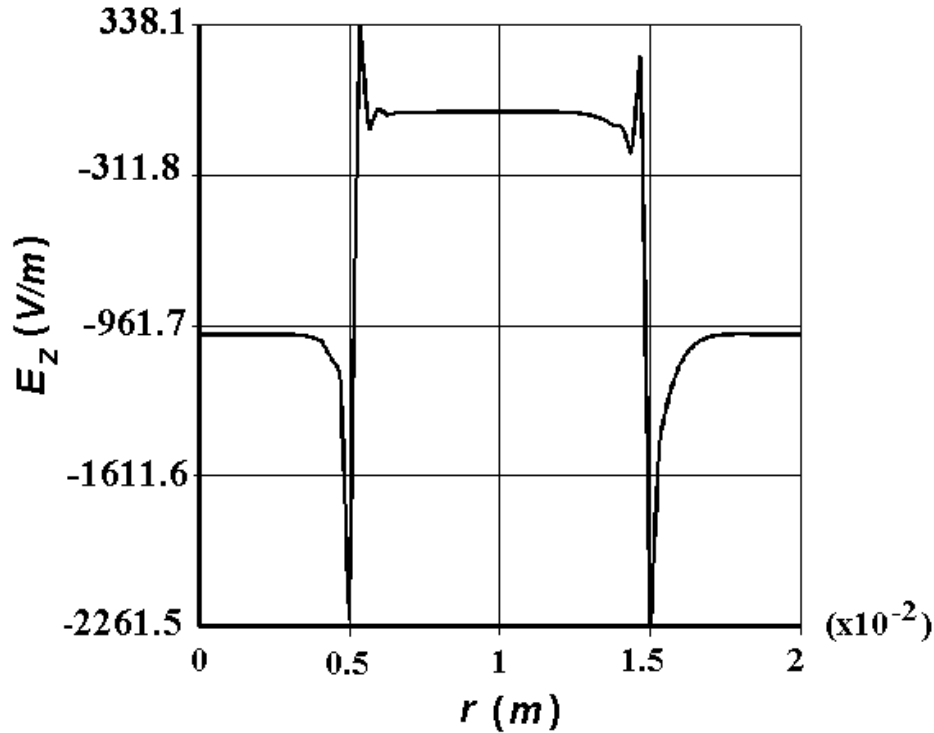


Figure 3.11. Behavior of the component  $E_z$  on the disk surface

```

PPATH,1,,0,H/2
PPATH,2,,R1,H/2
PPATH,3,,R2,H/2
PPATH,4,,R,H/2 ! Define a variable E_Z for plotting a graph along the path
PDEF,E_Z,EF,Y ! Define other variables (if needed)
PDEF,T_ZZ,S,Y $ PDEF,T_RR,S,X
PDEF,D_Z,D,Y $ PDEF,D_R,D,X $ PDEF,E_R,EF,X

PLPATH,E_Z ! Plot a graph of E_Z along the path

```

The finite element results presented in Fig. 3.11 for the dependence  $E_z = E_z(r)$  are not accurate in the vicinity of the electrode boundaries  $R_1 = 0.5 \cdot 10^{-2}$  (m) and  $R_2 = 1.5 \cdot 10^{-2}$  (m). If, for example, at  $r < R_1$  this curve is somewhat similar to a function with a root singularity  $k\sqrt{R_1^2 - r^2}$ , than a jump of the function at  $r > R_1$  is completely determined by the error of finite element approximations and the averaging techniques adopted here for calculation of the field gradients. However, far away from the electrode boundaries the field is determined with sufficient accuracy.

By analogy we can analyze the behavior of other gradient values of electromechanical fields:  $E_r$ ,  $D_z$ ,  $D_r$ ,  $\sigma_{zz}$ , etc.

### 3.1.2 Individual assignments

Write a program code in ANSYS APDL to compute a static deformation of a piezoelectric transducer with multi-electrode coating in 2D setting (axisymmetric or plane strain problem). Analyze the convergence of results for various density of finite element mesh. Plot the computation results (deformed shape, distribution of displacements, electric field vector, electric induction vector, von Mises stresses, graph of characteristic component of the electric field vector along the path with surface electrodes). Analyze the results and prepare a report.

The report should contain the name of the student, the full description of the problem and the results obtained in ANSYS.

The variants of individual tasks are presented in the Table 3.8. All sections of piezoelectric transducers are made of piezoceramics PZT-4, which material properties are provided in the above example problem (see program code). The electroded surfaces are shown in thick lines or dots, the values of electric potential or total electric charge are provided nearby. The rigidly fixed boundaries are marked by external hatching, the triangles outside the boundaries denote the fixing conditions in the corresponding point of the 2D disk section ( $\triangleleft$  or  $\triangleright$  denotes  $UX=0$ ,  $\triangle$  denotes  $UY=0$ ). The boundaries without any labels indicate homogeneous natural boundary conditions ( $\mathbf{n} \cdot \mathbf{D} = 0$  and/or  $\mathbf{n} \cdot \boldsymbol{\sigma} = 0$ ). For axisymmetric problems the axis of rotation  $Y$  is shown on the left by a dashed line.

**Table 3.8.** Variants of individual tasks for the practical assignment No. 1

No.	Scheme	Input data
1		Plane strain. $a_1 = a_4 = 8 \cdot 10^{-3}$ m, $a_2 = a_3 = 7 \cdot 10^{-3}$ m, $H = 3 \cdot 10^{-3}$ m, $V = 10$ V
2		Axisymmetric problem. $a_2 = a_3 = 8 \cdot 10^{-3}$ m, $H = 3 \cdot 10^{-3}$ m, $V = 5$ V

**Table 3.8.** Variants of individual tasks for the practical assignment No. 1 (continue)

<p>3</p>		<p>Plane strain.  <math>a_1 = a_4 = 7 \cdot 10^{-3}</math> m,  <math>a_2 = a_3 = 6 \cdot 10^{-3}</math> m,  <math>H = 2 \cdot 10^{-3}</math> m,  <math>V = 5</math> V</p>
<p>4</p>		<p>Axisymmetric problem.  <math>a_1 = a_3 = 0.02</math> m,  <math>a_2 = 0.03</math> m,  <math>H = 0.005</math> m,  <math>V = 10</math> V</p>
<p>5</p>		<p>Plane strain.  <math>a_1 = a_3 = 0.03</math> m,  <math>a_2 = 0.04</math> m,  <math>H = 0.004</math> m,  <math>V = 10</math> V</p>
<p>6</p>		<p>Axisymmetric problem.  <math>a_1 = a_3 = 6 \cdot 10^{-3}</math> m,  <math>a_2 = a_4 = 7 \cdot 10^{-3}</math> m,  <math>H = 2 \cdot 10^{-3}</math> m,  <math>V = 10</math> V</p>
<p>7</p>		<p>Axisymmetric problem.  <math>a_1 = 0.01</math> m,  <math>a_3 = 0.02</math> m,  <math>a_2 = 0.03</math> m,  <math>H = 0.005</math> m,  <math>V = 5</math> V</p>
<p>8</p>		<p>Plane strain.  <math>a_1 = a_3 = 0.03</math> m,  <math>a_2 = 0.04</math> m,  <math>H = 0.006</math> m,  <math>V = 10</math> V</p>

Table 3.8. Variants of individual tasks for the practical assignment No. 1 (continue)

9		<p>Plane strain.  <math>a_1 = a_3 = 7 \cdot 10^{-3}</math> m,  <math>a_2 = a_4 = 8 \cdot 10^{-3}</math> m,  <math>H = 3 \cdot 10^{-3}</math> m,  <math>V = 10</math> V</p>
10		<p>Axisymmetric problem.  <math>a_1 = a_2 = 8 \cdot 10^{-3}</math> m,  <math>a_3 = a_4 = 6 \cdot 10^{-3}</math> m,  <math>H = 3 \cdot 10^{-3}</math> m,  <math>V = 5</math> V</p>
11		<p>Axisymmetric problem.  <math>a_1 = a_3 = 0.01</math> m,  <math>a_2 = 0.02</math> m,  <math>H = 0.005</math> m,  <math>V = 5</math> V</p>
12		<p>Plane strain.  <math>a_1 = a_3 = 0.02</math> m,  <math>a_2 = 0.04</math> m,  <math>H = 0.008</math> m,  <math>V = 10</math> V</p>
13		<p>Axisymmetric problem.  <math>a_1 = a_3 = 9 \cdot 10^{-3}</math> m,  <math>a_2 = a_4 = 11 \cdot 10^{-3}</math> m,  <math>H = 3 \cdot 10^{-3}</math> m,  <math>V = 10</math> V</p>
14		<p>Plane strain.  <math>a_1 = a_4 = 11 \cdot 10^{-3}</math> m,  <math>a_2 = a_3 = 9 \cdot 10^{-3}</math> m,  <math>H = 2 \cdot 10^{-3}</math> m,  <math>V = 5</math> V</p>

**Table 3.8.** Variants of individual tasks for the practical assignment No. 1 (continue)

15		Plane strain. $a_1 = a_3 = 0.015$ m, $a_2 = 0.03$ m, $H = 0.004$ m, $V = 5$ V
----	--	---

### 3.2 Practical assignment No. 2.

#### Plane problem of heating and cooling of a thermoelastic body

##### Objectives of the assignment

1. Study the main features of solving transient problems of thermoelasticity in ANSYS APDL on the interaction of solids with acoustic media in ANSYS APDL. The example problem is a plane problem of slow heating and cooling of a body in the shape of letter “R” (input file FE\_Mod\_CP\_2.inp). Estimate the possibilities of solving the problems where mechanical and temperature fields are not fully-coupled and dynamic terms in the motion equations are neglected.
2. Write a program in ANSYS APDL for an individual assignment problem (transient problem for a 2D thermoelastic body under the plane strain conditions).
3. Perform the computations, analyze the results and prepare a report.

##### 3.2.1 Brief information on the solution techniques for the transient problems of thermoelasticity for isotropic bodies

The statement of the transient problems of thermoelasticity was provided previously in section 1.4. This statement contained field equations (1.110), (1.111), constitutive relations (1.112), (1.113), formulas (1.114), (1.115), boundary conditions (1.120)–(1.124), and initial conditions (1.125).

Let us note that many thermoelastic materials are isotropic and their modules from (1.112), (1.113), (1.115) have the following structure

$$c_{ijkl} = \lambda \delta_{ij} \delta_{kl} + \mu (\delta_{ik} \delta_{jl} + \delta_{il} \delta_{jk}), \quad (3.7)$$

$$\gamma_{ij} = \gamma\delta_{ij}, \quad k_{ij} = k\delta_{ij}, \quad (3.8)$$

where  $\lambda, \mu$  are Lamé's coefficients ( $\mu = G$  is also called the shear modulus),  $\gamma$  is the coefficient of thermal stresses,  $k$  is the thermal conductivity coefficient,  $\delta_{ij}$  is Kronecker delta.

For isotropic materials, constitutive relations (1.112), (1.113) in the component-wise form can be written as

$$\sigma_{ij} = \lambda\varepsilon_{kk}\delta_{ij} + 2\mu\varepsilon_{ij} - \gamma\theta\delta_{ij}, \quad (3.9)$$

$$S = \gamma\varepsilon_{kk} + \frac{\rho c_\varepsilon}{T_0}\theta, \quad (3.10)$$

where  $\varepsilon_{kk} = \operatorname{div} \mathbf{u} = \nabla \cdot \mathbf{u} = \sum_{k=1}^3 \varepsilon_{kk}$ .

Then, using (1.118), (1.119), (3.7), (3.8), the system of differential equations of linear thermoelasticity with respect to the components of displacements  $u_i$  and temperature  $\theta$  for isotropic media can be presented in the form

$$\underline{\rho u_{i,tt}} - (\lambda u_{k,k})_{,i} - [\mu(u_{i,j} + u_{j,i})]_{,j} + (\gamma\theta)_{,i} = \rho f_i, \quad i = 1, 2, 3, \quad (3.11)$$

$$\underline{\rho c_\varepsilon \theta_{,t}} - (k\theta_{,j})_{,j} + T_0 \gamma u_{k,kt} = W. \quad (3.12)$$

In (3.11), (3.12) we have underlined the terms that can be omitted without significant loss of accuracy. For example, as it was noted in section 1.4, the underlined term in (3.12) in the majority of thermoelastic problems appears to be small and can be left out of consideration (theory of thermal stresses). In such model in (3.12) we can formally set  $T_0 = 0$ , which will reduce (3.12) to the classical equation of transient thermal conductivity. It is clear that Eq. (3.12) with  $T_0 = 0$  together with boundary conditions (1.122)–(1.124) and initial conditions (1.125) for the temperature gives an uncoupled thermoelastic problem where the field  $\theta$  is determined independently from the displacement field  $\mathbf{u}$ .

The system (3.11), (3.12) can be additionally simplified if we omit the underlined summand in (3.11). In this case the motion equation (3.11) turns into a more simplified equation of statics (more precisely, quasi-statics). Such simplification is appropriate for many transient problems when the external heat influences change in time much slower compared to the characteristic times for the elastic waves propagation.

Let us give several comments regarding the material properties of isotropic media. As it can be seen from (3.11), (3.12), the isotropic thermoelastic media are characterized by six material modules: the porosity  $\rho$ ; the Lamé's parameters  $\lambda, \mu$ ; the coefficient of thermal stresses  $\gamma$ ;

the thermal conductivity coefficient  $k$  and the specific heat  $c_\varepsilon$ , calculated at constant strains. However, more often instead of the parameters  $\lambda$ ,  $\mu$ ,  $\gamma$  and  $c_\varepsilon$  the following values are used: the Young's modulus  $E$ ; the Poisson's ratio  $\nu$ ; the coefficient of thermal extension  $\alpha$  and the specific heat  $c_\sigma$ , calculated at constant stresses. These modules are present in the constitutive relations that connect the pairs  $(\varepsilon_{ij}, S)$  and  $(\sigma_{ij}, \theta)$ :

$$\varepsilon_{ij} = -\frac{\nu}{E}\sigma_{kk}\delta_{ij} + \frac{(1+\nu)}{E}\sigma_{ij} + \alpha\theta\delta_{ij}, \quad (3.13)$$

$$S = \alpha\sigma_{kk} + \frac{\rho c_\sigma}{T_0}\theta. \quad (3.14)$$

From (3.9), (3.10), (3.13), (3.14) it can be obtained that these modules can be expressed through one another by formulas:

$$E = \frac{\mu(3\lambda + 2\mu)}{\lambda + \mu}, \quad \nu = \frac{\lambda}{2(\lambda + \mu)}, \quad \alpha = \frac{(1 - 2\nu)}{E}\gamma, \quad c_\sigma = c_\varepsilon + \frac{3T_0\alpha\gamma}{\rho}. \quad (3.15)$$

In ANSYS APDL the material properties  $\rho$ ,  $E$ ,  $\nu$ ,  $\alpha$ ,  $k$  and  $c_\sigma$  can be set by the commands **MP**, *Lab*, *MAT*, *C0*, where *Lab* is the name of the module, *MAT* is the number of the group of material properties, *C0* is the value of the module with the name *Lab*. Here *Lab* = **DENS** defines the porosity  $\rho$ ; *Lab* = **EX** is the Young's modulus  $E$ ; *Lab* = **NUXY** or *Lab* = **PRXY** is the Poisson's ratio (for isotropic media **NUXY**=**PRXY**); *Lab* = **ALPX** is the coefficient of thermal extension; *Lab* = **KXX** is the thermal conductivity coefficient; *Lab* = **C** is the specific heat, calculated at constant stresses.

All these modules can also depend on temperature according to the polynomial law when using the command **MP**, *Lab*, *MAT*, *C0*, *C1*, *C2*, *C3*, *C4*. Then the value with the name *Lab* will be calculated by the formula  $C0 + C1\theta + C2\theta^2 + C3\theta^3 + C4\theta^4$ , and the problem becomes nonlinear by  $\theta$ , if any value among *C1*, *C2*, *C3*, *C4* will differ from zero.

The following finite elements are available in ANSYS for solving coupled thermoelastic problems: **PLANE223** with KEYOPT(1)=11 is a 2D quadrilateral element with 8 nodes; **SOLID226** with KEYOPT(1)=11 is a hexahedron with 20 nodes; **SOLID227** with KEYOPT(1)=11 is a tetrahedron with 10 nodes. These elements enable to solve transient problems, problems of steady-state oscillations and stationary problems of thermoelasticity.

Obsolete finite elements, such as **PLANE13** with KEYOPT(1)=4 (2D quadrilateral element with 4 nodes), **SOLID5** with KEYOPT(1)=0

(hexahedron with 8 nodes) and **SOLID98** with `KEYOPT(1)=0` (tetrahedron with 10 nodes), can be applied for solving transient and stationary problems of thermal stresses. The use of the elements **PLANE223**, **SOLID226** and **SOLID227** can also lead to the theory of thermal stresses, if we set  $T_0 = 0$ . The latter can be done by applying the command **TOFFST, 0**.

For simulating the problems of thermal stresses when the dynamic summand in (3.11) is omitted, but in (3.12) with  $T_0 = 0$  a transient equation for temperature is used, we can set small porosity  $\tilde{\rho} = \kappa\rho$ , where  $\kappa \ll 1$ , and  $c_p$  can be substituted by  $\tilde{c}_p = \kappa^{-1}c_p$ . Then Eq. (3.12) will hold as  $\tilde{\rho}\tilde{c}_p = \rho c_p$ , and  $c_p = c_\varepsilon$  for  $T_0 = 0$ .

There are other approaches to solving in ANSYS the problems of thermoelasticity with various degree of coupling which had been developed before the finite elements **PLANE223**, **SOLID226** and **SOLID227** were introduced. The description of these approaches can be found in ANSYS documentation in the section **Coupled-Field Analyses Guide**.

### 3.2.2 Example problem and solution methods

#### Problem description

Let us consider a transient problem of thermoelasticity for a plane domain in the shape of the letter “R”. The geometry of the domain in the Cartesian coordinate system  $Oxy$  is shown in Fig. 3.12(a). The sizes of the body are defined by the following parameters: the height is  $HL = 0.14$  (m); the width is  $WL = 0.08$  (m); the width of the walls is  $WWL = 0.02$  (m); the additional size along the height is  $HAL = 0.07$  (m). Curvilinear parts of the domain are defined by the parts of the ellipses with the ellipticity parameter  $PEL = (HAL/2)/(WL - WWL)$ , which define the ratio of the ellipse  $y$ -axis radius to the ellipse  $x$ -axis.

Let us assume that the material of the domain is steel (isotropic material) with the Young’s modulus  $E = 2 \cdot 10^{11}$  (N/m<sup>2</sup>), the Poisson’s ratio  $\nu = 0.29$ , the density  $\rho = 7800$  (kg/m<sup>3</sup>), the coefficient of thermal conductivity  $k = K_{XX} = 46.7$  (W/(m · K)), the coefficient of thermal expansion  $\alpha = 1.51 \cdot 10^{-5}$  (1/K) and the specific heat  $c_\sigma = 462$  (J/(kg · K)), calculated at constant stresses.

It is assumed that the temperature  $\theta$  on the bottom edge always equals 0°C. At the initial time moment  $t = 0$  the body was at rest. Then starting from the initial time moment till the time  $t = TES1 = 10$  (s) the temperature on the top edge has been increasing linearly from zero to 90°C.



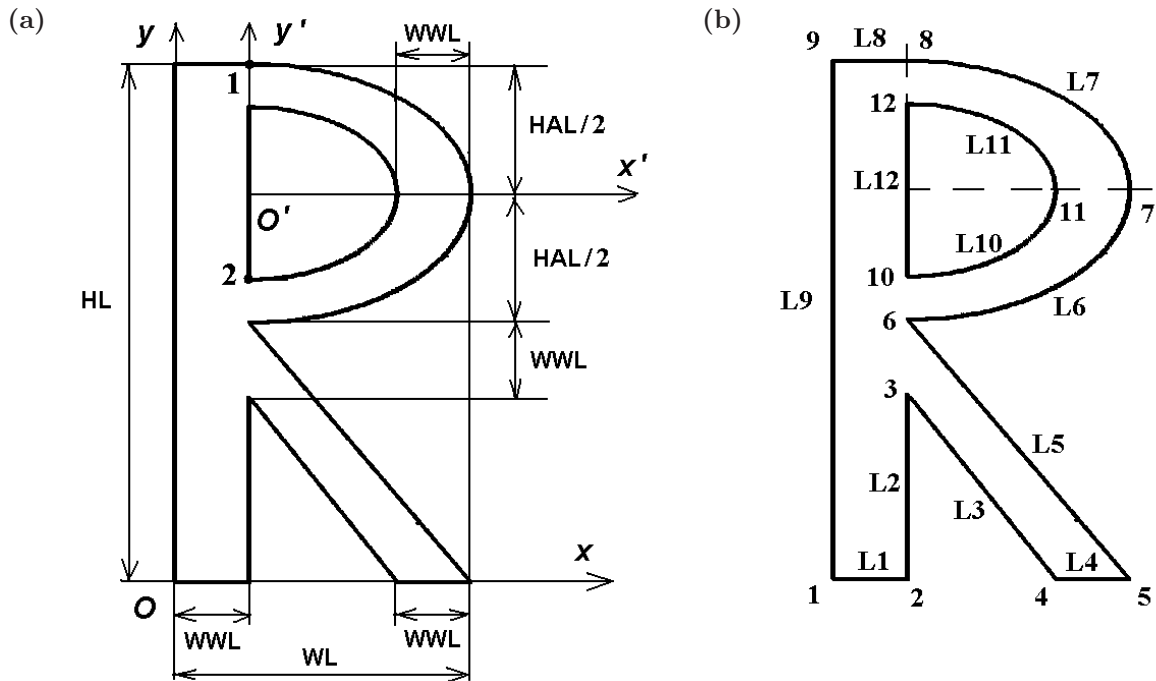


**Figure 3.12.** Geometry of the domain: (a) scheme of the domain; (b) numbering of keypoints and lines

After that the top edge was subjected to the conditions of convective heat transfer with the heat transfer coefficient  $h_f = 60$  (W/(m<sup>2</sup>·K)) and the ambient temperature  $\theta_b = 0^\circ\text{C}$ . The rest of the boundary for all considered time moments is thermally insulated, i. e. the normal component of the heat flux vector is equal to zero:  $\mathbf{n} \cdot \mathbf{q} = 0$ . The bottom edge of the body is considered to be rigidly fixed all the time.

The aim of the problem is to determine the fields of temperatures and displacements in the time interval  $t \in [0, TES2]$ ,  $TES2 = 120$  s, plot the graphs of time dependencies for the temperature  $\theta$  and the displacements  $u_y$  for two control points  $\mathbf{x}_1 = [WWL, HL]$  and  $\mathbf{x}_2 = [WWL, HL - HAL/2 - (WL - 2 * WWL) * PEL]$  (see Fig. 3.12(a), where the points are marked by numbers 1 and 2).

In order to investigate the influence of the coupling and dynamic effects, it is necessary to compare results for three different problems:

- 1) transient thermoelastic problem with full coupling;
- 2) transient thermoelastic problem with partial coupling when the problem for the temperature field does not depend on mechanical fields, i. e. it coincides with transient problem of thermal conductivity;
- 3) thermoelastic problem with partial coupling when the problem for the temperature field does not depend on mechanical fields, i. e. it

coincides with nonstationary problem of thermal conductivity, and the motion equations are considered in quasi-static statement.

The example of problem solving is provided in the file FE\_Mod\_CP\_2.inp.

### Text of input file FE\_Mod\_CP\_2.inp

```
! File   FE_Mod_CP_2.inp
! Test problem No. 2
! TWO-DIMENSIONAL PROBLEM
! THERMOELASTIC BODY
! Transient problem

! Invert background from black to white
/RGB,INDEX,100,100,100,0
/RGB,INDEX,0,0,0,15

/PREP7
! All values in SI system

TES1=10   ! time value at the end of the first step
TES2=120 ! time value at the end of the second step
! substeps for time steps
DT1=1    ! substep value for the step 1
DT2=2    ! substep value for the step 2

! Conditions for thermal analysis
T_INP1=0  ! Temperature on the bottom edge
T_INP2=90 ! Temperature on the right top edge (for time step 1)

T_EXT=0 ! Ambient temperature for convective heat transfer conditions
H_F=60  ! Coefficient of convective heat transfer

! Temperature difference from zero to absolute zero
TOFFST, 273
! For TOFFST=0 a heat equation is a thermal conductivity equation
! TOFFST, 0

! Material properties (steel)
E1=2.1e11 ! Young's modulus
NU1=0.29 ! Poisson's ratio
RH01=7.8e3 ! Density
K1=46.7 ! Thermal conductivity coefficient
C1=462 ! Specific heat
ALPH1=1.51e-05 ! Coefficient of thermal expansion

MP,EX,1,E1
```

```

MP,DENS,1,RHO1
MP,NUXY,1,NU1
MP,KXX,1,K1
MP,C,1,C1
MP,ALPX,1,ALPH1

! Commands to analyze the capabilities for not taking into account
! dynamic terms in the motion equations

! KAPPA=1e-6
! MP,DENS,1,RHO1*KAPPA
! MP,C,1,C1/KAPPA

ET,1,PLANE223,11,,2 ! Quadrilateral finite element with 8 nodes
                   ! Degrees of freedom UX, UY, TEMP, plane strain

! Geometrical sizes of the body in the shape of letter 'R'
HL=0.14 ! Height
WL=0.08 ! Width
WWL=0.02 ! Width of the walls of letter 'R'
HAL=0.07 ! Additional size along the height

! Meshing parameters
DMESH=WWL/4

PEL=(HAL/2)/(WL-WWL) ! Ellipticity parameter for curvilinear part
LOCAL,11,1,WWL,HL-HAL/2,,,,PEL ! Elliptical CS with number 11
CSYS,0 ! Change active coordinate system to Cartesian

! Build the geometry of the domain
! External part - area 1
K,1,0,0
K,2,WWL,0
K,3,WWL,HL-HAL-WWL
K,4,WL-WWL,0
K,5,WL,0
K,6,WWL,HL-HAL
K,7,WL,HL-HAL/2
K,8,WWL,HL
K,9,0,HL
L,1,2 $ L,2,3 $ L,3,4 $ L,4,5 $ L,5,6

CSYS,11
L,6,7 $ L,7,8
CSYS,0
L,8,9 $ L,9,1
AL,1,2,3,4,5,6,7,8,9

```

```
! Hole - area 2
K,10,WWL,HL-HAL/2-(WL-2*WWL)*PEL
K,11,WL-WWL,HL-HAL/2
K,12,WWL,HL-HAL/2+(WL-2*WWL)*PEL
CSYS,11
L,10,11 $ L,11,12
CSYS,0
L,12,10
AL,10,11,12
ASBA,1,2 ! Subtract area 2 from area 1

! Set the size of finite elements
ESIZE,DMESH

AMESH,ALL

! Conditions for rigidly fixed boundary
NSEL,S,LOC,Y,0 ! Select the nodes on the bottom (along Y-axis)
D,ALL,UX,0
D,ALL,UY,0 NSEL,ALL ! Select all nodes of the model

! Select the nodes to monitor the results
! Node N1_MON is in the upper part of the domain
! Y=HL, X=WWL
NSEL,S,LOC,Y,HL,HL
NSEL,R,LOC,X,WWL
*GET,N1_MON,NODE,,NUM,MIN
! Node N2_MON is below at X=WWL

NSEL,S,LOC,Y,HL-HAL/2-(WL-2*WWL)*PEL
NSEL,R,LOC,X,WWL
*GET,N2_MON,NODE,,NUM,MIN
NSEL,ALL

FINISH

! Solution of coupled thermoelastic problem
/SOLU ! Enter the solver
ANTYPE,TRANS ! Select the analysis type: transient analysis
KBC,0 ! Specify linearly interpolated (ramped) load

! Damping coefficient in time integration scheme
!TINTP,0.005 ! TINTP=0.005 - default value
TIME,TES1 ! Time at the end of step 1
DELTIM,DT1 ! Substep for step 1
```

```
NSEL,S,LOC,Y,0      ! Select the nodes on the bottom (by Y-axis)
D,ALL,TEMP,T_INP1 ! For all selected nodes set TEMP=T_INP1

NSEL,S,LOC,Y,HL,HL ! Select the nodes on the top (by Y-axis)
NSEL,R,LOC,X,0,WWL
D,ALL,TEMP,T_INP2  ! For all selected nodes set TEMP=T_INP2

NSEL,ALL
! Write to the database the results of nodal solution
! for all substeps
OUTRES,BASIC,ALL
SOLVE

! Step 2
TIME, TES2
DELTIM,DT2 KBC,1 ! Constant values of external influences

NSEL,S,LOC,Y,HL,HL ! Select the nodes on the top (by Y-axis)
NSEL,R,LOC,X,0,WWL
DDEL,ALL,TEMP ! Remove the conditions TEMP=T_INP2

SF,ALL,CONV,H_F,T_EXT ! Convective heat transfer in the selected nodes

NSEL,ALL

SOLVE
SAVE
FINISH

/POST26
/SHOW,WIN32C ! Specify device for graphical output
/TRIAD,OFF      ! Do not show the global coordinate triad

/PLOPTS,INFO,2    ! Use Auto-legend format
/PLOPTS,LEG2,OFF
/PLOPTS,LOGO,OFF  ! Do not show ANSYS logo
/PLOPTS,FRAME,OFF ! Do not show frame
/PLOPTS,DATE,OFF  ! Do not show date
/COLOR,CURVE,WHIT,1,6 ! Curve color for graphs -- white
                        ! (black after inversion)
/COLOR,GRID,WHIT ! Grid color -- white (black after inversion)
/GMARKER,1,2,3 ! Label 2 for curve 1 -- boxes, for every 3rd value
/GMARKER,2,4,3 ! Label 4 for curve 2 -- crosses, for every 3rd value
/GRID,1 ! Grid by X and Y (full grid)

/XRANG,0, TES2
/AXLAB,Y, Temperature (degree) ! Label for Y-axis
```

```

/AXLAB,X,Time (sec) ! Label for X-axis
NSOL,2,N1_MON,TEMP,,TEMP1 ! Variable 2 -- temperature in node N1_MON
NSOL,3,N2_MON,TEMP,,TEMP2

NSOL,4,N1_MON,U,Y,UY1 ! Variable 4 -- displacement UY in node N1_MON
NSOL,5,N2_MON,U,Y,UY2

PLVAR,2,3 ! Plot graphs of variables 2, 3 versus time (variable 1)

! Remove comments to show UY in control nodes
! /AXLAB,Y,UY (m)
! PLVAR,4,5

```

This program solves a coupled linear problem of thermoelasticity in assumption of plane strain when  $\mathbf{u} = \{u_x(x, y, t), u_y(x, y, t), 0\}$ ,  $\theta = \theta(x, y, t)$ .

As in the example from practical assignment 1, here we begin with building the solid model and then proceed to the finite element model. The solid model is obtained by constructing geometrical objects using the bottom to top method. Firstly the keypoints are created, then the keypoints are connected by lines (see Fig. 3.12(b)), and after that the areas are generated.

To construct a solid model, we will build two simply connected domains. The first domain is bounded by the outer lines of the letter “R”, and the second domain is bounded by the inner lines of the letter “R”. Then we use Boolean operation of subtraction (**ASBA** command) to obtain the resulting domain in the shape of the letter “R” with a hole. The curved lines are defined as segments of two ellipses in the corresponding elliptical coordinate system.

The finite element model is generated using free meshing in quadrilateral elements **PLANE223** with appropriate options. The global element size *DMESH* defines the maximal element edge length and specifies the density of the mesh. The structure of the finite element mesh for  $DMESH = WWL/4$  is shown in Fig. 3.13 (Fig 3.13(a) shows elements, Fig 3.13(b) shows nodes).

Fig. 3.13 also shows external influences at various time steps. (To show boundary conditions in the interactive mode execute: *Plot* → *Elements* or *Plot* → *Nodes*, *PlotCtrls* → *Symbols* → tick *All Applied BCs*. To plot the conditions of convective heat transfer with arrows, in menu path *Surface Load Symbols* specify *Convect FilmCoef* and for *Show pres and convect as* select *Arrows*.)

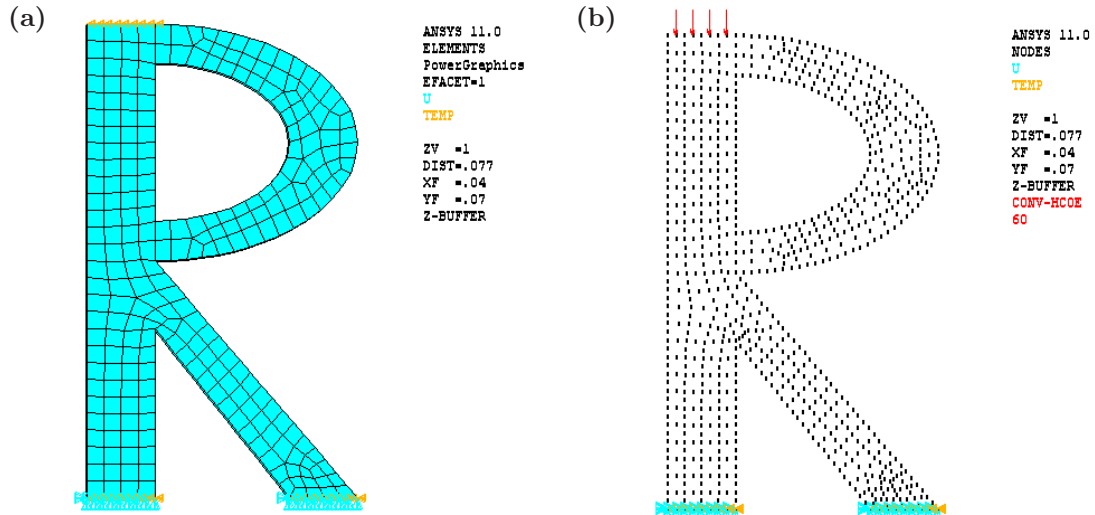


**Figure 3.13.** Finite element model:

- (a) elements and boundary conditions at the first time step;
- (b) nodes and boundary conditions at the second time step

The solution of transient problem is divided in two time steps  $t \in [0, TES1]$  and  $t \in [TES1, TES2]$ . At every time step the finite element system of ordinary differential equations of transient thermoelasticity (1.165), (1.166) is integrated by time with the substep  $\Delta t_j$  ( $\Delta t_1 = 1$  s,  $\Delta t_2 = 2$  s) by the modified Newmark scheme [1].

We note that different boundary conditions are set at the first and at the second time step on the top edge of the domain. At the first time step the temperature (Fig. 3.13(a)) is specified with linear change by time (**KBC,1**), and at the second time step instead of the temperature the condition of the convective heat transfer (Fig. 3.13(a)) is specified, which ensures the cooling of the body. The parameters of this boundary condition (the coefficient of heat transfer and the ambient temperature) are constant at the second time step, which is defined by the command **KBC,0**.

After solving the problem, the program enters the time-history postprocessor **POST26** to plot the graphs of the temperature dependence on time in characteristic points  $\mathbf{x}_1$  and  $\mathbf{x}_2$ . These dependences are shown in Fig. 3.14(a), where the boxes denote the graph for  $\theta_h(\mathbf{x}_1, t)$ , and the crosses denote the graph for  $\theta_h(\mathbf{x}_2, t)$ . After executing two commented commands from the program file, we can obtain the graphs of the time dependences for the displacements  $u_{yh}(\mathbf{x}_1, t)$  and  $u_{yh}(\mathbf{x}_2, t)$ . These curves are provided in Fig. 3.14(b), where by analogy the boxes denote the graph for  $u_{yh}(\mathbf{x}_1, t)$  and the crosses denote the graph for  $u_{yh}(\mathbf{x}_2, t)$ .

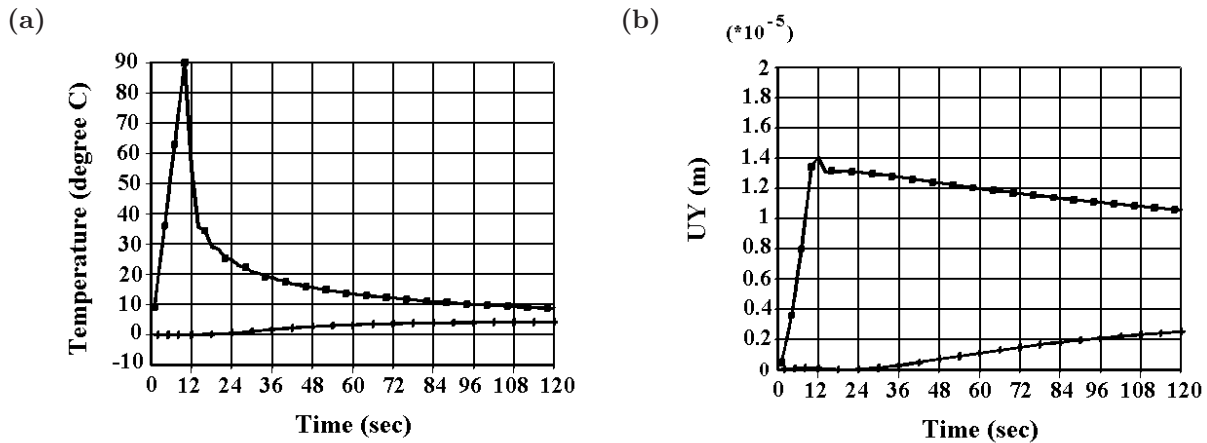


**Figure 3.14.** Temperature and displacements in characteristic points:  
 (a)  $\theta_h(\mathbf{x}_j, t)$ ; (b)  $u_{yh}(\mathbf{x}_j, t)$

As it can be seen from Fig. 3.14, at the stage of cooling the temperature on the top edge decreases much faster than the displacements  $u_y$  decline. Besides, inside the body the temperature and the displacements are gradually getting aligned, moreover the temperature and the displacements inside the body can even increase at the stage of cooling for a certain time interval.

Then using the interactive mode in General postprocessor **POST1** we can plot the pictures of various nodal values distribution (NSOL) for every substep. In order to do this it is necessary to read the data for the selected substep, for example, by menu path *General PostProc*  $\rightarrow$  *Read Results*  $\rightarrow$  *By Pick*  $\rightarrow$  then select the time substep value  $\rightarrow$  *Read*  $\rightarrow$  *Close*. After that we can plot the distribution of the values of interest NSOL in a usual way. For example, to plot the contour plot of the temperature field, execute *General PostProc*  $\rightarrow$  *Plot Results*  $\rightarrow$  *Contour plot*  $\rightarrow$  *Nodal Solution*  $\rightarrow$  *DOF Solution*  $\rightarrow$  *Nodal Temperature*; to plot the vector plot of the heat flux, execute *General Postproc*  $\rightarrow$  *Plot Results*  $\rightarrow$  *Vector Plo*  $\rightarrow$  *Predefined*  $\rightarrow$  *Flux & gradient*  $\rightarrow$  *Thermal flux TF*; etc.

Fig. 3.15 demonstrates some results for the time moment at the end of the first time step  $t = TES1$ , i. e. in the end of the heating stage: Fig. 3.15(a) shows the distribution of the temperature field, Fig. 3.15(b) shows the vector plot for the heat flux. Similar results at the final monitoring stage of the cooling process  $t = TES2$  are shown in Fig. 3.16.

These and other figures clearly demonstrate the process of the heat distribution in the body. It is only necessary to take into account that the color palette in different pictures every time corresponds to completely different ranges of values.



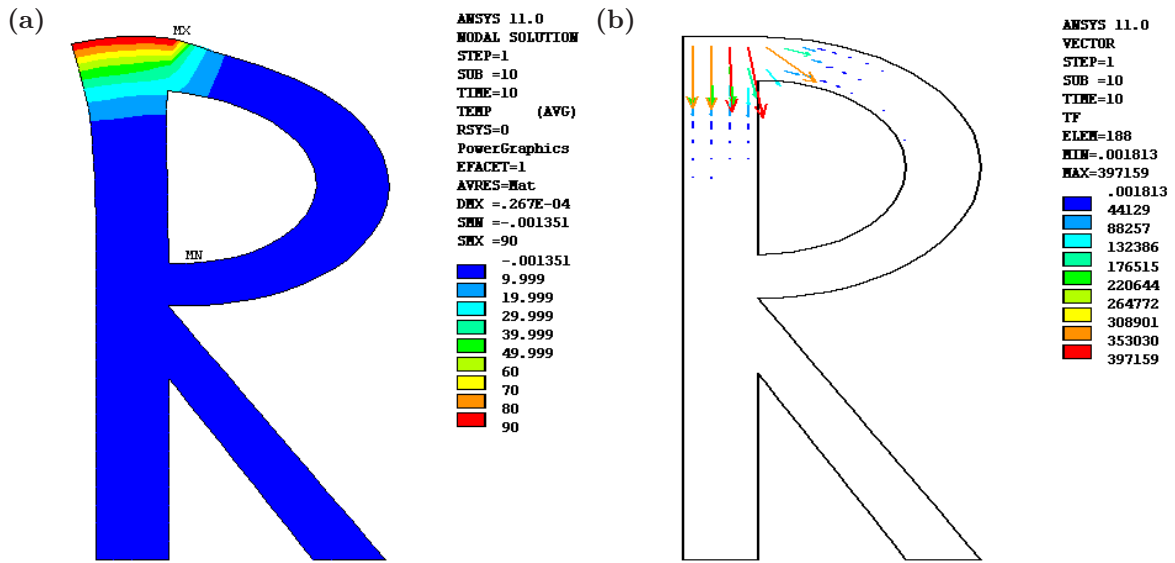


Figure 3.15. Some results at the end of the heating stage:  
(a) temperature; (b) heat flux vector

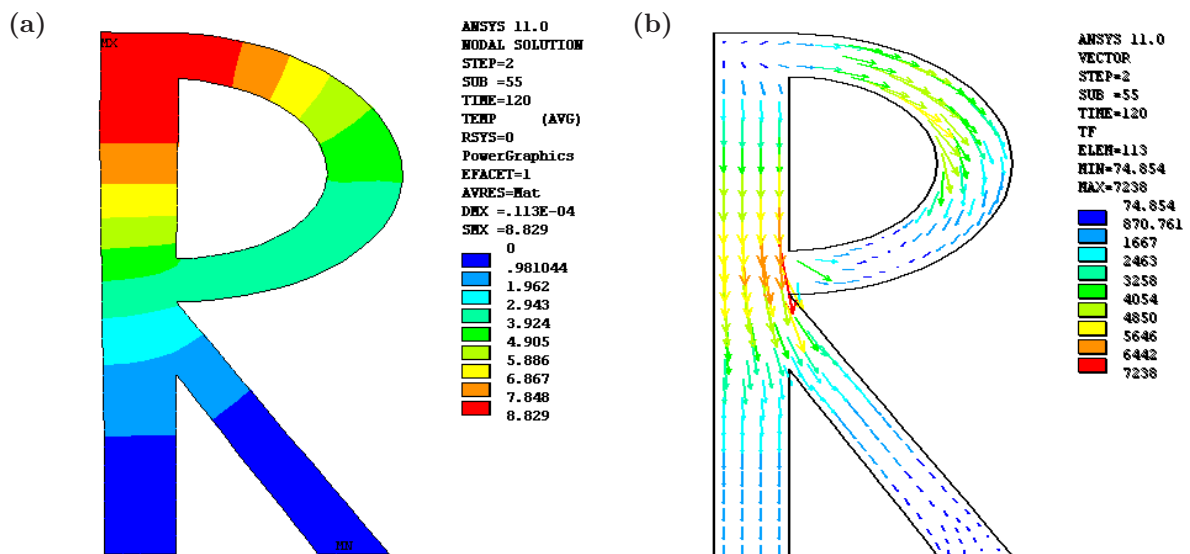


Figure 3.16. Some results at the end of the monitoring stage:  
(a) temperature; (b) heat flux vector

If in the file **FE\_Mod\_CP\_2.inp** we remove the comment sign in the line

```
! TOFFST, 0
```

i. e. execute the command **TOFFST, 0**, then ANSYS will calculate thermal stresses.

If we additionally remove the comments in the lines

```
! KAPPA=1e-6
```

```
! MP,DENS,1,RHO1*KAPPA
```

! MP,C,1,C1/KAPPA

then the problem of thermoelasticity with partial coupling will be solved, when the temperature field does not depend on the mechanical fields, and for the displacements the quasistatic equation is used. The computations show that the same results will be obtained for the temperature and the stresses in the control points, i. e. the resulting curves for  $\theta_h(\mathbf{x}_j, t)$  and  $u_{yh}(\mathbf{x}_j, t)$  will visually coincide.

Finally, we note that here the accuracy of the obtained results depends on many parameters. The maximal size of the elements  $DMESH$  determines the errors of discretization by spatial variables and the use of the finite elements that are quadratic by canonical coordinates gives theoretical error of the order  $O(DMESH^2)$ . The time tubsteps  $\Delta t_j$  give the estimation of the error of discretization by time, which are similar to the estimation of the error of discretization by spatial variables. These estimations are valid only when the solution has limited derivatives of the required degree of smoothness. However, for the areas with corner points and with the change of the types of the boundary conditions the solutions can have local singularities, i. e. they even can have no first derivatives limited in the domain.

Besides, the accuracy of the computations is also sensible to the parameters of the numerical scheme of the modified Newmark method of time integration. In the program the default parameters are used that correspond to the command **TINTP,0.005**. However, for large solution oscillations the parameter of numerical damping of the scheme can be increased or other values for the parameters in the command **TINTP** can be changed.

The results of the numerical experiments for various finite element sizes, time substeps and modified Newmark scheme parameters show sufficient accuracy of the temperature and displacement fields which is acceptable for the test example with the given values.

### 3.2.3 Individual assignments

It is required to calculate thermal stresses induced by thermal influence for a 2D construction in the shape of the letter indicated below. Consider a transient coupled problem of thermoelasticity and its simplified models similar to the previously provided example. For input data take the values similar to those from the test example. The geometrical sizes of the areas can be chosen individually.

Use ANSYS command mode to create solid and finite element models, set the boundary conditions, solve the problem and plot the results using Time-history postprocessor **POST26**. Use ANSYS interactive mode to view the results in General postprocessor **POST1** and plot solid and finite element models.

Analyze the convergence for various values of finite element mesh density, time substeps and modified Newmark scheme parameters. Provide a valid version of the finite element mesh with boundary conditions for various time steps. Analyze the results (graphs of the temperature and displacement dependences on time in the characteristic points, vector plot for the heat flux field) and prepare a report.

The report should contain the name of the student, the full description of the problem and the results obtained in ANSYS.

The variants of individual tasks are presented in the Table 3.9. The domains have the shapes of Latin and Greek letters.

**Table 3.9.** Variants of individual tasks for the practical assignment No. 2

No	1	2	3	4	5	6	7	8
Domain shape	<b>B</b>	<b>C</b>	<b>D</b>	<b>G</b>	<b>J</b>	<b>O</b>	<b>P</b>	<b>Q</b>
No	9	10	11	12	13	14	15	
Domain shape	<b>S</b>	<b>U</b>	$\Omega$	$\Psi$	$\Phi$	$\rho$	$\theta$	

### 3.3 Practical assignment No. 3. Steady-state oscillations of an elastic transmitter in acoustic medium

#### Objectives of the assignment

1. Study the main features of solving the problems on the interaction of solids with acoustic media in ANSYS APDL:
  - acoustic finite elements, including the elements with an option of interaction with solid elements;
  - defining non-reflecting boundary conditions for simulation of “infinite” domains;
  - selecting the parameters and structure of finite element meshes;
  - choosing the solver options;
  - postprocessing features.

The example problem is a two-dimensional problem of steady-state oscillations for an elastic transmitter submerged into acoustic medium (input files FE\_Mod\_CP\_3\_sm.inp, FE\_Mod\_CP\_3\_ha.inp, FE\_Mod\_CP\_3\_hi.inp).

2. Write a program in ANSYS APDL for an individual assignment problem (two-dimensional problem of steady-state oscillations for an elastic transmitter submerged into acoustic medium).
3. Perform the computations, analyze the results and prepare a report.

### 3.3.1 Brief information on the solution techniques for the problems of interaction of solids with acoustic media

Among numerous acoustic problems, the problems of interaction of a solid deformable transmitter with acoustic media are of great interest. Transmitters are usually elastic or piezoelectric bodies that make steady-state oscillations or transient movements under the applied governing influences. If these bodies are submerged into acoustic media than, as it was mentioned in section 1.6, the boundaries of solid and liquid media interact with each other. As a result, acoustic waves are spread in acoustic media, and these waves should be analyzed for the problems of this type (distribution of pressure, pressure gradients, velocity, sound pressure level).

Very often the transmitters have much smaller sizes in comparison with external acoustic medium, and the phenomena of reflection of acoustic waves from their remote boundaries are not of great interest. In such cases we can artificially “cut” the sizes of acoustic medium and set “non-reflecting” boundary conditions on new boundaries. Such conditions ideally should simulate the processes of propagation of acoustic waves through these boundaries without reflection.

The problems of interaction of solids with acoustic media are dynamic problems (problems of steady-state oscillations or transient problems). Therefore, in order to ensure appropriate accuracy of the solution, the finite element sizes should be selected not only from the error estimations for static problems of type  $O(h_s^p / \sin \varphi)$ , where  $h_s$  is the maximal element size,  $\varphi$  is the minimal angle at the element vertex, but should also be related to the lengths of characteristic waves. For example, if  $c_0$  is the velocity of acoustic waves, and the transmitter oscillates with the frequency  $f$ , then the characteristic wave lengths  $\lambda$  can be found by the formula:  $\lambda = c_0 / f$ . Then, depending on the finite element type, its recommended size  $h_d$  for the correct account for oscillation of the acoustic field values can be taken

as  $h_d = \lambda/10$  (for the elements with middle nodes) or  $h_d = \lambda/20$  (for the elements without middle nodes). For small values of the frequencies  $f$  the size  $h_d$  can considerably exceed  $h_s$ , and therefore cannot be taken into account. However, for large frequencies there can be situations when  $h_d \ll h_s$ , i. e. the element size related to the oscillations of the acoustic field values for the oscillation period is the defining value.

Therefore in the considered problems it is required to determine the boundaries of the interaction of solids and acoustic media, non-reflecting boundaries (if there is a necessity) and set reasonable parameters of finite element meshes.

It should be noted that the capabilities of ANSYS software in solving acoustic problems expanded significantly in the recent years. For this book ANSYS 11.0 is used, and therefore main attention is paid to the acoustic analysis implemented in this version of ANSYS. However, the facilities of newer ANSYS versions will be briefly discussed as well.

In ANSYS 11.0 there are two main types of fluid elements: **FLUID29** and **FLUID30**, of the dimension 2-D and 3-D, respectively. **FLUID29** is a quadrilateral element with four nodes and has a triangular version. **FLUID30** is an 8-node hexahedral element and has versions with prismatic and tetrahedral forms. The elements **FLUID29** and **FLUID30** can be in contact with similar solid elements (both with elastic and piezoelectric), for example, with **PLANE13**, **PLANE42**, **SOLID5**, **SOLID45**, etc. Naturally, in order to ensure consistency of finite element meshes here the elements of the same shape should be selected.

For acoustic elements, that are in contact with solid elements, it is necessary to use the option `KEYOPT(2)=0` (interaction permission). This leads to a non-symmetric finite element matrix. For all other acoustic elements we can set `KEYOPT(2)=1`, which will permit to obtain symmetric finite element matrices. As the solution of algebraic systems with symmetric matrices requires much less memory space and computation time, it is recommended to use symmetric matrices wherever possible.

For acoustic elements in ANSYS it is necessary to set the values for the material parameters (**MP**), which are *DENS* (the fluid density  $\rho_0$ ) and *SONC* (the speed of sound  $c_0$ ).

If there is a sound absorption at the media interface (the boundary  $\Gamma_{ai}$  with the impedance  $Z$ ), then we use additional material parameter *MU* to set the absorption coefficient  $\beta = Z/Z_0$ ,  $Z_0 = \rho_0 c_0$ . The value  $\beta$  is usually determined from experimental measurements. The absorption is

greater when the value of  $\beta$  is close to one. For one-dimensional problems the value  $\beta = 1$  ensures total absorption of plane acoustic waves at the impedance boundary  $\Gamma_{ai}$ .

More modern approaches are related to unconventional acoustic “infinite” elements **FLUID129** and **FLUID130**, that can be used together with **FLUID29** and **FLUID30** to simulate infinitely extended domains. These elements implement non-reflecting boundary conditions of the second kind that give more accurate results compared to conventional impedance boundaries  $\Gamma_{ai}$ . The development of numerical methods for simulating infinitely extended domains is a topic for special research [15]. The approach presented in [16] is implemented in finite elements **FLUID129** and **FLUID130**.

The elements **FLUID129** and **FLUID130** can contact only with acoustic elements **FLUID29** and **FLUID30**, correspondingly, but not with elastic or piezoelectric solid elements. The external boundary of the acoustic finite element mesh, covered by the elements **FLUID129** or **FLUID130**, should have the shape of a circumference (for 2D or axisymmetric elements) or sphere (for 3D). The radius of a circumference or a spherical boundary of a bounded domain, as well as the coordinates of a circumference or sphere center, should be set in the element constants with the command **R** .

As it is written in ANSYS documentation, the use of infinite elements gives good results both for low and high frequencies. It is mentioned that good solution accuracy is achieved when the infinite elements are located approximately at the distance  $\lambda/5$  outside the domain occupied by solid. Here  $\lambda = c_0/f$  is the dominant wave length for the pressure waves. For example, in the case of a submerged annular ring or spherical shell of the radius  $R_s$ , the radius of the external boundary  $R_a = RAD$  for the infinite elements can be approximately equal to  $R_s + \lambda/5$ . More accurate estimations can be obtained in numerical experiments for various values of  $R_a$ . Besides, it should be taken into account that in plane problems at large distances from the point source the acoustic fields attenuate in the point  $\xi$  as  $1/\sqrt{R}$ , where  $R = \sqrt{(x_1 - \xi_1)^2 + (x_2 - \xi_2)^2}$ , and in 3D problems the acoustic fields attenuate as  $1/r$ , where  $r = \sqrt{(x_1 - \xi_1)^2 + (x_2 - \xi_2)^2 + (x_3 - \xi_3)^2}$ .

In ANSYS Postprocessor, analyzing the solution results for the problems on the interaction of solids with acoustic media has particular features, which are related to the fact that the field functions associated with solids and acoustic media are defined in different domains. Therefore,

for example, if we need to show the mode shapes of elastic or piezoelectric body, first it is necessary to select only elastic or only piezoelectric elements and plot the mode shapes only after that. Similarly, if we need to plot the pressure fields **PRES** in acoustic medium, then it is necessary to select the acoustic elements and then apply the commands like **PLNSOL,PRES**.

The higher versions of ANSYS contain a lot of improvements for acoustic analysis: the models of acoustic fluids with absorption (**MP**, **VISC**, *MAT*, *C0*); the elements **FLUID220** and **FLUID221** with middle nodes for 3D problems; symmetric solvers for the problems of interaction of solid and fluid media (FSI); new impedance boundary conditions, as, for example, an ideal absorbing layer “perfectly matched layer” (PML), etc. Moreover, recently developed Application Customization Toolkit (ACT) now provides a range of convenient tools for performing acoustic computations in ANSYS Workbench.

Unfortunately, the documentation on new facilities for acoustic analysis in ANSYS is poor in details. Therefore for more in-depth acquaintance with acoustic analysis in ANSYS we recommend to refer to a voluminous monograph [14] with examples available by the link: <http://www.mecheng.adelaide.edu.au/avc/software>.

### 3.3.2 Example problem and solution methods

#### Problem description.

Let us consider a pipe immersed in sea water. The domain filled with water is so large then it can be considered infinitely extended in all directions. The pipe consists of two layers of different materials. The inner radius of the pipe is  $R_1 = 0.25$  (m), the external radius of the pipe is  $R_3 = 0.27$  (m), and the middle radius at the layer interface is  $R_2 = 0.26$  (m). The first layer  $R_1 \leq r \leq R_2$  is made of isotropic material (steel) with the Young’s modulus  $E_1 = 2 \cdot 10^{11}$  (N/m<sup>2</sup>), the Poisson’s ratio  $\nu_1 = 0.29$  and the density  $\rho_1 = 7860$  (kg/m<sup>3</sup>). The second layer  $R_2 \leq r \leq R_3$  is made of another isotropic material (copper) with the Young’s modulus  $E_2 = 1.2 \cdot 10^{11}$  (N/m<sup>2</sup>), the Poisson’s ratio  $\nu_2 = 0.33$  and the density  $\rho_2 = 8900$  (kg/m<sup>3</sup>). Let us assume that the density of sea water is  $\rho_0 = \rho_a = 1030$  (kg/m<sup>3</sup>), and the sound speed in sea water is  $c_0 = c_a = 1560$  (m/s).

As the pipe has rather large length along the axial direction and the external influences are uniformly applied along the axis, we can consider a 2D plane strain problem for a pipe cross-section (Fig. 3.17). The domain

occupied by fluid is bounded by the radius  $R_a$ . On the boundary  $r = R_a$  we will use non-reflecting boundary conditions, which will be simulated either by impedance boundary conditions or by special acoustic finite elements for infinite domains.

The aim of the problem is to analyze the displacement fields in the solid and the pressure fields in the fluid in an assumption of steady-state oscillations in the vicinity of the smallest resonance frequency  $f_r$ , the oscillation modes of which can be excited by two concentrated forces  $F = \tilde{F} \exp[i2\pi ft]$  with the amplitudes  $\tilde{F} = 100$  N/m, applied in two points on the inner boundary of the ring (cross-section of the pipe) in the opposite directions, as it is shown in Fig. 3.17.

### Example of problem solving using ANSYS

First of all, let us note that the problem is symmetric with respect to the axes  $X$  and  $Y$ . Therefore it is enough to consider a quarter of the model, for example, at  $X \geq 0, Y \geq 0$ . It is necessary to take into account that as the force  $F$  acts on both halves of the model  $Y \geq 0$  and  $Y \leq 0$ , therefore for the considered part we need to take a half of the force value  $F/2$ .

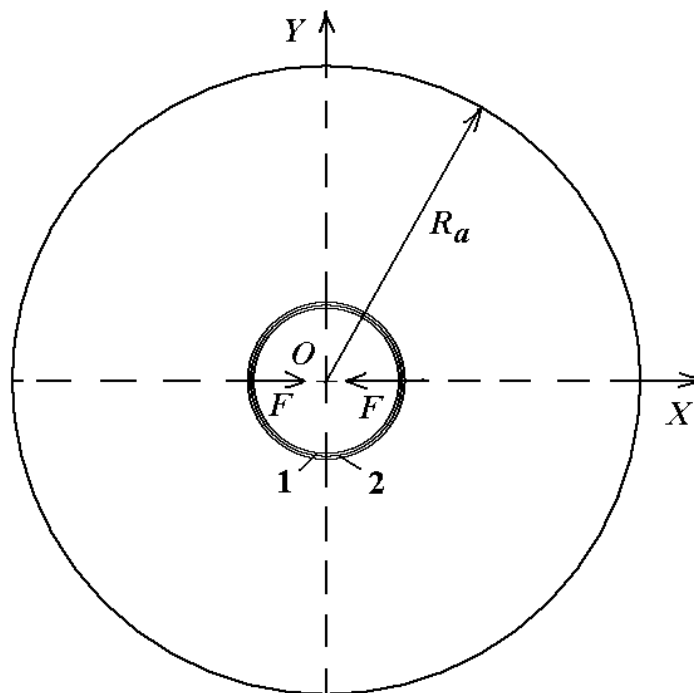


Figure 3.17. Geometry of the problem



We will begin with the calculation of the natural frequencies of the transmitter without account for fluid, by executing the file **FE\_Mod\_CP\_3\_sm.inp**.

### Text of input file **FE\_Mod\_CP\_3\_sm.inp**

```

! File    FE_Mod_CP_3_sm.inp
! Test problem No.~3
! PLANE PROBLEM
! OSCILLATIONS OF A COMPOUND RING (CYLINDER)
!
! Calculation of natural frequencies of the body without fluid

! Invert background from black to white
/RGB,INDEX,100,100,100,0
/RGB,INDEX,0,0,0,15

/PREP7
F_R='FE_Mod_CP_3_sm' ! file name for results

! Parameters for geometrical sizes (all in SI system)

R1=0.25 ! inner radius of the ring
R2=0.26 ! middle radius of the ring
R3=0.27 ! outer radius of the ring

NFREQ=4 ! number of output frequencies
FBEG=0.1 ! start value for the frequency range
FEND=1e10 ! end value for the frequency range

! Material properties of the body
! Material constants of steel
R01=7.86e3 ! density
E1=2e11 ! Young's modulus
NU1=0.29 ! Poisson's ratio
! Material constants of copper
R02=8.9e3
E2=1.2e11
NU2=0.33

MP,DENS,1,R01 ! density of the medium 1
MP,EX,1,E1 ! Young's modulus of the medium 1
MP,NUXY,1,NU1 ! Poisson's ratio of the medium 1
MP,DENS,2,R02 ! density of the medium 2
MP,EX,2,E2 ! Young's modulus of the medium 2
MP,NUXY,2,NU2 ! Poisson's ratio of the medium 2

```

```

ET,1,PLANE42,,,2 ! Elastic finite element with 4 nodes, plane strain

! Parameters of finite element mesh
SM=1.00 ! Scaling multiplier
HDIV=2*SM ! Number of elements along the thickness (for one material)

TDIV=32*SM ! Number of elements along the circumferential direction

/OUTPUT,F_R,res
*VWRITE
(1X,' MODAL ANALYSIS (Block Lanczos, Plane42)')
*VWRITE,NFREQ
(1X,' NFREQ= ',F4.0)
*VWRITE,HDIV,TDIV
(1X,' HDIV= ',F4.0,' TDIV= ',F4.0)
/OUTPUT
*DIM,FR,ARRAY,NFREQ ! Array for natural frequencies

! Geometry of the model
CSYS,1 ! Change active coordinate system to cylindrical
K,1,R1 $ K,2,R2 $ K,3,R3
K,4,R3,90 $ K,5,R2,90 $ K,6,R1,90
L,6,1 $ L,1,2 $ L,2,5 $ L,5,6 $ L,2,3 $ L,3,4 $ L,4,5
A,1,2,5,6
A,2,3,4,5
CSYS,0 ! Change active coordinate system to Cartesian

! Divide lines
LESIZE,1,,,TDIV $ LESIZE,3,,,TDIV $ LESIZE,6,,,TDIV

LESIZE,2,,,HDIV $ LESIZE,5,,,HDIV
LESIZE,4,,,HDIV $ LESIZE,7,,,HDIV
MSHKEY,1
MSHAPE,0,2D
ASEL,S,AREA,,2 ! Select new set of areas - area 2
AATT,2,,1 ! Associate material 2 and element type 1 (MAT=2, TYPE=1)
! with selected area
ASEL,ALL ! Select all areas
AMESH,ALL ! Mesh all areas
FINISH

/SOLU
ANTYPE,MODA ! Modal analysis
! Block Lanczos method
! Number of frequencies NFREQ in the interval FBEG,FEND
MODOPT,LANB,NFREQ,FBEG,FEND

```

```

! Conditions of symmetry
LSEL,S,LOC,Y,0
LSEL,A,LOC,X,0
DL,ALL,,SYMM
LSEL,ALL

SOLVE
FINISH

/POST1
! Output the table of resonance frequencies into the file
*DO,I,1,NFREQ
  SET,,I
  *GET,FR(I),MODE,I,FREQ
  FRI=FR(I)
  /OUTPUT,F_R,res,,append
  *VWRITE,I,FRI
  (1X,F4.0,' ',E12.5)
  /OUTPUT
*ENDDO

! Plot pictures of mode shapes
/PNUM,MAT,1 ! Enumerate elements by material properties

/NUMBER,1 ! Show numbers only by color
/TRIAD,OFF ! Do not show the global coordinate triad
/PLOPTS,LOGO,OFF ! Do not show ANSYS logo
/PLOPTS,DATE,OFF ! Do not show date
/PLOPTS,FRAME,OFF ! Do not show frame
/WINDOW,1,LTOP ! Place Window 1 at the left top of the screen
SET,,1 ! read data for the first mode
PLDISP,2 ! show mode shape together with undeformed shape

/WINDOW,1,OFF ! Make Window 1 passive
/NOERASE ! Don not erase window content
/WINDOW,2,RTOP ! Place Window 2 at the right top of the screen
SET,,2 ! read data for the second mode
PLDISP,2
/WINDOW,2,OFF
/WINDOW,3,LBOT ! Place Window 3 at the left bottom of the screen
SET,,3 ! read data for the third mode
PLDISP,2
/WINDOW,3,OFF
/WINDOW,4,RBOT ! Place Window 4 at the right bottom of the screen
SET,,4 ! read data for the fourth mode
PLDISP,2

```

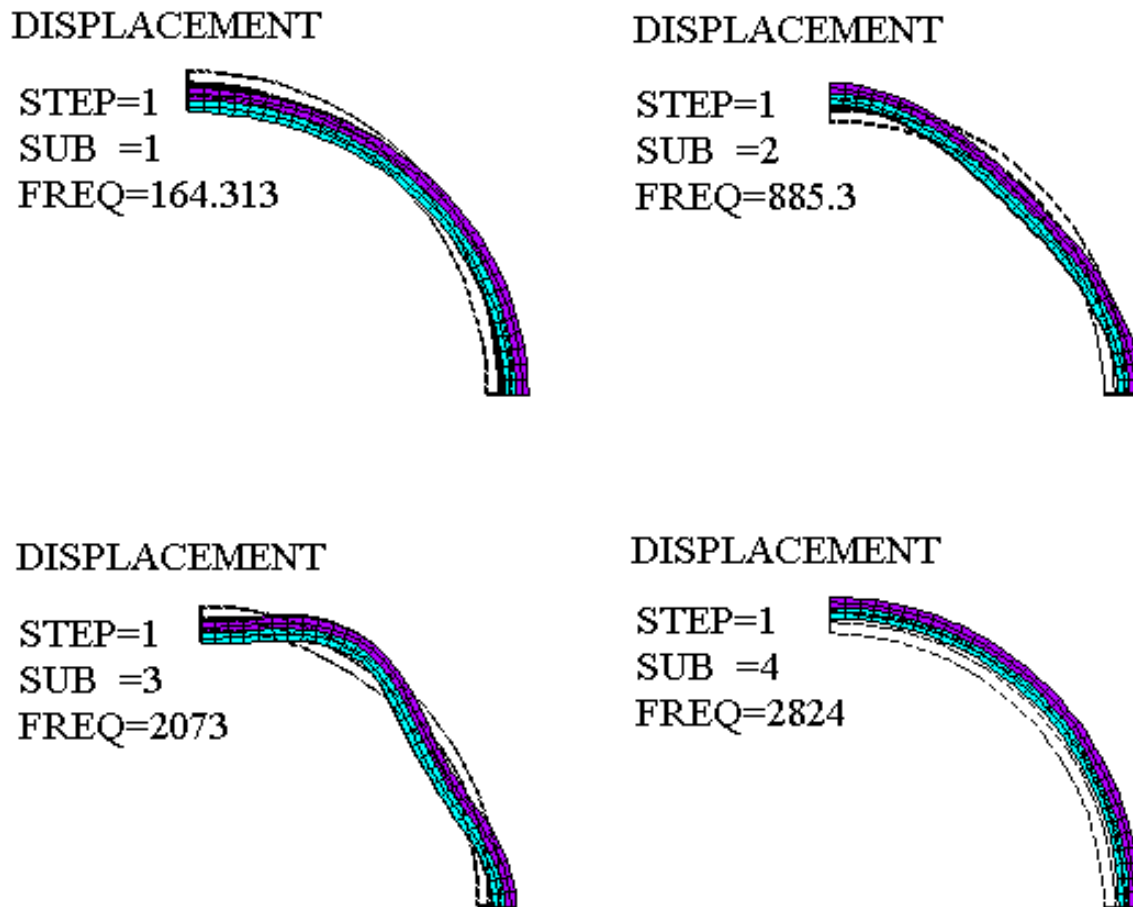


Figure 3.18. Natural mode shapes of the transmitter without fluid

```
! Return to default settings (one window at full screen)
/WINDOW,1,ON
/WINDOW,1,FULL
/WINDOW,4,OFF

! Execute this command to erase the content of the window
! ERASE
```

After executing this file in ANSYS we obtain the values of the first four natural frequencies and the mode shapes at these frequencies of the transmitter without account for fluid (Fig. 3.18). Here the elements that have different material properties are shown in different colors: material 1 is shown by turquoise, and material 2 is shown by violet. We note that the starting value FBEG of the frequency range, in which we search for natural frequencies, was taken slightly greater than zero in order not to search zero frequencies of a rigid body motion. (Although in this problem, as we consider only a quarter of a model with symmetry boundary conditions, there can be no zero frequencies, and here it is done only for convenience of using the commands from the provided file for other problems.)

It is clear that the concentrated forces shown in Fig. 3.17 can excite oscillations at all first four natural frequencies under relevant values of  $f$ . In the presence of fluid the values of all resonance frequencies will decrease, and, presumably, the expected value of the real part of the first natural frequency of the transmitter in the fluid can be around 130 Hz (For the transmitter without fluid the first natural frequency computed by the program FE\_Mod\_CP\_3.sm.inp was  $f_{sr1} = 164.313$  Hz).

Similarly we could have conducted modal analysis (solve an eigenvalue problem) for the transmitter in fluid and refine the value of the expected first natural frequency. Omitting this step, let us move to solving the problem of steady-state oscillations for an elastic transmitter in acoustic medium. We choose a computation frequency interval  $f_{beg} \leq f \leq f_{end}$ ;  $f_{beg} = 100$  Hz;  $f_{end} = 150$  Hz; and the number of values on the interval  $n_{freq} = 100$ . Therefore, the problem of steady-state oscillations for the transmitter in fluid will be solved  $n_{freq} = 100$  times with the step by frequency  $\Delta f = (f_{end} - f_{beg})/n_{freq} = 0.2$  Hz for the frequencies  $f_k = f_{beg} + k\Delta f$ ,  $k = 1, 2, \dots, n_{freq}$ .

By the resonance frequency  $f_r$  we will call the value of the frequency from an array  $f_k$ ,  $k = 1, 2, \dots, n_{freq}$ , which enables to achieve maximal value of the amplitude of the displacement  $\tilde{u}_y$  or acoustic pressure  $\tilde{p}p$  ( $u_y = \tilde{u}_y \exp[i2\pi ft]$ ;  $p = \tilde{p} \exp[i2\pi ft]$ ) at the top point of the transmitter  $X = 0$ ,  $Y = R_s$ . We have to remember that even if finite element computations were completely accurate, there would still be an incorporated absolute error of the frequency determination  $\Delta f = 0.2$  Hz, or a relative error  $(\Delta f / f_{beg}) \cdot 100\% = 0.2\%$ .

ANSYS documentation determines the distance, at which infinite elements should be located, as no less than  $R_s + \lambda/5$ , where  $R_s$  is the external diameter of the ring,  $\lambda = c_0/f$  is the dominant wavelength of the pressure waves. In this problem the external radius of the ring is  $R_s = R_3 = 0.27$  m, the speed of sound in water is  $c_0 = c_a = 1560$  m/s, the dominant frequency can be estimated as  $f = 130$  Hz. Then  $R_3 + \lambda/5 = 0.27 + 1560/130/5 = 2.67$  (m). However, in this problem under very low frequency oscillations we can expect that this distance would be much larger than the allowable distance for the infinite elements location. Therefore we will take  $R_a = 4R_s = 1.08$  m as the base value of the radius  $R_a$  for the location of acoustic elements **FLUID129** or impedance acoustic boundaries. The results obtained for this value will be compared with the results obtained at  $R_a = 2R_s$  and  $R_a = 8R_s$ .

Under a very large wavelength value  $\lambda = c_0/f \approx 12$  (m) a restriction on the finite element size  $h_d = \lambda/20 \approx 0.6$  (m) is larger than the value of the external radius of the ring  $R_s = R_3 = 0.27$  (m). As a basic example for each material of the ring we will consider the area division along the thickness  $HDIV = 2SM$ , the line division along the circumferential direction of the ring and acoustic area  $TDIV = 32SM$ , and the division of acoustic area  $HADIV = 32SM$ , where  $SM = 1$ . The finite elements in acoustic area will be built with an increase of their length along the radial directions with the multiplier  $SPACE = 3$ . For the convergence analysis the parameter  $SM$  will be changed towards both larger ( $SM = 2$ ) and smaller ( $SM = 0.5$ ) values.

The main program for calculating the steady-state oscillations of the ring in acoustic medium **FE\_Mod\_CP\_3\_ha.inp** is used for simulation of non-reflecting boundaries of acoustic finite elements **FLUID129**.

### Text of input file FE\_Mod\_CP\_3\_ha.inp

```
! File    FE_Mod_CP_3_ha.inp
```

```

! Test problem No. 3
! PLANE PROBLEM
! OSCILLATIONS OF A COMPOUND RING (CYLINDER) IN ACOUSTIC MEDIUM
!
! Calculation of natural frequencies of the body with fluid
! Infinite elements FLUID129

! Invert background from black to white
/RGB,INDEX,100,100,100,0
/RGB,INDEX,0,0,0,15

/PREP7
F_R='FE_Mod_CP_3_ha_4_SM1' ! file name for output results

! Parameters for geometrical sizes (all in SI system)

R1=0.25 ! inner radius of the ring
R2=0.26 ! middle radius of the ring
R3=0.27 ! outer radius of the ring
KRA=4 ! coefficient for the computation of the radius RA
RA=KRA*R3 ! radius for external boundary of the fluid

FP=100 ! Force value
NFREQ=100 ! number of output frequencies
FBEG=100 ! start value for the frequency range
FEND=150 ! end value for the frequency range

! Material properties
! Material constants of steel
R01=7.86e3 ! density
E1=2e11 ! Young's modulus
NU1=0.29 ! Poisson's ratio
! Material constants of copper
R02=8.9e3
E2=1.2e11
NU2=0.33
! Material constants of fluid
ROA=1030
CA=1560
AD=1

MP,DENS,1,R01 ! density of medium 1
MP,EX,1,E1 ! Young's modulus of medium 1
MP,NUXY,1,NU1 ! Poisson's ratio of medium 1

MP,DENS,2,R02 ! density of medium 2
MP,EX,2,E2 ! Young's modulus of medium 2

```

```

MP,NUXY,2,NU2    ! Poisson's ratio of medium 2

MP,DENS,3,ROA    ! density of acoustic medium
MP,SONC,3,CA     ! speed of sound in acoustic medium
MP,MU,3,AD       ! absorbing coefficient at the impedance boundary

ET,1,PLANE42,,,2 ! Elastic finite element with 4 nodes, plane strain
ET,2,FLUID29,,,1 ! Acoustic finite element with 4 nodes, without UX & UY
ET,3,FLUID29     ! Acoustic finite element with 4 nodes, with UX & UY
ET,4,FLUID129   ! Acoustic finite element for infinite boundaries
R,4,RA          ! Radius of infinite boundary for finite element FLUID129

! Parameters of finite element mesh
SM=1.00         ! scaling multiplier
HDIV=2*SM       ! Number of FEs along the thickness (for one material)

TDIV=32*SM      ! Number of FEs along the circumferential direction
HADIV=32*SM     ! Number of FEs along the radial direction for acoustic medium
SPACE=3         ! Multiplier to increase the length of acoustic FE
                ! along the radial direction

/OUTPUT,F_R,res
*VWRITE
(1X,' HARMONIC ANALYSIS (Plane42, Fluid29)')
*VWRITE,KRA
(1X,' RA/R3= ',F4.0)
*VWRITE,NFREQ
(1X,' NFREQ= ',F4.0)
*VWRITE,HDIV,TDIV,HADIV
(1X,' HDIV= ',F4.0,' TDIV= ',F4.0,' HADIV= ',F4.0)
/OUTPUT

! Geometry of the model
CSYS,1 ! Change active coordinate system to cylindrical
K,1,R1 $ K,2,R2 $ K,3,R3
K,4,R3,90 $ K,5,R2,90 $ K,6,R1,90
L,6,1 $ L,1,2 $ L,2,5 $ L,5,6 $ L,2,3 $ L,3,4 $ L,4,5
A,1,2,5,6 $ A,2,3,4,5
K,7,RA $ K,8,RA,90
L,3,7 $ L,7,8 $ L,8,4
A,3,7,8,4
CSYS,0 ! Change active coordinate system to Cartesian

! Line division
LESIZE,1,,,TDIV $ LESIZE,3,,,TDIV $ LESIZE,6,,,TDIV
LESIZE,2,,,HDIV $ LESIZE,5,,,HDIV
LESIZE,4,,,HDIV $ LESIZE,7,,,HDIV

```

```

LESIZE,9,, ,TDIV
LESIZE,8,, ,HADIV,SPACE
LESIZE,10,, ,HADIV,1/SPACE
MSHKEY,1
MSHAPE,0,2D
ASEL,S,AREA,,2 ! Select new set of areas - area 2
AATT,2,,1 ! Associate material 2 and element type 1 (MAT=2, TYPE=1)
           ! with the selected area
ASEL,S,AREA,,3 ! Select new set of areas - area 3
AATT,3,,2 ! Associate material 3 and element type 2 (MAT=3, TYPE=2)
           ! with the selected area
ASEL,ALL ! Select all areas
AMESH,ALL ! Mesh all areas

! Change acoustic finite elements on the border of the ring to type 3

LSEL,S,LINE,,6 ! Select line 6 - border of the ring and acoustic medium
NSLL,S,1 ! Select nodes on the selected lines
ESLN,S,0 ! Select finite elements that are attached to the selected nodes
ESEL,U,TYPE,,1 ! Unselect elements of type 1 from the selected set

EMODIF,ALL,TYPE,3 ! Modify all selected elements to type 3
ALLSEL

! Fluid-Structure Interface (FSI)
CSYS,1
NSEL,S,LOC,X,R3 ! Select the nodes at the border of solid and fluid bodies

ESLN ! Select elements attached to the selected nodes
ESEL,R,TYPE,,3 ! Select finite elements that have TYPE=3
SF,ALL,FSI ! Set the flag FSI for the contact nodes
NSEL,ALL
ESEL,ALL
CSYS,0

FINISH

/SOLU
ANTYPE,HARMIC ! Steady-state oscillations
HROPT,FULL
HARFRQ,FBEG,FEND
NSUBST,NFREQ
KBC,1

! Symmetry conditions
LSEL,S,LOC,Y,0
LSEL,A,LOC,X,0

```



```
DL,ALL,,SYMM
LSEL,ALL

CSYS,1
KSEL,S,LOC,X,R1
KSEL,R,LOC,Y,0
FK,ALL,FX,-FP/2 ! Divide FP into 2, as we consider half of the model

KSEL,ALL
CSYS,0

! Define infinite elements FLUID129
CSYS,1
NSEL,S,LOC,X,RA ! Select nodes at the impedance boundary
TYPE,4 $ REAL,4 $ MAT,3
ESURF
ESEL,ALL
NSEL,ALL
CSYS,0

OUTRES,BASIC,ALL
SOLVE
SAVE
FINISH

/POST26
/SHOW,WIN32C
/TRIAD,OFF ! Do not show the global coordinate triad

/PLOPTS,INFO,2 ! Use auto-legend
/PLOPTS,LEG2,OFF
/PLOPTS,LOGO,OFF ! Do not show ANSYS logo
/PLOPTS,DATE,OFF ! Do not show date
/PLOPTS,FRAME,OFF ! Do not show frame

/COLOR,CURVE,WHIT,1,6
/COLOR,GRID,WHIT
/GRID,1

CSYS,1
NSEL,S,LOC,X,R3
NSEL,R,LOC,Y,90 ! Node with number N_RES1 is the point (0,R3) in Cartesian CS
*GET,N_RES1,NODE,,NUM,MIN
NSEL,S,LOC,X,RA
NSEL,R,LOC,Y,90 ! Node with number N_RES2 is the point (0,RA) in Cartesian CS
*GET,N_RES2,NODE,,NUM,MIN
NSEL,ALL
```

```

CSYS,0

/XRANG,FBEG,FEND
/AXLAB,X,Frequency (Hz)
/AXLAB,Y,Displacement UY (m)
NSOL,2,N_RES1,UY
ABS,3,2,,ABSUY
*GET,FRES,VARI,3,EXTREM,TMAX ! Define resonance frequency

/OUTPUT,F_R,res,,append
*VWRITE,FRES
(1X,' FRES= ',E12.5)
PRVAR,2
/OUTPUT PLCPLX,2 ! Real part
PLVAR,2

! PLVAR,3 ! Amplitude UY

! Commands to plot the pressure at the same point
! NSOL,4,N_RES1,PRES
! /AXLAB,Y,Acoustic pressure PRES (Pa)
! PLVAR,4

```

This program constructs finite element mesh shown in Fig. 3.19 where on the left (a) the elements colors indicate material properties and on the right (b) the colors indicate the element types. Besides, Fig. 3.19(b) shows the boundary with the nodes of acoustic elements **FLUID29,,0**, for which the fluid-structure interface flag FSI has been set.

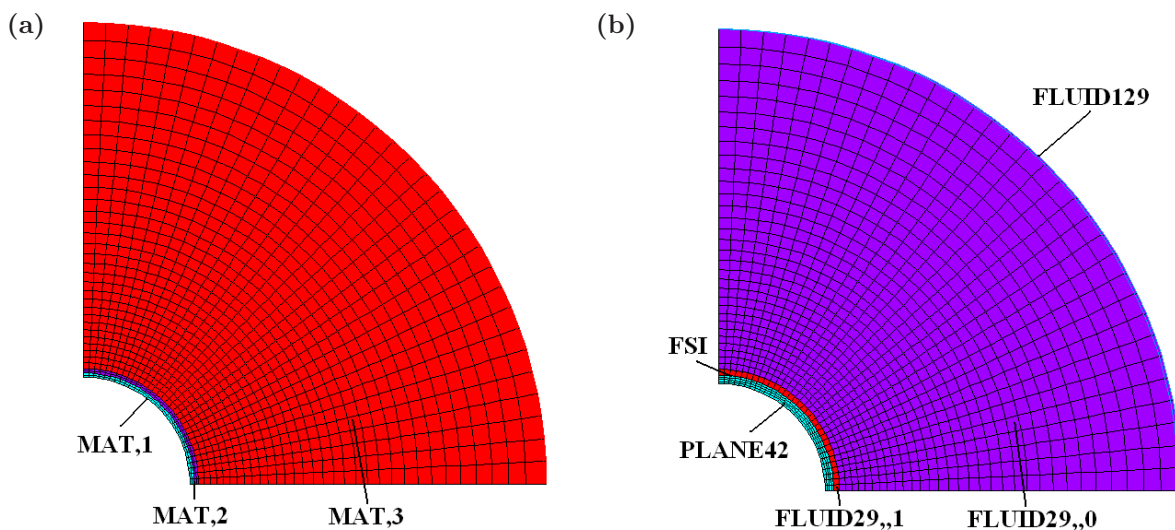


**Figure 3.19.** Finite element mesh: (a) highlight MAT; (b) highlight TYPE

Let us recall that in order to plot finite element mesh in interactive mode we need to execute *Plot*  $\rightarrow$  *Elements*. For showing the material properties of the elements by colors without showing the material numbers select *PltCtrls*  $\rightarrow$  *Numbering*  $\rightarrow$  *Elem/Attrib numbering*  $\rightarrow$  *Material numbers*  $\rightarrow$  *[NUM] Numbering shown with*  $\rightarrow$  *Colors only*  $\rightarrow$  *OK*, and for showing the element types by colors without showing the element type numbers select *PltCtrls*  $\rightarrow$  *Numbering*  $\rightarrow$  *Elem/Attrib numbering*  $\rightarrow$  *Element type num*  $\rightarrow$  *Material numbers*  $\rightarrow$  *[NUM] Numbering shown with*  $\rightarrow$  *Colors only*  $\rightarrow$  *OK*.

At the end of the program in postprocessor **/POST26** the data on the frequency characteristic of the displacement  $\tilde{u}_y$  in the point of the transmitter ( $X = 0, Y = R_3$ ) are written in the output file **FE\_Mod\_CP\_3\_ha\_4\_SM1.res**, and  $\text{Re}\tilde{u}_y$  is displayed as a graph (Fig. 3.20(a)). Execution of the command **PLVAR,3** gives the graph of the frequency dependence  $|\tilde{u}_y|$  at the same point (Fig. 3.20(b)). Besides, the resonance frequency value is written to the variable FRES and also to the output file. As a result we get that the resonance frequency value is equal to  $f_r = 126.5$  Hz.

The following file enables to obtain for the resonance frequency FRES a graph of the real part of the pressure along the  $Y$ -axis of the acoustic domain, i. e. the dependence  $\text{Re}\tilde{p}(0, y), y \in [R_3, R_a]$ .

### Text of input file FE\_Mod\_CP\_3\_Post.inp

```
! File      FE_Mod_CP_3_Post.inp
! Postprocessor plot of acoustic pressure
! along the path between the nodes N_RES1, N_RES2 at the frequency FRES
! N_RES1, N_RES2, FRES - should be determined earlier
/POST1
/COLOR,CURVE,WHIT,1,6 ! graph color -- white (black after inversion)
/COLOR,GRID,WHIT, ! grid color -- white (black after inversion)
/PLOPTS,TITLE,OFF ! no graph title
/PLOPT,FRAME,OFF ! no frame
/AXLAB,X,Y ! label for X-axis
/AXLAB,Y,Re PRES ! label for Y-axis
/XRANG /DSCALE,,OFF ! Remove displacement scaling (scale displacements by 0)

! Read results for real part at the frequency FRES
SET,NEAR,,0,FRES

! Commands to determine a path with keypoints
PATH,YY,2,,120
PPATH,1,N_RES1
```

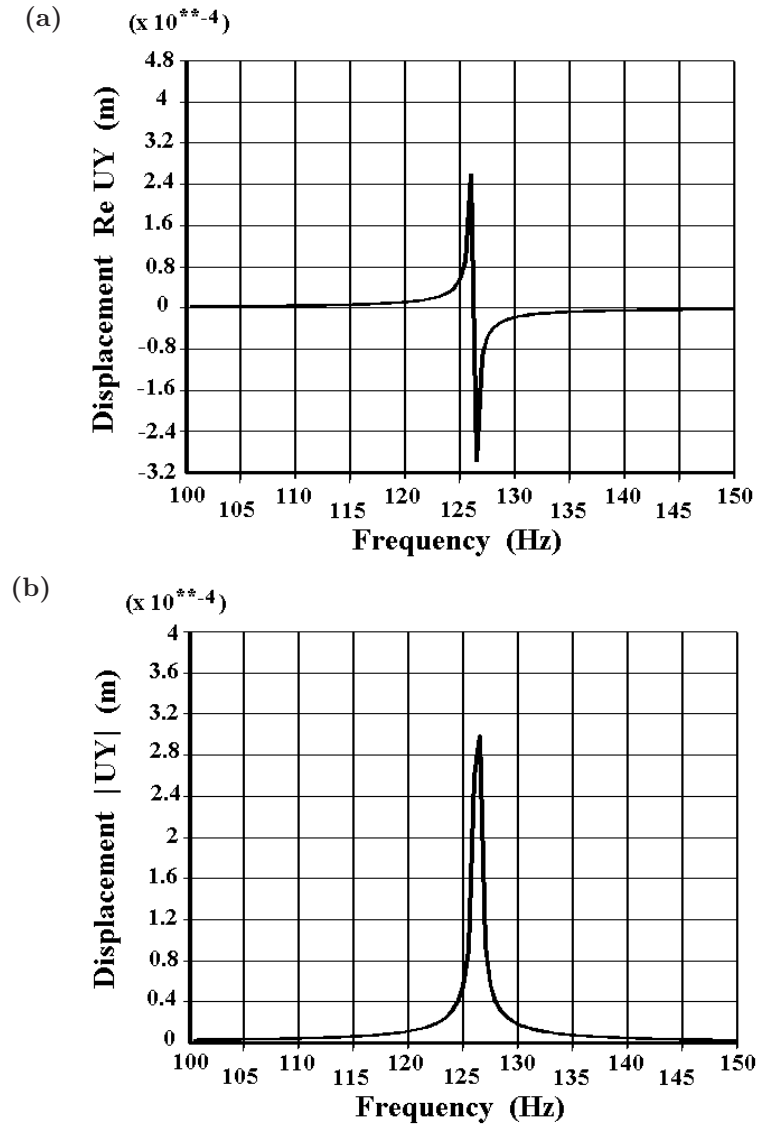


Figure 3.20. Frequency characteristic  $\tilde{u}_y$ : (a)  $\text{Re}\tilde{u}_y$ ; (b)  $|\tilde{u}_y|$

```

PPATH,2,N_RES2
! Determine the value of RePRES to plot the graph along the path
PDEF,RePRES,PRES

PLPATH,RePRES ! Plot the graph RePRES along the path

! Plot picture of pressure distribution (uncomment)
! ESEL,S,TYPE,,2,4
! PLNSOL,PRES
! Read results for imaginary part at the frequency FRES
! SET,NEAR,,1,FRES
! PLNSOL,PRES

```

The resulting graph is shown in Fig. 3.21. As expected, the pressure rather rapidly decreases along the path.

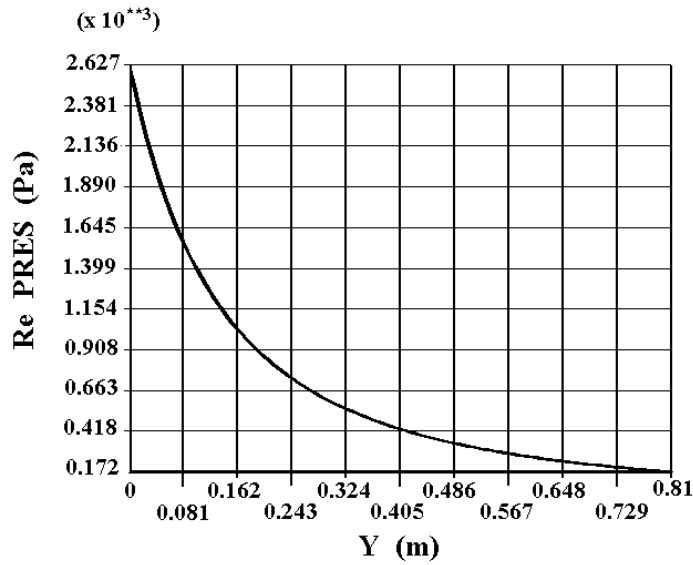


Figure 3.21. Acoustic pressure  $\text{Re}\tilde{p}$  along  $Y$ -axis

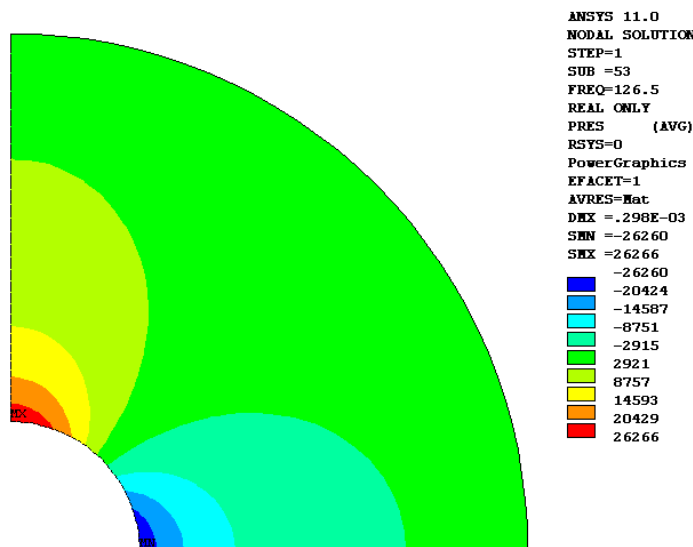
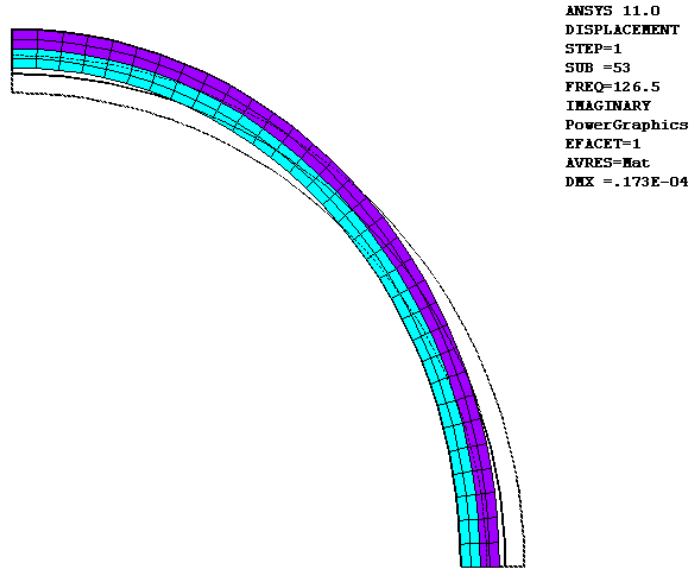


Figure 3.22. Distribution of the real part of the pressure at the frequency  $f_r = 126.5$  Hz

Let us plot the distribution of real and imaginary parts of the pressure at the resonance frequency. According to the last commands of the above file, using the command **ESEL,S,TYPE,,2,4** we firstly select only acoustic elements (type 2–4) and then we execute **PLNSOL,PRES**. As a result, we obtain the distribution of the real part of the pressure at the resonance frequency, which is shown in Fig. 3.22.

After executing the commands **SET,NEAR,,,1,FRES** and **PLNSOL,PRES**, we can obtain similar picture for the imaginary part of the pressure



**Figure 3.23.** Deformed shape of the ring at the resonance frequency  $f_r = 126.5$  Hz, (real part)

at the resonance frequency and ensure that the pressure values will be much smaller.

At last, we plot the picture of the deformed shape at the resonance frequency. To do this, firstly it is necessary to select only solid elements (of element type 1) **ESEL,S,TYPE,,1** and set automatic displacement scaling **/DSCALE,,AUTO**. Secondly, we need to read the results at this frequency for the real part of the solution **SET,NEAR,,0,FRES** and plot the picture of the deformed shape with an undeformed edge (Menu path: *Plot Results* → *Deformed Shape* → *Def+undef edg* → *OK* or execute the command **PLDISP,2**). In order to achieve more similarities with the first natural mode shape of the transmitter without fluid that is shown in the top left quarter in Fig. 3.18, we can paint the elements according to the numbers of their material properties without showing the material numbers: *PltCtrls* → *Numbering* → *Elem/Attrib numbering* → *Material numbers* → *[NUM] Numbering shown with* → *Colors only* → *OK*.

The result of these actions is shown in Fig. 3.23. From this figure it can be seen that the deformed shape in general repeats the first natural mode shape of the transmitter without fluid, which is shown in Fig. 3.18 (the natural mode shape is determined up to an arbitrary factor, therefore the sign of its displacements is not important).

The numerical experiments with varying the mesh density parameter  $SM$  show that  $f_r = 127$  Hz for  $SM = 0.5$ ,  $f_r = 126.5$  Hz for  $SM = 1$ ,  $f_r = 126$  Hz for  $SM = 2$ . As it can be seen, with the decrease of the

maximal size of finite elements the frequency decreases. This fact also follows from theoretical conclusions on the convergence character for the natural frequencies. However, this change in the value of the first natural frequency appears to be less than 1 %, which indicates a satisfactory choice of the parameters of the finite element mesh (even more coarse mesh is acceptable).

If we vary the sizes of acoustic domain at  $SM = 1$  by changing the parameter  $KRA = R_a/R_3$  from 2 to 8, than we can note that the value  $f_r = 126.5$  Hz will not change. Therefore, the selected sizes of acoustic domain are also quite satisfactory and even smaller sizes are acceptable. (However, here we do not analyze maximal values of the displacements and acoustic pressure that are calculated with larger error).

Finally, instead of locating acoustic elements **FLUID129** at the far boundary of the acoustic domain  $r = R_a$  we can set impedance boundary conditions by changing several commands in the file FE\_Mod\_CP\_3\_ha.inp:

```
! Define infinite element FLUID129
CSYS,1
NSEL,S,LOC,X,RA ! Select nodes at the impedance boundary
TYPE,4 $ REAL,4 $ MAT,3
ESURF
ESEL,ALL
NSEL,ALL
CSYS,0

! Impedance boundary conditions
CSYS,1
NSEL,S,LOC,X,RA ! Select nodes at the impedance boundary

SF,ALL,IMPD,1 ! Set impedance boundary condition
NSEL,ALL
CSYS,0
```

The computations show that for the considered problem both variants are acceptable for simulating a non-reflecting acoustic boundary. However, the first approach appears to be more accurate.

### 3.3.3 Individual assignments

Write a program code in ANSYS APDL to compute a problem of interaction of a solid with an acoustic medium in a steady-state oscillation mode in a 2D setting (axisymmetric or plane strain problem).

As the first step, solve the problem on natural oscillations of a solid. Find several first natural frequencies and estimate the possibility of their

excitation by external influences  $F = \tilde{F} \exp[i2\pi ft]$  or  $p_\Gamma = \tilde{p}_\Gamma \exp[i2\pi ft]$ . As a result, select a frequency interval in the vicinity of the first (among the excited frequencies) resonance frequency.

Estimate the value of the radius for locating the acoustic finite elements **FLUID129** or impedance acoustic boundaries and the finite element sizes.

Obtain the amplitude-frequency characteristics of the displacements in the characteristic point. For the resonance frequency get the deformed shape of the solid, the pressure distribution in the acoustic medium and the graph of the change of the acoustic pressure along the characteristic path.

Perform the computations for various densities of the finite element mesh and for several values of the acoustic medium radius. Find optimal values.

Analyze the results and prepare a report. The report should contain the name of the student, the full description of the problem and the results obtained in ANSYS.

For simulation use the following values of the material constants for isotropic media defined in SI system:

- steel with the Young's modulus  $E = 2 \cdot 10^{11}$  (N/m<sup>2</sup>), the Poisson's ratio  $\nu = 0.29$  and the density  $\rho = 7860$  (kg/m<sup>3</sup>);
- copper with the Young's modulus  $E = 1.2 \cdot 10^{11}$  (N/m<sup>2</sup>), the Poisson's ratio  $\nu = 0.33$  and the density  $\rho = 8900$  (kg/m<sup>3</sup>);
- titanium with the Young's modulus  $E = 1.12 \cdot 10^{11}$  (N/m<sup>2</sup>), the Poisson's ratio  $\nu = 0.32$  and the density  $\rho = 4500$  (kg/m<sup>3</sup>);
- sea water with the speed of sound  $c_a = 1560$  (m/s) and the density  $\rho_a = 1030$  (kg/m<sup>3</sup>);
- fresh water with the speed of sound  $c_a = 1500$  (m/s) and the density  $\rho_a = 1000$  (kg/m<sup>3</sup>);
- air with the speed of sound  $c_a = 340$  (m/s) and the density  $\rho_a = 1.2$  (kg/m<sup>3</sup>).

The variants of individual tasks are presented in Table 3.10. (When possible, use the symmetry of the problem!)

The concentrated forces  $\tilde{F}$  here have the dimension N/m, as in reality for a plain strain state they are distributed along the line parallel to the axis  $z$ , and for an axisymmetric problem they are distributed along the circumference with the radius  $R_f$  equal to the coordinate  $X$  of the point of the application of the force in meridional section. In ANSYS for an axisymmetric problem the force value must be multiplied by the circumference length  $2\pi R_f$ . Therefore, in the case of defining the



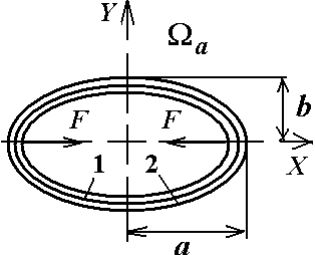
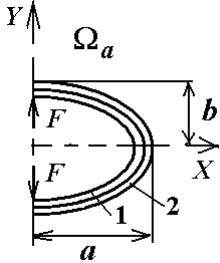
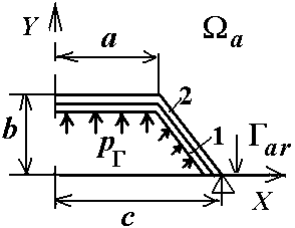
concentrated force  $\tilde{F}$  for an axisymmetric problem the value  $2\pi R_f \tilde{F}$  should be used, and for a plane strain state use the value  $\tilde{F}$ . (An exception for an axisymmetric problem is the case of defining the force  $\tilde{F}$  on the axis of rotation, i. e. at  $R_f = 0$ . Here  $\tilde{F}$  has the dimension N, and precisely this value of  $\tilde{F}$  is used.)

Everywhere in Table 3.10  $\Omega_a$  is an acoustic domain,  $\Gamma_{ar}$  is the surface of an acoustic domain with the boundary conditions of a rigid wall (1.204).

**Table 3.10.** Variants of individual tasks for the practical assignment No. 3

No.	Scheme	Input data
1		<p>Axisymmetric problem.</p> <p>The transmitter is made of titanium, the external dome radius is <math>R_1 = 0.2</math> m, its thickness is <math>h = 0.01</math> m, <math>a = 0.3</math> m.</p> <p>Acoustic medium (sea water) fills the domain from the side of external normal to the surface of the transmitter of the radius <math>R_1</math>, <math>\tilde{p}_\Gamma = 50</math> N/m<sup>2</sup>.</p>
2		<p>Axisymmetric problem.</p> <p>The transmitter is made of steel, the external dome radius is <math>R_1 = 0.2</math> m, its thickness is <math>h = 0.01</math> m, <math>a = 0.3</math> m.</p> <p>Acoustic medium (fresh water) fills the domain from the side of external normal to the surface of the transmitter of the radius <math>R_1 - h</math>, <math>\tilde{p}_\Gamma = 50</math> N/m<sup>2</sup>.</p>
3		<p>Plane strain.</p> <p>The transmitter is made of titanium, its thickness is <math>h = 0.02</math> m, <math>a = 0.4</math> m, <math>b = c = 0.3</math> m.</p> <p>Acoustic medium (air) fills the domain from the side of external normal to the surface of the transmitter, <math>\tilde{F} = 100</math> N/m.</p>
4		<p>Plane strain.</p> <p>The transmitter is made of copper, its thickness is <math>h = 0.01</math> m, <math>a = 0.2</math> m, <math>b = c = 0.15</math> m.</p> <p>Acoustic medium (air) fills the domain from the side of external normal to the upper surface of the transmitter, <math>\tilde{F} = 150</math> N/m.</p>

**Table 3.10.** Variants of individual tasks for the practical assignment No. 3 (continue)

<p>5</p>		<p>Plane strain.                  The cross section of the transmitter is a two-layer hollow ellipse.                  The boundary of the interaction of the transmitter with an acoustic medium:  <math>(x/a)^2 + (y/b)^2 = 1</math>,                  where <math>a = 0.4</math> m, <math>b = 0.2</math> m.                  External layer 2 is steel, its thickness is <math>h_2 = 0.02</math> m.                  Internal layer 1 is copper, its thickness is <math>h_1 = h_2</math>.                  Acoustic medium (fresh water) fills the domain <math>(x/a)^2 + (y/b)^2 \geq 1</math>,  <math>\tilde{F} = 100</math> N/m.</p>
<p>6</p>		<p>Axisymmetric problem.                  The cross section of the transmitter is a two-layer hollow ellipse.                  The boundary of the interaction of the transmitter with an acoustic medium:  <math>(x/a)^2 + (y/b)^2 = 1</math>,                  where <math>a = 0.5</math> m, <math>b = 0.25</math> m.                  External layer 2 is titanium, its thickness is <math>h_2 = 0.02</math> m.                  Internal layer 1 is copper, its thickness is <math>h_1 = h_2</math>.                  Acoustic medium (sea water) fills the domain <math>(x/a)^2 + (y/b)^2 \geq 1</math>,  <math>\tilde{F} = 80</math> N/m.</p>
<p>7</p>		<p>Axisymmetric problem.                  The cross-section of the transmitter is a two-layer body.                  External layer 2 is titanium, its thickness is <math>h_2 = 0.02</math> m.                  Internal layer 1 is copper, its thickness is <math>h_1 = h_2</math>.  <math>a = 0.3</math> m, <math>b = 0.2</math> m, <math>c = 0.5</math> m.                  Acoustic medium (fresh water) fills the domain from the side of external surface of the transmitter, <math>\tilde{p}_\Gamma = 75</math> N/m<sup>2</sup>.</p>

**Table 3.10.** Variants of individual tasks for the practical assignment No. 3 (continue)

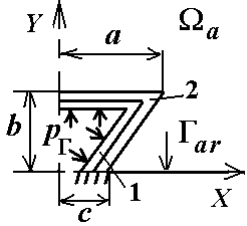
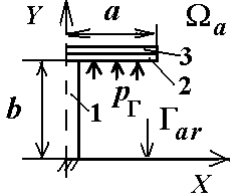
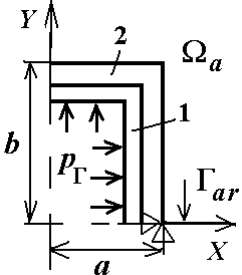
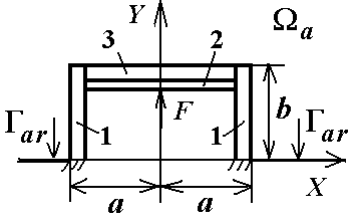
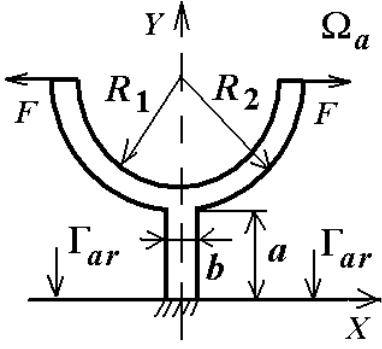
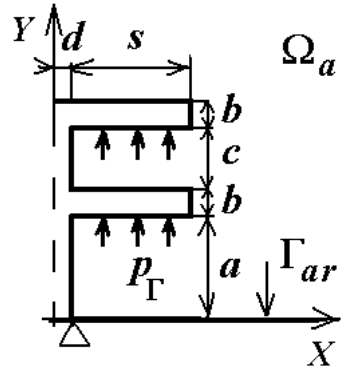
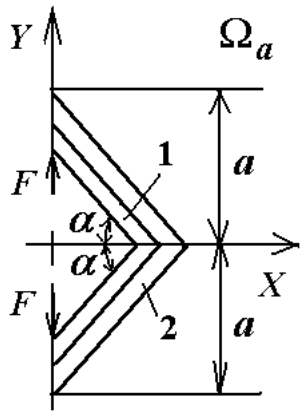
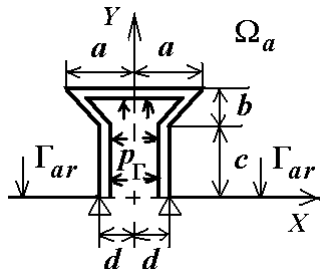
8		<p>Axisymmetric problem.</p> <p>The cross section of the transmitter is a two-layer body.</p> <p>External layer 2 is steel, its thickness is <math>h_2 = 0.02</math> m.</p> <p>Internal layer 1 is copper, its thickness is <math>h_1 = h_2</math>.</p> <p><math>a = 0.6</math> m, <math>b = 0.5</math> m, <math>c = 0.3</math> m.</p> <p>Acoustic medium (sea water) fills the domain from the side of external surface of the transmitter, <math>\tilde{p}_\Gamma = 50</math> N/m<sup>2</sup>.</p>
9		<p>Axisymmetric problem.</p> <p>The cross section of the transmitter is a three-layer body.</p> <p>Leg 1 is steel, the radius is <math>r_1 = 0.02</math> m, <math>b = 0.5</math> m.</p> <p>The lower hat 2 is copper, its thickness is <math>h_2 = 0.01</math> m, <math>a = 0.4</math> m.</p> <p>The upper hat 3 is titanium, its thickness is <math>h_3 = h_2</math>.</p> <p>Acoustic medium (fresh water) fills the domain from the side of external surface of the transmitter, <math>\tilde{p}_\Gamma = 70</math> N/m<sup>2</sup>.</p>
10		<p>Axisymmetric problem.</p> <p>The cross section of the transmitter is a two-layer body.</p> <p>External layer 2 is titanium, its thickness is <math>h_2 = 0.05</math> m.</p> <p>Internal layer 1 is steel, its thickness is <math>h_1 = 0.04</math> m, <math>a = 0.3</math> m, <math>b = 0.5</math> m.</p> <p>Acoustic medium (sea water) fills the domain from the side of external surface of the transmitter, <math>\tilde{p}_\Gamma = 120</math> N/m<sup>2</sup>.</p>
11		<p>Plane strain.</p> <p>The cross section of the transmitter is a three-layer body.</p> <p>Leg 1 is steel, its thickness is <math>h_1 = 0.04</math> m, <math>b = 0.2</math> m,</p> <p>The lower hat 2 is copper, its thickness is <math>h_2 = 0.02</math> m, <math>a = 0.3</math> m.</p> <p>The upper hat 3 is titanium, its thickness is <math>h_3 = h_1</math>,</p> <p>Acoustic medium (fresh water) fills the domain from the side of external surface of the transmitter, <math>\tilde{F} = 150</math> N/m.</p>

Table 3.10. Variants of individual tasks for the practical assignment No. 3 (continue)

<p>12</p>		<p>Plane strain.                      The transmitter is made of titanium,  <math>a = 0.3</math> m, <math>b = 0.1</math> m,  <math>R_1 = 0.5</math> m, <math>R_2 = 0.6</math> m.                      Acoustic medium (air)                      surrounds the surface of the transmitter,  <math>\tilde{F} = 100</math> N/m.</p>
<p>13</p>		<p>Axisymmetric problem.                      The transmitter is made of steel,  <math>a = 0.3</math> m, <math>b = 0.05</math> m, <math>c = 0.2</math> m,  <math>d = 0.05</math> m, <math>s = 0.35</math> m.                      Acoustic medium (sea water)                      surrounds the surface of the transmitter,  <math>\tilde{p}_\Gamma = 100</math> N/m<sup>2</sup>.</p>
<p>14</p>		<p>Axisymmetric problem.                      The cross-section of the transmitter is                      a two-layer body.                      External layer 2 is titanium,                      its thickness is <math>h_2 = 0.05</math> m.                      Internal layer 1 is steel, its thickness is  <math>h_1 = 0.05</math> m, <math>a = 0.5</math> m, <math>\alpha = 45^\circ</math> m.                      Acoustic medium (fresh water)                      fills the domain from the side of external                      surface of the transmitter, <math>\tilde{F} = 100</math> N/m.</p>
<p>15</p>		<p>Plane strain.                      The transmitter is made of steel,                      its thickness is <math>h = 0.02</math> m,  <math>a = 0.4</math> m, <math>b = 0.2</math> m, <math>c = 0.5</math> m, <math>d = 0.2</math> m.                      Acoustic medium (fresh water)                      fills the domain from the side of external                      surface of the transmitter, <math>\tilde{p}_\Gamma = 60</math> N/m<sup>2</sup>.</p>

## References

1. ANSYS Rel. 11.0. Theory Reference for ANSYS and ANSYS Workbench. SAS IP Inc. Canonsburg, 2007. 1110 p.
2. *Aubin J.-P.* Approximation of elliptic boundary-value problems. Wiley-Interscience, New York-London-Sydney, 1972. 360 p.
3. *Bathe K.J., Wilson E.L.* Numerical methods in finite elements analysis. Prentice-Hall, Englewood Cliffs, New Jersey, 1976. 528 p.
4. *Belokon A.V., Nasedkin A.V.* Some properties of the natural frequencies of electroelastic bodies of bounded dimensions. Journal of Applied Mathematics and Mechanics. 1996. V. 60, No. 1. pp. 145–152.
5. *Benzi M., Golub G.H., Liesen J.* Numerical solution of saddle point problems. Acta Numerica. 2005. V. 14. pp. 1–137.
6. *Berlincourt D.A., Curran D.R., Jaffe H.* Piezoelectric and piezomagnetic materials and their function in transducers. Physical Acoustics. Vol. 1, Part A. Academic Press, NY, 1964. pp. 233–256.
7. *Cadi W.* Piezoelectricity. An introduction to the theory and applications of electromechanical phenomena in crystals. N.-Y.-London: McGraw-Hill, 1946. 806 p.
8. *Ciarlet P.* The finite element method for elliptic problems. North-Holland publishing company, 1978.
9. *Coussy O.* Poromechanics. J.Wiley and Sons, 2004.
10. *De Gennes P.G.* Pierre Curie and the role of symmetry in physical laws. Ferroelectrics. 1982. V. 40, N 3/4. P. 125–129.
11. *Dieulesaint E., Royer D.* Elastic waves in solids – Applications to signal processing. Wiley, 1980.
12. *Encyclopedia of Acoustics.* Ed. M.J. Crocker, John Wiley & Sons, New York, 1997. 2096 p.
13. *Fickera G.* Existence theorems in elasticity. In: Handbuch der Physik V1a/2. Springer, Berlin, 1972. pp. 347–388.
14. *Howard C.Q., Cazzolato B.S.* Acoustic analyses using Matlab<sup>®</sup> and Ansys<sup>®</sup>. CRC Press, Taylor & Francis Group., 2015.
15. *Ilgamov M.A., Gilmanov A.N.* Non-reflecting boundary conditions for computational domains. Fizmatlit, Moscow, 2003. 240 p. (in Russian)
16. *Kallivokas L.F., Bielak J., MacCamy R.C.* Symmetric local absorbing boundaries in time and space. Journal of Engineering Mechanics. 1991. V. 117(9). P. 2027–2048.
17. *Kaltenbacher M.* Numerical simulation of mechatronic sensors and actuators. Springer, Berlin - Heidelberg - New York, 2004.

18. *Keller I.E.* Tensor calculus. Lan, St. Petersburg, 2012. 175 p. (in Russian)
19. *Lebedev L.P., Cloud M.J., Eremeyev V.A.* Tensor analysis with applications in mechanics. New Jersey: World Scientific, 2010, 381 p.
20. *Madenci E., Guven I.* The finite element method and applications in engineering using ANSYS. Springer, 2006.
21. The mechanics of coupled fields in structural elements. V.5. Electroelasticity. *Grinchenko V.T., Ulitko A.F., Shulga N.A.* Naukova Dumka, Kiev, 1989. 279 p. (in Russian)
22. *Nasedkin A.V.* Some finite element methods and algorithms for solving acousto-piezoelectric problems. Piezoceramic Materials and Devices, Ed. I. A. Parinov, Nova Science Publ., NY, 2010, pp. 177–218.
23. *Norrie D.H., De Vries G.* An introduction to finite element analysis. Academic Press, London, 1978. 301 p.
24. *Nowacki W.* Dynamic problems of thermoelasticity. Noordhoff, 1975. 436 c.
25. *Nowacki W.* Theory of elasticity. Mir, Moscow, 1975. 872 p. (in Russian)
26. *Nowacki W.* Electromagnetic effects in solids. Mir, Moscow, 1986. 160 p. (in Russian)
27. *Oden, J. T.* Finite elements of nonlinear continua. McGraw-Hill Book Company, New York, 1972. 432 p.
28. *Parton V.Z., Kudryavtsev B.A.* Electromagnetoelasticity: Piezoelectrics and electrically conductive solids. Gordon and Breach Science Publ., 1988. 503 c.
29. *Pissanetzky S.* Sparse matrix technology. Academic Press, New York, 1984. 312 p.
30. *Srinivas P., Sambana K.Ch., Datti R.K.* Finite element analysis using ANSYS® 11.0. PHI Learning Pvt. Ltd., 2010.
31. *Stolarski T.A., Nakasone Y., Yoshimoto S.* Engineering analysis with ANSYS software. Elsevier, 2006.
32. *Strang G., Fix G.* An analysis of the finite element method. Prentice-Hall, inc. Englewood Cliffs, N.J., 1973.
33. *Zienkiewicz O.C.* The Finite element method in engineering science. McGraw-Hill, 1977. 521 p.
34. *Zienkiewicz O.C., Morgan K.* Finite elements and approximation. J. Wiley and Sons, N.Y., 1983.
35. *Zienkiewicz O.C., Taylor R.L.* The finite element method. V. 1. The Basic. 2000.

36. *Zienkiewicz O.C., Taylor R.L.* The finite element method. V. 2. Solid Mechanics. 2000.
37. *Zienkiewicz O.C., Taylor R.L.* The finite element method. V. 3. Fluid Dynamics. 2000.
38. *Zubov L.M., Karyakin M.I.* Tensor calculus. Vuzovskaya kniga, Moscow, 2006. 120 p. (in Russian)